Energy, Environment, and Sustainability
Series Editor: Avinash Kumar Agarwal

Pravesh Chandra Shukla
Giacomo Belgiorno
Gabriele Di Blasio
Avinash Kumar Agarwal *Editors*

Alcohol as an Alternative Fuel for Internal Combustion Engines

Springer

Energy, Environment, and Sustainability

Series Editor

Avinash Kumar Agarwal, Department of Mechanical Engineering, Indian Institute of Technology Kanpur, Kanpur, Uttar Pradesh, India

AIMS AND SCOPE

This books series publishes cutting edge monographs and professional books focused on all aspects of energy and environmental sustainability, especially as it relates to energy concerns. The Series is published in partnership with the International Society for Energy, Environment, and Sustainability. The books in these series are edited or authored by top researchers and professional across the globe. The series aims at publishing state-of-the-art research and development in areas including, but not limited to:

- Renewable Energy
- Alternative Fuels
- Engines and Locomotives
- Combustion and Propulsion
- Fossil Fuels
- Carbon Capture
- Control and Automation for Energy
- Environmental Pollution
- Waste Management
- Transportation Sustainability

Review Process

The proposal for each volume is reviewed by the main editor and/or the advisory board. The chapters in each volume are individually reviewed single blind by expert reviewers (at least four reviews per chapter) and the main editor.

Ethics Statement for this series can be found in the Springer standard guidelines here https://www.springer.com/us/authors-editors/journal-author/journal-author-helpdesk/before-you-start/before-you-start/1330#c14214.

More information about this series at http://www.springer.com/series/15901

Pravesh Chandra Shukla · Giacomo Belgiorno ·
Gabriele Di Blasio · Avinash Kumar Agarwal
Editors

Alcohol as an Alternative Fuel for Internal Combustion Engines

Springer

Editors
Pravesh Chandra Shukla
Department of Mechanical Engineering
Indian Institute of Technology Bhilai
Raipur, Chhattisgarh, India

Gabriele Di Blasio
Istituto di Scienze e Tecnologie per
l'Energia e la Mobilità Sostenibili (STEMS)
Consiglio Nazionale Delle Ricerche
Napoli, Italy

Giacomo Belgiorno
PUNCH Torino S.p.A.
Turin, Italy

Avinash Kumar Agarwal
Department of Mechanical Engineering
Indian Institute of Technology Kanpur
Kanpur, Uttar Pradesh, India

ISSN 2522-8366 ISSN 2522-8374 (electronic)
Energy, Environment, and Sustainability
ISBN 978-981-16-0930-5 ISBN 978-981-16-0931-2 (eBook)
https://doi.org/10.1007/978-981-16-0931-2

Preface

Global pollution, depletion, and uneven distribution of petroleum reserves across the world have led to the research in the field of alternative fuels. Alcohol has emerged as an important potential alternative fuel for internal combustion (IC) engines. This book attempts to include the researches carried out in the field of alcohol utilization as an alternative fuel in IC engines.

The International Society for Energy, Environment and Sustainability (ISEES) was founded at Indian Institute of Technology Kanpur (IIT Kanpur), India, in January 2014 with an aim to spread knowledge/ awareness and catalyze research activities in the fields of energy, environment, sustainability, and combustion. The society's goal is to contribute to the development of clean, affordable, and secure energy resources and a sustainable environment for the society and to spread knowledge in the above-mentioned areas and create awareness of the environmental challenges, which the world is facing today. The unique way adopted by the society was to break the conventional silos of specializations (engineering, science, environment, agriculture, biotechnology, materials, fuels, etc.) to tackle the problems related to energy, environment, and sustainability in a holistic manner. This is quite evident by the participation of experts from all fields to resolve these issues. ISEES is involved in various activities such as conducting workshops, seminars, and conferences in the domains of its interests. The society also recognizes the outstanding works done by the young scientists and engineers for their contributions in these fields by conferring them awards under various categories.

Fourth International Conference on "Sustainable Energy and Environmental Challenges" (IV-SEEC) was organized under the auspices of ISEES from November 27–29, 2019, at NEERI, Nagpur. This conference provided a platform for discussions between eminent scientists and engineers from various countries including India, USA, China, Italy, Mexico, South Korea, Japan, Sweden, Greece, Czech Republic, Germany, Netherland, and Canada. In this conference, eminent speakers from all over the world presented their views related to different aspects of energy, combustion, emissions, and alternative energy resource for sustainable development and cleaner environment. The conference presented one high-voltage plenary talk by Mrs. Rashmi Urdhwareshe, Director, Automotive Research Association of India (ARAI), Pune.

The conference included 28 technical sessions on topics related to energy and environmental sustainability including one plenary talk, 25 keynote talks, and 54 invited talks from prominent scientists, in addition to 70+ contributed talks and 80+ poster presentations by students and researchers. The technical sessions in the conference included fuels, engine technology and emissions, coal & biomass combustion/gasification, atomization and sprays, combustion and modeling, alternative energy resources, water & water and wastewater treatment, automobile and other environmental applications, environmental challenges & sustainability, nuclear energy & other environmental challenges, clean fuels & other environmental challenges, water pollution and control, biomass and biotechnology, waste to wealth, microbiology, biotechnological and other environmental applications, waste & wastewater management, cleaner technology & environment, sustainable materials & processes, energy, environment and sustainability, technologies & approaches for clean, sensors and materials for environmental, biological processes and environmental sustainability. One of the highlights of the conference was the Rapid-Fire Poster Sessions in (i) engine/fuels/emissions, (ii) environment, and (iii) biotechnology, where 50+ students participated with great enthusiasm and won many prizes in a fiercely competitive environment. 300+ participants and speakers attended this three-day conference, where 12 ISEES books published by Springer, Singapore, under a special dedicated series "Energy, environment and sustainability" were released. This was the third time in a row that such a significant and high-quality outcome has been achieved by any society in India. The conference concluded with a panel discussion on "Balancing Energy Security, Environmental Impacts & Economic Considerations: Indian Perspective," where the panelists were Dr. Anjan Ray, CSIR-IIP Dehradun; Dr. RR Sonde, Thermax Ltd.; Prof. Avinash Kumar Agarwal, IIT Kanpur; Dr. R Srikanth, National Institute of Advanced Studies, Bengaluru; and Dr. Rakesh Kumar, NEERI Nagpur. The panel discussion was moderated by Prof. Ashok Pandey, Chairman, ISEES. This conference laid out the roadmap for technology development, opportunities, and challenges in energy, environment and sustainability domain. All these topics are very relevant for the country and the world in the present context. We acknowledge the support received from various funding agencies and organizations for the successful conduct of the Fourth ISEES Conference (IV-SEEC), where these books germinated. We would therefore like to acknowledge SERB, Government of India (special thanks to Dr. Sandeep Verma, Secretary); NEERI Nagpur (special thanks to Dr. Rakesh Kumar, Director), CSIR, and our publishing partner Springer (special thanks to Swati Mehershi).

The editors would like to express their sincere gratitude to a large number of authors from all over the world for submitting their high-quality work in a timely manner and revising it appropriately at a short notice. We would like express our special thanks to Dr. Chetan Patel, Dr. Nikhil Sharma, Dr. Deep Seth, Dr. Akhilendra Pratap Singh, Dr. Rakesh Kumar Maurya, Dr. Mohit Raj Saxena, Dr. Roberto Ianniello, Dr. Tomesh Kumar Sahu, Dr. Atul Dhar, and Dr. Vikram Kumar who reviewed various chapters of this monograph and provided their valuable suggestions to improve the manuscripts.

This book covers different aspects related to utilization of alcohol fuels in internal combustion (IC) engines with a focus on combustion, performance, and emission investigations. The main objective of this book is to present the engine combustion, performance, and emission characteristics of IC engines fueled by alcohol-blended fuels such as methanol, ethanol, and butanol. A section of the book highlights the importance of alcohol fuel for reducing the emission levels also. The possibility of alcohol fuels for the marine applications has also been discussed in this book. All the chapters written in this book include descriptions from the recent literatures and publications. Some of the chapters have shown the significance of alcohol fuels for advanced combustion concepts also. Engine researchers throughout the world will be benefitted from this book who are working in the field of alternative fuels. Editors expect interests in this book from automobile professionals and researchers in various academic institutions who are exploring their professional career or research in the field of engine research and alternative fuels for automobiles.

Raipur, India — Pravesh Chandra Shukla
Turin, Italy — Giacomo Belgiorno
Naples, Italy — Gabriele Di Blasio
Kanpur, India — Avinash Kumar Agarwal

Contents

Editors and Contributors

About the Editors

Dr. Pravesh Chandra Shukla is Assistant Professor in the Department of Mechanical Engineering at Indian Institute of Technology (IIT) Bhilai, India. Dr. Shukla received his Ph.D. from IIT Kanpur. He has also worked as Senior Research Associate at IIT Kanpur. He was Postdoctoral Researcher in the Division of Combustion Engines, Department of Energy Sciences, Lund University, Sweden. He briefly worked in Ecole Centrale de Nantes, France, in the field of dual fuel combustion. He is a recipient of Young Scientist Award from the International Society for Energy, Environment and Sustainability. Dr. Shukla mainly works in the field of internal combustion engines and alternative fuels for transportation. He worked on the development of additives for high compression ratio heavy duty engines fueled with alcohol. He is involved in investigating the emission characteristics for alternative fuels like biodiesel, HVO and alcohols for conventional and advanced heavy duty compression ignition engines. He has published over 28 technical articles in journals of national and international repute and conference proceedings.

Dr. Giacomo Belgiorno is Technology System Engineer in the Department of Advanced Engineering in PUNCH Torino S.p.A., formerly General Motors Global Propulsion Systems—Torino. He received his M.S. in Mechanical Engineering from University of Campania Luigi Vanvitelli in 2014, and Ph.D. in Energy Science and Engineering from University of Naples "Parthenope" in 2018. During the Ph.D. program, he worked in Istituto Motori as Research Associate and Guest Researcher in Lund University, Sweden. Subsequently, he worked in CNH Industrial. He has authored two book chapters and more than 20 conference and journal articles.

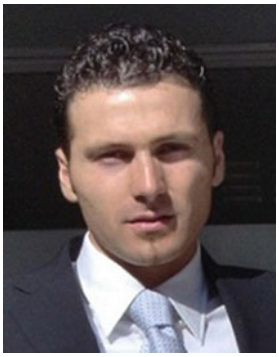

Dr. Gabriele Di Blasio is currently Research Scientist at the National Research Council of Italy. His main research interest is focused on advanced technologies for propulsion and energy conversion systems. Dr. Di Blasio worked as the responsible R&D engineer at ETRA and leads a project on the development of a dual fuel system for heavy duty engines. He is a regular reviewer of indexed journals of national and international repute. He has authored over 50 publications in peer-reviewed journals, conference proceedings and book chapters. He is a member of the SAE International. He has contributed to private and public projects in cooperation with universities, research centers and OEMs.

Prof. Avinash Kumar Agarwal joined the Indian Institute of Technology (IIT) Kanpur, India in 2001 after working as Postdoctoral Fellow at the Engine Research Center, University of Wisconsin at Madison, USA. His interests are IC engines, combustion, alternate and conventional fuels, lubricating oil tribology, optical diagnostics, laser ignition, HCCI, emissions and particulate control and large bore engines. Prof. Agarwal has published 290+ peer-reviewed international journal and conference papers, 42 edited books and 78 books chapters and has 10,000+ Scopus and 15,300+ Google Scholar citations. He is Fellow of SAE (2012), Fellow of ASME (2013), Fellow of ISEES (2015), Fellow of INAE (2015), Fellow of NASI (2018), Fellow of Royal Society of Chemistry (2018) and Fellow of American Association of Advancement in Science (2020). He is a recipient of several prestigious awards such as Clarivate

Analytics India Citation Award-2017 in Engineering and Technology, NASI-Reliance Industries Platinum Jubilee Award-2012; INAE Silver Jubilee Young Engineer Award-2012; Dr. C. V. Raman Young Teachers Award: 2011; SAE Ralph R. Teetor Educational Award-2008; INSA Young Scientist Award-2007; UICT Young Scientist Award-2007; INAE Young Engineer Award-2005. Professor Agarwal received Prestigious Shanti Swarup Bhatnagar Award-2016 in Engineering Sciences. For his outstanding contributions, Prof. Agarwal is conferred upon Sir J. C. Bose National Fellowship (2019) by SERB.

Contributors

Avinash Kumar Agarwal Department of Mechanical Engineering, Indian Institute of Technology Kanpur, Kanpur, India

Carlo Beatrice Istituto di Scienze e Tecnologie per l'Energia e la Mobilità Sostenibili (STEMS), Consiglio Nazionale Delle Ricerche, Naples, Italy

Giacomo Belgiorno Currently in PUNCH Torino S.p.A., Turin, Italy;
Istituto di Scienze e Tecnologie per l'Energia e la Mobilità Sostenibili (STEMS), Consiglio Nazionale Delle Ricerche, Naples, Italy

Timothy Bodisco School of Engineering, Deakin University, Geelong, VIC, Australia

Richard J. Brown Biofuel Engine Research Facility, Queensland University of Technology, Brisbane, QLD, Australia

Balendra V. S. Chauhan Automotive Fuels and Lubricants Application Division, CSIR-Indian Institute of Petroleum, Dehradun, India

Cengiz Deniz Maritime Faculty, Istanbul Technical University, Istanbul, Turkey

Atul Dhar School of Engineering, Indian Institute of Technology Mandi, Mandi, India

Gabriele Di Blasio Istituto di Scienze e Tecnologie per l'Energia e la Mobilità Sostenibili (STEMS), Consiglio Nazionale Delle Ricerche, Naples, Italy

Giuseppe Di Luca Istituto di Scienze e Tecnologie per l'Energia e la Mobilità Sostenibili (STEMS), Consiglio Nazionale Delle Ricerche, Naples, Italy

Ayat Gharehghani School of Mechanical Engineering, Iran University of Science and Technology, Tehran, Iran

Roberto Ianniello Istituto di Scienze e Tecnologie per l'Energia e la Mobilità Sostenibili (STEMS), Consiglio Nazionale Delle Ricerche, Naples, Italy

Alireza Kakoee School of Mechanical Engineering, Iran University of Science and Technology, Tehran, Iran

Ravindra Kshatri Department of Mechanical Engineering, Indian Institute of Technology Bhilai, Raipur, India

Rakesh Kumar Maurya Department of Mechanical Engineering, Indian Institute of Technology Ropar, Rupnagar, India

B. Prabakaran Department of Automobile Engineering, Hindustan Institute of Technology and Science, Chennai, Tamil Nadu, India

S. Rajkumar Mechanical Engineering, Sri Sivasubramaniya Nadar College of Engineering, Chennai, India

Tomesh Kumar Sahu Department of Mechanical Engineering, Indian Institute of Technology Bhilai, Raipur, India

Mohit Raj Saxena Department of Mechanical Engineering, Indian Institute of Technology Ropar, Rupnagar, India

Nahil Serhan Wärtsilä Catalyst Systems R&D, Vaasa, Finland

Nikhil Sharma Department of Mechanical Engineering, Malaviya National Institute of Technology Jaipur, Jaipur, Rajasthan, India

M. K. Shukla Automotive Fuels and Lubricants Application Division, CSIR-Indian Institute of Petroleum, Dehradun, India;
School of Engineering, Indian Institute of Technology Mandi, Mandi, India

Pravesh Chandra Shukla Department of Mechanical Engineering, Indian Institute of Technology Bhilai, Raipur, India

J. Thangaraja Mechanical Engineering, Vellore Institute of Technology, Vellore, India

Ali Zare School of Engineering, Deakin University, Geelong, VIC, Australia

Burak Zincir Maritime Faculty, Istanbul Technical University, Istanbul, Turkey

Chapter 1
Introduction to Alcohol as an Alternative Fuel for Internal Combustion Engines

Pravesh Chandra Shukla, Giacomo Belgiorno, Gabriele Di Blasio, and Avinash Kumar Agarwal

The transportation sector is one of the main contributors to global CO_2 emissions and is expected to further increase due to the growth of population and life quality standards. Therefore, to prevent the negative impacts of climate change, the reduction of CO_2 emissions is the top priority. For these reasons, the automotive sector is facing new challenges; advanced internal combustion engines, electrification of the drive train, and replacing fossil fuels can help to meet greenhouse gas emission standards and simultaneously reduce pollutants.

The second chapter is about *Ethanol in Dual-Fuel and Blend Fueling Modes for Advanced Combustion in Compression Ignition Engines*. This chapter discusses two ethanol fueling modes, dual fuel, and blend which are applied in a compression ignition engine to evaluate the effect of different engine calibration parameters on the thermodynamic and emissions. The dual-fuel combustion employing high ethanol, rail pressure, and EGR levels leads to important benefits, minimizing the emissions and noise and maximizing the efficiency. The results demonstrate ethanol being a promising alternative to fossil fuels for the globally lower emissions in compliance with the actual advanced engine technologies. Similar to this, another author investigated *PM characteristics and relation with oxidative reactivity—alcohol as a*

P. C. Shukla (✉)
Department of Mechanical Engineering, Indian Institute of Technology Bhilai, Raipur, India
e-mail: pravesh@iitbhilai.ac.in

G. Belgiorno
Currently in PUNCH Torino S.p.A., Corso Castelfidardo, 36, 10129 Turin, Italy

G. Belgiorno · G. Di Blasio
Istituto di Scienze e Tecnologie per l'Energia e la Mobilità Sostenibili (STEMS), Consiglio Nazionale Delle Ricerche, Via G. Marconi, 4, 80125 Naples, Italy

A. K. Agarwal
Department of Mechanical Engineering, Indian Institute of Technology Kanpur, Kanpur, India

P. C. Shukla et al. (eds.), *Alcohol as an Alternative Fuel for Internal Combustion Engines*, Energy, Environment, and Sustainability,
https://doi.org/10.1007/978-981-16-0931-2_1

renewable fuel. This review chapter explains the PM physical and chemical properties and highlights their correlation with the oxidative reactivity toward oxygen. This review chapter summarizes different theories and assumptions proposed in the literature to correlate the soot physico-chemical parameters with the assigned oxidative reactivity toward oxygen.

Maritime transportation is the most important transportation type since 90% of world trade is carried. In another chapter, the details about *Methanol as a Fuel for Marine Diesel Engines* are discussed. This chapter covers information about the status of maritime transportation, international maritime emission rules and regulations, emission mitigation technologies and methods, methanol at maritime transportation, methanol properties, and combustion concepts, and the methanol partially premixed combustion strategy for maritime transportation. The main findings of the chapter are using alternative fuels, such as methanol, which can reduce different types of regulated emissions at maritime transportation without applying additional equipment while providing more efficient marine diesel engines, and the methanol partially premixed combustion (PPC) strategy showed high engine efficiency than the conventional marine gas oil-fueled diesel engine with lower CO_2 and NO_x emissions.

The internal combustion engines remain preferred prime movers for on-road and off-road applications over many decades. However, for reducing the usage of fossil fuels and the harmful pollutants emitted by the conventional engines, it has become imperative that the alternative strategies are developed. In another chapter, investigation related to *The Potential of Various Alcohol Fuels for Low-Temperature Combustion Engines* is discussed. Moreover, the alcohol fuels are effective in advanced combustion strategy like low-temperature combustion (LTC). It is opined that alcohol fuels make use of the full merits of LTC which is attributed to the increased octane number, wider equivalence ratio, broad operational range with reduction in emission, higher auto-ignition resistance, and longer ignition delay. Hence, this chapter is aimed to present significant details on combustion and emission characteristics of alcohol-fueled engines operated on advance combustions strategy of LTC. This chapter provided the essential details of the alcohol fuel as alternate fuels for internal combustion engines. Alcohol fuels are characterized by their renewability, closer to the properties of gasoline, better adaptability with diesel, and advantages of emission reduction.

Similar to this, a chapter related to *Challenges in blending the Diesel–Ethanol blends using Butanol* as co-solvent along with diesel for replacing the neat diesel to fuel compression ignition engines suitable for low-temperature application is also present in the book. This study was conducted in various steps, viz. test of solubility of diesel–ethanol blends containing various proportions of ethanol from 0 to 50% in increments of 5% in a temperature range of 5–35 °C using butanol as co-solvent in the proportions from 0 to 10% in increments of 1%; different phases of study have been followed to utilize diesel–ethanol blends as fuel in compression ignition (CI) engine in this study. Experiments have been conducted with diesel–ethanol without co-solvent and with butanol as co-solvent. The effects of engine operating parameters such as injection pressure (IP), injection timing (IT), compression ratio (CR), and intake air temperature (IAT) on engine performance, combustion, and emission were

studied. As a sum up, although the efficiency produced by D45E45B10 is found to be marginally lower, the emissions of smoke, HC, and CO produced are found to be marginally higher compared to that of diesel.

Alcohols produced from organic matter have been actively considered as solution to energy demand and an attractive alternative to conventional fuel. These fuels are considered to be green, clean, and renewable. In another chapter, *Recent Development for Use of Alcohol-Based Renewable Fuels in Compression Ignition Engine* is discussed. This chapter is a review of recent research work available in the literature and explains about alcohol as a fuel and its utilization in diesel engine, causes of emission in diesel engine, and after-treatment devices to reduce this emission. Topics such as material compatibility and economical aspect of alcohol as a fuel in diesel engine are discussed. The present review shows that alcohol is a promising fuel to be blended with diesel; however, material compatibility and combustion process have to be optimized to take the advantage of oxygen present in fuel to reduce emission. Low-temperature combustion strategy in internal combustion engines provides lower emissions beside high engine performance according to chemically control combustion temperature. This strategy is divided into three engine types which are premixed charge compression ignition (PCCI), homogenous charge compression ignition (HCCI), and reactivity-controlled compression ignition (RCCI) engines. Low-temperature combustion strategies usually used two various fuels with low and high reactivities.

In another chapter, *Alcohol fuels in low-temperature combustion engines* are discussed. This chapter categorized LTC strategies in which alcohol fuels are used as alternative fuel. Alcohol fuel application in various countries is dependent on the country's geographical situation and their policies; Brazil, China, USA, European Union, and Japan are the most areas of using alcohol fuels. In this way, government policies were effective on people demands of this type of fuels with providing special vehicles; for example, using flexible-fuel engines in Brazil could increase alcohol fuel demand, especially ethanol up to 88%; a flexible-fuel engine is a dual-fuel engine with separated fuel tank. Biobutanol is a very promising renewable fuel for spark-ignition engines due to quite similar properties to conventional gasoline. In another chapter, titled *Effect of n-Butanol and Gasoline Blends on SI Engine Performance and Emissions*, it discusses the possibility of usage of biobutanol in unmodified spark-ignition (SI) engines while blending them with gasoline up to 70% (v/v). Detailed characterization of combustion-related fuel properties of butanol and gasoline butanol blends has been carried out. The engine test results of butanol blends with gasoline are comparable to that of baseline gasoline.

In most of the cases, butanol blends are a better choice over gasoline in terms of emissions and performance. Being an oxygenated fuel, butanol gives better combustion efficiency and reduces most of the emissions except NO, which can be taken care of by means of after-treatments. The results of this study indicate that butanol blending with gasoline at higher butanol concentrations (>50%) is not feasible in unmodified SI engines designed for gasoline. Production and consumption cycle of biobutanol, as a whole, result in smaller emission than the conventional fuels of fossil

origins as it is a biofuel. In another chapter, *Ethanol Fumigation and Engine Performance in a Diesel Engine* is discussed. This chapter studied the effect of ethanol fumigation on engine performance using a modern compression ignition engine. Performance-related parameters were investigated at ethanol substitutions of 0, 10, 20, 30, and 40% (by energy) under 25, 50, 75, and 100% load at 1500 and 2000 rpm. Using E10 and E20 in some of the operating modes decreased FMEP and BSFC, while using E40 increased FMEP and BSFC. This study investigated the effect of ethanol fumigation on engine performance parameters using a modern turbocharged.

CI-engine is an emerging strategy to improve engine efficiency along with the simultaneous in-cylinder reduction of NO_x and PM emissions. In dual-fuel operation, low-reactivity fuel (such as methanol and ethanol) and high-reactivity fuel (such as diesel) are used in the same engine cycle. In another chapter, *Low and Medium Carbon Alcohol Fueled Dual-Fuel Compression Ignition Engine* is discussed. This chapter presents a detailed analysis of performance, combustion, and emission characteristics of low- and medium-carbon alcohol–diesel-fueled dual-fuel CI engine. This chapter also briefly explains the production of alcohol fuel and the benefits of their inimitable properties. The influence of engine operating parameters on the heat release rate, combustion duration, and cyclic combustion variations has been discussed in this chapter. This chapter presents the performance, combustion, and emissions characteristics of low- and medium-carbon alcohol–diesel-fueled dual-fuel CI engine. Diesel engines are one of the most preferred internal combustion (IC) engines for heavy-duty transport vehicles due to its higher torque characteristics and better thermal efficiency over gasoline engines. Despite having advantages in terms of efficiency and durability, it contributes to emissions in the environment, primarily particulate matter (PM) and oxides of nitrogen (NO_x). Another chapter, titled *Impact of Ethanol on Combustion, Performance, and Emission Characteristics of Diesel Engine*, aims to review about the combustion and emission characteristics of ethanol–diesel-blended fuels in CI engines. Studies show that an increasing fraction of ethanol in diesel tends to reduce CO and HC emissions, while NO_x emissions are reported slightly higher compared to baseline diesel. Higher ignition delay (ID) and lower combustion duration (CD) are observed for ethanol blends.

Chapter 2
Ethanol in Dual-Fuel and Blend Fueling Modes for Advanced Combustion in Compression Ignition Engines

Roberto Ianniello, Giacomo Belgiorno, Giuseppe Di Luca, Carlo Beatrice, and Gabriele Di Blasio

2.1 Introduction: Ethanol–Diesel Dual Fuel and Blending

The automotive industry is always looking for cleaner and more efficient technologies that effectively improve ambient air quality to reduce greenhouse gas (GHG) emissions and contribute to energy saving. So, the technologies relating to fuels and engines are facing a double challenge of improving consumption and reducing emissions. Considering the strict regulation emission and the poorness of primary energy resources, the new concept development and highly efficient combustion systems have become increasingly important (Blasio et al. 2017; Belgiorno et al. 2020). The alternative combustion concept is generally focused on better spray atomization and the preparation of the air–fuel mixing, lower local equivalence ratios, lower peak temperatures in the combustion chamber, and higher combustion rates. A strategic way to achieve the targets just proposed is using alternative fuels, among them, ethanol.

Ethanol is a potential alternative fuel for combustion engines that can offset the demand for petroleum-based because it can be produced from biomass, hence providing the potential to reduce particulate emissions in compression ignition engines (Mani Sarathy et al. 2014). Many researchers have investigated the effect of ethanol using different injection configurations, port fuel, or direct injections to achieve low emission and high thermal efficiency combustion (Asad et al. 2015; Pedrozo et al. 2017).

R. Ianniello (✉) · G. Belgiorno · G. Di Luca · C. Beatrice · G. Di Blasio
Istituto di Scienze e Tecnologie per l'Energia e la Mobilità Sostenibili (STEMS), Consiglio Nazionale Delle Ricerche, Via G. Marconi, 4, 80125 Naples, Italy
e-mail: roberto.ianniello@stems.cnr.it

G. Belgiorno
Currently in PUNCH Torino S.p.A., Corso Castelfidardo, 36, 10129 Turin, Italy

P. C. Shukla et al. (eds.), *Alcohol as an Alternative Fuel for Internal Combustion Engines*, Energy, Environment, and Sustainability,
https://doi.org/10.1007/978-981-16-0931-2_2

Asad et al. (2015) studied the effect of ethanol in dual-fuel mode combustion using a single-cylinder light-duty engine adopting high EGR levels and single diesel injection near firing top dead center (TDC). The authors observed elevated levels of HC and CO emissions at low loads, as well as ultra-low NO_x and soot with diesel-like thermal efficiency. Pedrozo et al. (2017) evaluated the optimization of diesel injection timings for efficient dual-fuel combustion, observing that the pre-injection of diesel before the main injection is essential to reduce peak pressure rise rate. High ethanol energy fractions effectively lowered NO_x emissions, and EGR further reduced NO_x emissions with a negligible impact on engine efficiency.

As concerns, the ethanol–diesel DI, Waterland et al. (2003) analyzed the safety aspects and assessed the performance of ethanol–diesel mixtures in order to optimize overall efficiency. Another aspect to consider is the chemical properties of the ethanol when compared to diesel. Satgé de Caro et al. (2001) evaluated the effect of ethanol on diesel fuel properties, such as lubricity, material compatibility, viscosity, safety, and stability. They assessed the impact of the fuel on emission and engine performance. Also, the authors proposed a new additive formulation to guarantee proper operation of a compression ignition engine, because the ethanol addition affects key properties as blend cetane number, viscosity, lubricity, stability, and energy content.

In this monograph, two different combustion modes, dual fuel and blended, have been described applying as alternative fuels the ethanol combined to the diesel fuel. The aim is to give the reader an overview of the pros and cons of the two presented combustion modes, showing the comparison of the individual calibration parameters (e.g., EGR, rail pressure, injection pattern, etc.) on the different combustion modes tested. The one-factor-at-a-time method has been used; this approach permits to evaluate the response for each factor varied. An exhaustive overview of emissions, efficiencies, and combustion behaviors, adopting two different fueling modes, is presented.

2.2 Engine Test Rig and Fuel Proprieties

In this monograph, the combustion process, emissions, and efficiencies of compression ignition engines fueled with ethanol in dual fuel and blending have been discussed. The experiments have been performed on a single-cylinder compression ignition engine with a displacement of about 0.5 l representative of the unit displacement of modern light-duty compression ignition engines. Figure 2.1 shows the schematic layout of the experimental setup. The auxiliary engine systems are not automatically connected to the engine, as shown in Fig. 2.1, to guarantee the maximum flexibility without affecting the load conditions. The engine is equipped with a conventional fuel injection system (direct) and a port fuel injection system to operate in dual-fuel mode. Table 2.1 shows the engine geometrical characteristics. The electronic control unit, developed by real-time FPGA control, allows the setting of all the engine control parameters. This approach offers great flexibility for all operating conditions.

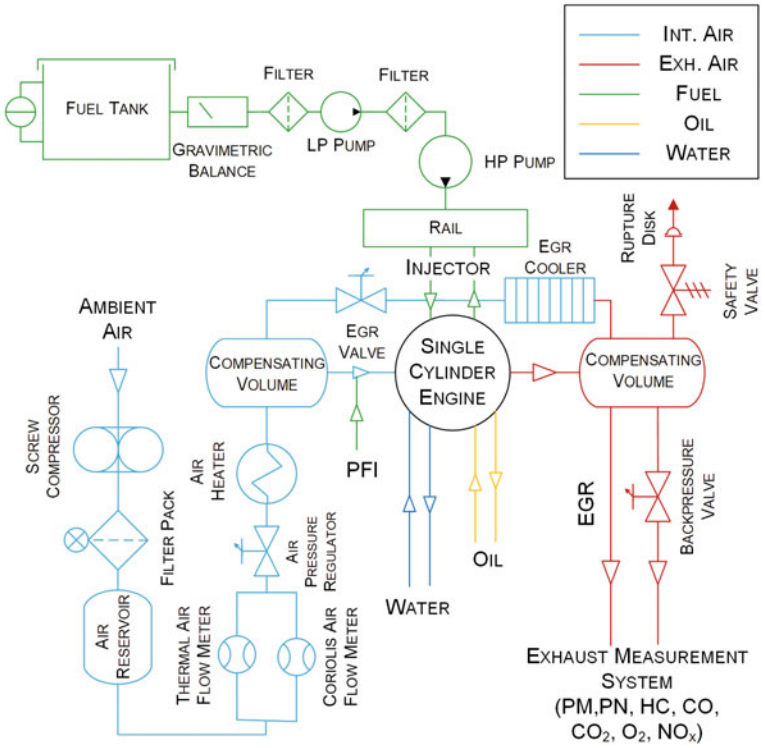

Fig. 2.1 Test cell layout

Table 2.1 Engines' geometrical characteristics

Displaced volume [l]	0.5
Bore × stroke [mm] × [mm]	82 × 90.4
Compression ratio	16.5
Diesel fuel injection system	Common rail
Diesel injector	Solenoid with 7 holes
Ethanol PFI injector	Solenoid multi-hole
Fuels tested	Ethanol, diesel

The ethanol fuel has been injected on the intake manifold using a port fuel injection (PFI) system, suitably calibrated for ethanol fuel delivery. The diesel fuel has been directly injected into the combustion chamber using the engine's common rail fuel system and the solenoid injector. The PFI and diesel injector specifications are given in Table 2.1.

The data has been processed to compute combustion metrics such as the indicated mean effective pressure (IMEP), the start of combustion (SOI), the heat release rate (HRR), and the combustion phasing (CA50). The combustion duration is defined as

Table 2.2 Fuel properties (Epping et al. 2002; Yates et al. 2010)

Properties	Diesel	Ethanol
Research octane number [-]	–	108–109
Molar mass [g/mol]	170	46.07
H/C [−]	1.8	3
O/C [−]	0	0.5
LHV [MJ/kg]	42.9	26.9
(A/F)s [−]	14.5	9.0
Viscosity [mPa/s]	3.91	1.36
Density [kg/m^3]	810	785
Boiling point [°C]	180–360	78
Heat of vaporization [kJ/kg]	270	840
ΔH_{vap}/LHV [kJ/MJ]	6.29	31.23
Specific heat [kJ/kg K]	2.2	2.5

the duration from CA10 to CA90 (crank angle where the 10 and 90% of the total heat release occurs, respectively), while the ignition delay (ID) as the crank angle difference between CA10 and the start of injection (SOI).

Engine-out emissions (THC, CO, NO_x) have been considered for the results presented in this monograph.

The monograph focuses on the sensitivities of the ethanol blending ratio, injection parameters, and EGR on engine efficiencies and engine-out emissions for both ethanol fueling modes, dual fuel and blending.

Table 2.2 shows the relevant chemical–physical properties of the fuels tested for the experimental results presented in this monograph. The intrinsic fuel property that plays an important role in the mixing and combustion process is the heat of vaporization, ΔH_{vap} expressed in kJ/kg, giving an effect on the charge cooling; the charge cooling effect could be measured normalizing the heat of vaporization with lower heating value (LHV). This fuel property ΔH_{vap}/LHV is an indicator of the difficulty of igniting the ethanol fuel at conventional intake temperature and compression ratio conditions, and the ethanol is ~5 times higher than the conventional diesel fuel. The cooling effect of ethanol reduces the in-cylinder thermodynamic temperatures, and in turn, the in-cylinder heat transfer losses compared to conventional diesel combustion (CDC) increasing the engine efficiency (Caton 2012).

2.3 Dual-Fuel Combustion Mode

An experimental investigation has been performed to further assess, in comparison with literature results, the ethanol effects as secondary premixed fuel in dual-fuel mode. A steady-state engine point has been selected for the investigation, which has speed 1500 rpm and engine load 6.2 bar IMEP. A Euro6 diesel engine parameter

Table 2.3 Dual-fuel engine operating conditions and constraints

Engine parameters	Values		
Engine speed [rpm]	1500		
IMEP [bar]	6.2		
EGR [%]	0	0	20
Diesel injection pressure [bar]	500–1000	500	500
Diesel injection strategy	Main	Pilot–main	Main
SOI ethanol [deg aTDC]	−360		
PFI pressure [barG]	5		
Intake manifold temperature [K]	333		
Boost pressure [barG]	0.3		
Combustion noise max. [dBA]	90		
PRR_{max} [bar/deg]	8.0		
COV_{IMEP} max. [%]	3.5%		

calibration has been used to ensure direct transferrable outputs to real light-duty engine applications. In particular, the injection, boost, back pressure, etc., parameters are derived from a multi-cylinder engine with the same combustion architecture. Table 2.3 reports the main engine control settings of the operating point tested.

The premixed ethanol level has been varied from the conventional diesel combustion toward the maximum value. The level of premixing, defined as fuel substitution ratio (FSR), can be quantified on an energy basis according to the following equations:

$$\mathrm{FSR} = \frac{m_p \cdot \mathrm{LHV}_p}{m_p \cdot \mathrm{LHV}_p + m_d \cdot \mathrm{LHV}_d} \tag{2.1}$$

where the m_p and m_d indicate the mass flow rate of premixed fuel (P) and direct injection (DI) fuel, respectively, while the LHV_d and LHV_p correspond to the lower heating value for each fuel. Furthermore, the average LHV value is calculated by:

$$\mathrm{LHV}_{\mathrm{mix}} = \frac{m_p}{m_{\mathrm{tot}}} \cdot \mathrm{LHV}_p + \left(1 - \frac{m_p}{m_{\mathrm{tot}}}\right) \cdot \mathrm{LHV}_d \tag{2.2}$$

The effects of different ethanol energy fractions, diesel injection strategies, injection pressure, and EGR rates have been investigated. Efficiencies and emission analysis have been carried out to determine the effectiveness of using ethanol and calibration parameters on a light-duty diesel engine. Table 2.3 shows the parameters that have been investigated, as well as the levels. Ethanol fuel has been injected employing a port fuel injector (PFI), with a fixed injection timing ($\mathrm{SOI}_{\mathrm{ethanol}}$) of −360° before the firing top dead center (bTDC) and injection pressure 5 bar, with an air–fuel mixture intake manifold temperature of 333 K for all test conditions. Two levels of diesel fuel

injection pressure are investigated, 500 and 1000 bar. Single- and multiple-compact injection pattern strategies are employed for this test campaign. The start of injection of diesel (SOI_{diesel}) and the injection durations for both fuels have been varied to achieve the reference combustion phasing and IMEP values, respectively. Other injection parameters, pilot injection, energizing time (ET), dwell time among the pulses, and $SOI_{ethanol}$ have been kept constant. During the test campaign, practical constraints such as the maximum pressure rise rate (PRR) or combustion noise values have been observed. The PRR value has been limited to about 8 bar/deg, which corresponds to 90 dBA, according to the comfort standards. The coefficient of variation (COV_{IMEP}) has been limited to 3.5%.

The test methodology flowchart is schematized in Fig. 2.2. The first step of the test campaign consists of warming up the engine in diesel mode to stabilize the coolant

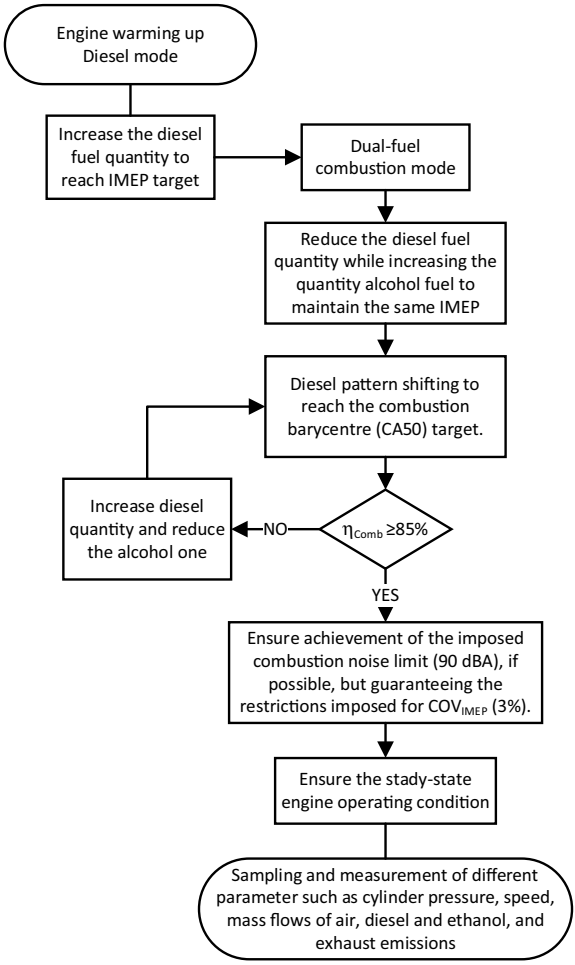

Fig. 2.2 Flowchart of the dual-fuel combustion test execution

temperatures (oil and water cooling) at about 85 °C. Switching to dual-fuel mode, the energy fraction of ethanol has been varied from zero to nearly 70% according to the imposed limit on combustion noise, PRR, and combustion stability (Table 2.3). Once the maximum ethanol fraction is achieved, a one-factor-at-a-time parameterization has been performed for the start of injection, injection pattern, rail pressure, and EGR.

In the following sections, the main effect of the engine control parameters on combustion, emission, and performance of a dual-fuel ethanol–diesel compression ignition engine is presented. A parametric analysis has been performed at a constant speed (1500 rpm) and load (6.2 bar of IMEP) to evaluate the maximum possible ethanol fraction, following the methodology illustrated in Fig. 2.2, the injection pattern, fuel injection pressure, and EGR effects.

2.3.1 Maximum Ethanol Fraction

This section describes the steps that the authors have followed to define the maximum substitution fraction of diesel with ethanol according to the imposed limits on combustion (combustion noise, peak PRR, and combustion stability); see Table 2.3.

The fuel substitution ratio (FSR) has been assessed in a steady-state test point at different levels of combustion phasing (from 4° to 14° aTDC), employing a constant diesel injection pattern (only main injection), diesel injection pressure (500 bar), boost and back pressures, intake temperature, at 1500 rpm and 6.2 bar IMEP (see Table 2.3). Since the one-factor-at-a-time method has been chosen to evaluate the calibration parameter effect, the first analysis has been conducted using only one pulse without EGR. In this way, it is possible to discriminate the single effects of the ethanol fraction with no influence of other parameters. The combustion phasing has been kept constant, and as the reference one, this choice is based on keeping to some extent constant the thermodynamic efficiency constant. Once the maximum FSR and optimal CA50 have been selected, this has been used for the analysis presented for the next dual-fuel sections.

The maximum FSR and gross-indicated efficiency (η_{gross}) function of CA50 are displayed in Fig. 2.3. The comparative results among the combustion phasing show that advanced CA50 allows, on average, a higher FSR as well as the efficiency. A flat trend for the FSR is observed, in a range 70–74%, for CA50 values from 4 up to 10°, while for higher values, the ethanol amount has been reduced to respect the imposed target (combustion noise).

The gross-indicated efficiency, shown in Fig. 2.3, is characterized by a flat trend for advanced combustion phasing, in the range 33–34%; as it shifts to later positions, the trend decreases until reaching a minimum at 14°, about 31.5%. This decrease is mainly due to an increase in the combustion duration, which values are reported in Table 2.4, with a consequent increase in the wall heat losses and a reduction in thermodynamic efficiency.

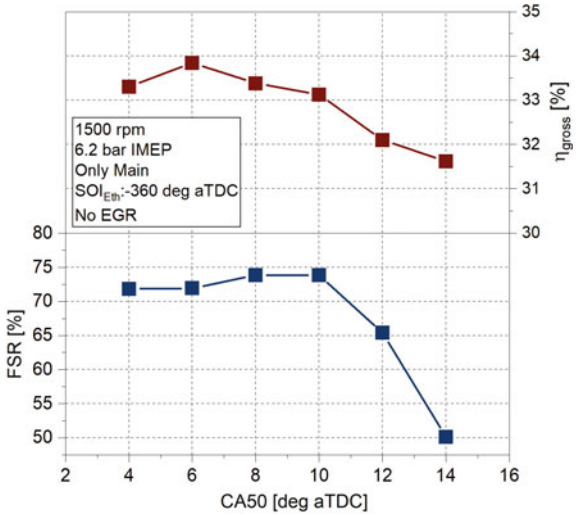

Fig. 2.3 η_{gross} and maximum FSR function of CA50, 1500 rpm, 6.2 bar IMEP

Table 2.4 CA90-10 and COV_{IMEP} function of CA50, 1500 rpm, 6.2 bar IMEP

CA50 [deg aTDC]	CA90-10 [deg]	COV_{IMEP} [%]
4	17.6	2.3
6	17.2	2.9
8	17.9	2.8
10	19.8	3.2
12	20.4	2.6
14	21.2	1.7

The CA50 sweep diagram is an easy way to identify the optimal combustion phasing range for the tested point. Therefore, as already introduced in the previous section, CA50 equal to 6° aTDC has been chosen as a reference point, because it guarantees a maximum gross-indicated efficiency and a high value of ethanol fraction.

2.3.2 Injection Strategy

This section presents the effects of a more complex, double pilot plus main injection pattern in comparison with the standard single-pulse injection one usually employed for dual-fuel application. The aim of using a complex injection pattern, characterized by multiple close injections, is to realize a more compact combustion process allowing an improved mixture stratification and lowering the heat losses to the chamber walls. Additionally, a reduction of the combustion noise is possible too (Vassallo et al. 2018). The injection pattern schematics adopted, energizing current (EC), are shown in Fig. 2.4. These investigations have been performed at CA50,

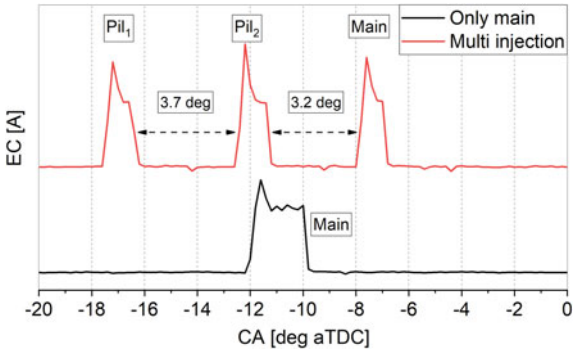

Fig. 2.4 Schematic of the injection patterns' dual-fuel mode

equal to 6° aTDC, identified in Sect. 2.3.1, at the constant rail pressure (500 bar), $SOI_{ethanol}$, FSR, and load without EGR (see Table 2.3) in a manner to discriminate the injection pattern effect.

Different combustion modes, adopting different injection patterns, are observed in Fig. 2.5. The single-injection strategy shows a longer ignition delay, allowing a higher air–fuel mixing degree and, consequently, more low reactive fuel at low equivalence ratios. The diesel is so diluted that no sustained combustion can be obtained. The multi-injection strategy instead leads to a high degree of high reactive fuel stratification in the combustion chamber. The employment of a more complex injection strategy reduces the ignition delay, with a consequent earlier start of combustion as HRR profiles are demonstrated in Fig. 2.6. An improvement of the ethanol combustion is observed in the premixed pilot region, which influences the flame propagation through the air–fuel mixture. Therefore, the HRR trace is less sharp, characterized by a lower peak value than in the reference case, resulting in a substantial reduction in combustion noise of about 4 dBA. Longer and higher diffusive combustion than

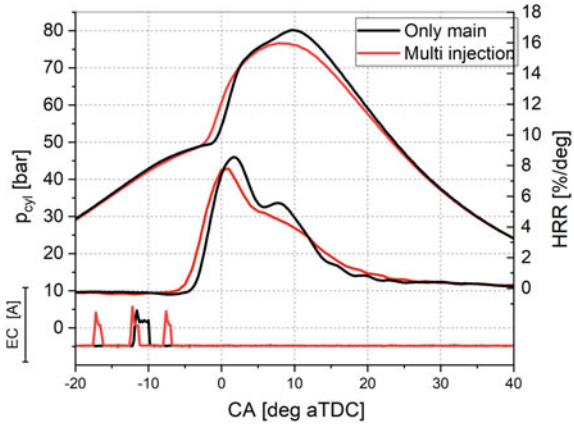

Fig. 2.5 In-cylinder pressure, apparent HRR, and injection pattern for multi- and single-injection strategies in dual-fuel mode at 1500 rpm and 6.2 bar IMEP

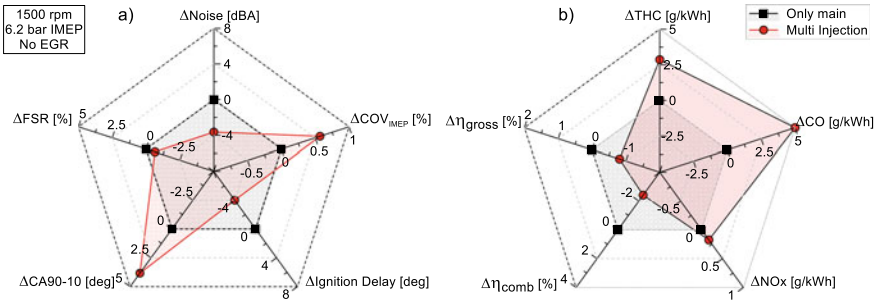

Fig. 2.6 Delta combustion noise, COV_{IMEP}, ID, CA90-10, FSR, emissions, and efficiencies for multi-injection strategy compared to the only main injection at 70% of FSR

the reference case is noted, which causes an increase in the particulate matter, even if it is to be considered negligible being in a soot-less zone.

Figure 2.6a shows the variances by adopting the multi-injection strategy compared to the single injection at constant FSR, in terms of combustion noise, COV_{IMEP}, ignition delay, and combustion duration. The higher combustion duration of the multi-injection pattern, of about 5°, due to the more significant diffusive phase, as observed in the heat release rate (Fig. 2.5), increases the heat transfer losses from the charge to the combustion chamber walls (Chang et al. 2012). Then, a higher amount of fuel burns further into the expansion stroke, increasing exhaust gas losses and exhaust temperatures (Knight et al. 2010).

The FSR can be as high as 73% within the imposed combustion limit listed in Table 2.3; the combustion process covariance is within 3.5%. Also, the combustion noise is below the maximum acceptable value, even at high FSR. A reduction of PRR is observed by adopting a multi-injection strategy. It is related to a lower premixed combustion phase leads to a longer combustion duration of about 4°. The combustion noise reduces about 4 dBA (Fig. 2.6a). The combustion temperature, for the complex pattern, is not as high as that of the single injection one, which could potentially decrease NO_x emissions (Nehmer and Reitz 1994). Since the tests are at constant equivalence ratio and temperature, the NO_x concentration in Fig. 2.6b is similar to both injection strategies. The smoke emissions have not been included in the graph, as the tests have been performed without EGR and with a high level of ethanol fraction (above 70%), and the values obtained are lower than 0.2 FSN (soot-less zone). An increase for THC emission of about 25% is observed compared to the single-injection strategy. Therefore, the increase in HC emissions is believed mainly caused by ethanol trapped in parasitic volumes and crevices due to injections very close to TDC. Also, for the specific CO emissions, a similar trend can again be observed, with an increase of about 25%. This raise should be due to the flame quenching of the highly diluted ethanol–air mixing. Previous studies had already shown that low-temperature combustion concepts with high mixture homogenization temperatures on the cylinder wall and piston surface are too low to allow for sufficient oxidation of CO to CO_2 (Bhave et al. 2006). The delta η_{gross} is also shown in Fig. 2.6b. It reduces

about 1% units for the multi-injection strategy compared to the reference one due to the longer combustion duration resulting in a reduction of the thermodynamic efficiency (higher exhaust losses). In conclusion, it can be stated that the single diesel injection strategy for dual-fuel combustion with high ethanol percentage guarantees better efficiencies and engine-out emissions than a diesel multi-injection pattern.

2.3.3 Injection Pressure

In this section, the effect of diesel injection pressure has been investigated in dual-fuel combustion at part load. Two levels of variation have been used for the tested points (Table 2.3). The energizing time of pilot pulses, as well as $SOI_{ethanol}$, CA50, and the load, has been kept constant, to achieve the same FSR as the reference test. Figure 2.7 shows the changes in in-cylinder pressure and heat release rate of dual-fuel combustion at different injection pressures. In terms of the combustion process, as HRR profile shows, the higher diesel injection pressure seems not producing relevant changes. It is noticed that the change in slope related to higher injection pressure, even if the combustion starts earlier at the lower rail pressure, has observed a rising of the heat release rate due to better atomization of high reactive fuel. The start of injection was retarded of 4° to reach the CA50 target. HRR trace also shows a combustion duration increase of about 4° due to the slow diffusive phase that overtakes the reference trace, as reported in the spider plot in Fig. 2.8.

Figure 2.8 shows the indicated specific emissions and the engine performance for the two tested points. A slight difference in terms of combustion noise is observed between the two different rail pressures tested. The COV_{IMEP} at different injection pressures is given in Fig. 2.8a. It is considered that the cooling effect of the low reactive fuel injected into intake port lowers the inlet temperature leading to higher combustion instabilities. However, COV_{IMEP} decreases at a higher rail pressure of

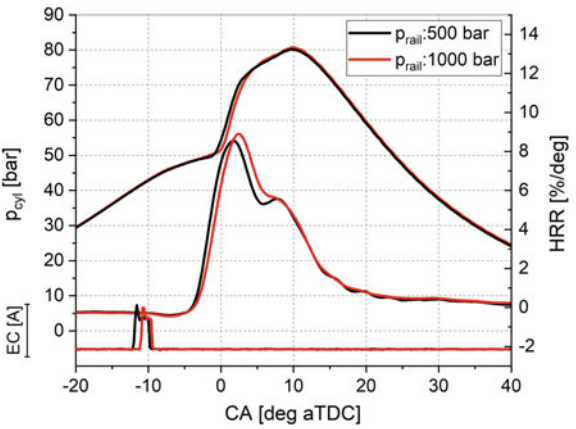

Fig. 2.7 In-cylinder pressure, apparent HRR, and injection pattern for two levels of injection pressure in dual-fuel mode (72% FSR) at 1500 rpm and 6.2 bar IMEP

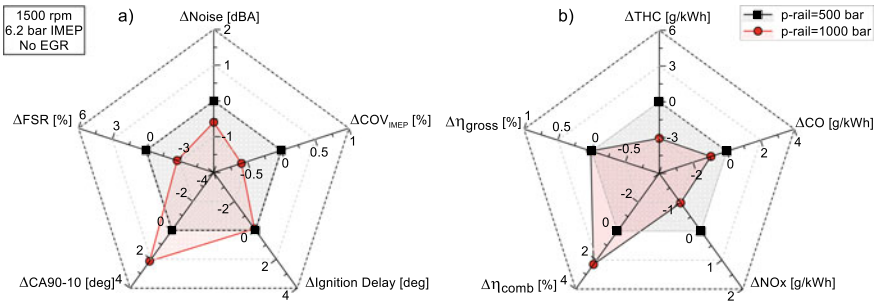

Fig. 2.8 Delta combustion noise, COV_{IMEP}, ID, CA90-10, FSR, emissions, and efficiencies for 1000 bar compared to the 500 bar of injection pressure

about 0.6% due to the better spray atomization and penetration inside the combustion chamber, involving more premixed fuel during the ignition process.

As depicted in Fig. 2.8b, the injection pressure does not have a clear effect on NO_x emission at constant CA50 and FSR. The HC and CO emissions slightly decrease with rail pressure increase mainly due to the higher fuel oxidation rate of the premixed ethanol present in the squish volume of the combustion chamber (Di Blasio et al. 2013; Belgiorno et al. 2018). The lower CO emissions, of about 1 g/kWh, at higher pressure, are mainly due to the better atomization obtained and, therefore, to better air–fuel mixing and to a longer combustion duration, which guarantees greater oxidation of CO into CO_2. It can be noted a sharp decrease in the unburned hydrocarbon emissions, 3 g/kWh lower, as the injection pressure increases. This is due to more diesel quantity covering a broader region of the combustion chamber, thanks to the higher rail pressure and the greater in-cylinder temperature related to a higher fuel–air ratio that promotes the complete oxidation of hydrocarbons. For both test points, no differences are evidenced in terms of gross efficiency, as shown in Fig. 2.8b, with a benefit in terms of combustion efficiency (η_{comb}), 2% higher, due to mainly the lower CO and HC emissions.

2.3.4 Exhaust Gaseous Recirculation

In the following section, the effect of the EGR has been analyzed, keeping constant all engine boundary conditions. The EGR is usually applied to dilute the in-cylinder charge to control NO_x emissions; however, usually, it is associated with a smoke penalty. The ethanol addition is even more effective when EGR is used, and this is because of the lower oxygen availability. The EGR effect on combustion, emissions, and efficiencies is described, and no EGR and 20% of EGR are shown at 1500 rpm, 6.2 bar of IMEP with 70% of ethanol percentage.

As shown in Fig. 2.9a, the EGR rate does not involve variations in terms of ID, keeping constant the CA50. The PRR decreases with the EGR rate at constant FSR;

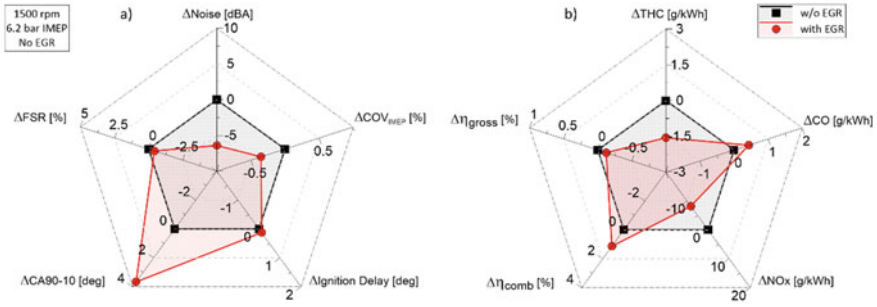

Fig. 2.9 Delta combustion noise, COV_{IMEP}, ID, CA90-10, FSR, emissions, and efficiencies with EGR compared to the without EGR

in terms of combustion noise, a benefit of 6 dBA can be noted. Increasing the EGR rate leads to a rise of combustion duration of about 4°, mainly due to the lower in-cylinder temperature near the end of the compression stroke. It also allows greater stability of the combustion process, with a reduction of almost 0.5% of COV_{IMEP} compared to the case without EGR.

Figure 2.9b displays the effect of the EGR rate on emissions and engine performance of dual-fuel combustion mode. The HC emissions slightly decrease with EGR, and the measured value is below 1.5 g/kWh because of the ethanol concentration that is relatively low in combination with the longer duration of combustion. Therefore, longer oxidation time reduces the HC concentration. As shown in Fig. 2.9b, a slight difference of about 0.5 g/kWh is observed in terms of CO emissions adopting the EGR. The ability to oxidize CO decreases with the increase of CO_2, which reduces in-cylinder pressure and temperature. It is mainly due to the lower combustion temperature making it harder to burn ethanol/diesel mixture to oxidize CO. Concerning the engine performance, the gross efficiency is well aligned with and without EGR. In contrast, for combustion efficiency, the efficiency improvement, of about 1.2%, is mainly related to the reduction of HC emissions.

The use of EGR has a positive impact on the emissions and engine performance, except for HC and CO emissions, which are much greater than conventional diesel combustion (Martin et al. 2018).

2.4 Ethanol–Diesel Blend

A simpler fueling mode to utilize ethanol fuel in a compression ignition engine is to blend it in diesel. However, the maximum blending ratio is limited, due to the low ethanol miscibility with the diesel fuel. To increase the percentage of the ethanol fraction blended with diesel, an emulsifier is needed because the alcohol's polarity increases exponentially with a reduced carbon chain length due to the oxygen atom in the molecule (Collins 2017). The type of emulsifier used has specific effects on

Table 2.5
Ethanol–biodiesel–diesel blend engine operating conditions and constraints

Engine parameters	Values		
Engine speed [rpm]	2000	1500–2000	2000
IMEP [bar]	4.0–7.0	3.3–4.0	4–0–7.0
Ethanol percentage [%]	0–15–30	30	30
EGR [%]	0	0	0–50
Diesel injection strategy	Pilot–main	Pilot–main/only main	Pilot–main
Intake manifold temperature [K]	333		
Combustion noise max. [dBA]	90		
PRR_{max} [bar/deg]	8.0		
COV_{IMEP} max. [%]	3.5%		

global engine performances. In this regard, experiments have been conducted using ethanol–diesel blends with biodiesel and gasoline as emulsifiers, explicating their effects (Belgiorno et al. 2018a; Shamun et al. 2018).

In this monograph, the authors have focused on ethanol–diesel blends employing as emulsifier soybean fatty acid methyl ester (FAME or biodiesel). The test has been performed using the single-cylinder engine test rig, which main engine specifications are listed in Table 2.1. The analysis is conducted at partial load conditions listed in Table 2.5. The part load area is a critical area for both dual-fuel and blending combustion modes contributing significantly on the emissions and efficiencies over the actual emission homologation cycles.

Two levels of ethanol percentage have been adopted diesel, biodiesel, and EtOH (DBE) blend in 68:17:15 ratio and diesel, biodiesel, and EtOH blend in 56:14:30 ratio. Both blends are stable in the proposed blending ratios. The one-factor-at-a-time method has been used. This method evaluates the engine response for each factor varied, in particular, the effect of ethanol percentage, injection strategy (single and pilot–main pulses), exhaust gaseous recirculation on the combustion process, engine-out emissions, engine heat rejection analysis, and the gross-indicated efficiency. The maximum value of ethanol percentage (30%) has been used to investigate the effect of EGR and injection strategy. Table 2.5 shows the engine operating conditions and constraints used during the experiments.

2.4.1 Ethanol Blend Substitution Ratio

In this section, an overview of the ethanol–diesel blend ratio on combustion, emissions, and engine efficiencies has been analyzed. Three different ethanol–diesel blend ratios have been considered 100% diesel, 15%, and 30% of ethanol (EtOH). To stabilize the blend between diesel and ethanol, biodiesel has been used as an emulsifier. The diesel–biodiesel–ethanol blends are identified as DBE15 (diesel, biodiesel and EtOH blend in 68:17:15 ratio) and DBE30 (diesel, biodiesel and EtOH blend in 56:14:30 ratio).

To analyze the effect of ethanol blend level, the experiments have been conducted keeping constant all engine boundary conditions: in-cylinder air, boost pressure, fuel injection parameters, combustion phasing, and IMEP. Two test points are analyzed at 2000 rpm, 4 and 7 bar of IMEP, representative of partial load engine operating conditions. The analysis aims a complete overview of combustion behavior between the ethanol–diesel blend and the CDC. The delta in terms of combustion noise, COV_{IMEP}, ignition delay, combustion duration, and exhaust temperature between the two levels of ethanol blend and the CDC is presented (see Fig. 2.10).

At low engine load (4 bar IMEP), increasing the ethanol blend percentage higher COV_{IMEP} has been observed of about 1.1% up to 3.2% for DBE15 and DBE30, respectively. The higher COV_{IMEP} at the high level of ethanol blend percentage is related to the ethanol cooling effect as already established for the dual-fuel combustion; therefore, the combustion becomes unstable. Increasing the engine load (7 bar IMEP), the in-cylinder temperature increases and the combustion stability improves; the COV_{IMEP} is comparable and within acceptable values (below 3%).

The ID, in crank angle degree, has been evaluated as differences between crank angles of the start of the main injection and crank angle at which 10% of the charging heat is released (CA10). The ID is a function of the cetane number (CN) and by the in-cylinder thermodynamic conditions. The diesel fuel has a relatively lower ID due to the higher CN. Increasing the ethanol percentage, the ignition delay is prolonged due to the combustion characteristics such as a higher cooling effect of in-cylinder and a larger fraction of premixed flame.

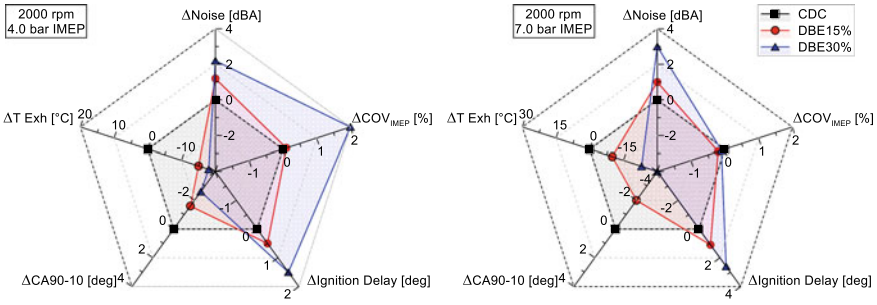

Fig. 2.10 Delta combustion noise, COV_{IMEP}, ID, CA90-10, and exhaust temperature at part loads for two levels of ethanol–diesel blends compared to the CDC

The combustion duration CA10-90, in crank angle degree, has been calculated as differences between the crank angles at which 90 and 10% of the charging heat is released. DBE blends show lower combustion duration compared to the diesel fuel, due to the ID. When the ID is prolonged, the combustion shows a marked premixed flame with a positive impact on CA10-90, CA50, and exhaust temperature reduction as well. Short combustion is characterized by an advanced CA90, and lower exhaust temperature is expected. A reduction in the range of 10–20 °C has been measured moving from the CDC to DBE30. Lower exhaust temperature is related to the improvement of the thermodynamic efficiency (lower exhaust losses).

Another combustion parameter linked to the ignition delay is the combustion noise. With a high ID, a higher premixed flame is observed, and the ethanol–diesel blend combustion shows an increase of combustion noise in the range of 2 – 3 dBA between DBE30 and diesel fuel.

Figure 2.11 shows the engine-out emissions (THC, CO, and NO_x), $\eta_{comb,}$ and η_{gross} for the two levels of ethanol blend substitution ration, also including the CDC as reference. As mentioned above, the results refer to the experimental test performed without EGR, to avoid the influence of EGR on the combustion process; for this reason, a higher value of NO_x has been measured above 5 g/kWh. Looking at NO_x emissions, the ethanol can be an enabler for the NO_x reduction, increasing the ethanol percentage to the blend, the reduction ranges between 20 and 30%, for both operating points shown as a consequence of the charge cooling effect that reduces the in-cylinder temperatures in comparison with the CDC (Yilmaz et al. 2014; Ishida et al. 2010).

The smoke level has not been plotted for brevity, and smoke below 0.2 FSN has been measured both for CDC and all ethanol–diesel blend, due to the higher lambda (no EGR). Notwithstanding the low level of smoke, a further reduction has been measured, increasing the ethanol content in the blend. The smoke reduction is related to the combination of the short two-atom carbon chain of ethanol and oxygen content of biodiesel used as an emulsifier. Increasing the ethanol fraction in the fuel results in a higher THC and CO emissions two times more compared to the CDC, 0.4 and 3.0 g/kWh, respectively. The higher ID of the ethanol–diesel blend gives

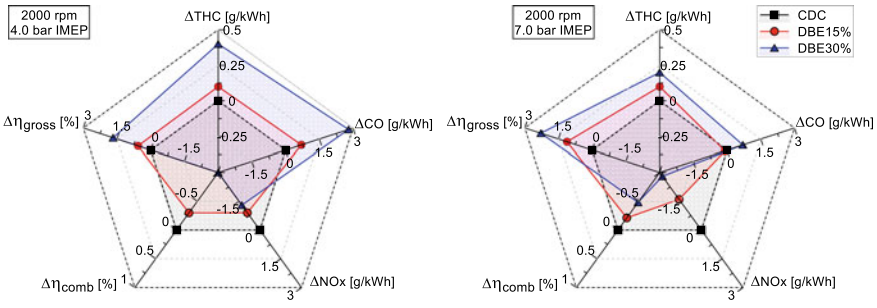

Fig. 2.11 Delta THC, CO, NO_x, and delta η_{comb} and η_{gross} at part loads for two levels of ethanol–diesel blends compared to the CDC

the fuel more time to enter the crevice volumes causing higher THC emissions. The cooling effect of ethanol reduces the in-cylinder temperature penalizing the complete oxidation of the CO to the CO_2.

The η_{gross} is also presented in Fig. 2.11. It increases by about 1% unit per 15% of the ethanol fraction. Higher premixed combustion phasing with consequence shorter combustion duration improves the thermodynamic efficiency of ethanol–diesel blends compared to the CDC. To evaluate better and in detail the η_{gross} improvements working with ethanol blends instead of CDC, the energy distribution has been evaluated (including the incomplete combustion, exhaust, and in-cylinder heat transfer losses and gross-indicated efficiency).

Increasing the ethanol fraction, higher combustion losses have been obtained due to the higher CO and THC compared to the CDC. The gross indicated efficiency improvement of about 2% units is observed passing from CDC to the 30% ethanol blend ratio, which is related to the simultaneous reduction of in-cylinder heat transfer (HT) and exhaust losses (short combustion duration).

2.4.2 Injection Strategy

In this section, two different injection patterns have been studied to analyze the combustion behavior, emissions, and engine efficiencies for a combustion engine fueled with ethanol–biodiesel–diesel blend. The ethanol fraction is kept constant equal to 30%.

The injection patterns studied are single (main only) and double (pilot–main) injections. The two explored k-points are at 1500 and 2000 rpm and 3.3 and 4.0 bar of IMEP, respectively, and no EGR has been used. Figure 2.12 shows the overall results in terms of combustion noise, COV_{IMEP}, ignition delay, combustion duration, and exhaust temperature, for the two injection strategies (pilot–main and main only). Typically, the pilot injection quantity varies in the range of 1–3 mm^3/stroke. The pilot injection is generally used to control the combustion noise and peak pressure

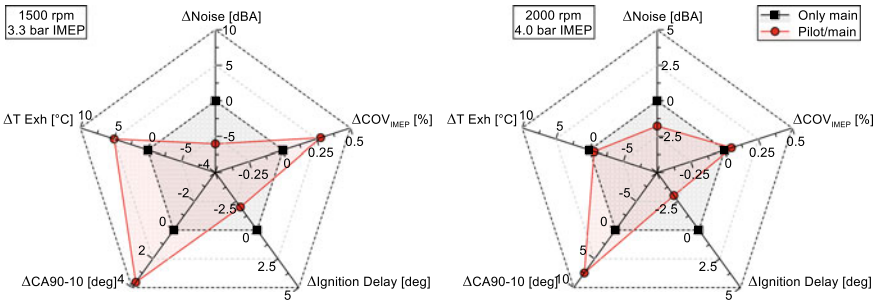

Fig. 2.12 Delta combustion noise, COV_{IMEP}, ID, CA90-10, and exhaust temperature at part loads of pilot/main injections compared to only main injection

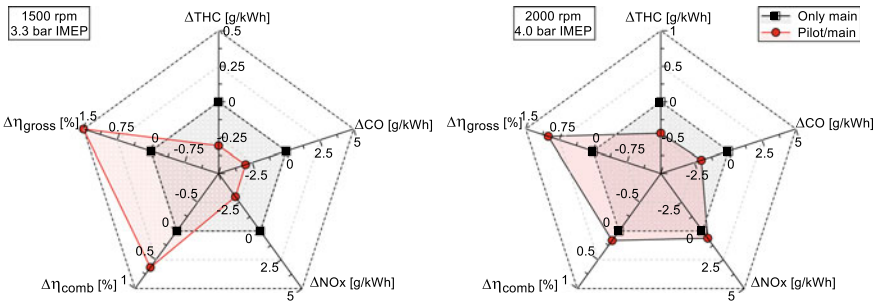

Fig. 2.13 Delta THC, CO, NO_x, and delta η_{comb} and η_{gross} at part loads of pilot–main injections compared to only main injection

rise rate (Selim 2003); then, the main injection controls the engine load. Looking at the combustion noise (Fig. 2.12), higher noise up to 6 dBA has been measured switching from the double- to the single-injection case.

The pilot injection gives a lower contribution to the cooling effect compared to the main injection. The only main injection strategy shows a higher cooling effect of the charge extending the ID of about 3° compared to the pilot–main strategy. The only main injection shows a separation between the end of injection and the start of combustion, with a higher premixed phase of heat release rate, consists of a premixed flame mode typically characteristic of partially premixed combustion (Belgiorno et al. 2017, 2018b).

The COV_{IMEP} and exhaust temperature are well aligned between the single- and double-injection strategy. The single-injection strategy shows a higher premixed combustion phase compared to the pilot–main injection strategy at lower engine speed, promoting the NO_x production (Fig. 2.13).

Engine-out emissions (THC, CO, and NO_x), combustion, and gross-indicated efficiencies are plotted in Fig. 2.13, for the two injection strategies (pilot–main and main only). Switching from double- to single-injection strategy, the ID increases. The higher cooling effect of main injection strategy postpones the start of combustion, and the fuel has more time to enter the crevice volume with a negative impact on CO and THC emissions compared to the double injection.

The η_{gross} increases from about 0.75 up to 1.5% units more with the double-pulse injection instead of a single-injection strategy, and it is mainly related to the combination of lower incomplete combustion (lower CO and THC) and heat transfer losses (lower peak temperature).

2.4.3 Exhaust Gas Recirculation

The main enabler to minimize the NO_x engine-out emissions is the exhaust gas recirculation (EGR). The EGR increases the specific heat ratio, γ, of the intake air.

The air can absorb the energy produced by the combustion reducing the in-cylinder peak temperatures (Murayama et al. 1995). One of the drawbacks of the EGR is the reduction of air–fuel ratio, promoting the soot formation. Higher EGR content reduces the in-cylinder oxygen concentration, and the fuel is poorly oxidized, also promoting the high level of CO and THC (Murayama et al. 1995). In this section, the EGR effect on combustion, emissions, and efficiencies is described, and no EGR and high level of EGR (about 50%) are shown at 2000 rpm, 4, and 7 bar of IMEP with DBE30.

Figure 2.14 shows the overall results in terms of combustion noise, COV_{IMEP}, ignition delay, combustion duration, and exhaust temperature, with and without EGR. The EGR rate reduces the in-cylinder A/F ratio, penalizing the combustion stability at low load (4 bar of IMEP). Increasing the EGR, reduce the ignition delay due to the higher intake temperature, fasting the evaporation phase of ethanol. The CA10-90 slightly decreases of about 1 crank angle degree compared to the test without EGR with a reduction of exhaust temperature of about 10 °C.

Engine-out emissions (THC, CO, and NO_x), combustion, and gross-indicated efficiencies are plotted in Fig. 2.15, with and without EGR at part load with 30% of ethanol. With 50% of EGR ratio, the NO_x level passing from 7 g/kWh to below

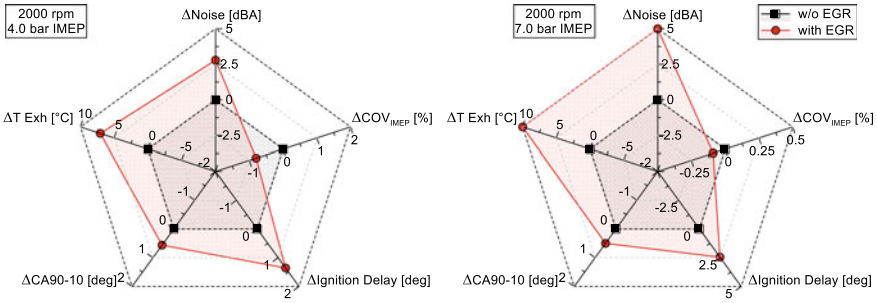

Fig. 2.14 Delta combustion noise, COV_{IMEP}, ID, CA90-10, and exhaust temperature at part loads with EGR compared to without EGR

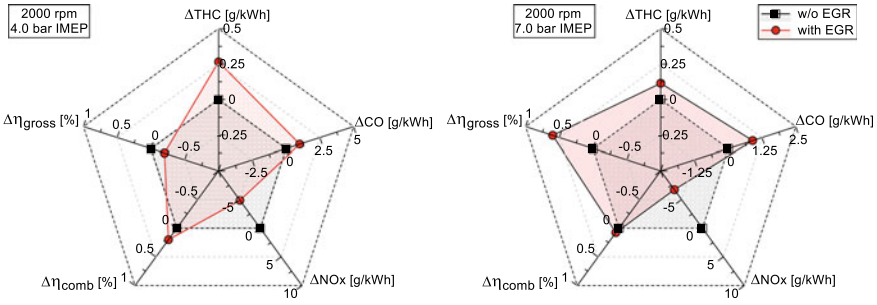

Fig. 2.15 Delta THC, CO, NO*x*, and delta η_{comb} and η_{gross} at part loads with EGR compared to without EGR

1 g/kWh without drawback in terms of smoke, this is related to the high ethanol content (30%) to the fuel blend, because the ethanol produces a larger fraction of premixed flame.

The η_{gross} is well-aligned with and without EGR at low engine load (4.0 bar IMEP), while at 7.0 bar IMEP, it increases by about 1.0% units employing the EGR rate. The efficiency improvement is related to the simultaneous reduction of in-cylinder heat transfer and exhaust losses.

2.5 Summary

The monograph reports the effects of the ethanol fraction, injection patterns, EGR analysis for both fueling strategies, dual-fuel combustion ethanol–diesel, and ethanol–biodiesel–diesel blend. The tests have been performed on a single-cylinder engine light-duty compression ignition engine at part load since the part load areas are a most critical area for both dual-fuel and blending combustion modes contributing significantly on the emissions and efficiencies over the actual emission homologation cycles. The impact of the ethanol rate and fueling mode on engine efficiency and emissions is investigated. The one-factor-at-a-time method has been used. This method evaluates the engine response for each factor varied.

This monograph analyzes the sensitivity among the engine control parameters on the engine response, emissions, efficiencies, and combustion indicators (stability, ignition delay, combustion duration, and stability).

To have a comprehensive overview of all results presented, two Pugh matrixes are presented for the two fueling strategies analyzed (Tables 2.6 and 2.7). Five criteria have been chosen, THC + CO, NO_x, η_{gross}, $COV_{IMEP,}$ and combustion noise. The following leveraging parameters have been considered: ethanol fraction, multi-injection strategy, higher rail pressure (only for dual-fuel mode), and higher EGR.

Table 6 Pugh matrix ethanol–diesel dual-fuel combustion

Criteria	Datum	Ethanol%	Multi-injection	p-rail	EGR
THC + CO		−	−	+	+
NO_x		S	S	+	+
η_{gross}		−	−	S	S
COV_{IMEP}		S	S	+	S
Combustion noise		S	+	S	+
Sum of all positives		0	1	3	3
Sum of all negatives		2	2	0	0
Sum of all neutrals		3	2	2	2
Total		−2	−1	3	3

Table 7 Pugh matrix ethanol–biodiesel–diesel blend combustion

Criteria	Datum	Ethanol%	Double injections	EGR
THC + CO		−	+	S
NO_x		+	+	+
η_{gross}		+	+	+
COV_{IMEP}		S	S	S
Combustion noise		−	+	−
Sum of all positives		2	4	2
Sum of all negatives		2	0	1
Sum of all neutrals		1	1	2
Total		0	4	1

Each concept has been compared to different datums. In summary, the ethanol fraction impact on combustion and emissions has been compared to the CDC, while, the multi-injection strategy has been compared to the single injection pattern, then, the results of high rail pressure are referred to the low rail pressure level and finally, the results obtained with EGR are compared with the baseline without EGR. When no significative difference of criteria between the datum and generic concept can be appreciated, the symbol (S) has been used. Then, a strategy that reduces the emissions, $COV_{IMEP,}$ and noise and as well as improves the gross efficiencies the symbol (+) is used, vice versa (−).

For what concerns the dual-fuel Pugh matrix (see Table 2.6), it can be stated that the dual-fuel mode shows comparable NO_x, combustion noise, and COV_{IMEP} compared to the CDC. Penalties in terms of unburnt and efficiency are noted. Higher levels of fuel injection pressure and EGR reduce THC, CO, and NO_x emissions without a relevant impact on efficiency and improved combustion stability and noise. The multi-injection strategy shows emissions and efficiency penalties, a reduction of the combustion noise, and aligned combustion stability compared to the single injection. Concluding, the combination of a single-injection strategy, high rail pressure, and EGR permits to minimize the engine-out emissions and combustion noise while maximizing the gross-indicated efficiency.

The Pugh matrix of the blend fueling mode is shown in Table 2.7. High level of ethanol blend ratio shows higher combustion noise, THC, and CO compared to the CDC, but with fuel consumption and NO_x reductions compared to the CDC. The double-injection strategy permits to reduce the engine-out emissions (THC, CO, and NO_x) and combustion noise, while the combustion stability is pretty aligned with a single-injection strategy. High level of EGR combined to the low reactive fuel as ethanol gives to the combustion process typical characteristics of partially premixed combustion showing a reduction of NO_x and fuel consumption compared to the no EGR. Summarizing, employing high ethanol percentage to the diesel fuel, with double-injection strategy and higher EGR, a positive impact on gross-indicated efficiencies and emissions has been observed.

References

Asad U, Kumar R, Zheng M, Tjong J (2015) Ethanol-fueled low temperature combustion: a pathway to clean and efficient diesel engine cycles. Appl Energy 157:838–850. ISSN 0306-2619. https://doi.org/10.1016/j.apenergy.2015.01.057

Belgiorno G, Dimitrakopoulos N, Di Blasio G, Beatrice C, et al (2017) Parametric analysis of the effect of pilot quantity, combustion phasing and EGR on efficiencies of a gasoline PPC light-duty engine. SAE Technical Paper 2017-24-0084. https://doi.org/10.4271/2017-24-0084

Belgiorno G, Di Blasio G, Shamun S, Beatrice C et al (2018a) Performance and emissions of diesel-gasoline-ethanol blends in a light duty compression ignition engine. Fuel 217:78–90. https://doi.org/10.1016/j.fuel.2017.12.090

Belgiorno G, Dimitrakopoulos N, Blasio GD, Beatrice C, Tunestål P, Tunér M (2018b) Effect of the engine calibration parameters on gasoline partially premixed combustion performance and emissions compared to conventional diesel combustion in a light-duty Euro 6 engine. Appl Energy 228:2221–2234. ISSN 0306-2619. https://doi.org/10.1016/j.apenergy.2018.07.098

Belgiorno G, Di Blasio G, Beatrice C (2018c) Parametric study and optimization of the main engine calibration parameters and compression ratio of a methane-diesel dual fuel engine. Fuel 222:821–40. https://doi.org/10.1016/j.fuel.2018.02.038. ISSN 0016-2361

Belgiorno G, Boscolo A, Dileo G, Numidi F et al (2020) Experimental study of additive-manufacturing-enabled innovative diesel combustion bowl features for achieving ultra-low emissions and high efficiency. SAE Technical Paper 2020-37-0003. https://doi.org/10.4271/2020-37-0003

Bhave A, Kraft M, Montorsi L, Mauss F (2006) Sources of CO emissions in an HCCI engine: a numerical analysis. Combust Flame 144(3):634–637. https://doi.org/10.1016/j.combustflame.2005.10.015

Caton JA (2012) The thermodynamic characteristics of high efficiency, internal-combustion engines. Energy Convers Manage 58:84–93. https://doi.org/10.1016/j.enconman.2012.01.005

Chang J., Kalghatgi G, Amer A, Viollet Y (2012) Enabling high efficiency direct injection engine with naphtha fuel through partially premixed charge compression ignition combustion. SAE Technical Paper 2012-01-0677. https://doi.org/10.4271/2012-01-0677

Collins CD (2017) Implementing phytoremediation of petroleum hydrocarbons. Humana Press. ISBN: 978-1-59745-098-0

Di Blasio G, Beatrice C, Molina S (2013) Effect of port injected ethanol on combustion characteristics in a dual-fuel light duty diesel engine. SAE Technical Paper 2013-01-1692. https://doi.org/10.4271/2013-01-1692

Di Blasio G, Beatrice C, Belgiorno G, Pesce FP, Vasallo A (2017) Functional requirements to exceed the 100 kw/l milestone for high power density automotive diesel engines. SAE Int J Engines 10(5):2342–2353. https://doi.org/10.4271/2017-24-0072

Epping K, Aceves S, Bechtold R, Dec J (2002) The potential of HCCI combustion for high efficiency and low emissions. SAE Technical Paper 2002-01-1923. https://doi.org/10.4271/2002-01-1923

Ishida M, Yamamoto S, Ueki H, Sakaguchi D (2010) Remarkable improvement of NOxPM trade-off in a diesel engine by means of bioethanol and EGR. Energy 35(12):4572–4581

Knight BM, Bittle JA, Jacobs TJ (2010) Efficiency consideration of later-phased low temperature diesel combustion. In: ASME, Internal combustion engine division fall technical conference, ICEF2018-9657. https://doi.org/10.1115/ICEF2010-35070

Mani Sarathy S, Oßwald P, Hansen N, Kohse-Höinghaus K (2014) Alcohol combustion chemistry. Prog Energy Combus Sci 44:40–102. ISSN 0360-1285. https://doi.org/10.1016/j.pecs.2014.04.003

Martin J, Boehman A, Topkar R, Chopra S et al (2018) Intermediate combustion modes between conventional diesel and RCCI. SAE Int J Engines 11(6):835–860. https://doi.org/10.4271/2018-01-0249

Murayama T, Zheng M, Chikahisa T, Oh Y et al (1995) Simultaneous reductions of smoke and NOx from a DI diesel engine with EGR and dimethyl carbonate. SAE Technical Paper 952518. https://doi.org/10.4271/952518

Nehmer D, Reitz R (1994) Measurement of the effect of injection rate and split injections on diesel engine soot and NO_x emissions. SAE Technical Paper 940668. https://doi.org/10.4271/940668

Pedrozo VB, May I, Zhao H (2017) Exploring the mid-load potential of ethanol-diesel dual-fuel combustion with and without EGR. Appl Energy 193:263–275. ISSN 0306-2619. https://doi.org/10.1016/j.apenergy.2017.02.043

Satgé de Caro P, Mouloungui Z, Vaitilingom G, Berge J.C (2001) Interest of combining an additive with diesel–ethanol blends for use in diesel engines. Fuel 80(4):565–574. ISSN 0016-2361. https://doi.org/10.1016/S0016-2361(00)00117-4

Selim MYE (2003) Effect of exhaust gas recirculation on some combustion characteristics of dual fuel engine. Energy Convers Manage 44(5):707–721. https://doi.org/10.1016/S0196-8904(02)00083-3

Shamun S, Belgiorno G, Di Blasio G, Beatrice C et al (2018) Performance and emissions of diesel-biodiesel-ethanol blends in a light duty compression ignition engine. Appl Therm Eng 145:444–452. https://doi.org/10.1016/j.applthermaleng.2018.09.067

Vassallo A, Beatrice C, Di Blasio G, Belgiorno G et al (2018) The key role of advanced, flexible fuel injection systems to match the future CO_2 targets in an ultra-light mid-size diesel engine. SAE Technical Paper 2018-37-0005. https://doi.org/10.4271/2018-37-0005

Waterland LR, Venkatesh S, Unnasch S (2003) Safety and performance assessment of ethanol/diesel blends (e-diesel). No. NREL/SR-540–34817. National Renewable Energy Lab., Golden, CO. (US)

Yates A, Bell A, Swarts A (2010) Insights relating to the autoignition characteristics of alcohol fuels. Fuel 89(1):83–93. https://doi.org/10.1016/j.fuel.2009.06.037

Yilmaz N, Vigil FM, Donaldson AB, Darabseh T (2014) Investigation of CI engine emissions in biodieselethanoldiesel blends as a function of ethanol concentration. Fuel 115:790–793

Chapter 3
PM Characteristics and Relation with Oxidative Reactivity—Alcohol as a Renewable Fuel

Nahil Serhan

3.1 Introduction

Diesel smoke, so-called particulate matter (PM), can be presented as a combination of carbonaceous material (soot) blended with several types of inorganic and organic substances, resulting in mutagenic and carcinogenic elements by nature (Silverman 2012). Soot inception is generally defined as a combination of different physical and chemical reactions that result in the transition of the fuel HCs from the vapor phase into a complex solid carbon structure (Omidvarborna et al. 2014; Shandilya and Kumar 2013). This mechanism takes place within the fuel-rich regions presented in the diesel combustion process when enough temperature (1000–2800 K) and pressure conditions (50–100 bars) are available (Omidvarborna et al. 2014; Shandilya and Kumar 2013). The detailed mechanism by which the soot is produced is still under debate in the literature despite that a significant number of publications have examined this process (Haynes and Wagner 1981; Omidvarborna et al. 2015). Reader is referred to (Omidvarborna et al. 2015) for a general summary of the soot pyrolysis/oxidation process in compression ignition engines.

3.1.1 PM Elemental Composition

Soot generally comprises carbon (C) as the main component and to a lesser extent some traces of hydrogen can be also detected, resulting in an overall density of 1.84 $\pm$ 0.1 g/cm^3 (Choi 1994). When the particulates are immature (during the initial stages of the soot inception process), hydrogen is considered one of the basic soot

N. Serhan (✉)
Wärtsilä Catalyst Systems R&D, Vaasa, Finland
e-mail: nahil.serhan@wartsila.com

P. C. Shukla et al. (eds.), *Alcohol as an Alternative Fuel for Internal Combustion Engines*, Energy, Environment, and Sustainability,
https://doi.org/10.1007/978-981-16-0931-2_3

components (C/H ratio ~1). However, as the soot becomes more mature, the corresponding carbon portion increases while hydrogen's level drops (Omidvarborna et al. 2015). In addition, soot also contains a soluble organic fraction (SOF) that mainly originates from the fuel aromatic compounds and the different unburnt hydrocarbon species of the fuel (Daido 2000; Tree and Svensson 2007). Both oxygen, as strongly bonded oxygen functionalities, and sulfur, in the form of sulfates, can be found on the soot surface. Moreover, different types of metals such as zinc (Zn), iron (Fe), silicon (Si), calcium (Ca), chromium (Cr), and phosphorus (P) can be detected in the soot elemental composition (Omidvarborna et al. 2014; Shandilya and Kumar 2013; Xi and Zhong 2006). These types of metals are generally referred to as the "ash" portion in the aggregate and mainly result from the engine wear, lubrication oil, and the various inorganic compounds of the fuel (Mühlbauer 2016). The combination of the soot particulates (the solid part) with SOF and ash is the so-called PM. Following the findings of Roessler et al. (1981), a representative diesel PM holds on weight basis 70% C, 20% O_2, 3% Sulfur (S), 1.5% H_2, <1% N_2, <1% trace metal.

3.1.2 PM Morphology

PM profile can be generally described as a fractal aggregate with an average size of 80–300 nm (nm). Each aggregate can include up to 4000 carbonized spherules, so-called primary soot particulates (Wagner 1979). In a typical diesel engine, the sum of primary particulates grouped in a single aggregate falls in the range of 22–100 (Song 2003). This number is influenced by the total in-cylinder air to fuel (A/F) ratio: The leaner the combustion, the lesser the agglomeration (Roessler 1981; Song 2003). The diameter of the spherules varies from 10 to 80 nm; however, in normal diesel operation, the typical diameter range is 15–50 nm (Walker et al. 1966). Soot morphological analysis—the soot agglomerate geometry—includes several physical parameters such as the fractal dimension (D_f), gyration radius (R_g), number of primary particulates within the aggregate (n_{p0}), and primary particulate size (d_{p0}). A schematic presentation of R_g and d_{p0} is shown in Fig. 3.1.

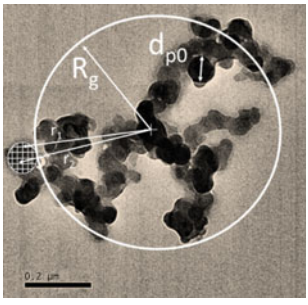

Fig. 3.1 Schematic of a diesel soot particulate magnified by TEM to 0.2 µm scale showing the different morphological parameters Serhan (2019)

D_f demonstrates what growth mechanism governs the production of the aggregate particulates through the combustion course (Meakin et al. 1989). Larger magnitudes imply that the particulates are more likely to be spherical in shape and smaller magnitudes indicate a stretched chainlike structure (Meakin et al. 1989). R_g is a representative of the average length that links the centroid of the aggregate with the center of each spherule (Lee et al. 2013), highlighting the average size of the whole aggregate. As for n_{p0}, as its name shows, this parameter is an indication of the number of spherules comprised in an aggregate. d_{p0} is the average size of these spherules.

3.1.3 PM Nanostructure

Apart from the morphology, it is also important to understand the nanoscale ordering of the primary particulates (nanostructure) as the soot formation process and the corresponding oxidative reactivity is partly reflected in the nanostructure. Each primary particulate includes around 10^5–10^6 carbon atoms in its structure (Walker et al. 1966). These atoms are chemically bonded with each other following a hexagonal fashion arrangement, usually referred to as "platelet" or "graphene layer" (Fig. 3.2) (Glassman and Yetter 2008). In general, the carbon atoms in each of these layers are positioned within a two-dimensional plane, known as "basal plane" and "edge plane". Typically, these platelets are parallel to each other and stack in a group of 2–5 platelets (Xi and Zhong 2006). This configuration is generally known as a "crystallite". The interlayer spacing separating the graphene layers in the diesel soot, usually defined by d_{002}, is slightly larger than that of the graphite (0.335 nm) and falls in the range of 0.35–0.36 nm (Glassman and Yetter 2008). The interlayer spacing is a measurement of the degree of graphitization, and smaller values indicate more graphitic structure. Diesel spherules usually hold around 10^3 crystallites that have an

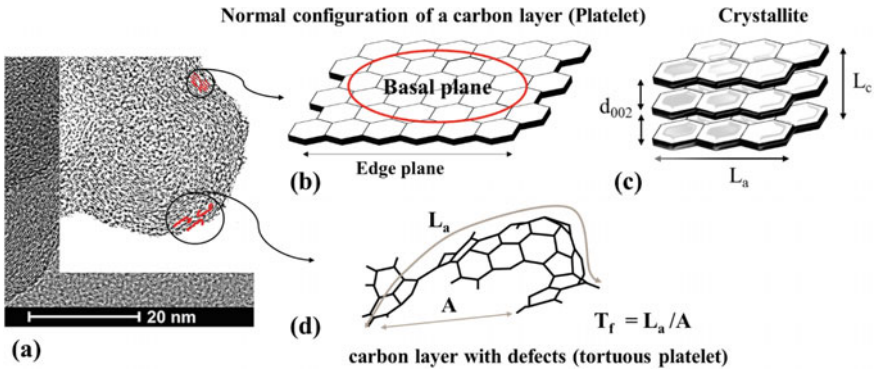

Fig. 3.2 Representation of **a** the primary particulate nanostructure (binary picture), **b** carbon atoms in the basal and edge plane of a platelet, **c** crystallite arrangement, and **d** curved layer configuration, reproduced from (Gaddam et al. 2016)

approximate thickness (L_c) of 12 nm each (Xi and Zhong 2006). These crystallites form the outer shell of the primary particulate, and they are usually arranged parallel to each other and surround the particulate's center (Amann and Siegla 1982). The inner core of the spherule ranges from 18 to 30 nm and incorporates several fine particulates characterized with an amorphous assembly. This configuration reveals that the central part is structurally and chemically less stable than the outer shell (Amann and Siegla 1982). In addition to d_{002} and L_c, two different parameters should be also examined in the nanostructure analysis:

- The crystallite basal plane length is also known as "the fringe length" (L_a): It is a measure of the physical extent of the atomic carbon layer (Gaddam et al. 2016).
- The curvature of the carbon layer, also known as "the fringe tortuosity" (T_f), indicates the existence of a non-six membered ring (i.e., five and seven membered rings)—defected ring (Gaddam et al. 2016; Al-Qurashi and Boehman 2008; Vander Wal and Tomasek 2004).

3.2 PM Oxidative Reactivity

Particulate filter (PF) regeneration (i.e., PM oxidation) can be achieved via two different methods: passive or active regeneration. In the passive version, the particulates are regularly oxidized with NO_2 when the exhaust temperature varies from 200 to 450 °C. The needed NO_2 is usually delivered to the PF by the help of the DOC which converts the engine out NO into NO_2. However, in case the filter backpressure is above the normal range and the available NO_2 and exhaust temperature are not enough (i.e., urban and extra urban cycles), the regeneration is accomplished through the active method. Oxygen presented in the exhaust is used to regenerate the filter; however, exhaust temperature of 550 °C or higher is required. To achieve that, fuel is injected in the exhaust pipe to be oxidized through the DOC (exothermic process) with a view to achieve the required temperature level (= >550 °C) to launch the PM oxidation reactions.

Soot oxidative reactivity is generally known as the ability of the PM to combust in an oxidizing environment (i.e., usually air) (Al-Qurashi et al. 2011). In simple terms, it defines the needed time and temperature required to fully oxidize a known mass of PM. The knowledge of the soot oxidation behavior is the key factor in optimizing the PF design and the regeneration cycles to reduce the encountered fuel penalties from this application. Increasing the soot oxidative reactivity toward oxygen results in the full oxidation of the soot at lower temperatures, thus lowering the fuel penalties and vice versa. It is widely accepted that different engine technologies, operating modes, and fuel types result in particulates that strongly differ in their physical and chemical properties (Burtscher 2005; Matti 2007). This usually includes a variation in the particulate's elemental composition, morphology and carbon layer arrangement (i.e., nanostructure of the primary particulate). The dependency of the soot oxidative reactivity toward the different physico-chemical characteristics is detailed in Sects. 3.2.1, 3.2.2, and 3.2.3.

3.2.1 PM Oxidative Reactivity Dependence Upon Morphology

Numerous researchers suggest that R_g and d_{p0} change according to the parent fuel type (Fayad 2015, 2017; Savic 2016) and the engine operating conditions (Leidenberger 2012; Lapuerta et al. 2007). Hence, many authors base their analysis on these physical parameters (R_g and dp_0) to explain the difference in the particulate's reactivity. Lapuerta et al. (2012) and Rodríguez-Fernandez et al. (2017) spotted a noticeable reduction in R_g and dp_0 along with a significant improvement in the PM reactivity when operating the engine with synthetic fuel (gas to liquid—GTL), biodiesel blends (such as hydrotreated vegetable oil (HVO), and conventional biodiesel originated from animal fat methyl ester). It was suggested that due to the reduction in dp_0 or R_g, a larger specific surface area (SSA) was available for the oxidizers (i.e., O_2, etc.) to react with, thus easing and enhancing the oxidation process. Both authors calculated the SSA assuming that the particulate shape is spherical. Rodríguez-Fernandez et al. (2017) also assumed that a higher level of D_f (i.e., more chain-like structure) can also increase the SSA, however did not take into account this parameter in the final analysis. On the contrary, other researchers reported that increasing the biodiesel portion in diesel fuel results in larger PM (Ye 2014; Lin et al. 2008). However, the soot oxidation activity was better than that produced from the conventional diesel fuel (Ye 2014). Lu et al. (2012) highlight that along with the particulate's size range, various rates of oxidation can be presented. Leidenberger et al. (2012) reported that by increasing the fuel injection pressure, smaller PM size is produced and as a result better oxidative reactivity is achieved compared to lower injection pressures. In another study, Ye et al. (2014) reported that as the fuel pressure increases, the soot reactivity increases accordingly yet, the size of the primary particulate remains constant, highlighting a negative correlation with the reactivity recorded.

3.2.2 PM Oxidative Reactivity Dependence Upon Elemental Composition

In addition to morphology, soot elemental composition, mainly the surface functional group, has been also recognized as a vital parameter governing the soot oxidation mechanism. Morjan et al. (2004) suggested that the presence of oxygen molecules in the reactive mixture can significantly alter the final soot structure. The electron affinity of this moiety can increase the surface chemical activity and therefore alter the soot physical configuration in a way that more curved layers are obtained. Furthermore, the chemisorbed oxygen can be easily bonded to the carbon edge sites due to the presence of unpaired sp^2 electrons. As a result, the reactivity of the edge plane is increased, thus enhancing the reactivity of the whole particulate (Barrientos 2014). Muller et al. (Müller 2006) reported that oxygenated functional groups including C–O–C, C–OH, and C=O are likely to be very reactive agents that facilitate the soot oxidation. Smith and Chughtai (1995) found that the soot reactivity is influenced by

the concentration of oxygen and hydrogen radicals linked to the non-six-membraned PAH rings in the soot surface. They reported that an increase in these elements will reduce the energy required to launch the soot oxidation process, in other words, the energy required to desorb the oxygen functionality from the surface as a combustion product (i.e., CO, CO_2) will be reduced. Several other publications (Wang 2012) also studied the impact of the surface oxygen functional groups and depicted that these species significantly enhance the soot oxidation process. Soot reactivity has been also reported in several studies (Stanmore et al. 2001) to be influenced by the amount of volatile organic fraction (VOF) condensed onto the surface of the aggregates. It was seen that during the oxidation process, the adsorbed VOF devolatilizes and as a result new micropores opening are generated onto the soot surface. As a result, the soot specific surface area in which the oxygen can diffuse and react is increased—this in turn accelerates the kinetics of the oxidation mechanism. On the other hand, the inorganic elements (ash), especially the metal species, show to have a catalytic impact that can significantly enhance the particulate's oxidative reactivity (Liati et al. 2012; Hansen et al. 2013). Hansen et al. (2013) studied the oxidative reactivity of different soot samples with and without the presence of different inorganic species that simulate the various ash components comprised in biodiesel fuel and engine oil. The author depicts that biodiesel ash components, such as sodium carbonate (Na_2CO_3), potassium carbonate (K_2CO_3), and tri-potassium phosphate (K_3PO_4) have a positive impact on the oxidation reactions, while the oil-derived ash such as calcium sulfate ($CaSO_4$) can negatively affect the soot oxidation kinetics (i.e., slower rates).

3.2.3 PM Oxidative Reactivity Dependence Upon Nanostructure

It is of importance to understand the reactivity of the carbon atoms upon their position within the graphene layer (basal and edge plane) to further understand the influence of the nanostructure parameters (d_{002}, L_a and T_f) toward the particulate's oxidation reactivity. To start with, the carbon atoms positioned in the edge sites hold a significantly higher reactivity (around 100–1000 times more reactive) compared to that located in the basal plane (Vander Wal and Tomasek 2003; Gogoi 2015). This is mainly due to the presence of unpaired sp^2 electrons that allows the edge site atoms to easily bond with the upcoming oxygen molecules (Vander Wal and Tomasek 2003; Marsh and Kuo 1989; Ma 2014). However, this is not the case for the atoms placed within the basal plane as they can only share Π (pi) electrons forming chemical bonds (Vander Wal and Tomasek 2003; Marsh and Kuo 1989; Ma 2014). In addition, edge site atoms also present a greater accessibility for oxygen attack (Vander Wal and Tomasek 2003; Marsh and Kuo 1989; Ma 2014). In summary, the overall reactivity of the primary particulate, and as a subsequence of the whole aggregate, can be predicted by evaluating the amount of carbon atoms situated in the basal

plane with respect to these in the edge sites (Vander Wal and Tomasek 2003). This could be mainly concluded by analyzing the crystallite basal plane length (i.e., L_a): Shorter layers indicate the presence of higher amounts of carbon atoms in the edge sites and as a result better oxidative reactivity is expected (Vander Wal and Tomasek 2003; Marsh and Kuo 1989; Ma 2014; Strzelec, et al. 2017). In addition, wavy layers (increasing T_f) indicate the presence of defects in the layer, as presented earlier in Fig. 3.2 (Gaddam et al. 2016; Al-Qurashi and Boehman 2008; Vander Wal and Tomasek 2004). This kind of structure is reported to reduce the electronic resonance stability of the C–C bonds positioned within the basal plane as their atomic orbitals (i.e., electron cloud) are overlapped. Consequently, the C–C bonds are weakened which in turn increases their reactivity and makes them more vulnerable toward oxidation (Vander Wal and Tomasek 2003; Strzelec, et al. 2017). On the other hand, during the oxidation process, curvy layers can be more easily stripped out from the outer surface of the particulate compared to flat layers, hence improving the particulate's reactivity (Lapuerta 2012). d_{002} is also considered as a critical parameter when evaluating the soot structure. Larger values of d_{002} indicate that the particulate ordering is less stable in a manner that eases the access of the oxygen moieties into the edge site position leading to more reactive particulates (Vander Wal and Mueller 2006).

3.3 Alcohol Impact on PM Tendency

In general, oxygenated fuels are likely to yield more complete combustion compared to traditional diesel, even in the fuel-rich regions of the flame. This is mainly attributed to two phenomena: (a) the extra amount of oxygen-borne species (O and OH) helps in oxidizing the already formed soot precursors into combustion products instead of being transformed into aromatics and soot (Herreros 2015). (b) The molecular C–O moieties presented in the oxygenates structure are expected to survive the fuel-rich ignition phase by that suppressing the rate of soot formation (Westbrook et al. 2006; An 2015). With regard to the fuel composition, it has been seen that at equivalent oxygen content, alcohols (i.e., single bond oxygen connection C–OH) reduce PM more effectively than alkyl esters (double bond oxygen connection, C=O) (Buchholz et al. 2004). Pepiot-Desjardins et al. (2008) screened a wide variety of oxygenated additives blended with hydrocarbon fuels. It was seen that the PM suppression is mainly influenced by the base fuel and by the nature of the oxygenated groups. Similar work has been also reported by other authors (Barrientos and Boehman 2013). Both works suggest that at equivalent oxygen content, alcohols and ether groups are more effective than esters in reducing soot formation. Also, it was seen that that branched molecules have higher tendency to produce soot. Review regarding the impact of alcohol combustion on PM emissions is detailed in the Table 3.1

Table 3.1 Summary of the research work showing the impact of alcohol combustion on PM emissions

No	Fuel	Engine parameters	Emission findings	Remarks	References
1	Diesel, used cooking oil, and 20% of ethanol in biodiesel (E-biodiesel)	Steady state—6 bar indicated mean effective pressure (IMEP)- 1500 rpm	Particulate number (PN) diesel > PN biodiesel > PN 20% E-biodiesel		Sua et al. (2013)
2	Diesel, biodiesel, and 5–15% of E-biodiesel	Steady state—BMEP from 25 to 240 Nm & 0.8 to 7 bar—1800 rpm Steady state—70% load—1800	PM E-biodiesel = PM biodiesel < PM diesel		Zhua (2013)
3	Diesel, pure soybean oil biodiesel; B5 and ternary blend with 89% of diesel, 5% of biodiesel and 6% of ethanol (B5E6)	Steady state—25, 50 and 75% of the rated power for different loads—3000 rpm	PN B5E6 < PN B100 < PN B5	B5 and B5E6 show similar PN peaks, however B5 show to have higher concentration in the particles > 150 nm compared to B5E6 and B100	Guarieiro et al. (2014)
4	Diesel, 20% biodiesel–diesel blend (B20); B20 blends contained 5, 10, and 15% by volume of butanol	Steady state—0.9 to 7 bar brake mean effective pressure (BMEP)—1800 rpm	Reduction in elemental carbon (EC) for butanol/biodiesel blends compared to B20 and diesel		Zhang (2014)
5	Diesel, biodiesel from waste cooking oil, diesel–biodiesel–ethanol blends: DBE0 (85% diesel; 15% biodiesel; 0% ethanol, volume basis), DBE5 (80% D; 15% B; 5% E), DBE10 (75%D; 15% B; 10% E), and DBE20 (65% D; 15%B; 20% E)	Steady state—no load (0%)—1800 rpm	PM & PN DB mix < PM & PN Biodiesel < PM & PN diesel	this reduction could be attributed to lower aromatics and Sulfur content resulted from ethanol addition	Tse and Cheung (2015)

(continued)

Table 3.1 (continued)

No	Fuel	Engine parameters	Emission findings	Remarks	References
6	Diesel, 5% biodiesel–diesel blend (B5), pure biodiesel and additivated ethanol	Steady state—25, 50, and 75% of the rated power for different loads—3000 rpm	PM addit. Eth < PM biodiesel < PM diesel	Addit. ethanol: 91.06% ethanol, the additives were nitrate of tetrahydrofurfuryl (NTHF) 7.92% and castor oil 0.99%. Higher emission in biodiesel-blended fuels as with respect to addit. ethanol could be due to the higher viscosity of biodiesel	Amaral et al. (2016)
7	Diesel, 10% and 20% butanol–diesel blend (volume basis), 10 and 20% pentanol–diesel blend	Steady state—0.8 to 6.5 bar BMEP—1800 rpm	Butanol blends reduce EC emissions, solid and volatile PN compared with pentanol–diesel blend		Zhang and Balasubramanian (2016)
8	Diesel, biodiesel, 10, 20, and 30% pentanol–biodiesel blends	Steady state—0% to 100% load—1500 rpm	PN pentanol–biodiesel < PN biodiesel < PN diesel		Zhu et al. (2016)
9	Diesel, 10, 20, and 30% butanol–diesel blends	13-mode European Stationary Cycle (ESC)	Smoke opacity, PM and PN decrease massively with butanol–diesel blends, especially the 30% mix		Saxena (2016)
10	Diesel, 10, 20, and 30% butanol-diesel blends		PM 30% mix < PM 20% mix < PM 10% mix < PM diesel	PN emissions at 1472 rpm, 1865 rpm and 2257 rpm respectively at a 25% of full load	Nabi et al. (2017)

3.4 Alcohol Impact on PM Characteristics

It is generally accepted that the combustion of oxygenated diesel blends results in more reactive soot particulates compared to conventional diesel fuelling (Savic 2016; Lapuerta 2012; Barrientos 2014; Liati et al. 2012; Vander Wal and Mueller 2006; Man 2015). Numerous researchers (Savic 2016; Barrientos 2014; Vander Wal and Mueller 2006; Man 2015) proved that this ameliorated reactivity was mainly influenced by the initial arrangement of the graphene layers (soot nanostructure) which was seen to be structurally less ordered compared to that presented in a diesel soot particulate. Limited research work has been made regarding alcohol impact on PM reactivity. Selection of the most appealing articles has been summarized in the following paragraph.

Vander Wal and Tomasek (2003) show that the soot oxidative reactivity mainly depends on the initial carbon layer arrangement which in turn relies on the nature of the fuel combusted. Under similar testing conditions, they found that the particulates generated from ethanol combustion present faster oxidation rates compared to those produced from benzene and acetylene combustion. HRTEM analysis revealed that this is mainly due to more curved layers presented in case of ethanol-derived soot. This has been linked to the presence of defects in the carbon layers (five-membraned layers) which in turn impose the bond strain and reduce the electronic resonance stabilization, thus weakening the C–C bonds and making them more vulnerable toward oxidation reaction. In addition, it was also reported that the curvature of the carbon layers presents a more influential factor that dictates the particulate's oxidative reactivity when compared to the basal plane diameter. Yet, in another research work, Vander Wal and Tomasek (2004) highlight that the oxidative reactivity and the nanostructure of the primary particulates are majorly determined by the synthesis conditions upon which the soot was incepted, such as temperature and residence time in the combustion chamber. It was found that at low-temperature conditions (~1250 °C), the combustion yields amorphous particulates that comprise short and disconnected carbon layers (which is stacked in a non-uniform direction), regardless of the operating fuel type or the mixture flow rate. However, an increase in the combustion temperatures (~1650 °C) leads to particulates with different structural order according to the flow speed and the nature of the fuel incorporated. For example, indene, benzene, and acetylene tend to produce highly ordered particulates (less reactive) at low flow rates (i.e., increasing the soot residence time), whereas soot with curved carbon layers (more reactive) is yielded at higher flows. As for ethanol, irrespective of the flow rate, more reactive soot characterized with curved graphene layers was always emitted. In both studies, the authors confirm the dependence of the soot reactivity upon its initial nanostructure ordering. Luo et al. (2018) study the impact of adding up to 30% vol. acetone–butanol–ethanol (ABE) to diesel fuel on soot oxidation reactivity. Soot originated from the ABE blend shows lower activation energy (i.e., more reactive) compared to those produced from diesel combustion.

Increasing the ABE concentration in the blend leads to reduction in the C=C functional groups while oxygen-borne species, O/C and H/C ratios increased correspondingly. Soot nanostructure turns into more amorphous core, $d\mathrm{p}_0$ and L_a decrease while T_f increases. The structural changes seen with the presence of ABE support the higher reactivity recorded. Lapuerta et al. (2019) investigated the impact of butanol/diesel blends on soot characteristics. It was seen that with increasing the butanol portion, the soot turns to be more ordered compared to diesel. This has been concluded from X-ray diffraction (XRD) analysis that shows longer L_a and high-resolution transmission electron microscopy (HRTEM) analysis that shows decrease in d_{002}. According to these structural changes, soot resulted from butanol blends suppose being less reactive than diesel particles. However, the thermal analysis shows the opposite, where butanol blend-derived particles show higher reactivity than diesel particles. In this study, the soot nanostructure did not follow the reactivity trend. As for the soot chemical composition, surface bonded oxygenated functional groups increase with the presence of butanol.

3.5 Summary

This review chapter summarized the different theories and assumptions proposed in the literature to correlate the soot physico-chemical parameters with the assigned oxidative reactivity toward oxygen. In case of diesel originated soot, nanostructure is considered the governing parameter to dictate soot oxidative reactivity. However, in case of alcohol/diesel blends, nanostructure tends to be of less importance and the soot chemical composition, mainly surface attached oxygen-borne species, turned to the main factor governing soot reactivity. Soot originated from ethanol/diesel blends present more amorphous core and more curved layers compared to diesel originated soot, resulting in higher oxidative reactivity. As for butanol/diesel blends, the soot nanostructure appears to be same as diesel soot or even more ordered; however, butanol/diesel originated soot tends to be more reactive toward oxygen. This has been directly related to the higher oxygen-borne species detected in the soot composition. As for soot concentration in the exhaust stream, alcohol/diesel blends suppress the PM and PN mass mainly by increasing the in-cylinder rate of soot oxidation (O and OH radicals enhance the oxidation rate) and by suppressing the formation of soot precursors in the fuel-rich regions (C–O moieties require higher energy to break up compared to C–C). With regard to the fuel composition, it has been seen that at equivalent oxygen content, alcohols are more effective than esters (i.e., biodiesel) in reducing soot formation.

References

Al-Qurashi K, Boehman AL (2008) Impact of exhaust gas recirculation (EGR) on the oxidative reactivity of diesel engine soot. Combust Flame 155(4):675–695. https://doi.org/10.1016/j.combustflame.2008.06.002

Al-Qurashi K, Lueking AD, Boehman AL (2011) The deconvolution of the thermal, dilution, and chemical effects of exhaust gas recirculation (EGR) on the reactivity of engine and flame soot. Combust Flame 158(9):1696–1704. https://doi.org/10.1016/j.combustflame.2011.02.006

Amann CA, Siegla DC (1982) Diesel particles—what they are and why. Aerosol Sci Technol 1:73–101. https://doi.org/10.1080/02786828208958580

Amaral BSN, Novaes FJM, Ramos MCKV, de Aquino Neto FR, Gioda A (2016) Comparative profile of pollutants generated by a stationary engine fueled with diesel, biodiesel, and ethanol. J Aerosol Sci 100:155-1-163. https://doi.org/https://doi.org/10.1016/j.jaerosci.2016.07.009

An H et al (2015) Modeling study of oxygenated fuels on diesel combustion: effects of oxygen concentration, cetane number and C/H ratio. Energy Convers Manage 90:261–271. https://doi.org/10.1016/j.enconman.2014.11.031

Barrientos EJ (2014) Impact of oxygenated fuels on sooting tendency and soot oxidative reactivity with application to biofuels. Doctoral dissertation, The Pennsylvania State University. Retrieved from https://etda.libraries.psu.edu/files/final_submissions/9482

Barrientos EJ, Lapuerta M, Boehman AL (2013) Group additivity in soot formation for the example of C-5 oxygenated hydrocarbon fuels. Combust Flame 160:1484–1498. https://doi.org/https://doi.org/10.1016/j.combustflame.2013.02.024

Buchholz B, Mueller C, Upatnieks A, Martin G, Pitz W, Westbrook C (2004) Using carbon-14 isotope tracing to investigate molecular structure effects of the oxygenate dibutyl maleate on soot emissions from a DI diesel engine. SAE technical paper, 2004-01-1849

Burtscher H (2005) Physical characterization of particulate emissions from diesel engines: a review. J Aerosol Sci 36(7):896–932. https://doi.org/10.1016/j.jaerosci.2004.12.001

Choi MY et al (1994) Simultaneous optical measurement of soot volume fraction and temperature in premixed flames. Combust Flame 99:174–186

Daido S et al (2000) Analysis of soot accumulation inside diesel engines. Soc Automot Eng Jpn 21(3):303–308. https://doi.org/10.1016/S0389-4304(00)00048-5

Fayad MA et al (2015) Role of alternative fuels on particulate matter (PM) characteristics and influence of the diesel oxidation catalyst. Environ Sci Technol 49(19):11967–11973. https://doi.org/10.1021/acs.est.5b02447

Fayad MA et al (2017) Manipulating modern diesel engine particulate emission characteristics through butanol fuel blending and fuel injection strategies for efficient diesel oxidation catalysts. Appl Energy 190:490–500. https://doi.org/10.1016/j.apenergy.2016.12.102

Gaddam CK, Huang C-H, Vander Wal RL (2016) Quantification of nano-scale carbon structure by HRTEM and lattice fringe analysis. Pattern Recogn Lett 76:90–97. https://doi.org/10.1016/j.patrec.2015.08.028

Glassman I, Yetter RA (2008) Combustion, vol 4th edition. Academic Press

Gogoi B et al (2015) Effects of 2,5-dimethylfuran addition to diesel on soot nanostructures and reactivity. Fuel 159:766–775. https://doi.org/10.1016/j.fuel.2015.07.038

Guarieiro LLN, de Almeida Guerretriro ET, dos Santos Amparo KK, Manera VB, Regis ACD, Santos AG, Ferreira VP, Leão DJ, Torres EA, de Andrade JB (2014) Assessment of the use of oxygenated fuels on emissions and performance of a diesel engine. Microchem J 117:94–99. https://doi.org/https://doi.org/10.1016/j.microc.2014.06.004

Hansen BB, Jensen AD, Jensen PA (2013) Performance of diesel particulate filter catalysts in the presence of biodiesel ash species. Fuel 106:234–240. https://doi.org/10.1016/j.fuel.2012.11.038

Haynes BS, Wagner HGG (1981) Soot formation. Prog Energy Combust Sci 7(4):229–273. https://doi.org/10.1016/0360-1285(81)90001-0

Herreros JM et al (2015) Extending the environmental benefits of ethanol–diesel blends through DGE incorporation. Appl Energy 146:335–343. https://doi.org/10.1016/j.apenergy.2015.02.075

Lapuerta M, Martos FJ, Herreros JM (2007) Effect of engine operating conditions on the size of primary particles composing diesel soot agglomerates. J Aerosol Sci 38(4):455–466. https://doi.org/10.1016/j.jaerosci.2007.02.001

Lapuerta M et al (2012) Effect of fuel on the soot nanostructure and consequences on loading and regeneration of diesel particulate filters. Combust Flame 159(2):844–853. https://doi.org/10.1016/j.combustflame.2011.09.003

Lapuerta M et al (2019) Analysis of soot from the use of butanol blends in a euro 6 diesel engine. Energy Fuels 33:2265–2277. https://doi.org/10.1021/acs.energyfuels.8b04083

Lee D, Choi SC, Lee CS (2013) Impact of SME blended fuel combustion on soot morphological characteristics in a diesel engine. Int J Automot Technol 14(5):757–762. https://doi.org/10.1007/s12239?013?0083?2

Leidenberger U et al (2012) Experimental studies on the influence of diesel engine operating parameters on properties of emitted soot particles. Combust Sci Technol 184(1):1–15. https://doi.org/10.1080/00102202.2011.611551

Liati A et al (2012). Microscopic investigation of soot and ash particulate matter derived from biofuel and diesel: implications for the reactivity of soot. J Nanoparticle Res 14(11). https://doi.org/https://doi.org/10.1007/s11051-012-1224-7

Lin YC, Lee C-F, Fang T (2008) Characterization of particle size distribution from diesel engines fueled with palm-biodiesel blends and paraffinic fuel blends. Atmos Environ 42(6):1133–1143. https://doi.org/10.1016/j.atmosenv.2007.10.046

Lu T, Cheung CS, Huang Z (2012) Size-resolved volatility, morphology, nanostructure, and oxidation characteristics of diesel particulate. Energy Fuels 26(10):6168–6176. https://doi.org/10.1021/ef3010527

Luo J et al (2018) Effect of acetone–butanol–ethanol addition to diesel on the soot reactivity. Fuel 226:555–563. https://doi.org/10.1016/j.fuel.2018.04.036

Ma Z et al (2014) Effects of diesel oxidation catalyst on nanostructure and reactivity of diesel soot. Energy Fuels 28:4376–4382. https://doi.org/10.1021/ef500467a

Man XJ et al (2015) Effect of waste cooking oil biodiesel on the properties of particulate from a DI diesel engine. Aerosol Sci Technol 49(4):199–209. https://doi.org/10.1080/02786826.2015.1016214

Marsh H, Kuo K (1989) Introduction to carbon science. Butterworth-Heinemann, pp 107–151

Matti MM (2007) Chemical characterization of particulate emissions from diesel engines: a review. J Aerosol Sci 38(11):1079–1118. https://doi.org/10.1016/j.jaerosci.2007.08.001

Meakin P, Donn B, Mullholland G (1989) Collisions between point masses and fractal aggregates. Langmuir 5(2):510–518. https://doi.org/https://doi.org/10.1021/la00086a038

Morjan I et al (2004) Gas composition in laser pyrolysis of hydrocarbon-based mixtures: influence on soot morphology. Carbon 42(7):1269–1273. https://doi.org/10.1016/j.carbon.2004.01.020

Mühlbauer W et al (2016) Correlations between physicochemical properties of emitted diesel particulate matter and its reactivity. Combust Flame 167:39–51. https://doi.org/10.1016/j.combustflame.2016.02.029

Müller JO et al (2006) Diesel engine exhaust emission: oxidative behavior and microstructure of black smoke soot particulate. Environ Sci Technol 40(4):1231–1236. https://doi.org/10.1021/es0512069

Nabi MNZ, Hossain FM, Bodisco TA, Ristovski ZD, Brown RJ (2017) A parametric study on engine performance and emissions with neat diesel and diesel-butanol blends in the 13-Mode European stationary cycle. Energy Convers Manag 148:251–259. https:doi.org/https://doi.org/10.1016/j.enconman.2017.06.001

Omidvarborna H, Kumar A, Kim D-S (2014) Characterization of particulate matter emitted from transit buses fueled with B20 in idle modes. J Environ Chem Eng 2(4):2335–2342. https://doi.org/10.1016/j.jece.2014.09.020

Omidvarborna H, Kumar A, Kim D-S (2015) Recent studies on soot modeling for diesel combustion. Renew Sustain Energy Rev 48:635–647. https://doi.org/10.1016/j.rser.2015.04.019

Pepiotdesjardins P et al (2008) Structural group analysis for soot reduction tendency of oxygenated fuels. Combust. Flame 154(1–2):191–205. https://doi.org/10.1016/j.combustflame.2008.03.017
Rodríguez-Fernández J, Lapuerta M, Sánchez-Valdepeñas J (2017) Regeneration of diesel particulate filters: effect of renewable fuels. Renew Energy 104:30–39. https://doi.org/10.1016/j.renene.2016.11.059
Roessler DM et al (1981) Optical properties and morphology of particulate carbon: variation with air/fuel ratio. Springer, US
Savic N et al (2016) Influence of biodiesel fuel composition on the morphology and microstructure of particles emitted from diesel engines. Carbon 104:179–189. https://doi.org/10.1016/j.carbon.2016.03.061
Saxena MRM, Mauriya RK (2016) Effect of SE emissions from a stationary conventional diesel engine. Aerosol Air Qual Res 16:2255–2266. https:doi.org/https://doi.org/10.4209/aaqr.2016.04.0144
Serhan N (2019) Destruction of diesel soot aggregates with the use of fuel-borne oxygen and the application of hydrogen assisted SCR catalyst. Ph.D. thesis, University of Birmingham. Retrieved from https://etheses.bham.ac.uk/id/eprint/9430
Shandilya K, Kumar A (2013) Particulate emissions from tailpipe during idling of public transit buses fueled with alternative fuels. Environ Progr Sustain Energy 32(4):1134–1142. https://doi.org/10.1002/ep.11696
Silverman DT et al (2012) The diesel exhaust in miners study: a nested case-control study of lung cancer and diesel exhaust. J Natl Cancer Inst 104(11):855–868. https://doi.org/10.1093/jnci/djs034
Smith DM, Chughtai AR (1995) Surface structure and reactivity of black carbon. Colloids Surf 105(1):47–77. https://doi.org/10.1016/0927-7757(95)03337-1
Song H (2003) Diesel soot oxidation under controlled conditions. Doctoral dissertation, Brunel University. Retrieved from https://bura.brunel.ac.uk/handle/2438/4814
Stanmore BR., Brilhac JF, Gilot P (2001) The oxidation of soot: a review of experiments, mechanisms and models. Carbon 39:2247–2268. https://doi.org/https://doi.org/10.1016/S0008-6223(01)00109-9
Strzelec A et al (2017) Nanostructure and burning mode of light-duty diesel particulate with conventional diesel, biodiesel, and intermediate blends. Int J Engine Res 18(6). https://doi.org/https://doi.org/10.1177/1468087416674414
Sua J, Zhub H, Bohac SV (2013) Particulate matter emission comparison from conventional and premixed low temperature combustion with diesel, biodiesel and biodiesel–ethanol fuels. Fuel 113:221–227. https://doi.org/10.1016/j.fuel.2013.05.068
Tree DR, Svensson KI (2007) Soot processes in compression ignition engines. Prog Energy Combust Sci 33(3):272–309. https://doi.org/10.1016/j.pecs.2006.03.002
Tse HL, Leung CW, Cheung CS (2015) Investigation on the combustion characteristics and particulate emissions from a diesel engine fueled with diesel-biodiesel-ethanol blends. Energy Convers Manag 83. https://doi.org/https://doi.org/10.1016/j.energy.2015.02.030
Vander Wal RL, Mueller CJ (2006) Initial investigation of effects of fuel oxygenation on nanostructure of soot from a direct-injection diesel engine. Energy Fuels 20(6):2364–2369. https://doi.org/10.1021/ef060201+
Vander Wal RL, Tomasek AJ (2003) Soot oxidation: dependence upon initial nanostructure. Combust Flame 134(1–2):1–9. https://doi.org/10.1016/s0010-2180(03)00084-1
Vander Wal RL, Tomasek AJ (2004) Soot nanostructure: dependence upon synthesis conditions. Combust Flame 136(1–2):129–140. https://doi.org/10.1016/j.combustflame.2003.09.008
Wagner HGG (1979) Soot formation in combustion. Symposium (International) Combust 17(1):3–19. https://doi.org/https://doi.org/10.1016/S0082-0784(79)80005-3
Walker PL, Austin LG, Nandi SP (1966) Chemistry and physics of carbon, vol 2. Pergamon Press Ltd.
Wang X et al (2012) Identification of active oxygen species for soot combustion on $LaMnO_3$ perovskite. Catal Sci Technol 2(9):1822. https://doi.org/10.1039/c2cy20353g

Westbrook CK, Pitz WJ, Curran HJ (2006) Chemical kinetic modeling study of the effects of oxygenated hydrocarbons on soot emissions from diesel engines. J Phys Chem 110:6912–6922

Xi J, Zhong BJ (2006) Soot in diesel combustion systems. Chem Eng Technol 29(6):665–673. https://doi.org/10.1002/ceat.200600016

Ye P et al (2014) Impact of rail pressure and biodiesel fueling on the particulate morphology and soot nanostructures from a common-rail turbocharged direct injection diesel engine. Int J Engine Res 17(2):193–208. https://doi.org/10.1177/1468087414564229

Zhang ZHB, R. (2014) Influence of butanol addition to diesel-biodiesel blend on engine performance and particulate emissions of a stationary diesel engine. Appl. Energy 119:530–536. https://doi.org/10.1016/j.apenergy.2014.01.043

Zhang ZHC, Chua SM, Balasubramanian R (2016) Comparative evaluation of the effect of butanol-diesel and pentanol-diesel blends on carbonaceous particulate composition and particle number emissions from a diesel engine. Fuel 176:40–47. https://doi.org/https://doi.org/10.1016/j.fuel.2016.02.061

Zhu LXY, Cheung CS, Guan C, Huang Z (2016) Combustion, gaseous and particulate emission of a diesel engine fueled with n-pentanol (C5 alcohol) blended with waste cooking oil biodiesel. Appl Therm Eng 102:73–79. https:doi.org/https://doi.org/10.1016/j.applthermaleng.2016.03.145

Zhua L et al (2013) Effects of ethanol–biodiesel blends and diesel oxidation catalyst (DOC) on particulate and unregulated emissions. Fuel 113:690–696. https://doi.org/10.1016/j.fuel.2013.06.028

Chapter 4
Methanol as a Fuel for Marine Diesel Engines

Burak Zincir and Cengiz Deniz

Abbreviations

A/F_S	Stoichiometric air–fuel ratio
CCS	Carbon capture system
CI	Compression ignition
COV IMEP	Coefficient of variation indicated mean effective pressure
DISI	Direct injection spark ignition
DME	Dimethyl ether
ECA	Emission control area
EEDI	Energy efficiency design index
EEOI	Energy efficiency operational indicator
EFTA	European Free Trade Association
EGR	Exhaust gas recirculation
EMSA	European Maritime Safety Agency
η_{GIE}	Gross-indicated efficiency
FuelMEP	Fuel mean effective pressure
HCCI	Homogenous charge compression ignition
HFO	Heavy fuel oil
IACS	The International Association of Classification Societies
IMEP	Gross-indicated mean effective pressure
IMO	International Maritime Organization
LHV	Lower heating value
LSMGO	Low-sulfur marine gas oil
MARPOL	International Convention for the Prevention of Pollution from Ships
MEPC	Marine Environment Protection Committee

B. Zincir (✉) · C. Deniz
Maritime Faculty, Istanbul Technical University, Istanbul, Turkey
e-mail: bzincir@itu.edu.tr

P. C. Shukla et al. (eds.), *Alcohol as an Alternative Fuel for Internal Combustion Engines*, Energy, Environment, and Sustainability,
https://doi.org/10.1007/978-981-16-0931-2_4

MGO	Marine gas oil
MON	Motor octane number
MRV	Monitoring, reporting, verification
NaOH	Caustic soda
PFI-SI	Port fuel injection-spark-ignited combustion
PPC	Partially premixed combustion
PRR	Pressure rise rate
RCCI	Reactivity-controlled compression ignition
RON	Research octane number
SAMS	Scavenge air moisturizing system
SCR	Selective catalytic reduction
SEC	Specific energy consumption
SEEMP	Ship energy efficiency management plan
SI	Spark ignition
SOFC	Solid oxide fuel cell
SVO	Straight vegetable oil
UNCTAD	The United Nations Conference on Trade and Development
WHRS	Waste heat recovery system

4.1 The Status of the Maritime Transportation

The transportation sector is indispensable for the mobility of people and goods worldwide. It connects people and provides persons or goods to reach the farthest destination of the world. Maritime transportation is an essential piece of the transportation sector and constitutes a major part of worldwide trade. 90% of the worldwide trade (Deniz and Zincir 2016), 90% of the outer freight, and 40% of the inner freight of the European Union (Fan et al. 2018) have been done by maritime transportation. According to 2019 data of the United Nations Conference on Trade and Development (UNCTAD), 96,295 ships are in operation which is equal to 1.97 billion deadweight tons (dwt) (United Nations Conference on Trade and Development (UNCTAD) 2019). Also, it is indicated that the annual maritime transportation volume growth was 2.6% in 2019, and it is estimated that an annual average growth rate will be 3.4% for the period 2019–2024.

On the other hand, maritime transportation has an important share of worldwide emissions. International Maritime Organization (IMO) states that maritime transportation consumes 300 million tons of fuel annually and leads to 938 million tons of CO_2, 19 million tons of NO_X, 10.2 million tons of SO_X, 1.4 million tons of PM, and 936 thousand tons of CO emissions in 2012 (International Maritime Organization (IMO) 2014). At a study of European Energy Agency (EEA) (2019), the maritime transportation has the contribution of 20.98% of the worldwide NO_X emissions, 11.80% of the worldwide SO_X emissions, 8.57 and 4.63% of the worldwide PM2.5 and PM10 emissions, respectively, and lastly, 1.94% of the worldwide CO emissions.

The status of maritime transportation was given in this section. Maritime transportation is an integrated part of global trade, and it is expected that the trade volume will be in the growing trend for the near future. It also means that the fuel consumption and engine emissions will be in increasing trend. To overcome this issue, international maritime emission rules and regulations are stricter day by day. The next section introduces rules and regulations about CO_2, NO_X, SO_X, and PM emissions to control and mitigate shipboard emissions.

4.2 International Maritime Emission Rules and Regulations

The fuel consumption and shipboard emissions have been in escalation since the ship number has increased year by year. Nowadays, shipboard emissions are the most important issue for maritime transportation. The International Maritime Organization (IMO) has been working on emission mitigation and control by implementing international maritime emission rules and regulations. The international maritime emission rules and regulations are becoming stricter day by day. There are rules and regulations for CO_2, NO_X, and SO_X emissions. There are not any specific rules or regulations for PM emissions, but it has been regulated by the SO_X regulation. All rules and regulations about these emissions were addressed in the International Convention for the Prevention of Pollution from Ships (MARPOL), Annex VI—Regulations for the prevention of air pollution from ships (May 2005). This section is going to give detailed information about international maritime emission rules and regulations.

4.2.1 Carbon Dioxide Emission Rules and Regulations

The carbon content of the fuel is the reason for the CO_2 emissions. To achieve zero CO_2 formation as a combustion product, the fuel does not contain carbon atoms in its structure. Almost all maritime transportation fuels contain carbon atoms, and the CO_2 formation is inevitable. It is awaited that the CO_2 emissions will raise with 50–250% compared to the 2008 level (International Maritime Organization (IMO) 2014). However, the CO_2 emissions can be decreased by reducing fuel consumption of the main engine and auxiliary engines of a ship or using low-carbon content fuels. Increasing energy efficiency on ships results in lower fuel consumption and reduced CO_2 emissions.

The Regulations on Energy Efficiency for Ships in MARPOL Annex VI regulates the CO_2 emissions from ships on and after January 1, 2013 (International Maritime Organization (IMO) 2011). The regulation aims to control and mitigate CO_2 emissions from the existing and new building ships. Two mandatory terms the energy

Table 4.1 EEDI reduction phases (Bazari 2016)

Phase	Year	Reduction amount (%)
0	2013–2015	0
1	2015–2020	10
2	2020–2025	15–20
3	2025–	30

efficiency design index (EEDI) and the ship energy efficiency management plan (SEEMP) and a voluntary term the energy efficiency operational indicator (EEOI) were defined by the regulation.

The EEDI is a measure for the new building ships. It aims to standardize and increase the use of energy-efficient engines and equipment on the new building ships. The vessel energy efficiency level is calculated by taking fuel consumption, fuel carbon content, ship speed, and the cargo carrying capacity of the ship (MAN 2014). Its unit is grams of CO_2 per ton-mile, and the lower value indicates a more efficient ship. There are "attained EEDI" and "required EEDI" in the regulation. The attained EEDI is the actual EEDI calculated for new building ships. And the required EEDI is the allowable maximum EEDI limit for the specific ship type. The required EEDI limit has decreased every five years phase by phase. Shipowners can use any technology which is suitable for their new building project for not exceeding the maximum EEDI limit. The phases are shown in Table 4.1.

The SEEMP was defined for the CO_2 emission control of the existing ships doing international maritime transportation. It is a mandatory plan for all ships, and it aims to encourage and increase the energy-efficient operation on the ships. The SEEMP contains measures such as optimizing ship speed, weather routing, trim optimization, hull and propeller cleaning, and using waste heat recovery system. Lastly, EEOI was introduced as a voluntary voyage-based calculation with the regulation. It aims to reduce CO_2 emissions emitted at a voyage (Zincir and Deniz 2016). The shipowners or operators can track their ship efficiency performance in grams of CO_2 per ton-mile basis. This voluntary term was the first building block of the mandatory rules, Monitoring, Reporting, Verification (MRV) Regulation and IMO Data Collection System (DCS). The CO_2 emission performance of a ship can be calculated by EEOI.

On July 1, 2015, the MRV Regulation entered into force by the European Union, Norway, and Iceland (Gl 2020). The regulation aims to record and control the annual CO_2 emissions of ships larger than 5000 GRT calling to the EU, Norway, and Iceland ports. The monitoring phase was started on January 1, 2018, by monitoring annual fuel consumption, voyage day, fuel carbon content, and CO_2 emission data of the ship. The second phase of reporting has started in 2019. The shipowners and operators have to submit their ship annual report to Thetis MRV application of the European Maritime Safety Agency (EMSA) (Gl 2017). The reporting phase encourages shipowners and operators to increase energy efficiency measures on a ship, reduce fuel consumption, or use lower carbon content fuel. And lastly, annual ship reports were verified and the verification document has been required by the port authorities after June 30, 2019.

Table 4.2 Greenhouse gas strategy of the IMO (International Council on Clean Transportation (ICCT) 2018)

Term	Year	Target	Strategy	Status
Short	2018–2023	New vessels	New EEDI phases	−10% in 2015 −20% in 2020 −30% in 2030
Short	2018–2023	In-service vessels	Operational efficiency measures	SEEMP planning required
Short	2018–2023	In-service vessels	Improvement of existing fleet program	–
Short	2018–2023	In-service vessels	Speed reduction	–
Short	2018–2023	Engine and fugitive emission	Measures to address volatile organic compound and methane emissions	–
Mid	2023–2030	Fuels/new and in-service vessels	Alternative fuel implementation program	–
Mid	2023–2030	In service vessels	Further operational efficiency measures	SEEMP planning required
Mid	2023–2030	In service vessels/fuels	Market-based measures	–
Long	2030+	Fuels/new and in-service vessels	Zero carbon	–

IMO DCS is the latest regulation to mitigate CO_2 emissions worldwide. This regulation is amendments to MARPOL Annex VI by the resolution MEPC.278(70) which has been effective on and after March 1, 2018 (International Maritime Organization (IMO) 2020a). It is a similar regulation to MRV Regulation. The only difference is the IMO DCS covers all ports worldwide while MRV Regulation covers EU and EFTA ports. The first reporting period was started on January 1, 2019 (Gl 2020). Also, the IMO DCS requires an update to the existing SEEMP as the SEEMP Part II. The additional part contains data collection and reporting methods for the specific ship.

In April 2018, at the MEPC 72 meeting IMO has a greenhouse gas (GHG) strategy that aims to lessen CO_2 emissions per transport work at least 40% by 2030 and 70% by 2050 compared to 2008 levels (International Council on Clean Transportation (ICCT) 2018). IMO announced its short-, mid-, and long-term strategies (Table 4.2) to achieve success at their GHG strategy.

4.2.2 Nitrogen Oxide Emission Rules and Regulations

In 2000 at the MEPC.58 meeting, the MARPOL Annex VI was revised and the NO_X Technical Code was adopted (International Maritime Organization (IMO) 2017) and

Table 4.3 NO_X tier limits (International Maritime Organization (IMO) 2020b)

Tier	Ship construction date	Total weighted cycle emission limit (g/kWh) n = engine's rated speed (rpm)		
		$n < 130$	$n = 130–1999$	$n \geq 2000$
I	January 1, 2000	17.0	$45n^{(-0.2)}$	9.8
II	January 1, 2011	14.4	$44n^{(-0.23)}$	7.7
III	January 1, 2016	3.4	$9n^{(-0.2)}$	2.0

entered into force on October 10, 2008 (International Maritime Organization (IMO) 2008). The NO_X Technical Code, Regulation 13, of MARPOL Annex VI aims to limit the shipboard NO_X emissions. The ships which have the engine power above 130 kW are regulated by the code. The code determines the minimum standards for the manufacturing and usage of the code-compliant marine engines and certification of the engines on ships. The NO_X emission limits vary depending on the engine speed and emission tiers (International Maritime Organization (IMO) 2020b). Also, tier limits are different for outside the ECAs and inside ECAs. The NO_X limits can be shown in Table 4.3.

4.2.3 Sulfur Oxide and Particulate Matter Emission Rules and Regulations

The SO_X emissions are regulated by Regulation 14 of MARPOL Annex VI that entered into force in 2005 (International Maritime Organization (IMO) 2020c). This regulation limits the fuel sulfur content by mass (m/m) to mitigate the SO_X emissions from ships. The PM emissions are related to the fuel sulfur content; as a result, the PM emissions are also regulated. The sulfur limits are different for inside ECAs and outside ECAs. Table 4.4 shows the SO_X and PM emission limits.

On January 1, 2020, The IMO Sulfur Cap entered into force. The sulfur limit is 0.50% m/m at the non-ECAs and 0.10% m/m inside the ECAs for the used fuel. Also, it is forbidden to carry fuel that has higher sulfur content than the limits. Around

Table 4.4 SO_X and PM limits (International Maritime Organization (IMO) 2020c)

SO_X and PM limits outside ECAs	SO_X and PM limits inside ECAs
4.50% m/m prior to January 1, 2012	1.50% m/m prior to July 1, 2010
3.50% m/m on and after January 1, 2012	1.00% m/m on and after July 1, 2010
0.50% m/m on and after January 1, 2020	0.10% m/m on and after January 1, 2015

70,000 ships are affected worldwide by these new sulfur limits (Chryssakis et al. 2017).

4.3 Emission Mitigation Technologies and Methods for Ships

The international emission rules and regulations at the maritime transportation have been stricter day by day, and measures have to be taken to comply with the recent regulations to do international maritime trade. There are various ways to mitigate the different types of emissions from ships. This section discusses emission mitigation technologies and methods on ships.

4.3.1 CO_2 Emission Mitigation

CO_2 emissions are related to fuel consumption. The efficient fuel combustion or increasing the efficiency of the systems and operations on a ship is the key element for reduced CO_2 emissions. The design measures, engine and engine room machinery modifications, operational measures, and new technologies are the main classification of the technologies and methods to reduce the CO_2 emission. Table 4.5 shows the CO_2 mitigation technologies and methods for ships.

4.3.1.1 Design Measures

The design measures consist of ship size, ship weight reduction, optimum ship dimensions, improved aft-body, aerodynamic superstructure design, hydrodynamic bulb and bow design, improved propeller design, optimization of propeller, rudder and hull interaction, pre- and post-swirl devices, and contra-rotating propellers.

The energy efficiency for ships is calculated as the CO_2 emission amount per tone-nautical mile. The ship size affects energy efficiency and CO_2 emissions. Larger ships are more efficient and emitting less CO_2 emissions since they can transport more cargo at the same speed and distance than the smaller ships. It was stated that 4–5% higher transport efficiency can be provided by a 10% larger ship (Lassesson and Andersson 2009). Ship weight reduction is also an important measure. The loading capacity will increase if the low-weighted materials are used on a ship and it will affect the energy efficiency and CO_2 emissions of a ship. The optimum ship dimensions with a high length/breadth ratio reduce the resistance and increase the hull efficiency and decrease the CO_2 emissions.

The air resistance of the superstructure reduces energy efficiency and increases CO_2 emissions. An aerodynamic superstructure design improves energy efficiency

Table 4.5 CO_2 mitigation technologies and methods for ships (Lassesson and Andersson 2009; Maritime Knowledge Center (MKC) 2017; Winkel et al. 2015)

CO_2 mitigation technologies and methods			
Design measures	Engine and engine room machinery modifications	Operational measures	New technologies
Ship size	Common rail	Speed reduction	Air lubrication
Ship weight	Engine derating	Voyage optimization	Diesel-electric propulsion
Ship dimensions	Fans, pumps, and compressors	Weather routing	Hybrid auxiliary power generation
Aft-body	Waste heat recovery system	Hull coating and cleaning	Renewable energy
Superstructure		Propeller polishing	Carbon capture system
Bulb and bow		Machinery maintenance	Alternative fuels
Propeller design		Trim and ballast optimization	
Optimization of propeller, rudder, and hull interaction		Shore connection	
Pre- and post-swirl devices			
Contra-rotating propellers			

by the lower air resistance. The improved aft-body and hydrodynamic bulb and bow design reduce the hull–water resistance and again increase the energy efficiency.

The improved propeller design, optimization of propeller, rudder and hull interaction, pre- and post-swirl devices, and contra-rotating propellers aim to improve the water flow to the propeller, reduce the rotational losses from the propeller, and increase the propeller efficiency.

4.3.1.2 Engine and Engine Room Machinery Modifications

Common rail system, engine derating, optimization of the fans, pumps, compressors, and waste heat recovery system (WHRS) are the CO_2 mitigation measures at the engine room of a ship.

The common rail system is an electronically controlled fuel injection system that arranges the fuel injection timing, pressure, and duration independently from the position of the piston (Winkel et al. 2015). This system can determine the optimum fuel injection timing, fuel pressure, and fuel injection duration depending on the

engine load. It provides more efficient combustion of the fuel which results in lower CO_2 emissions.

The engine derating is an engine modification that limits the maximum engine power and changes the continuous load of the engine. The combustion parameters are also changed according to the new load range. The engine derating is a speed reduction technique. It provides more optimum and efficient working of the ship main engine at slower speeds of a ship. Lower ship speed results with lower fuel consumption at the total voyage distance and lower CO_2 emissions.

In addition to the main engine modifications, engine room machinery can be optimized for energy-efficient operation. Fans, pumps, and compressors are important elements of an engine room with high electricity consumption. Instead of running at full load all the time, if they changed with variable speed ones, they will work according to the instantaneous need. A study showed that there is a high amount of wasted energy from the seawater pump working at full load (Durmusoglu et al. 2015). This energy is not wasted if the pump is changed with the variable speed pump.

The WHRS is the system that recovers some of the thermal energy from the wasted energy in the exhaust gases. The recovered thermal energy can be used for the electric generation at the turbogenerators, additional mechanical energy to the ship main engine or heating, and freshwater generation on a ship. The WHRS can provide energy saving up to 15% of the engine power (Lassesson and Andersson 2009).

4.3.1.3 Operational Measures

The operational measures are the easiest methods to reduce the CO_2 emissions which can be done by the ship crew and ship management companies. These measures are speed reduction, voyage optimization, weather routing, hull coating and cleaning, propeller polishing, trim and ballast optimization, and shore connection at ports.

The speed reduction (slow steaming) is an effective way to reduce total fuel consumption at a distance. Lower fuel consumption means lesser CO_2 emissions emitted to the atmosphere. It is stated that one knot of speed reduction equals to 11% fuel consumption at the same distance (Lassesson and Andersson 2009). Another report indicated that 10% of speed reduction reduces 20% of fuel consumption and emissions and 30% of speed reduction decreases more than 50% of fuel consumption and harmful emissions (Maritime Knowledge Center (MKC) 2017).

Voyage optimization and weather routing are other operational measures concerning ship navigation. Optimum planning of the voyage including reducing waiting times at ports, or before strait and canal passages is important for the decrease at the fuel consumption. Weather routing is finding optimal routes according to the weather condition. Winds, waves, and currents affect the fuel consumption of a ship; thus, the weather routing can be used as an operational measure for CO_2 reduction.

Maintenance operations on a ship can provide lower fuel consumption and higher ship efficiency. Hull coating and cleaning and propeller polishing are the maintenance

operations directly related to fuel consumption. Roughness and biofouling on the hull and propeller increase the resistance that results in higher fuel consumption and CO_2 emissions. A study indicates that periodic hull cleaning leads to 9% of fuel-saving, while dry-docking leads to 17% of fuel-saving (Adland et al. 2018). Machinery maintenance, cleaning, and replacement of parts with the new ones at the scheduled intervals can provide 5–10% lesser fuel consumption and CO_2 emission (Wireman 2011).

Another operational measure is trim and ballast optimization on ships which is a mandatory part in SEEMP. The trim is the difference between the height of the bow and the stern of a ship when it is measured from the waterline. The optimum trim is essential for the reduced resistance at the hull. An optimum trim can provide a 1–5% energy reduction on a ship (Lassesson and Andersson 2009). The optimum ballast is also an important issue on a ship. The ballast water is an extra weight on a ship, and the ballast water uptake has to be arranged according to the optimum trim condition.

The shore connection known as cold-ironing is a shore-based operational measure. The electricity requirement of a ship is taken from the shore by a special cable. Since the diesel generator does not work on a ship, this results with zero fuel consumption and zero CO_2 emission from the ship. On the other hand, the shore electricity should be produced from renewable sources to assume that the operation results with zero CO_2 emission.

4.3.1.4 New Technologies

The new technologies are not common, but it is in the increasing trend in maritime transportation in recent years. The new technologies which are mentioned in this chapter are air lubrication system, diesel-electric machinery, hybrid auxiliary power generation, renewable energy, carbon capture systems (CCS), and alternative fuels. Alternative fuels will be mentioned later.

The air lubrication system is designed to reduce friction between hull and water. It is a system that air is delivered via pumps to out of the hull. The air bubbles are delivered between the hull and water due to the lower resistance between hull–air–water than the hull–water (Lassesson and Andersson 2009). The total efficiency saved is 9% with the air lubrication system (Winkel et al. 2015).

Diesel-electric propulsion is a propulsion system consisting of electric motors powered by diesel engines. The electric motors are connected to the propellers. The diesel-electric propulsors are able to work at higher total efficiency than the conventional propulsion type because it can respond quicker at load changes, especially at maneuvering operation of a ship. The maneuvering operation is the navigation of a ship near coastal areas, such as port entry, canal, or strait passages. Another new technology is the hybrid auxiliary power generation on a ship by using fuel cells and batteries. The hydrogen, methanol, or natural gas fuel cells can be used to generate energy that is supportive of the main engine. Since the maximum theoretical efficiency is higher for fuel cells, it increases the energy efficiency of a ship and reduces the CO_2 emissions (Lassesson and Andersson 2009).

Nowadays, renewable energy such as wind and solar power is used on ships. Soft sails, rigid wing sails, kites, and Flettner rotors are some of the equipment and systems for getting wind energy as an auxiliary energy to the ship main engine. Also, solar panels are placed on the deck of the ship to change solar energy to the electricity by storing at the batteries. These systems reduce fossil fuel consumption of a ship and increase the use of zero-carbon energy.

Carbon capture systems (CCSs) are mostly used in power plants, steel, and cement industries, but there are some studies to apply CCS on ships (Zhou and Wang 2014; Akker 2017; Feenstra et al. 2019). Basically, a CCS captures the CO_2 emission from the ship funnel as an after-treatment system. The CO_2 capture rate varies from 80 to 95% depending on the system specifications (American Society of Civil Engineers (ASCE) 2014). It does not measure to reduce the CO_2 emission, but a measure to capture and store onboard.

4.3.2 NO_X Emission Mitigation

NO_X emission consists of NO and NO_2 emissions. Although there are two types of emissions in NO_X, NO has a higher proportion than NO_2; therefore, NO kinetics are dominant at NO_X formation. The NO_X formation highly depends on maximum in-cylinder temperature and oxygen content and also related to the pressure rise rate (PRR) and maximum in-cylinder pressure since high PRR and maximum in-cylinder pressure result in sudden high in-cylinder temperature. There are various mitigation technologies and methods to overcome NO_X formation at marine diesel engines. Pre-combustion techniques, combustion intervention techniques, and after-treatment technologies which are shown in Table 4.6 can be used on a marine diesel engine. Alternative fuels will be discussed further in detail.

Pre-combustion techniques for NO_X reduction are water/steam injection to the intake air, fuel–water emulsion, engine modification, and alternative fuel usage. The marine diesel engine manufacturer, MAN B&W, has a system named "Scavenge Air Moisturizing System (SAMS)" which injects seawater into the intake air of an

Table 4.6 NO_X mitigation methods for ships

Pre-combustion	Combustion intervention	After-treatment
Water/steam injection to the intake air	Exhaust gas recirculation system	Selective catalytic reduction system
Fuel–water emulsion	Water/steam injection into the cylinder	
Engine modification		
Alternative fuels		

engine. The purpose is to reduce local maximum combustion temperature in the combustion chamber by the cooling effect of the water (MAN 2014). The lower maximum combustion temperature limits the NO_X formation. Also, steam can be introduced to the intake air to do the same effect as water vapor. This method decreases engine efficiency and increases the specific fuel consumption (SFC) and PM emission (Andreoni et al. 2008). The water/steam injection can be also used as a combustion intervention technique. The water/steam is injected during the combustion process as the combustion intervention to do the same effect as the pre-combustion technique.

Fuel–water emulsion is the homogenous fuel–water mixture is used as a fuel at marine diesel engines. It has a similar effect to the SAMS. Reduction at the maximum combustion temperature is provided that results in lower NO_X emission with slightly increased SFC. The study results show that 30% NO_X reduction was provided with 20–80% water–fuel emulsion (Kim et al. 2018) at a four-stroke diesel engine. MAN states that 10% NO_X reduction was achieved for each 10% water added at their two-stroke marine diesel engine (MAN 2014).

The engine modification is the NO_X mitigation method at pre-combustion and combustion intervention stages. Optimum engine modification can achieve to lower NO_X emission. Optimized fuel injection valves and nozzles, the number and size of the spray holes, fuel injection retardation, compression ratio reduction, increase of injection pressure, induction swirl optimization, and intake air system modification are some of the engine modifications (MAN 2014; Andreoni et al. 2008).

Exhaust gas recirculation (EGR) system is a combustion intervention technology. It recirculates some of the exhaust gases, after cools down and cleans, delivers into the cylinder to reduce the oxygen content in the cylinder, and decreases the nitrogen oxidation inside the cylinder (Zincir 2019). NO_X reduction of up to 70% can be achieved with EGR (MAN 2014). The system decreases engine efficiency and NO_X emissions while increasing SFC, CO_2, and PM emissions (Zincir 2014).

The selective catalytic reduction (SCR) system is an after-treatment system that uses ammonia or urea to mitigate NO_X emission by the chemical reaction. It can remove 90–95% of NO_X emission (MAN 2014). The system has side effects on the engine such as reduced engine efficiency, increased SFC, and CO_2 emissions (Zincir 2019).

4.3.3 SO_X Emission Mitigation

The SO_X emission depends on fuel sulfur content. Using low-sulfur heavy fuel oil or marine diesel oil is an option to reduce SO_X emission. The sulfur scrubber as an after-treatment technology is another way to decrease the SO_X emission from ships. There are wet-type scrubbers that use either seawater or freshwater with a caustic soda (NaOH) solution, and dry-type scrubbers use chemicals and capture SO_X and PM emissions inside the scrubber (Zincir 2014). Local regulations of California waters do not allow to use the scrubbers and force ship operators to use low-sulfur fuels. The sulfur scrubbers reduce engine efficiency and increase SFC and CO_2 emission.

The last way to mitigate SO_X emission is the usage of sulfur-free alternative fuels on ships (Andersson and Salazar 2015).

4.3.4 *Mitigation Method for All Regulated Emissions: Alternative Fuels*

Up to now, emission mitigation methods and technologies for various emission types were explained. It can be understood that an emission mitigation method or technology only decreases only one type of emission and it does not have any effect on other types of regulated emissions. Therefore, sometimes two types of technology, i.e., SCR for NO_X emission and sulfur scrubber for SO_X and PM emissions, are applied to a ship to comply with recent emission rules and regulations. It means high investment costs and enough space requirements on a ship. To overcome this issue, alternative fuels can be used as fuel. Using alternative fuels can reduce the different types of emissions at once without applying additional equipment for each emission target.

The alternative fuels for the maritime transportation are liquefied natural gas (LNG), methanol, liquefied petroleum gas (LPG), ethanol, ethane, dimethyl ether (DME), biodiesel, biogas, synthetic fuels, ammonia, and hydrogen (Chryssakis et al. 2014; Sverrisdottir 2018; Zincir and Deniz 2018; Bakhtov 2019). And the possible ones for the future are straight vegetable oil (SVO), bio-ethanol, and bio-ammonia (Maritime Knowledge Center (MKC) 2017). Although there is a large variety of alternative fuels for the maritime transportation, the most promising alternatives are LNG and methanol, due to their good supply infrastructure and biofuel counterparts as biomethane and biomethanol (Moirangthem 2016). Recent alternative fueled ship numbers are 169 LNG-fueled ship in operation and 216 ships in order, 10 methanol-fueled ship in operation and 6 in order, 12 LPG-fueled ships in operation and 14 ships in order, and 2 ethane fueled ships in operation and 2 in order (Zincir and Deniz 2018; DNV GL 2020).

LNG, LPG, and methanol can decrease NO_X emission by up to 90%, below the NO_X Tier III Limit. The CO_2 emission reduction is 23%, 20%, and 10% by using LNG, LPG, and methanol, respectively, and the sulfur-free structure of these fuels results with a 90–97% reduction at SO_X emission and 90% PM emission (ClassNK 2018). However, alternative fuels can increase engine efficiency and decrease SFC in contrary to the after-treatment technologies.

Table 4.7 compares the emission mitigation technologies with the regular marine diesel engine without any emission mitigation technology as the baseline. The most popular technologies and alternative fuels at maritime transportation are included in the comparison table. The emission types, engine efficiency, and space and modification requirement on a ship for the technology are the criteria. Yellow, orange, red, and green colors indicate low effect, moderate effect, high effect, and no effect, respectively. At space and modification requirement criterion, colors have reverse meaning.

Table 4.7 Comparison of the emission mitigation technologies and alternative fuels

Emission Mitigation Technologies	Comparison Criteria of the Emission Mitigation Technologies					
	CO_2 Emission	NO_X Emission	SO_X Emission	PM Emission	Engine Efficiency	Space & Modification Requirement
EGR	-	+	S	-	-	Moderate
SCR	-	+	S	S	-	High
Sulfur scrubber	-	S	+	+	-	High
WHRS	+	+	+	+	+	High
Engine modification	-/+	+/-	-/+	-/+	-/+	S
Low-sulfur conventional fuel	S	S	+	+	S	S
Renewable energy assist	+	+	+	+	+	High
LNG	+	+	+	+	+	High
Methanol	+	+	+	+	+	Moderate

(− = worse than the baseline, + = better than the baseline, S = the same as the baseline)

Yellow, orange, and red colors indicate high requirements, moderate requirements, and low requirements, respectively.

EGR as a NO_X emission mitigation technology has a medium reduction effect (70% of reduction) and slightly higher SFC, CO_2, and PM emissions, and slightly lower engine efficiency with no effect on SO_X emission. EGR has moderate space and modification requirements on a ship when it is compared with other technologies, such as SCR and sulfur scrubber. Increased CO_2 and PM emissions and reduced engine efficiency are the negative sides of the EGR.

SCR is another NO_X emission mitigation technology that has a high reduction effect (90–95% of reduction). It slightly increases CO_2 emission and decreases the engine efficiency, and there is no effect on SO_X and PM emissions. SCR has a high space and modification requirement on a ship since it has a complex system with equipment high in number. The CO_2 emission increase, engine efficiency reduction, and high space and modification requirement for the system elements are the disadvantages of SCR.

The sulfur scrubber highly reduces SO_X and PM emissions, slightly increases CO_2 emission, and reduces engine efficiency with no effect on NO_X emission. It has a high space and modification requirement on a ship the same as SCR. The disadvantages of the sulfur scrubber are slightly increased CO_2 emission, reduced engine efficiency, and high space and modification requirement of the system.

WHRS can reduce total fuel consumption onboard by getting energy from the wasted exhaust energy and use it at a steam generation that can be used at a turbo-generator for ship electricity production, additional mechanical energy to the ship main engine, heating, freshwater generation, etc. This results in slightly lower CO_2,

NO_X, SO_X, and PM emissions with slightly higher engine efficiency. The WHRS also needs high space and modification requirements on a ship.

The engine modification can affect the emission formation. The NO_X emission can be reduced with the trade-off of slightly higher SFC, CO_2, SO_X, and PM emissions and slightly lower engine efficiency by changing fuel injection timing or injection pressure. On the other hand, vice versa can be happened by doing engine modification on the main engine. There is no need for space and modification requirements on a ship.

Use of low-sulfur conventional fuel highly decreases the SO_X and PM emissions, but there is no effect on CO_2 and NO_X emissions, and engine efficiency. Also, there is no need for space and modification requirements on a ship since the same fuel system is used.

The renewable energies, wind and solar, assist to the main engine or auxiliary engines. This reduces total fuel consumption on a ship that results in slightly lower CO_2, NO_X, SO_X, and PM emissions with slightly higher engine efficiency. Renewable energy systems require high space and modification on a ship, and it is the disadvantage of these systems.

LNG is the most popular alternative fuel in maritime transportation. When it is compared with the conventional-fueled main engine, the use of LNG on a ship results in extremely lower CO_2, NO_X, SO_X, and PM emissions with slightly higher engine efficiency. The LNG storage and fuel system have a high space and modification requirements on a ship. It requires special LNG tanks for the storage, double-walled fuel piping with the LNG supply system to the main engine. The main engine must have a modified fuel injection system with the safety systems for LNG fuel. High space and modification requirement is the disadvantage of LNG fuel.

Methanol is the second most popular alternative fuel in maritime transportation nowadays. Methanol moderately reduces CO_2 emissions and highly decreases NO_X, SO_X, and PM emissions. Methanol fuel usage moderately increases engine efficiency if the optimum combustion conditions are provided. Methanol storage and fuel system require some space and modification on a ship, but they are less than LNG storage and fuel system. There is no need for special storage tanks; methanol can be stored in conventional fuel tanks after minor modifications. Similar fuel supply and safety equipment with LNG are needed for methanol.

The moderate space and modification requirement on a ship and moderate increase at the engine efficiency is the advantage of methanol on LNG. Methanol with biofuel option has more advantages since it is carbon–neutral fuel. Also, there are other production methods by using renewable electricity and carbon capture from the atmosphere or waste CO_2 which is called electrofuel (Verhelst et al. 2019).

4.4 Methanol at Maritime Transportation

Methanol is one of the promising alternative fuels at the maritime transportation and maritime projects, and commercial applications are in increasing trend. This section

gives recent information about maritime rules and regulations for methanol as a fuel for ships, marine projects, and commercial applications of methanol on ships.

4.4.1 Maritime Rules and Regulations for Methanol as a Fuel for Ships

IMO has prepared and implemented maritime rules and regulations for the ships doing worldwide trade. It has also had studies about rules for the usage of alternative fuels on ships. The International Code of Safety for Ships Using Gases or Other Low-Flashpoint Fuels (IGF Code) has been effective since January 2017. The IGF Code aims to determine an international minimum standard for ships using gas fuels or low-flashpoint liquids as a fuel. The Code contains mandatory criteria for the design and installation of machinery, equipment, and systems for ships using gases or other low-flashpoint fuels (IMO Web Site 2020). Firstly, the Code has concentrated on LNG, but the draft guidelines for the safety of ships using methyl/ethyl alcohol as fuel were prepared and sent to the Maritime Safety Committee for approval since these fuels are low-flashpoint fuels (IMO Web Site 2020).

In addition to the IMO rules, there are rules and guidelines of classification societies to standardize international maritime transportation. The classification societies do classification and statutory services of ships and help IMO about maritime safety and pollution prevention. They develop and apply their own rules, in addition to the IMO rules, and verify that the ships comply with the international and/or national regulations (International Association of Classification Societies (IACS) 2020). The classification societies determine their minimum standards which are usually higher than the IMO standards and check the structural hull strength, propulsion and steering systems, power generation, other auxiliary machinery systems, and ship safety systems. The classification societies have their own guidelines for methanol-fueled ships. The International Association of Classification Societies (IACS) members, DNV GL, and Lloyd's Register apply their own rules when they do the classification of these ships. DNV GL gives approval to the methanol-fueled ships by the certificate with the notation of LFL fueled (DNV GL 2014) and Lloyd's Register with the notation of LFPF (GF, ML) (Lloyd's Register 2019).

4.4.2 Marine Methanol Projects and Commercial Applications

Various methanol projects at the maritime industry have been done until now. The project subjects change from different combustion concepts to risk assessment of the use of methanol on ships. Besides, there are commercial applications now doing maritime trade. The section starts with the marine methanol projects.

METHAPU (2006–2010)

METHAPU was an EU project with 6 project partners. The project aimed to assess the maturity of methanol technology on a commercial vessel, validation of methanol solid oxide fuel cell (SOFC) technology, determination of the technical requirements of the use of methanol on commercial vessels, assessment of short-term and long-term environmental impacts, and determination of the future research pathways for methanol SOFC for larger ships (European Commission 2020).

EffShip (2009–2013)

EffShip was the Swedish-based project. The aim of the EffShip was to find the best solution to comply with SO_X and NO_X limits in the short-term and GHG reduction targets in the medium term and long term (Andersson and Salazar 2015). Various technologies and marine fuels were evaluated. Methanol was found as the best alternative fuel with its advantages of availability, existing infrastructure, price, easy application to a ship, and maturity of the system (Fagerlund and Ramne 2013).

e4ships and Pa-X-ell (2009–2016)

The e4ships project was funded by the German government. The aim of the project was to develop the most advanced and largest methanol fuel cell. The Pa-X-ell project was the subproject of e4ships. It focused on the application of the methanol fuel cell on a ferry named Mariella (Maritime Knowledge Center (MKC) 2018).

CleanShip (2010–2013)

CleanShip focused on clean shipping in the Baltic Sea. The ports in the Baltic Sea and the shipowners whose ships were operating in the Baltic Sea involved in the project. Methanol was considered as a possible alternative fuel for clean shipping in the Baltic Sea. Also, a methanol fuel cell as an auxiliary engine was tested in the project (Andersson and Salazar 2015; Paulauskas and Lukauskas 2013).

SPIRETH (2011–2014)

SPIRETH had commenced between 2011 and 2014. The aim of the project was to observe the laboratory test results of methanol and dimethyl ether (DME) from methanol use on a marine diesel engine (Andersson and Salazar 2015). In addition to this, the project contributed to the IMO's draft IGF Code by the risk and safety analysis in the project. The findings showed that methanol is a promising alternative fuel for the Nordic region and the Baltic Sea (Maritime Knowledge Center (MKC) 2018).

PILOT Methanol (2014–2015)

The PILOT Methanol project is a ship conversion and operation of the Ro-Pax ferry Stena Germanica. The ship was converted to the dual-fuel operation with methanol and diesel. Stena Germanica was the first methanol-fueled ship. The methanol fuel conversion requirements and procedures on a ship were determined, and a bunkering facility was formed. Besides, this project assisted in the regulation development

for the methanol fuel operation both on a ship and during bunkering (Andersson and Salazar 2015). The ship conversion was completed in April 2015, and she has operated since that date.

SUMMETH (2015–2017)

The SUMMETH project aimed to test and evaluate different methanol combustion concepts, including spark-ignition (SI) and compression ignition (CI) concepts, for the smaller engines (between 250 and 1200 kW), to investigate the total GHG reduction potential of methanol as a marine fuel, determine the conversion requirements for a ship, and assess the requirements for transport, distribution, and sustainable production of methanol for the maritime industry (SUMMETH 2020). The project partners were Lund University, Farjerederiet Trafikverket, Marine Benchmark, ScandiNAOS, Scania, Svenskt Marintekniskt Forum, SSPA, VTT, and the project was financed by Swedish Maritime Administration, Methanol Institute, Vastra Götalandsregionen, and Oiltanking.

MethaShip (2015–2017)

The project partners Meyer Werft, Lloyd's Register, and Flensburger Schiffbau-Gesellschaft involved in the MethaShip funded by the German government. The aim of the project was the assessment of the feasibility of new-building methanol-fueled ships. There were two cruise ships and Ro-Pax ferry designs developed as the project output (Andersson and Salazar 2015).

LeanShips (2015–2019)

LeanShips was an EU Horizon 2020 project with 49 partners. This project had different work packages, and one of them was "The potential of methanol as an alternative fuel." In this work package, a high-speed marine diesel engine had been modified to operate with the methanol–diesel dual-fuel engine concept. The laboratory tests were focused on engine efficiency and emissions. The methanol–diesel dual-fuel operation had an improvement of 12% in brake thermal efficiency, and NO and soot emissions averagely reduced by 60 and 77% at all load range, respectively (LeanShips Project website 2020).

GreenPilot (2016–2018)

The GreenPilot project comprised Svenskt Marintekniskt Forum, SSPA, ScandiNAOS, the Swedish Transport Administration, and the Swedish Maritime Administration. The project focused on the conversion of small boats to the methanol-fueled boats and engine efficiency and emissions of the converted boat. The conversion requirements were determined, and various methanol combustion concepts were evaluated in the project (Maritime Knowledge Center (MKC) 2018).

The research and development projects in the maritime industry have increased the maturity of methanol fuel in maritime transportation. There are 10 methanol-fueled ships in operation and 6 in order recently. The first methanol-fueled ship is Stena Germanica that has operated since April 2015. Its operation resulted in 3–5 g/kWh NO_X emission, below 1 g/kWh CO and THC emissions, low PM emission

from pilot MGO, and 99% SO_X reduction with higher engine efficiency (Stefenson 2016). Waterfront Shipping ordered three methanol dual-fuel chemical tankers and they started to operate them in April 2016 (Maritime Knowledge Center (MKC) 2018). These ships were the first new-building methanol-fueled ships in history. The ships can operate with methanol, fuel oil, marine diesel oil, or gas oil. After these pioneers, the methanol-fueled ship fleet has been in increasing trend.

4.5 Methanol Properties and Combustion Concepts

This section approaches methanol properties from the aspect of maritime transportation and explains the important fuel properties on ships. Besides, possible methanol combustion concepts for marine diesel engines are mentioned and compared.

4.5.1 Methanol Properties from the Aspect of Maritime Transportation

Methanol has been one of the top five produced chemicals worldwide (Independent Commodity Intelligence Services (ICIS) 2017), with an annual production capacity of about 95 million tons (Nash 2015) that includes the production of 20 million tons as a fuel or fuel blend (Landälv 2017). Methanol can be produced from fossil fuel sources, mostly from natural gas and coal, or renewable sources. It can also be produced from any carbonaceous sources including wood, agricultural, and municipal waste (Yao et al. 2017). This type of methanol is biomethanol. It is stated that biomethanol can reduce GHG emissions significantly compared to methanol from fossil fuels (Maritime Knowledge Center (MKC) 2018). Additionally, there is methanol that is produced by using renewable electricity, and carbon capture from the atmosphere or waste CO_2 is called electrofuel (Verhelst et al. 2019). Methanol from renewable sources is a way for sustainable maritime transportation with 100% renewable fuels (Andersson and Salazar 2015).

Methanol has been considered as a fuel option since the 1970s, and it was used as a motor fuel until the mid-1990s. Methanol constitutes a 7–8% transportation fuel pool of China, and up to 3% of methanol blend to gasoline is permitted in European countries (Aakko-Saksa et al. 2020). Nowadays, methanol is also one of the promising alternative fuels to conventional ones in maritime transportation. Table 4.8 shows methanol properties.

Emissions

Methanol has the chemical formula of CH_3OH. It has a high H/C ratio, and it does not form particulate matter since methanol is not a long-chain hydrocarbon (Verhelst et al. 2019). If molar mass and lower heating value (LHV) of methanol are considered,

Table 4.8 Properties of methanol (Verhelst et al. 2019)

Specifications	Methanol
Chemical formula	CH_3OH
RON	107–109
MON	92
H/C	4
O/C	1
LHV (MJ/kg)	19.9
A/F_S	6.45
Density (kg/m^3)	790
Vapor density (kg/m^3)	1.42
Boiling point at 1 bar (°C)	65
Heat of vaporization (kJ/kg)	1100
Dynamic viscosity (20 °C) (mPas)	0.57
Molecular weight (kg/kmol)	32.04
Oxygen content by mass %	49.93
Hydrogen content by mass %	12.58
Carbon content by mass %	37.48
Auto-ignition temperature (°C)	465
Flashpoint (°C)	12
Adiabatic flame temperature (°C)	1870

methanol emits 20% less CO_2 emission while its combustion when compared with diesel with similar engine efficiencies (Maritime Knowledge Center (MKC) 2018). Another report states that methanol combustion in an internal combustion engine results in an approximately 10% reduction at CO_2 emission compared with heavy fuel oil (HFO) or distillate fuel (Gl 2019). The oxygen atom in the methanol molecule promotes more efficient combustion with lesser air requirement that lowers CO_2 and PM emissions. Alcohol fuel, methanol, decreases soot emissions by the assist of the oxygen atom. Methanol combustion has reduced combustion temperature that offers lesser NO_X formation down to IMO Tier III Limit (Andersson and Salazar 2015). Using methanol in diesel engines is a promising way to reduce both soot and NO_X emissions together (Tuner 2015). The sulfur-free structure of methanol results in no SO_X emission from the methanol combustion, and a ship can comply with the new IMO sulfur emission cap. In addition to this, methanol combustion on diesel engines can reduce polycyclic aromatic hydrocarbons that are the main reason for diesel fuel toxicity (Wuebben 2016).

Efficiency

Liquid fuels absorb heat energy from inside of the cylinder after the injection during the evaporation event. This is called the heat of vaporization (kJ/kg). Methanol has almost 4 times higher heat of vaporization than the diesel fuel (Maritime Knowledge

Center (MKC) 2018). It means methanol absorbs more heat energy to vaporize and it results in a charge cooling effect and a lower in-cylinder temperature. Methanol combustion has a lower heat transfer loss, lower compression work, and higher engine efficiency related to the charge cooling effect (Shamun et al. 2018; Zincir et al. 2019a). Also, it raises the intake air density and volumetric efficiency of the engine (Verhelst et al. 2019). According to the MIT researchers, a diesel engine can be downsized from a 9-L engine to a 5.5-L engine and 30% more engine power with the use of methanol (Wuebben 2016). Besides, the charge cooling effect of methanol reduces NO_X emission since the combustion temperature is lower than the diesel fuel combustion. The use of methanol at maritime transportation brings more efficient and emission regulation compliant marine diesel engines in operation which will contribute to sustainable maritime transportation.

Unique properties

Methanol has other unique properties. Methanol has a significant molar expansion that increases in-cylinder pressure at the time of the combustion event without additional heat (Tuner 2015). Methanol is a high octane fuel that causes high auto-ignition resistance. On the other hand, the cetane number of methanol is low. Methanol has a higher laminar flame velocity than the conventional fuels that provide faster combustion, lower heat loss to the cylinder walls, and higher engine efficiency. The high octane and low cetane number of methanol make it an unsuitable fuel for compression ignition engines, but it can be burnt by doing hardware changes or/and fuel reforming (Maritime Knowledge Center (MKC) 2018). Methanol has low lubricity due to its lower kinematic viscosity. It has lower kinematic viscosity than diesel, so lubrication additives have to be used with methanol to prevent corrosion at injection pumps, injectors, and other fuel system equipment (Tuner 2015). Methanol is highly corrosive to some materials. The polar structure of methanol brings dry corrosion on the materials (Verhelst et al. 2019). Metals including zinc, copper, lead, aluminum, magnesium and elastomers, plastics, and rubber are extremely affected by methanol (Methanol Institute, Compatibility of metals & alloys in neat methanol service; Methanol Institute, Compatibility of elastomers in neat methanol service).

Safety on a ship

IMO indicates that marine fuels have to have a flashpoint higher than 60 °C on a ship (International Maritime Organization (IMO) 1974). Methanol is one of the low-flashpoint fuels. It has a flashpoint of 12 °C, and additional safety precautions have to be taken on a ship. Similar safety precautions to LNG-fueled ships are applied for the methanol-fueled ships. Besides its low flashpoint, methanol has an invisible flame and quite wide flammability limits between 6.7 and 36%. Although there are some considerations about the methanol safety on a ship, methanol vapor is heavier than air and methanol fire can be extinguished with water (Aakko-Saksa et al. 2020). High auto-ignition temperature reduces the risk of self-ignition or explosion of methanol. Other than its low flashpoint, methanol is in liquid at ambient temperature and pressure, and almost similar to HFO, and similar handling and safety practices could be applied (Andersson and Salazar 2015).

Storage and fuel operation on a ship

Methanol has similar physical properties to conventional marine fuels, such as HFO, and it can be stored at the same bunker tanks after minor modifications (Andersson and Salazar 2015; Stocker 2018; Zincir et al. 2019b). This means requirements for methanol storage tanks, equipment, and procedures are lesser than the LNG storage and have reduced capital cost. Additionally, since methanol is infinitely miscible in water, it is not harmful to the environment and can be stored in the double hull bottom of the ship (Verhelst et al. 2019; Landälv 2017). The LHV of methanol is less than half of the LHV of diesel; therefore, roughly twice the tank volume of the conventional fuel storage tank is required for the same distance of navigation. But the double hull bottom storage opportunity of methanol is an advantage for methanol storage on a ship. Lower LHV of methanol also affects the fuel injection capacity. New injectors with a higher fuel flow rate have to be used to provide the same engine power as conventional fuels.

Environmental impact

Methanol can be assumed as environmentally friendly fuel. Fuel spillages from ships are important environmental incidents for marine ecology. Methanol is biodegradable and has a short half-life time (1–6 days) in ground and water (Aakko-Saksa et al. 2020). Methanol dilutes quickly in water and breaks down into CO_2 and water (Landälv 2017). The methanol spillage forms less ecological threat; on the other hand, it can increase sea vegetation (Maritime Knowledge Center (MKC) 2018). Besides, when methanol is compared with LNG, the vapor slip of methanol does not increase the GHG effect.

Impact on health

Methanol is toxic for human beings and causes blindness when it is ingested as 10 mL and is fatal when it is ingested 60–100 mL. Methanol is also dangerous if a person uptakes methanol through the skin and by inhalation (Aakko-Saksa et al. 2020). Methanol is odorless below 2000 ppm in air, so when it is used as a fuel on a ship, the fuel system has to be completely closed-off, the ventilation system has to be placed, and nobody has to touch methanol (Andersson and Salazar 2015). Although it is toxic, it does not have a cancerous effect contrary to diesel.

Methanol is a significant alternative marine fuel which promises good combustion properties, high engine efficiency, low engine emissions, and low environmental impact when its spillage or vapor slip to the atmosphere. Drawbacks of methanol are low LHV, larger storage tanks than the conventional fuels, and toxicity.

4.5.2 *Methanol Combustion Concepts on Marine Diesel Engines*

The internal combustion engines convert chemical energy of the fuel to mechanical energy by the combustion of fuel as a thermodynamic process. Fuel properties are an important aspect of the combustion event. The properties of methanol and their effects on the combustion event were mentioned in the previous section. Besides the fuel properties, fuel combustion strategy compatibility is also crucial for high engine efficiency and low emission formation. There are three main combustion strategies for internal combustion engines. These are compression ignition (CI), spark ignition (SI), and homogenous charge compression ignition (HCCI). Three main combustion strategies form a combustion strategy triangle, and they are the corner points of the triangle (Johansson 2016). In addition to the main combustion strategies, there are intermediary combustion strategies between three main combustion strategies which are suitable to combust methanol in a diesel engine. The intermediary combustion strategies are dual-fuel combustion, direct injection spark ignition (DISI), reactivity-controlled compression ignition (RCCI), and partially premixed combustion (PPC). Figure 4.1 shows the combustion concepts for methanol. Since the book section focuses on marine diesel engines, the combustion strategies for the marine diesel engines will be discussed.

4.5.2.1 Methanol–Diesel–Additive Emulsion (MD95) Combustion Strategy

Before explaining the intermediary combustion strategies, a methanol-additive emulsion combustion strategy should be mentioned. It is a combustion strategy that can be applied during conventional CI combustion. This strategy uses 95% methanol and 5% diesel with the ignition improver as a fuel emulsion (Ellis et al. 2018). MD95 combustion strategy uses a very high compression ratio (28:1) to burn methanol, and the ignition improver also promotes the combustion. There are studies on Scania heavy-duty

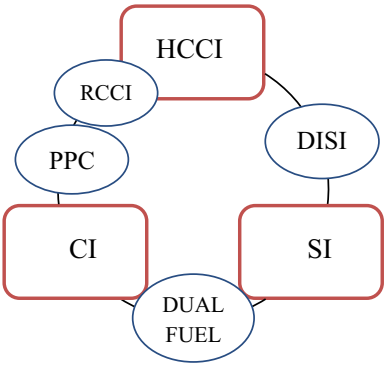

Fig. 4.1 Scheme of the combustion concepts (figure reproduced and adapted) (Zincir 2019; Johansson 2016)

engines with MD95 (Aakko-Saksa et al. 2020; Ellis et al. 2018). This combustion strategy can be used on smaller ships, but the main issue is high compression ratio and material durability in the long-term.

4.5.2.2 PFI-SI Methanol Combustion Strategy

PFI-SI means port fuel injection—spark-ignited combustion strategy. It is a combustion strategy similar to the conventional SI engines, but it can be applied to diesel engines. The diesel engine is modified to run as a SI and PFI engine. Methanol injected into the intake manifold and air–fuel mixture enters into the cylinder. And then, the mixture is ignited by a spark plug. In a study, the NO_X emission complied with the IMO Tier III Limit, and almost zero emission was recorded with similar engine efficiency and torque to a conventional CI (Ellis et al. 2018).

4.5.2.3 HCCI Combustion Strategy

HCCI, homogeneous charge compression ignition, combustion strategy is the third main combustion strategy. It is one of the first low-temperature combustion strategies (Lönn 2019). The HCCI is comparable to the SI engine, the mixture of fuel and air enters into the cylinder, and the combustion event is initiated by the raised pressure and temperature during the compression stroke.

The combustion starts in different areas in the combustion chamber at the same time and can be called a distributed reaction (Johansson 2016). Actually, in contrary to the strategy name, the combustion event is not homogenous; there are fast-burning zones and slow-burning zones in the combustion chamber. The in-cylinder charge is diluted to keep the reactivity speed to prevent high PRR and peak in-cylinder pressure during the combustion event (Zincir 2019). This brings low-temperature combustion that results in high engine efficiency and low soot and NO_X emissions (Tuner 2015). There are disadvantages of the HCCI which are difficulties in the combustion control, low power production range, high PRR, high HC, and CO emissions (Zincir et al. 2019a; Lönn 2019). The disadvantages of the HCCI limit commercial using of this combustion strategy.

4.5.2.4 Dual-Fuel Combustion Strategy

Dual-fuel combustion strategy, one of the intermediary combustion strategies, uses two different fuels that one of them has a higher cetane and lower octane than the other one. The main fuel is methanol as a high octane fuel, and the pilot fuel is diesel as a low octane and high cetane fuel. Methanol can be injected into the port or directly into the cylinder. Diesel is injected into the cylinder on to the methanol–air mixture in the cylinder and ignites the mixture (Tuner 2016). The pilot fuel amount for igniting the methanol–air mixture can be low as 1–2% of the total fuel (Johansson 2016). The

timing of the combustion event is determined by the diesel injection timing, and the methanol–air mixture is burned with flame propagation similar to SI engines (Zincir 2019).

Large marine diesel engine applications use this combustion strategy. Two top marine diesel engine manufacturers, MAN and Wartsila, have commercial methanol–diesel dual-fuel marine diesel engine applications on various ships, such as Stena Germanica and several tankers of Waterfront Shipping.

4.5.2.5 RCCI Combustion Strategy

Reactivity-controlled compression ignition (RCCI) combustion strategy comprises two different fuels with different octane numbers in various amounts to provide an optimum combustion event. This combustion strategy is similar to the dual-fuel strategy. High octane fuel is injected into the intake port and is premixed with air while low octane fuel is injected directly into the cylinder. Also, it is similar to the HCCI combustion strategy since the RCCI uses dilution and low-temperature combustion like the HCCI (Tuner 2015). The high engine efficiency, 60%, has been reported (Splitter et al. 2013), and similar emission characteristics to the HCCI combustion strategy have been achieved. Although the RCCI has high engine efficiency, this combustion strategy is impractical due to the two fuel tanks and fuel supply systems to the diesel engine.

4.5.2.6 DISI Combustion Strategy

Direct injection spark ignition (DISI) is a combustion strategy between SI and HCCI. Methanol is combusted by a spark plug mounted to the cylinder head of diesel engines. The combustion event started the same as SI engines with flame propagation and ends with similar to the HCCI combustion strategy. The in-cylinder mixture should be suitable for proper flame propagation and also be diluted to slow down the auto-ignition process (Johansson 2016). To heat the in-cylinder mixture, negative valve overlaps are often used to hold residual gases in the cylinder and the spark plug ignited the diluted in-cylinder mixture (Li 2018). The engine efficiency of more than 51% can be achieved with a stratified late injection of methanol in the DISI combustion strategy (Björnestrand 2017). But the operation range is narrow between the knock and misfire during the stratified combustion.

4.5.2.7 PPC Combustion Strategy

Partially premixed combustion (PPC) is a combustion strategy combining conventional CI and HCCI combustion strategies. The main principle of PPC is the separation of the start of combustion and end of injection (Tuner 2016). The aim of a comparatively earlier injection of methanol than the conventional CI during the

compression stroke is to constitute a partially homogenous air–fuel mixture in the cylinder before the combustion event. The combustion event starts with a stratified charge, but it is not diffusion-controlled, spray-driven combustion (Johansson 2016). The PPC strategy has simple combustion control, low NO_X and soot emissions, and good engine efficiency (Zincir et al. 2019a, b). Methanol has a high burning rate at the PPC strategy that leads to reduced heat transfer losses and lowers NO_X emission since high-temperature combustion period is lower (Shamun 2019). The PPC strategy achieved engine efficiency which was higher than 53% with methanol as a fuel (Shamun et al. 2017a). The split injection can be used to form an optimum combustion event with high engine efficiency and low engine emissions.

The methanol project named SUMMETH is one of the crucial projects for maritime transportation. Possible combustion strategies for marine diesel engines powered between the ranges of 250 and 1200 kW. The engine power range represents the main engine of small tonnage ships or auxiliary diesel engines for electricity generation on large ships. But this project is the only project that compares methanol combustion strategies for marine diesel engines in detail, so this study can also give an opinion about the marine engines larger than 1200 kW. Table 4.9 shows the compared methanol engine combustion strategies with additional after-treatment methods. There are more combustion strategies in the study (Ellis et al. 2018), but some of them are not included in the table. The alternative combustion strategies are compared with the conventional CI engine. The yellow color indicates a slightly higher or lower difference, the red color indicates a significantly higher or lower difference, and the green color indicates no difference during the comparison with the conventional CI engine.

Table 4.9 Comparison of methanol engine combustion strategies (Ellis et al. 2018)

Engine Type	Comparison Criteria of the Methanol Engine Combustion Strategies							
	Robustness	Efficiency	Power	Noise	HC	CO	NO_X	Soot
Conventional CI	B	B	B	B	B	B	B	B
MD95 with oxidation catalyst	-	S	-	S	S	S	+	+
MD95 with particulate filter / SCR	-	-	-	S	S	S	+	+
PFI-SI Lean burn	-	S	-	+	-	-	+	+
DISI Lean burn	-	+	-	+	-	-	+	+
Dual-fuel	-	-	-	+	-	-	S	+
DI Dual-fuel	S	S	S	S	-	-	+	+
PPC	-	+	S	-	S	S	+	+

(B = the baseline, − = worse than the baseline, + = better than the baseline, S = the same as the baseline)

The conventional CI engines have a robust operation; therefore, they are preferred to use at heavy duties, such as marine engines. The study compared the robustness of alternative combustion strategies. It can be seen that only DI dual-fuel strategy has the same robustness as the conventional CI engine. All other alternative combustion strategies, except PPC, have slightly lower robustness since these strategies can affect more from the start–stop operation and higher in-cylinder corrosion can be observed (Ellis et al. 2018). PPC has significantly lower robustness, due to its poor low load operation by the cycle-to-cycle in-cylinder pressure variation and sudden high pressure rise rates in the cylinder (Tuner 2015; Ellis et al. 2018).

The engine efficiency is only higher than the conventional CI at DISI lean burn and PPC concepts. PPC strategy has the highest engine efficiency in the study. There is an engine power reduction at all alternative combustion strategies, except DI dual fuel and PPC. The engine power is the same at these combustion strategies. The noise level is slightly higher at the PPC concept since the combustion is more aggressive (Ellis et al. 2018). The PFI-SI lean burn, DISI lean burn, and dual fuel have a lower noise level than the conventional CI.

It can be seen in Table 4.9 that the effect of the MD95 with particulate filter/SCR and PPC on the total emissions is higher than the other combustion concepts. They significantly reduced the NO_X and soot emissions, while HC and CO emissions remained the same as the conventional CI.

The study (Ellis et al. 2018) showed that the PPC strategy can achieve significantly higher engine efficiency than the conventional CI engines without a decline at the engine power. Also, this strategy can substantially reduce NO_X and soot emissions while HC and CO emissions remain the same. The only disadvantage of PPC is the lower robustness, due to its poor operation at the low loads. Although the previous studies (Tuner 2015; Ellis et al. 2018) indicated that the low load operation of the PPC strategy is problematic and results in high engine emissions, later studies (Zincir 2019; Zincir et al. 2019a, b) showed that the PPC strategy can operate well with high engine efficiency and low engine emissions. The next section will contain the findings of these studies.

4.6 The Methanol Partially Premixed Combustion Strategy for Maritime Transportation

The medium to high loads of the methanol PPC engines have been operated without any combustion issues and emission problems at the previous studies (Zincir 2019; Shamun et al. 2016, 2017a, b, 2018; Ellis et al. 2018). The methanol PPC strategy has shown high engine efficiency than the conventional CI engines with lower CO_2 and NO_X emissions. The sulfur-free structure of methanol does not emit SO_X emission, and the low-carbon chain structure of the methanol molecule extremely decreases PM emission formation. The measured PM emission at a methanol PPC study was 0.000004 g/kWh (Tuner et al. 2018), and another study states that the main reason for

the PM emissions is from the lubrication oil (Shamun et al. 2017a). The PM emission from the methanol PPC strategy can be assumed as zero, and this is an advantage for using EGR for further decrease of NO_X emission without PM emission trade-off. Otherwise, the low load methanol PPC is problematic due to the possibilities of poor combustion, engine stability problems, high CO, and unburned hydrocarbons. High octane fuels like methanol can cause combustion stability problems by its high auto-ignition resistance (Tang et al. 2017). Also, leaner in-cylinder air–fuel mixtures at the low load operation, which results in very long ignition delay, and retarded combustion phasing, occur combustion stability issues (An et al. 2018).

The methanol PPC was found as a promising combustion strategy in the previous section, except its significantly lower robustness when it is compared with a conventional CI engine. The studies (Tuner 2015; Ellis et al. 2018) indicate that the methanol PPC strategy has a poor operation and high engine emissions at the low load operation. The stable operation of methanol PPC with low engine emissions at medium to high loads has been proofed at the previous studies until now; for this reason only the low load operation will be discussed. This section will give some findings of previous low load studies to contradict these statements and proof that the methanol PPC can be an alternative combustion strategy for the marine engines at all engine loads.

4.6.1 Low Load Performance Comparison of the Conventional CI and Methanol PPC

Maritime transportation routes can be at either open seas or near coastal areas. Ship speed at open seas is at normal speeds, but nowadays reduced speed is used as an operational measure to decrease fuel consumption and mitigate CO_2 emission. This measure is called slow steaming that was proposed by the major shipping company, Maersk, in 2007 (Tezdogan et al. 2015). To reduce ship speed, the engine load is reduced to a certain level. According to MAN B&W, which is the marine engine manufacturer with the largest market share, the slow steaming can safely and reliably be done at below to a 10% engine load by taking necessary precautions (MAN, PrimeServ 2012).

The near coastal areas, such as straits, canals, and ports, are the other areas for the slow speed navigation. The main engine has to operate smoothly and with good combustion stability since these areas are dangerous and risky areas with shallow waters and close distance to the coastal lands. And this type of navigation forms an important part of the ship main engine operation. A study indicates that the low load operation of the main engine constitutes approximately 20% of the total engine operation of a ship (Baldi et al. 2013). In addition to this, emissions from the ships are a crucial problem for near coastal settlements. Maritime transportation activity near coastal areas increases health issues due to the raised harmful emissions, and vegetation areas are degraded.

The methanol PPC strategy can be a solution for greener shipping, especially in the near coastal areas. To find this, Zincir et al. (2019b) made a study about the low load operation of the methanol PPC strategy and the MGO-fueled conventional CI engine was compared. The experimental findings of the methanol PPC strategy are compared with the results of the empirical formulas of the conventional CI engine. The empirical formulas have been used in previous studies (Ammar 2019; Ammar and Seddiek 2017; EEA 2000). Detailed information about the formulas can be found in the study (Zincir et al. 2019b). The methanol PPC experiments were done at 2, 3, and 5 bar gross-indicated mean effective pressure (IMEP) which were assumed as 10, 15, and 25% load, respectively. The SFC, emissions, and efficiency of the engine fueled with marine gas oil were calculated by the empirical and theoretical equations in the study.

Engine performance

The engine performance criterion includes engine stability, gross-indicated efficiency (η_{GIE}), SFC, and specific energy consumption (SEC). The engine stability was measured by the coefficient of variation IMEP (COV IMEP). It is a term representing the stable engine operation, and the top limit is 5% (Przybyla et al. 2016). Equations (4.1)–(4.3) show how to calculate the COV IMEP.

$$\text{IMEP}_n = 1/V_{\text{d}} \int_0^{720} p\text{d}V \tag{4.1}$$

$$\overline{x} = 1/N \sum_1^N x_i \tag{4.2}$$

$$\text{COV IMEP} = \left(\sqrt{\sum_{i=1}^{N} (x_i - \overline{x})^2 / N} \right) / \overline{x} \cdot 100\% \tag{4.3}$$

where N is continuously sampled cycles during the experimental study ($N = 300$) and x_i is IMEP_n of a specific cycle.

Methanol is a high octane fuel that has a high auto-ignition resistance. To overcome this issue to combust methanol in diesel engines, intake air is heated to an optimum point. Intake temperature is one of the important intake parameters for high engine stability. The study showed that higher intake temperature results in more stable engine operation with reduced COV IMEP (Zincir et al. 2019a). The intake temperature was held constant at 150 °C to provide good engine stability.

The η_{GIE} of the methanol PPC strategy was calculated by Eq. (4.4), and the η_{GIE} of the MGO-fueled diesel engine was calculated by Eq. (4.5) (Klaus et al. 2013).

$$\eta_{\text{GIE}_{\text{MeOH}}} = \text{IMEP} / \text{FuelMEP} \tag{4.4}$$

$$\eta_{\mathrm{GIE_{MGO}}} = 3600/(\mathrm{LHV} \times \mathrm{SFC}) \tag{4.5}$$

The SFC for the methanol PPC strategy was derived from the experimental study, and the SFC of the MGO-fueled diesel engine was calculated by Eq. (4.6) (Ammar and Seddiek 2017; EEA 2000). The SEC is a measure in MJ/kWh basis which is calculated by Eq. (4.7) (Toolbax and (ETB) 2003).

$$\mathrm{SFC} = 14.1205/\ \%\ \mathrm{load}\ + 205.7169 \tag{4.6}$$

$$\mathrm{SEC} = (\mathrm{SFC} \times \mathrm{LHV})/1000 \tag{4.7}$$

The LHV of methanol is 19.9 and 42.8 MJ/kg for MGO at the SEC calculation.

The COV IMEP of methanol PPC strategy was below 5% at all low loads in the experimental study (Zincir et al. 2019b). It was 3.3%, 2.4%, and 1.4% from 10 to 25% engine load. The MGO-fueled diesel engine has been used for many years in maritime transportation, and there have not any engine stability issues at low load operation. The η_{GIE} of the methanol PPC and the MGO-fueled diesel is shown in Fig. 4.2.

It can be seen in the figure that the methanol PPC strategy has a higher η_{GIE} than the MGO-fueled diesel engine. η_{GIE} is 0.422, 0.459, and 0.463 at the engine loads 10%, 15%, and 25%, respectively, for the methanol PPC while it is 0.240, 0.280, and 0.320 at the same engine loads for the MGO-fueled diesel engine. The high heat of vaporization of methanol formed a cooling effect in the cylinder, reduced the maximum combustion temperature, lowered heat transfer loss, and also decreased

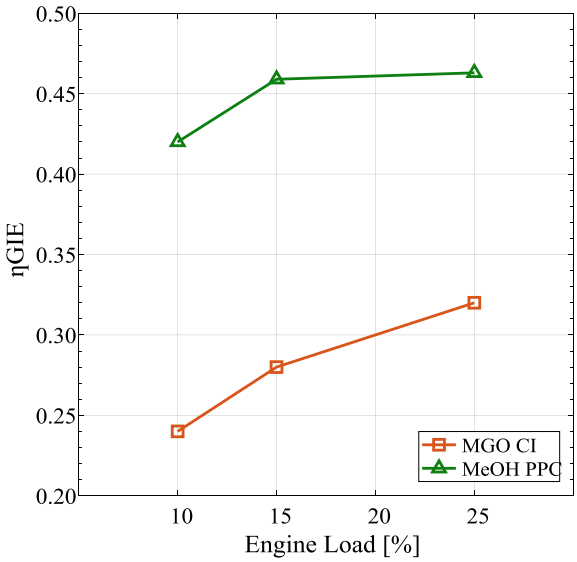

Fig. 4.2 Gross-indicated efficiency comparison of methanol PPC and MGO CI. Values are taken from Zincir et al. (2019b), and a new figure is formed

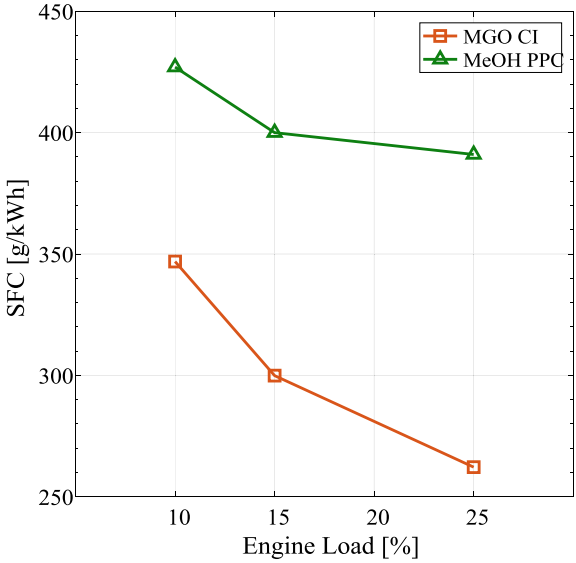

Fig. 4.3 Specific fuel consumption comparison of methanol PPC and MGO CI. (Values are taken from (Zincir et al. 2019b), and a new figure is formed)

compression work that resulted in higher engine efficiency than the MGO-fueled diesel engine. The methanol PPC has precedence over the MGO-fueled diesel engine at low load operations.

Another comparison between the methanol PPC strategy and the MGO-fueled diesel engine is the SFC comparison. Methanol has less than half of the LHV of diesel, so it is obvious that methanol has a higher fuel consumption. Figure 4.3 shows the SFC comparison of two fuels. The MGO-fueled diesel engine has the SFC of 347, 300, and 262 g/kWh, while the methanol PPC has the SFC of 427, 400, and 391 g/kWh from 10 to 25% engine load. The SFC seems higher at the methanol PPC strategy, but the SFC and the SEC should be considered together. Figure 4.4 shows the SEC comparison of both fuels. It can be seen that the methanol PPC strategy has the SEC of 8.5, 8.0, and 7.8 MJ/kWh while the MGO-fueled diesel engine has the SEC of 14.8, 12.8, and 11.2 MJ/kWh. Despite the higher SFC consumption of the methanol PPC, it has lower SEC consumption. This is because of the engine efficiency difference between two combustion strategies at the low load operation. Higher engine efficiency of the methanol PPC strategy provides lower energy required to provide the same engine load. Again, it is proofed that the methanol PPC concept is a promising tool for the stable and efficient combustion at the low load operation of the marine diesel engines.

Engine emissions

The regulated emissions in maritime transportation are CO_2, NO_X, SO_X, and PM emissions. The study (Zincir et al. 2019b) compares emissions of the methanol PPC strategy and the MGO-fueled diesel engine. The emissions of the methanol PPC strategy, except SO_X and PM emissions, were measured during the experiments. On

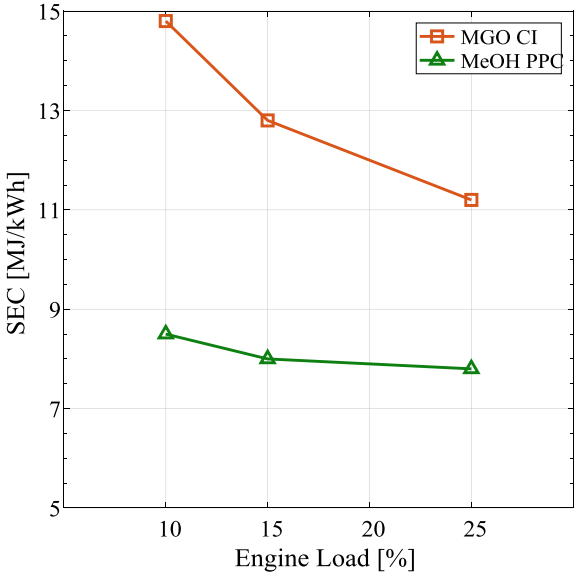

Fig. 4.4 Specific energy consumption comparison of methanol PPC and MGO CI. (Values are taken from (Zincir et al. 2019b), and a new figure is formed.)

Table 4.10 Emission factor coefficients (Revised from Zincir et al. 2019b)

Coefficient	NO_X	SO_X	PM	CO_2
a	0.1255	2.3735	0.0059	44.1
z	1.5	n/a	1.5	1.0
b	10.4496	−0.4792	0.2551	648.6

the other hand, the emissions of the MGO-fueled diesel engine were calculated by the empirical formulas. Equations (4.8) and (4.9) with the coefficients in Table 4.10 were used to calculate the emissions (Zincir et al. 2019b; Ammar 2019; Ammar and Seddiek 2017; ICF 2009).

$$E = a(\%\text{load})^{-z} + b \tag{4.8}$$

$$E_{SO_x} = a(\text{SFC} \times S\%) + b \tag{4.9}$$

where a, z, and b are the emission factor coefficients. $S\%$ is the fuel sulfur fraction that was taken as 0.1% to represent low-sulfur marine gas oil (LSMGO) and comply with the new sulfur regulation limit.

The specific CO_2 emissions of the methanol PPC strategy and the MGO-fueled diesel engine are shown in Fig. 4.5. The specific CO_2 emissions of the MGO-fueled diesel engine are 1112, 961, and 841 g/kWh, while it is 587, 550, and 520 g/kWh for methanol PPC at 10%, 15%, and 25% engine load, respectively. CO_2 emission is related to fuel consumption and the carbon content of the fuel. Although the methanol

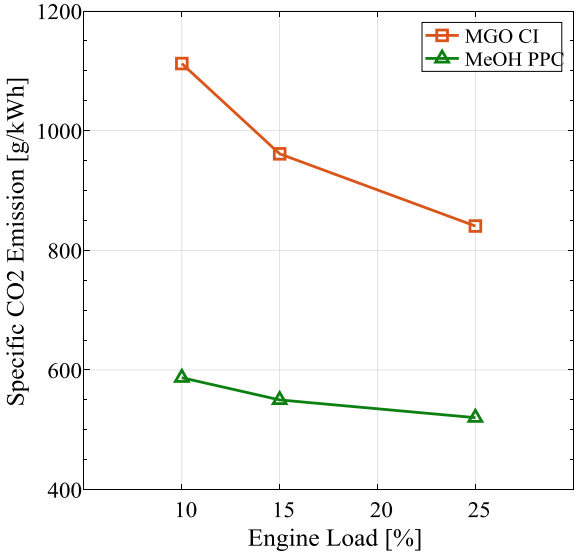

Fig. 4.5 Specific CO_2 emissions of methanol PPC and MGO CI. Values are taken from (Zincir et al. 2019b), and a new figure is formed

PPC strategy has a higher SFC than the MGO-fueled diesel engine, the carbon content of methanol is lower than MGO. The carbon content of methanol is 37.5%, while it is 85.7% for the MGO (Systems and (GCS) 2019). Besides, the methanol PPC engine efficiency is higher than the MGO-fueled diesel engine which results in lower CO_2 formation.

Figure 4.6 shows NO_X emissions of the methanol PPC strategy and the MGO-fueled diesel engine. The MGO-fueled diesel engine has the NO_X emission of 14.4,

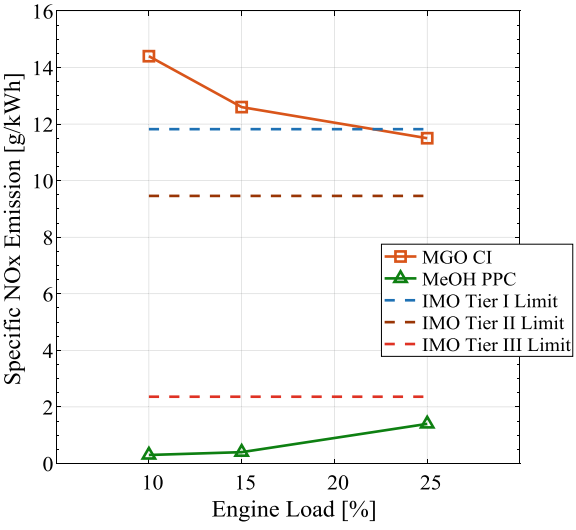

Fig. 4.6 Specific NO_X emissions of methanol PPC and MGO CI. Values are taken from Zincir et al. (2019b), and a new figure is formed

12.6, and 11.5 g/kWh from 10 to 25% engine load, respectively. The engine was considered operating at 800 rpm which was the same as the experimental studies with the methanol PPC. The IMO Tier I Limit is 11.8 g/kWh for the engine at 800 rpm. The MGO-fueled diesel engine does not fulfill with even the IMO Tier I Limit at 10 and 15% engine loads. However, the methanol PPC concept complies with the IMO Tier III Limit of 2.4 g/kWh. The NO_X emissions are 0.3, 0.4, and 1.4 g/kWh between 10 and 25% engine loads. The NO_X formation depends on high in-cylinder temperature. The high heat of vaporization of methanol decreases maximum combustion temperature, and it results in a lower NO_X formation. Also, the methanol PPC strategy has a shorter burn duration which means the maximum in-cylinder temperature period is shortened. The methanol PPC strategy complies with the recent NO_X emission limit at the low load operation without any after-treatment system.

The SO_X emission from the marine engines is more important after the new IMO Sulfur Cap regulation entered into force on January 1, 2020. Methanol has a sulfur-free structure that does not emit SO_X emission. It is naturally the SO_X emission regulation compliant fuel. Figure 4.7 shows the SO_X emission comparison of the methanol PPC strategy and the MGO-fueled diesel engine. The methanol PPC plot is drawn as zero at all loads in the study. The MGO in the study (Zincir et al. 2019b) was assumed as LSMGO (0.1% sulfur in the fuel) and complied with the sulfur regulation. The specific SO_X emission of the MGO-fueled diesel engine is 0.34, 0.23, and 0.14 g/kWh between 10 and 25% engine loads, and complies with the SO_X ECA Limit. Figure 4.8 shows the specific PM emissions of methanol PPC strategy and MGO-fuelled diesel engine. Methanol fuel does not emit PM emission due to its sulfur-free structure. The PM emission has the same ECA and non-ECA limits. It can be seen that the MGO-fuelled diesel engine does not comply with the PM

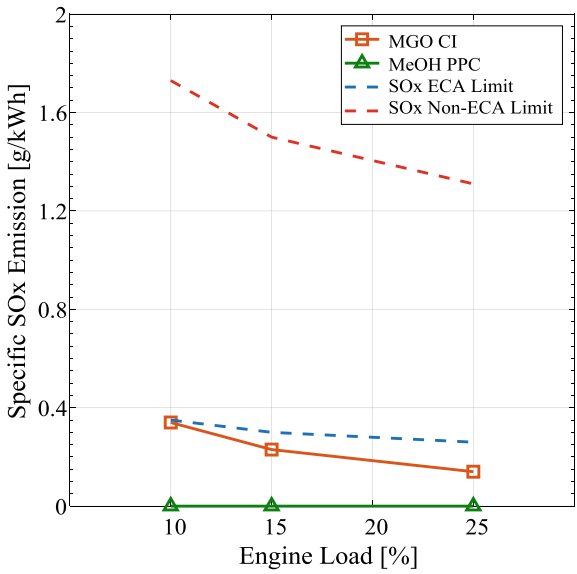

Fig. 4.7 Specific SO_X emissions of methanol PPC and MGO CI. Values are taken from Zincir et al. (2019b), and a new figure is formed

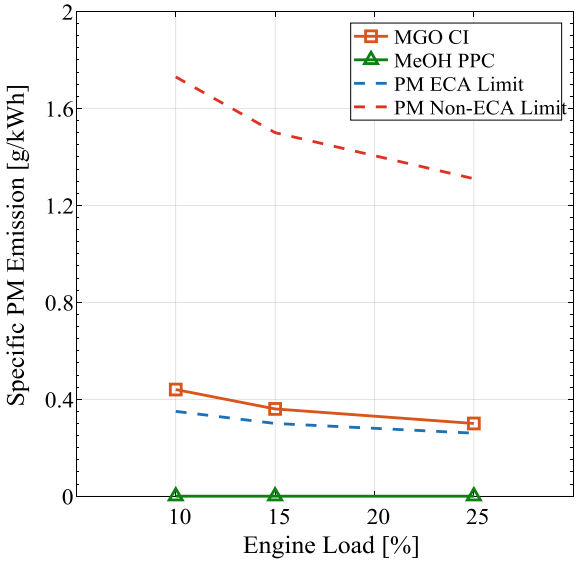

Fig. 4.8 Specific PM emissions of methanol PPC and MGO CI. Values are taken from Zincir et al. (2019b), and a new figure is formed

ECA limit. The MGO-fueled diesel engine has the PM emissions of 0.44, 0.36, and 0.30 g/kWh which are above the PM ECA limit of 0.35, 0.30, and 0.26 g/kWh at 10%, 15%, and 25% engine load.

The methanol PPC strategy proved itself at medium to high engine load at the previous studies. Also, it showed good emission performance when it was compared with the MGO-fueled diesel engine at the low load operation. Methanol has lower carbon content than the MGO, and the PPC strategy has higher gross-indicated efficiency that resulted in lower CO_2 emission than the MGO-fueled diesel engine. The NO_X emission was lower than the IMO Tier II Limit for the methanol PPC strategy, and the sulfur-free structure of methanol does not emit SO_X and PM emissions. The methanol PPC strategy is a promising fuel combustion strategy combination for the marine engines at the low load operation.

4.7 Summary

This chapter covered the status of maritime transportation, international maritime rules and regulations, emission mitigation technologies and methods on ships, methanol at maritime transportation, methanol properties, and combustion concepts, and the methanol partially premixed combustion strategy for maritime transportation.

Maritime transportation is an important way to perform international trade. It constitutes 90% of worldwide trade by 96,295 ships in various tonnages. Ships consume a huge amount of fuel and emit a high level of pollutants to the atmosphere. To decrease shipboard emissions, IMO has been working on international maritime

emission rules and regulations. The international maritime emission rules and regulations are becoming stricter day by day. The chapter gave detailed information about recent rules and regulations about CO_2, NO_X, SO_X, and PM emissions. Emission mitigation technologies and methods have been used to comply with the recent rules and regulations. There are design measures, engine and engine room machinery modifications, operational measures, and new technologies to reduce CO_2 emissions from ships, and pre-combustion, combustion intervention, and after-treatment methods to decrease NO_X emissions from ships. SO_X emissions are mitigated by using low-sulfur conventional fuels, SO_X scrubbers, or sulfur-free alternative fuels. Alternative fuels can reduce all types of emissions at once without any other methods. The most popular alternative fuels at maritime transportation are LNG and methanol. Methanol was compared with LNG and some emission mitigation technologies and was found as the most promising emission mitigation element.

Maritime-based methanol projects and methanol-fueled commercial applications are in increasing trend. The IGF Code entered into force in January 2017 by IMO. The Code contains mandatory criteria for the design and installation of machinery, equipment, and systems for ships using gases or other low-flashpoint fuels, such as methanol. There are also the classification society rules and guidelines for methanol.

Methanol emits low CO_2 and NO_X emissions and zero SO_X and PM emissions. This is important to comply with the recent international emission rules and regulations. Methanol provides higher engine efficiency than diesel thanks to its unique properties. Methanol has similar physical properties to conventional marine fuels, and it can be kept at the same bunker tanks after minor modifications. The only disadvantage is its LHV is less than half of the LHV of diesel, so double the onboard storage volume of the conventional fuel is required for the same distance. Methanol is environmentally friendly because it is biodegradable and does not give much damage to sea ecology. On the other hand, it is toxic for humans, and the ship crew has to be careful during the methanol operation.

Methanol can be combusted at diesel engines by various combustion strategies. The most promising combustion strategy is PPC. This strategy can provide higher engine efficiency than the conventional CI with no power reduction. Besides, it can reduce NO_X and soot emissions while HC and CO emissions remain the same. The methanol PPC strategy proved itself at medium to high engine loads. The only drawback according to the previous studies is lower robustness than the conventional CI, because of its poor low load performance. But it was shown in the chapter that the methanol PPC can be operated at the low loads with good engine stability of 3.3%, 2.4%, and 1.4%, high engine efficiency (0.422, 0.459, and 0.463) than the conventional CI (0.240, 0.280, and 0.320) at the engine loads 10%, 15%, and 25%, respectively.

The MGO-fueled diesel engine has the SFC of 347, 300, and 262 g/kWh, while the methanol PPC has the SFC of 427, 400, and 391 g/kWh at the same engine loads. On the other hand, the SEC of the methanol PPC is lower than the MGO-fueled diesel engine with 8.5, 8.0, and 7.8 MJ/kWh while it is 14.8, 12.8, and 11.2 MJ/kWh at the same engine loads. Although the SFC is higher at the methanol PPC, the high engine efficiency provides lower SEC.

The methanol PPC strategy has lower emissions than the MGO-fueled diesel engine, which complies with IMO Tier III Limit and IMO Sulfur Cap. The methanol PPC strategy has 587, 550, and 520 g/kWh CO_2 emissions and 0.3, 0.4, and 1.4 g/kWh NO_X emissions, while the MGO-fueled diesel engine has 1112, 961, and 841 g/kWh CO_2 emissions and 14.4, 12.6, and 11.5 g/kWh NO_X emissions at 10%, 15%, and 25% engine load, respectively. The SO_X and PM emissions are zero for the methanol PPC strategy.

Methanol is one of the promising alternative fuels for maritime transportation and the usage of methanol as a fuel will be increased in the future. Using biomethanol will further decrease CO_2 emissions drastically. In addition to this, the PPC strategy can be used at the marine engines with methanol to provide high engine efficiency and low engine emissions.

References

Aakko-Saksa PT, Westerholm M, Pettinen R, Söderström C, Roslund P, Piimakorpi P, Koponen P, Murtonen T, Niinistö M, Tuner M, Ellis J (2020) Renewable methanol with ignition improver additive for diesel engines. Energy Fuels 34:379–388

Adland R, Cariou P, Jia H, Wolff F (2018) The energy efficiency effects of periodic ship hull cleaning. J Clean Prod 178:1–13

Akker JT (2017) Carbon capture onboard LNG-fueled vessels, a feasibility study. MSc. Thesis, Marine Technology, Delft University of Technology, The Netherlands

American Society of Civil Engineers (ASCE) (2014) Carbon capture and storage. https://ebookcentral.proquest.com/lib/itup/detail.action?docID=3115707

Ammar NR (2019) An environmental and economical analysis of methanol fuel for a cellular container ship. Transp Res Part D 69:66–76

Ammar NR, Seddiek IS (2017) Eco-environmental analysis of ship emission control methods: case study RO-RO cargo vessel. Ocean Eng 137:166–173

Andersson K, Salazar CM (2015) Methanol as a marine fuel report. FCBI Energy

Andreoni V, Miola A, Perujo A (2008) Cost effectiveness analysis of the emission abatement in the shipping sector emissions. JRC Sci Tech Rep. EUR 23715 EN-2008. https://doi.org/10.2788/77899

An Y, Jaasim M, Raman V, Perez FEH, Sim J, Chang J, Im HG, Johansson B (2018) Homogenous charge compression ignition (HCCI) and partially premixed combustion (PPC) in compression ignition engine with low octane gasoline. Energy 158:181–191

Bakhtov A (2019) Alternative fuels for shipping in the Baltic sea region. Baltic Marine Environment Protection Commission Report

Baldi F, Bengtsson S, Andersson K (2013) The influence of propulsion system design on the carbon footprint of different marine fuels. In: Low carbon shipping conference, London 2013

Bazari Z (2016) IMO train the trainer (TTT) course on energy efficient ship operation, module 2—ship energy efficiency regulations and related guidelines

Björnestrand L (2017) Efficiency and emissions analysis of a methanol fuelled direct injection spark ignition heavy duty engine. Master Thesis, Department of Energy Sciences, Lund University, Sweden

Chryssakis C, Balland O, Tvete HA, Brandsæter A (2014) DNV GL strategic research & innovation position paper 17-2014, alternative fuels for shipping

Chryssakis C, Brinks HW, Brunelli AC, Fuglseth TP, Lande M, Laugen L, Longva T, Raeissi B, Tvete HA (2017) Low carbon shipping towards 2050. DNV GL Technical Report

ClassNK (2018) Alternative fuels and energy efficiency for the shipping industry: an overview of LNG, LPG and methanol fuelled ships. [Powerpoint slides]. https://gmn.imo.org/wp-content/uploads/2018/01/AnnexV-2-5-Alternative-Fuels-and-Energy-Efficiency.pdf
Deniz C, Zincir B (2016) Environmental and economical assessment of alternative marine fuels. J Clean Prod 113:438–449
DNV GL (2014) DNV GL to class new methanol-fuelled tankers. https://www.dnvgl.com/news/dnv-gl-to-class-new-methanol-fuelled-tankers-7579
DNV GL (2017) EU MRV regulation, get the details on monitoring, reporting and verifying in line with the new EU MRV regulation—the smart way to comply. DNV GL Technical Report, Apr 2017
DNV GL (2020) Alternative-fuelled ships. https://www.dnvgl.com/services/alternative-fuels-insight-128171
DNV GL (2020) EU MRV and IMO DCS. https://www.dnvgl.com/maritime/insights/topics/EU-MRV-and-IMO-DCS/index.html
DNV GL (2019) Alternative fuels in the Arctic. Technical report, 27.02.2019
Durmusoglu Y, Kocak G, Deniz C, Zincir B (2015) Energy efficiency analysis of pump systems in a ship power plant and a case study of a container ship. In: Proceedings 16th IAMU Annual General Assembly, Opatija, Croatia, 7–10 Oct 2015
EEA (2000) Analysis of commercial marine vessels emissions and fuel consumption data. Office of Transportation and Air Quality. U.S. Environmental Protection Agency. EPA420-R-00-002
Ellis J, Ramne B, Bomanson J, Molander P, Tuner M, Aakko-Saksa P, Svanberg M, Rydbergh T, Berneblad B (2018) SUMMETH—sustainable marine methanol. Final Report—Summary of the SUMMETH Project Activities and Results. Doc. Number: D6.2, 10.04.2018
Engineering Toolbax (ETB) (2003) Fuels—higher and lower calorific values. https://www.engineeringtoolbox.com/fuels-higher-calorific-values-d_169.html
European Commission (2020) CORDIS EU Research Results. METHAPU. https://cordis.europa.eu/project/id/31414
European Energy Agency (EEA) (2019) Emissions of air pollutants from transport. https://www.eea.europa.eu/data-and-maps/indicators/transport-emissions-of-air-pollutants-8/transport-emissions-of-air-pollutants-6#tab-related-briefings
Fagerlund P, Ramne B (2013) Effship project: summary and conclusions
Fan YV, Perry S, Klemes JJ, Lee CT (2018) A review on air emissions assessment: transportation. J Clean Prod 194:673–684
Feenstra M, Monterio J, Akker JTVD, Abu-Zahra M, Gilling E, Goetheer E (2019) Ship-based carbon capture onboard of diesel or LNG-fuelled ships. Int J Greenhouse Gas Control 85:1–10
Global Combustion Systems (GCS) (2019) Oil fuel properties. https://www.globalcombustion.com/oil-fuel-properties/
ICF (2009) Current methodologies in preparing mobile source port-related emission inventories. Environmental Protection Agency, U.S
IMO Web Site (2020a) International Code of Safety for Ships Using Gases or Other Low-flashpoint Fuels (IGF Code). https://www.imo.org/en/OurWork/Safety/SafetyTopics/Pages/IGF-Code.aspx
IMO Web Site (2020b) Media centre. https://www.imo.org/en/MediaCentre/MeetingSummaries/CCC/Pages/CCC-6th-session.aspx
International Association of Classification Societies (IACS) (2020) Classification societies—what, why and how? https://www.iacs.org.uk/media/3785/iacs-class-what-why-how.pdf
Independent Commodity Intelligence Services (ICIS) (2017) Chemical profile special. ICIS Chemical Business 2017 (26 May–1 June)
International Council on Clean Transportation (ICCT) (2018) The International Maritime Organization's initial greenhouse gas strategy. Apr 2018
International Maritime Organization (IMO) (2014) Third greenhouse gas study
International Maritime Organization (IMO) (1974) International convention for the safety of life at sea (SOLAS)

International Maritime Organization (IMO) (2008) Resolution MEPC.177(58), Annex 14, Adopted on 10 October 2008, amendments to the technical code on control of emission of nitrogen oxides from marine diesel engines (NO_X Technical Code)
International Maritime Organization (IMO) (2011) Resolution MEPC.203(62), Annex 19, Adopted on 15 July 2011. Amendments to the annex of the protocol of 1997 to amend the international convention for the prevention of pollution from ships, 1973, as modified by the protocol of 1978 relating thereto (inclusion of regulations on energy efficiency for ships in MARPOL annex VI)
International Maritime Organization (IMO) (2017) Consideration of how to progress the matter of reduction of GHG emissions from ships, existing IMO activity related to reducing GHG emissions in the shipping sector, 21 Feb 2017
International Maritime Organization (IMO) (2020a) IMO data collection system. https://www.imo.org/en/ourwork/environment/pollutionprevention/airpollution/pages/data-collection-system.aspx
International Maritime Organization (IMO) (2020b) Nitrogen oxides. https://www.imo.org/en/OurWork/Environment/PollutionPrevention/AirPollution/Pages/Nitrogen-oxides-(NOx)-%E2%80%93-Regulation-13.aspx
International Maritime Organization (IMO) (2020c) Sulphur oxides. https://www.imo.org/en/OurWork/Environment/PollutionPrevention/AirPollution/Pages/Sulphur-oxides-(SOx)-%E2%80%93-Regulation-14.aspx
Johansson, B (2016) Fuels and combustion. In Boot M (eds) Biofuels from lignocellulosic biomass: innovation beyond bioethanol. Wiley-VCH Verlag GmbH & Co. KGaA, pp 1–27
Kim M, Oh J, Lee C (2018) Study on combustion and emission characteristics of marine diesel oil and water-in-oil emulsified marine diesel oil. Energies 11:1830. https://doi.org/10.3390/en11071830
Klaus OL, Villetti L, Siqueira JAC, De Souza SNM, Santos RF, Nogueira CEC, Rosseto C (2013) Efficiency and fuel specific consumption of an engine running on fish biodiesel. Sci Res Essays 8(42):2120–2122. https://doi.org/10.5897/SRE2013.5550
Landälv I (2017) Methanol as a renewable fuel—a knowledge synthesis. Technical Report f3—The Swedish Knowledge Centre for Renewable Fuels
Lassesson H, Andersson K (2009) Energy efficiency in shipping—review and evaluation of the state of knowledge. Department of Shipping and Marine Technology, Division of Sustainable Ship Propulsion, Chalmers University of Technology
LeanShips Project website (2020) https://www.leanships-project.eu/demo-cases/demo-case-05/overview/
Li C (2018) Stratification and combustion in the transition from HCCI to PPC. PhD Thesis, Department of Energy Sciences, Lund University, Sweden
Lloyd's Register (2019) Rules for the classification of methanol fuelled ships. July 2019
Lönn S (2019) Investigation of PPC in an optical engine: with focus on fuel distribution and combustion characterization. PhD Thesis, Department of Energy Sciences, Lund University, Sweden
MAN (2014) Exhaust gas emission control today and tomorrow, application on MAN B&W two-stroke marine diesel engines. MAN Technical Report
MAN (2014) Waste heat recovery system (WHRS) for reduction of fuel consumption, emissions and EEDI. MAN Technical Report
MAN, PrimeServ (2012) Slow steaming benefitting retrofit solutions from MAN PrimeServ. Technical Paper, Sept 2012
Maritime Knowledge Center (MKC), TNO, TU Delft (2017) Framework CO_2 reduction in shipping. Project Final Report, MIIP019-2016
Maritime Knowledge Center (MKC), TNO, TU Delft (2018) Methanol as an alternative fuel for vessels. Public Final Report, MIIP001-2017
Methanol Institute (2016) Compatibility of elastomers in neat methanol service. Methanol Safe Handling Techn Bull

Methanol Institute (2016) Compatibility of metals & alloys in neat methanol service. Methanol Safe Handling Techn Bull

Moirangthem K (2016) Alternative fuels for marine and inland waterways. European Commission JRC, Petten

Nash, M (2015) IHS chemical: overview of the global methanol industry: the times they are a-changin' IHS Chem 2015

Paulauskas V, Lukauskas V (2013) CleanShip, clean Baltic Sea shipping. 3.6 Sustainable shipping and port development. Klaipeda Science and Technology Park, Klaipeda

Przybyla G, Postrzednik S, Zmudka Z (2016) The impact of air-fuel mixture composition on SI engine performance during natural gas and producer gas combustion. In: IOP Conference Series on Material Science and Engineering, vol 148(1):12082, Sept 2016

Shamun S (2019) Characterization of the combustion of light alcohols in CI engine: performance, combustion characteristics and emissions. PhD Thesis, Department of Energy Sciences, Lund University, Sweden

Shamun S, Shen M, Johansson B, Tuner M, Pagels J, Gudmundsson A, Tunestal P (2016) Exhaust PM emissions analysis of alcohol fueled heavy-duty engine utilizing PPC. SAE Int J Engines 9(4):2016. https://doi.org/10.4271/2016-01-2288

Shamun S, Haşimoğlu C, Murcak A, Andersson Ö, Tuner M, Tunestal P (2017) Experimental investigation of methanol compression ignition in a high compression ratio HD engine using a Box-Behnken design. Fuel 209:624–633

Shamun S, Novakovic M, Malmborg Berg V, Preger C, Shen M, Messing ME, Pagels J, Tuner M, Tunestal P (2017) Detailed characterization of particulate matter in alcohol exhaust emissions. In: COMODIA, June 2017

Shamun S, Zincir B, Shukla P, Valladolid PG, Verhelst S, Tuner M (2018) Quantification and analysis of the charge cooling effect of methanol in a compression ignition engine utilizing PPC strategy. In: Proceedings of the ASME 2018, Internal Combustion Engine Division Fall Technical Conference, ICEF2018, San Diego, CA, USA, 4–7 Nov 2018

Splitter D, Wissink M, Del Vescovo D, Reitz D (2013) RCCI engine operation towards 60% thermal efficiency. SAE Technical Paper 2013-01-0279, 2013. https://doi.org/10.4271/2013-01-0279

Stefenson, P (2016) Methanol: The marine fuel of the future, updates from the Stena Germanica (the world's first methanol-powered ferry). https://www.methanol.org/wp-content/uploads/2016/07/Updates-from-Stena-Germanica-Per-Stefenson.pdf

Stocker A (2018) Investigation of renewable fuels for a Scottish ferry service. MSc. Thesis, Department of Mechanical and Aerospace Engineering, University of Strathclyde, Scotland

SUMMETH (2020) Sustainable Marine Methanol Project website. https://summeth.marinemethanol.com/?page=home

Sverrisdottir SR (2018) Alternative fuels for ships. Orkustafnun, Energy in the West Nordics and the Arctic. [Powerpoint slides]. https://orkustofnun.is/media/banners/Hafid-Alternative-fuel-for-ships-30Nov2018.pdf

Tang Q, Liu H, Li M, Yao M (2017) Optical study of spray-wall impingement impact on early injection gasoline partially premixed combustion at low engine load. Appl Energy 185:708–719

Tezdogan T, Demirel YK, Kellett P, Khorasanchi M, Incecik A, Turan O (2015) Full-scale unsteady RANS CFD simulations of ship behavior and performance in head seas due to slow steaming. Ocean Eng 97:186–206

Tuner M (2015) Combustion of alternative vehicle fuels in internal combustion engines. A report on engine performance from combustion of alternative fuels based on literature review. Report from a pre-study to prepare for interdisciplinary research on future alternative transportation fuels project

Tuner M (2016) Review and benchmarking of alternative fuels in conventional and advanced engine concepts with emphasis on efficiency, CO_2, and regulated emissions. SAE Technical Paper 2016-01-0882. https://doi.org/10.4271/2016-01-0882

Tuner M, Aakko-Saksa P, Molander P (2018) SUMMETH—sustainable marine methanol deliverable D3.1 Engine technology, research, and development for methanol in internal combustion engines. Final Report

United Nations Conference on Trade and Development (UNCTAD) (2019) Review of maritime transportation 2019

Verhelst S, Turner JWG, Sileghem L, Vancoillie J (2019) Methanol as a fuel for internal combustion engines. Prog Energy Combust Sci 70:43–88

Winkel R, Van den Bos A, Weddige U (2015) Study on energy efficiency technologies for ships. ECOFYS—Energy efficiency technologies for ships, inventory and technology transfer, final report. CLIMA.B3/ETU/2014/0023r

Wireman T (2011) Tips on saving energy using preventive maintenance techniques. https://www.pem-mag.com/Features/Tips-on-saving-energy-using-preventive-maintenance-techniques.html#sthash.F31kH9ip.dpuf

Wuebben P (2016) A new look at methanol: accelerating petroleum reduction and the transition to low carbon mobility. Methanol Institute

Yao C, Pan W, Yao A (2017) Methanol fumigation in compression-ignition engines: a critical review of recent academic and technological developments. Fuel 209:713–732

Zhou P, Wang H (2014) Carbon capture and storage-Solidification and storage of carbon dioxide captured on ships. Ocean Eng 91:172–180

Zincir B (2019) An alternative fuel assessment model for ships and experiments on the effect of methanol on diesel engines. Ph.D. Thesis, Maritime Transportation Engineering Department, Istanbul Technical University, Turkey

Zincir, B (2014) Hidrojen karışımlı yakıtların gemilere uygulanabilirliğinin ve emisyon salınımlarına etkilerinin incelenmesi. MSc. Thesis in Turkish, Maritime Transportation Engineering Department, Istanbul Technical University, Turkey

Zincir B, Deniz C (2016) Investigation of effect of alternative marine fuels on energy efficiency operational indicator (EEOI). In: The second global conference on innovation in marine technology and the future of maritime transportation. Bodrum, Muğla, Turkey, 24–25 Oct 2016

Zincir B, Deniz C (2018) Maritime industry developments related to alternative fuels. In: Proceedings of INT-NAM, 3rd International Symposium on Naval Architecture and Maritime, Istanbul, Turkey, 24–25 Apr 2018

Zincir B, Shukla P, Shamun S, Tuner M, Deniz C, Johansson B (2019a) Investigation of effects of intake temperature on low load limitations of methanol partially premixed combustion. Energy Fuels 33:5695–5709

Zincir B, Deniz C, Tuner M (2019b) Investigation of environmental, operational and economic performance of methanol partially premixed combustion at slow speed operation of a marine engine. J Clean Prod 235:1006–1019

Chapter 5
The Potential of Various Alcohol Fuels for Low-Temperature Combustion Engines

S. Rajkumar and J. Thangaraja

5.1 Introduction

Due to higher compression ratio, better thermal efficiency, and good torque characteristics of diesel engine compared to its counterpart spark ignition (SI) gasoline engines, the diesel engines have become indispensable to meet the power demands for on-road and off-road applications. However, the oxides of nitrogen (NO_x) and smoke emission from the diesel engine are its major concerns. To surmount the depletion of fossil fuel resources and harmful emissions from these sources, the emission norms are tightened. Currently, the stringent emission norms keep the researchers in active mode to establish feasible solutions to mitigate the emissions from conventional fossil fuels. Several alternative strategies, namely alternate fuels, advanced combustion technology, and after treatment techniques, are practiced. In this regard, the alternate fuels from biomasses like alcohol and biodiesel are proved to be effective alternate fuels for internal combustion engines. Alcohol fuels have many advantages like renewable in nature, higher latent heat of evaporation (beneficial in NO_x reduction), and fuel-bound hydroxyl (OH) group (reduces smoke emission). However, direct usage of alcohols in compression ignition (CI) engines needs ignition aids due to their lower cetane and viscosity characteristics. Therefore, the alcohol–diesel blends or dual-fuel mode is preferred in CI engines. Biodiesel fuel is an efficient alternative fuel for CI engines. The biodiesel fuels have several advantages like renewable in nature, the presence of fuel-bound oxygen, and high miscibility with diesel. However, many

S. Rajkumar (✉)
Mechanical Engineering, Sri Sivasubramaniya Nadar College of Engineering, Chennai 603110, India
e-mail: rajkumars@ssn.edu.in

J. Thangaraja
Mechanical Engineering, Vellore Institute of Technology, Vellore 632014, India
e-mail: thangaraja.j@vit.ac.in

P. C. Shukla et al. (eds.), *Alcohol as an Alternative Fuel for Internal Combustion Engines*, Energy, Environment, and Sustainability,
https://doi.org/10.1007/978-981-16-0931-2_6

researchers have reported an increase in NO_x emission from biodiesel compared to that of diesel fuel. Blending alcohol with biodiesel fuels decreases the NO_x emission by reducing in-cylinder temperature. In diesel engines, the NO_x and soot emissions' formation is influenced by flame temperature and equivalence ratio, respectively. Hence, the simultaneous reduction of these emissions is possible by controlling the flame temperature and local equivalence ratio. This is achieved in an advanced low-temperature combustion (LTC) strategy. Numerous articles are available in the open literature on the effect of LTC on performance, combustion, and emission characteristics of CI engines (Amorim et al. 2017; Carlucci et al. 2014; Fang et al. 2013a). The LTC could be attained with the help of advanced combustion strategies like homogeneous charge compression ignition (HCCI), partially premixed combustion (PPC), premixed charge compression ignition (PCCI), and reactivity-controlled compression ignition (RCCI). In LTC mode, preparing homogeneous mixture is one of the primary tasks, which can be done effectively with alcohol fuels because of its higher volatility (Kumar and Rehman 2017). Alcohols are one of the favorable alternative fuels for LTC due to their higher octane number, wide equivalence ratio range, and widened operational range with emissions reduction capabilities (Pachiannan et al. 2019). Moreover, alcohol and biodiesel fuels are used in an internal combustion engine with minimal or without major modifications (Çelebi and Aydın 2019). Numerous articles on the use of alcohol fuels with diesel and biodiesel in both the SI and CI engines are accessible from the literature (Nour et al. 2019; Yusri et al. 2017; Shirazi et al. 2019). Hence, an effort is made to comprehend the outcome of alcohol fuels on combustion and emission characteristics of low-temperature combustion engines as shown in Fig. 5.1.

5.2 Overview of Alcohol Fuels

Methanol, ethanol, and butanol are the extensively utilized alcohols in both SI and CI engines. The chemical structure of alcohol is represented as $C_nH_{2n+1}OH$. The higher octane number of alcohol can reduce the knocking tendency in spark-ignition (SI) engines, whereas the presence of fuel oxygen content in alcohol diesel blends lowers the soot formation tendency in compression ignition engines. Concomitantly, blending alcohol results in lower emissions in both the version of internal combustion engines (Çelebi and Aydın 2019; Yusri et al. 2017).

5.2.1 Types of Alcohol Fuels

Among the oxygenated fuels, methanol came into the spotlight as a clean alternative fuel supplementing conventional fossil fuels and is produced from fossil or bioenergy resources. The merits of blending methanol with gasoline include high research octane number and hence higher engine efficiency, higher latent heat, and wider

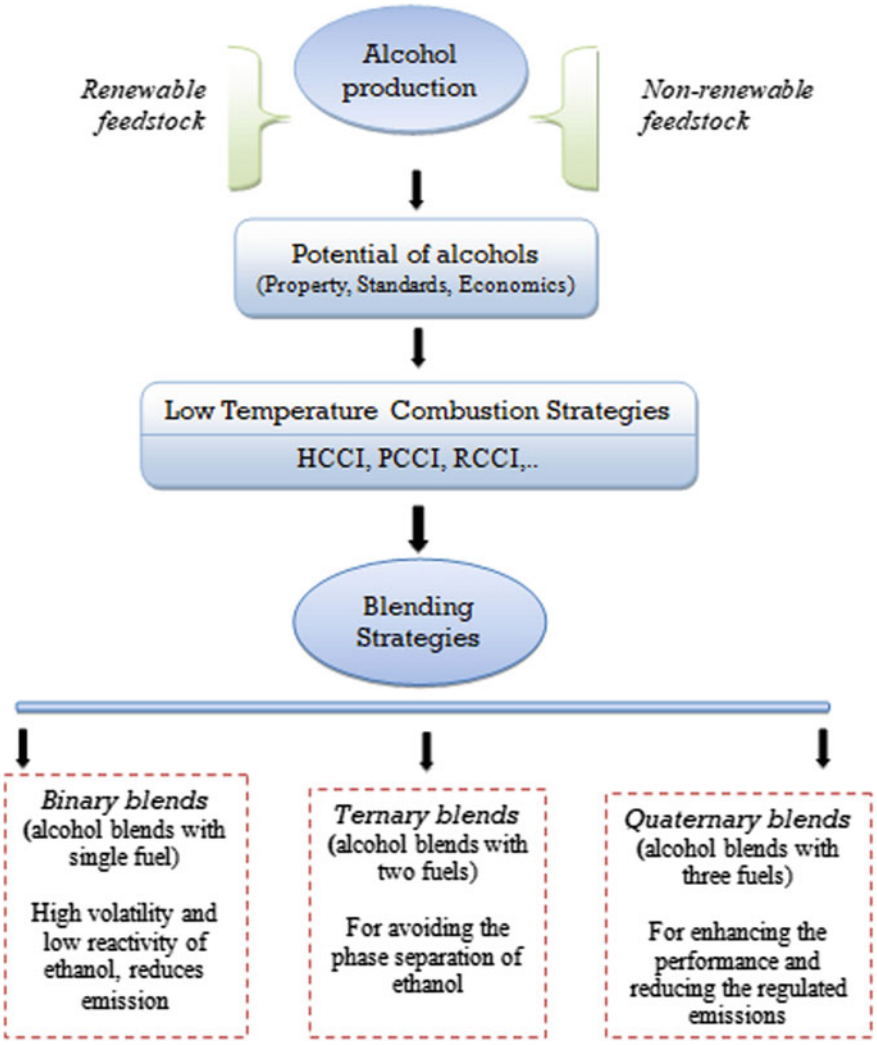

Fig. 5.1 An outline of the chapter

flammability limits than those of gasoline result in lower combustion temperature and thus lesser pollutant formation. Ethanol is a clear, colorless liquid and also known as grain alcohol. The USA and Brazil produce 85% of the world's ethanol as shown in Fig. 5.2. In USA, corn is used to produce the majority of ethanol, while in Brazil sugarcane is the preferred feedstock. *n*-propanol (1-propanol) and isopropanol (2-propanol) are the two isomers of propanol (C_3H_7OH). Though the energy density of propanol is higher than ethanol, they are not recommended in the automotive fuel segment due to their higher production cost. Hence, only very few studies are attempted in comparison to ethanol and butanol isomers (Shirazi et al. 2019). Among

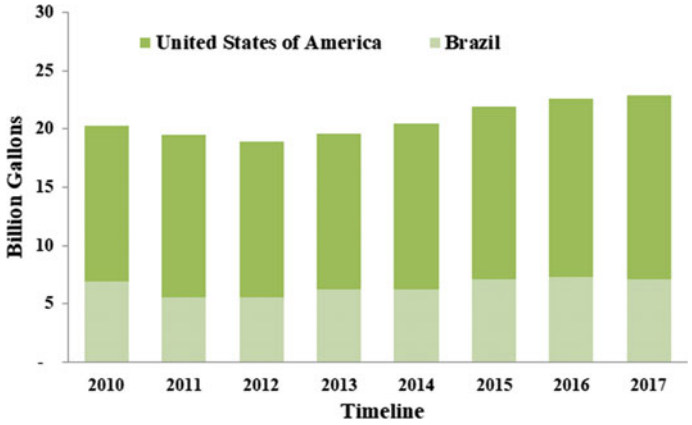

Fig. 5.2 Major ethanol-producing countries in the world (Annual Fuel Ethanol Production 2020)

the different isomers of butanol (C_4H_9OH), *n*-butanol and isobutanol are the potential blends for spark-ignition engines.

The other isomers, viz. secondary butanol and tertiary butanol, are not recommended due to their extremely low motor octane rating (32) and higher melting point (about 25 °C), respectively. Though butanol can be obtained from both fossil and renewable resources, production through biological pathways is highly preferred to mitigate greenhouse gas emissions. Biobutanol is produced through fermentation of straw, sorghum, sugar beets, wheat, corn, sugar cane, and cassava (Shirazi et al. 2019). In comparison with propanol and butanol, methanol is toxic and less volatile (Yusri et al. 2017). Table 5.1 provides the property comparison of methanol, ethanol, propanol, and butanol fuels. In particular, the four alcohols have higher octane number, heat of evaporation, and auto-ignition temperature than those of fossil fuels, and also they contain fuel-bound oxygen.

Among the alcohol groups, butanol has higher boiling point, thus requires higher temperatures for the evaporation. Longer ignition delay periods could be observed in the case of methanol and ethanol due to their higher heat of vaporization. Due to their higher heating values, propanol and butanol lower the fuel consumption for the same power output. The higher flash point of propanol and butanol offers safer storage and fuel transportation.

5.2.2 Standard Requirements

Flexible-fuel vehicles (FFVs) are designed to operate on alcohol and gasoline in any combination from a single fuel tank. As shown in Table 5.2, ASTM Standards provide

Table 5.1 Physicochemical properties of fuels (Yusri et al. 2017; Shirazi et al. 2019)

Properties	Fossil fuels		Alcohol fuels			
	Gasoline	Diesel	Methanol	Ethanol	Propanol	Butanol
Chemical formula	C_8H_{18}	$C_{12}H_{26}$	CH_3OH	C_2H_5OH	C_3H_7OH	C_4H_9OH
Molecular weight (g/mol)	114	170	32.04	46.07	60.10	74.12
Oxygen content (% wt.)	–	0	49.93	34.73	26.62	21.6
Cetane number	0–10	40–55	3.8	5–8	12	25
Research octane number	80–99	20–30	136	129	112	96
Boiling point (°C)	40–200	143	65	79	97	117
Density (kg/m^3)	~740	840	791.3	789.4	803.7	810
Viscosity @ 40 °C (mm^2/s)	~0.6	2.43	0.59	1.13	1.74	2.22
Lower heating value (MJ/kg)	42.7	42.5	20.01	26.08	29.82	33.01
Heat of vaporization @ 25 °C (kJ/kg)	349	243	1162.64	918.42	727.88	585.40
Flash point (°C)	−13 to 45	65–88	12	13	22	35
Auto-ignition temperature (°C)	257	~300	463	420	350	345
Stoichiometric air–fuel ratio	14.7	14.3	6.47	9.01	10.35	11.19

the specification for methanol fuel blends (M51–M85), ethanol fuel blends (E51–E83), butanol for use in automotive spark-ignition engines equipped with flexible-fuel and dedicated spark-ignition engines. For optimum vehicle operation, the alcohol content in the fuel blend is a vital parameter to ascertain the proper air–fuel ratio by the fuel metering system of the FFVs.

5.2.3 Economic Benefits of Alcohol Fuels

The pricing policy of biofuels is a crucial parameter to sustain their growth in comparison to conventional fossil fuels. European Union has set a goal to consume 10% of biofuels by 2020, and the USA is aiming for 36 billion gallons of biofuels by 2022 (Çelebi and Aydın 2019). Gallagher et al. (2005) emphasized the relation between capital costs and plant size for the economical production of biofuels. Typical biofuel

Table 5.2 Comparison of standard requirements of the alcohol fuel blends (ASTM Standard D5797-18 2018; ASTM Standard D5798-20 2020; ASTM Standard D7862-19 2019)

Properties	Methanol blends	Ethanol blends	Butanol
ASTM standard	D5797-18	D5798-19	D7862-18
Alcohol content (% by vol.)	51–85	51–83	94
Vapor pressure (kPa)	62–83	48–65	
Methanol content (% by vol., max)	–	0.5	0.4
Ethanol content (% by vol., max)	–	–	1.0
Lead (mg/L, max)	2.6	–	–
Phosphorus (mg/L, max)	0.2	–	–
Sulfur (mg/kg, max)	80	80	30
Acetic acid (mg/kg, max)	50	50	56 (mg/L)
Unwashed gum content (mg/100 mL, max)	20	20	–
Solvent washed gum content (mg/100 mL, max)	5	5	5
Total inorganic sulfate (mg/kg, max)	4	–	–
Water (% by mass, max)	0.5	1.0	1.0 (by vol.)
Total inorganic chloride (mg/kg, max)	1.0	1.0	8.0
Copper content (mg/L, max)	–	0.07	–
Existent sulfate (mg/kg, max)	–	–	4

productions in large scale were assumed to be 245 million L/year for ethanol and 110 million L/year for biodiesel (Pimentel and Patzek 2005). Lin et al. (2013) recommended utilizing waste feedstock (such as food waste or reused cooking oil) to lower the production cost of biofuels. Considering the Indian scenario, Thangaraja and Srinivasan (2019) found that the price of coconut biodiesel blend (B20) is slightly higher (0.017 $) in comparison to fossil diesel. Figure 5.3 summarizes the price variation between fossil and biofuel blends (E85 and B20) in major clean cities of the USA. It is interesting to observe that the price of biofuel blends is converging closer to fossil fuels in recent years.

5.2.4 Implementation of Alcohol Fuels in Combustion Engines

The current stringent emission norms led the researchers to shift their focus toward establishing alternative fuels and to develop advanced combustion strategies for subsiding the fossil fuel dependency and mitigating the deleterious emission from the internal combustion engines. In this regard, one of the promising alternate fuels such as alcohol deemed to be a suitable source to overcome the adverse impact of emission caused by internal combustion engines. However, the concurrent decrease

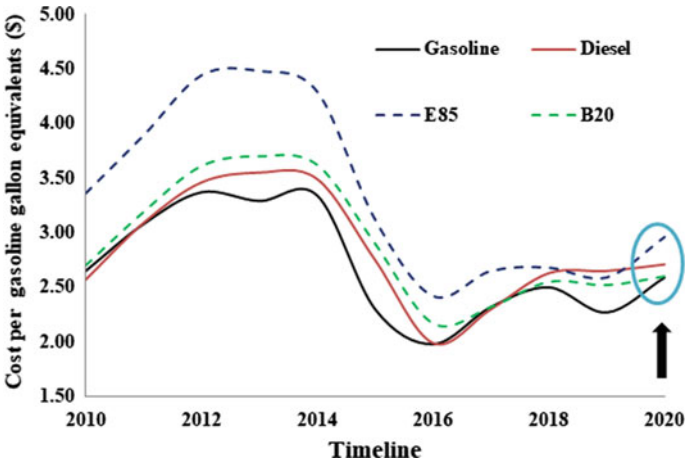

Fig. 5.3 Average retail fossil and biofuel blend prices in the USA (Clean Cities Alternative Fuel Price Reports 2020)

of NO_x and soot emissions is one of the major inherent drawbacks of the diesel engine. LTC is one of the advanced combustion strategies which show the potential of reducing NO_x and soot emissions. The LTC is accomplished with the help of altering the injection timing, a higher rate of exhaust gas recirculation (EGR), varying the fuel reactivity, etc. To abate the consequences of high rate of EGR and retarded injection timing, it is desirable to implement a fuel which has lower cetane number and higher volatility, like alcohol fuel (Zhang et al. 2012; Fang et al. 2013b). Moreover, alcoholic fuels are considered as suitable in LTC due to their desirable properties, namely high auto-ignition resistance and enhanced ignition delay, which helps in allowing adequate time for mixing the air and fuel and evaporating the fuel faster. Its hydroxyl group and higher latent heat of vaporization reduce the smoke emission especially at high loads (Lapuerta et al. 2010) and NO_x emission significantly vis-à-vis diesel fuel (Doğan 2011). Therefore, the next section describes the potential of alcohol fuels in achieving low combustion strategies and their effect on combustion and emission characteristics of internal combustion engines.

5.3 Usage of Alcohol Fuels in LTC Strategies

It is well known that the simultaneous reduction of NO_x and PM emissions necessitates avoiding both the high-temperature stoichiometric regions and local fuel-rich regions which are inherent in diesel combustion. It is informed that the low-temperature combustion improves fuel atomization and mixing, lowers the local equivalence ratio and reduces combustion temperature (Leermakers and Musculus

2015; Yousefi et al. 2018) which can abate the NO_x and particulate matter (PM) emissions simultaneously (El-Asrag and Ju 2014; Niemeyer et al. 2015). The alcohol fuels make use of the full merits of HCCI combustion due to their desirable properties such as higher octane number, wider range of equivalence ratios with a reduction in emissions (Maurya and Agarwal 2014). The alcohol fuel used in other mode of LTC such as RCCI engine increases the thermal efficiency along with decrease in harmful exhaust pollutants (Dou et al. 2017; Jamrozik 2017). As this chapter discusses the effect of alcohol fuels on LTC, for the sake of brevity the LTC concept is not explained in detail. Though several papers published on alcohol fuels, this work provides the effect of alcohol fuels which is characterized in terms of number of fuels used for blending. This section describes the suitability of alcohol fuel for LTC strategies and their effect on performance, combustion, and emission characteristics of engines under LTC mode.

5.3.1 Binary Blends

The binary blends consist of alcohol fuels blended with gasoline–diesel–biodiesel. This section describes the use of binary blends on LTC mode.

5.3.1.1 Diesel–Alcohol Blends

In the normal mode of combustion, it is reported that the alcohol fuels increase the intensity of premixed combustion phase due to increase in ignition delay period and heat release which in turn increases the combustion temperature (Ning et al. 2020). However, the high volatility and low reactivity of ethanol fuel suit LTC operation in diesel engines (Asad et al. 2015). Increasing the quantity of ethanol reduces the premixed phase of combustion and NO_x and soot emissions but it increases HC emission. The reduction of NO_x is attributed to the reduction in combustion temperature due to charge cooling. The higher premixed ratio (increase in ethanol fraction) increases the delay period and retards combustion due to higher resistance to auto-ignition of ethanol fuel and lower cetane number which in turn affects the auto-ignition process, respectively (Mancaruso and Vaglieco 2015). The binary blend diesel–ethanol (15% of ethanol) in a double-injection strategy reduced the NO_x and smoke emissions by 85% and 33%, respectively (Srihari and Thirumalini 2017). The reduced heat release rate, and combustion temperature and the higher latent heat of evaporation of ethanol fuel caused the NO_x reduction. The smoke reduction is attributed to the fuel-bound oxygen of ethanol fuel and improved fuel–air mixing. However, the HC and CO emissions are observed to increase at all the load conditions. It is suggested that increasing the inlet air temperature can decrease CO and HC emissions with a trade-off in NO_x emission (Maurya and Agarwal 2011).

The use of diesel with higher alcohols like isobutanol and *n*-pentanol blends (Rajesh Kumar and Saravanan 2016) established an increase in ignition delay and rate

of premixed combustion phase with retarded occurrences. Butanol blends increased the ignition delay, peak pressure, and combustion efficiency vis-à-vis pentanol blends which is attributed to low cetane number and higher oxygen content of butanol fuel compared to those of pentanol. The viscosity and density of isobutanol are lower compared to those of *n*-pentanol which enhance the spray behavior. While the butanol blends are noted to be comparable with the performance of diesel fuel, it is observed to be better than pentanol. In emission standpoint, butanol offered a huge reduction in NO_x than pentanol blends due to longer delay period, reduction in combustion flame temperature, and lower oxygen content of butanol blend. However, the lower oxygen content of butanol increased the smoke emission.

The RCCI strategy is one of the LTC variants, which addresses the several problems associated with HCCI and PCCI mode such as extending LTC to higher load, combustion phasing for a wide range of engine load conditions and excessive pressure rise rates at higher loads. Since the homogeneity of the fuel plays a major role in LTC, the use of port injected low reactivity fuel (LRF) and earlier direct injection of high reactivity (HRF) fuel is suggested for RCCI engines. The proper fuel blending provides the required fuel reactivity which can be changed by varying the quantity of LRF and HRF. These varying reactivities between LRF and HRF help control the various parameters of LTC for extending the range of engine load and speed conditions (Splitter and Reitz 2014). It is proved that the spatial stratification of the fuel reactivity influences the duration of combustion. For obtaining the necessary fuel reactivities, alcohol fuels, namely methanol, ethanol, and butanol, qualify as LRFs in the RCCI combustion concept. Among the variety of alcohol fuels, butanol is one of the potential low-reactivity fuels for RCCI mode due to its higher heating value, more energy density, low hydrophilicity, and non-corrosiveness (No 2016; Pan et al. 2017). The use of alcohol fuels achieves stable and extends the operation of RCCI engine (Dempsey et al. 2013; DelVescovo et al. 2015) due to their low reactivity and higher latent heat of evaporation. A small fraction of ethanol (about 10–20%) reduces the NO_x and smoke emissions in compliance with EURO VI emission norms with enhanced HC and CO emissions for a wide range of engine loads (Benajes et al. 2015). However, higher premixed ratios of ethanol are observed to increase CO and HC emission, while lowering NO_x and soot emissions significantly due to enhanced cooling effect and reduction in in-cylinder temperature, respectively (Qian et al. 2015). It is stated that the increasing the ethanol premixed ratio delays the phasing of combustion and reduces NO_x emission to an extremely low level, and hence the alcohol fuel becomes a good choice as LRF for RCCI engine (Zhu et al. 2015). The methanol–diesel combination in the RCCI engine emits low NO_x emission vis-à-vis gasoline–diesel pair (Li et al. 2016) which is attributed to reduced local combustion peak temperature and equivalence ratio. However, in general, CO and HC emissions increase (Tutak 2014; Işık and Aydın 2016) with ethanol fuel. In RCCI mode, it is found that the isobutanol–diesel blend is capable of mitigating CO, HC, NO_x, and particulate matter emissions vis-à-vis gasoline–diesel combination (Pan et al. 2020). The isobutanol–diesel retards the combustion phase with higher mean in-cylinder temperature along with the longer ignition delay and lower rate of pressure rise vis-à-vis gasoline–diesel. Recently, alcohol fuels are more focused as LRF for the RCCI

engine because of their superior physical and chemical properties (Liu et al. 2018; Zheng et al. 2018).

5.3.1.2 Biodiesel–Alcohol Blends

Biodiesel and higher alcohols have gained popularity among the other alternative fuels for diesel engines due to their renewable characteristics. It is concluded that adding the higher alcohols to biodiesel fuel lowers the density and viscosity of biodiesel and hence enhances the atomization and auto-ignition characteristics. It also assists the combustion process to occur in semi-LTC with reduced NO_x emissions (Atmanli and Yilmaz 2020). As shown in Fig. 5.4, the combination of higher alcohols has lowered the NO_x emission significantly than that of diesel (D) and waste cooking biodiesel (WB).

It is showed that the particle number concentrations are significantly reduced when two fuel-bound oxygen fuels, namely biodiesel and ethanol are used (Su et al. 2013). This explains the benefit of the fuel oxygen content in decreasing the PM emission. n-butanol reduced the NO_x and soot emissions by 75% and 98%, respectively, compared to those of diesel fuel in LTC mode due to low-combustion temperature and oxygen content. However, it is reported that an incomplete combustion during the premixed phase of combustion increased the CO and HC emissions (Soloiu et al. 2013). Use of *n*-butanol with high-pressure direct injection is suggested for LTC operation compared to diesel fuel (Han et al. 2013). The *n*-butanol decreases soot emission due to low boiling point, low viscosity, and higher latent heat of evaporation and significant improvement in the fuel–air mixing. As n-butanol easily blends with diesel (Rakopoulos et al. 2010; Merola et al. 2014) because of its less hydrophilicity

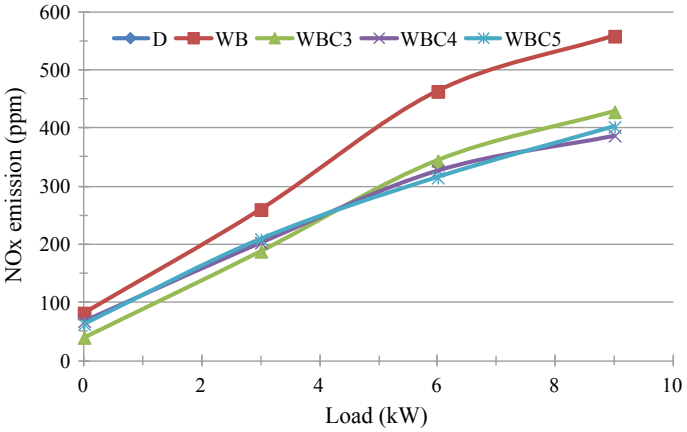

Fig. 5.4 NO_x emission from the various fuels (Atmanli and Yilmaz 2020). Legend: D—Diesel, WB—waste cooking biodiesel, WBC3—biodiesel + propanol, WBC4—biodiesel + *n*-butanol and WBC5—biodiesel + *n*-butanol

and higher miscibility nature compared to ethanol, n-butanol has good potential for LTC engines. Usage of alcohol fuels like n-butanol reduces the particulate matter emission to nearly zero levels (Han et al. 2013) and also reduces PM emission significantly even at a higher rate of EGR rate (Huang et al. 2016).

5.3.1.3 Gasoline–Alcohol Blends

The most important drawback of the HCCI engine is the extension of its operating range over a wide range of engine loads. This can be surmounted by employing alcohol–gasoline fuel blends with the optimal start of injection and blend ratio (Turkcan et al. 2014). In this study, ~80% of the total fuel (of the ethanol–gasoline blend) is injected in suction stroke, and the balance fuel is injected towards the later stage of compression stroke to control the ignition timing. It is concluded that for the fixed start of injections, the blend ratio affected the control of HCCI combustion phases significantly. However, *n*-butanol–gasoline blend auto-ignites earlier vis-à-vis ethanol–gasoline blends and reduced the combustion duration (He et al. 2015). *n*-butanol–gasoline blends also decreased the indicated mean effective pressure (IMEP) and indicated thermal efficiency (ITE).

5.3.2 Ternary Blends

In order to avoid the separation of ethanol from diesel fuel, an emulsifier or a surfactant is essential for increasing the premixed ratio of ethanol (Satgé De Caro et al. 2001; Xing-Cai et al. 2004). Fortunately, biodiesel stabilizes the diesel and ethanol mixture and helps in achieving a homogeneous mixture of ethanol–diesel blends (Fernando and Hanna 2005; Kwanchareon et al. 2007). The increase in smoke emission at higher load during LTC operation can be mitigated with the help of oxygenated fuels like biodiesel, and hence, it extends the higher operational load limit of LTC engines (Ickes et al. 2009). It is proved that biodiesel and ethanol blends reduce the smoke emission vis-à-vis conventional diesel combustion (Xue et al. 2011; Zhu et al. 2011). In an investigation, with the blends of ethanol–diesel–biodiesel (waste cooking oil) and EGR (Fang et al. 2013b), among the various blends of biodiesel–ethanol–diesel, it is observed that the ethanol blends lower the NO_x and smoke emissions about 8.55 and 31.79% (for BDE10—blend of 10% ethanol + 10% biodiesel + remaining diesel) and 23.08 and 73.44% (for BDE20—blend of 20% ethanol + 10% biodiesel + remaining diesel) due to lower energy release and higher latent heat of evaporation of alcohol fuel, respectively. Similar kinds of results, i.e., decrease in NO_x and smoke emissions and increase in HC and CO emissions, are also reported with diesel–rape seed biodiesel–ethanol blends (Pidol et al. 2012).

In ethanol RCCI combustion mode, it is observed that the engine knock is completely eliminated with reduced heat losses (Işık and Aydın 2016). Increase in quantity of ethanol reduced NO emission for all the tested fuel blends. BSFC is

found to increase in 30% ethanol RCCI operation for all fuels vis-à-vis 50% ethanol RCCI operation. In 50% ethanol RCCI operation, the BSFC is comparable to that of single fuel mode. This shows the effect of blending modes on the performance of the engines. It is shown that 5% rice wine alcohol with 75% diesel and 20% neem methyl ester increases the brake thermal efficiency by 8% and decreases the brake specific fuel consumption by 3.33% compared to those of diesel fuel. However, NO_x emission increased because of the presence of oxygenated biodiesel. The NO_x emission of 20, 5, and 10% biodiesel fuel (with 5% rice wine and remaining fraction is diesel) are noted to be 6.4%, 4.26, and 2.14% higher than vis-à-vis base line diesel fuel (Reang et al. 2020).

5.3.3 *Quaternary Blends*

The experimental investigation (Appavu et al. 2019) established that the use of higher alcohol like pentanol as a quaternary blend with diesel, biodiesel, and vegetable oil overcomes the demerits involved with neat biodiesel operation. It is noted that at full load condition, the quaternary blends reduced the NO_x emission by 11.23%. This is ascribed to higher latent heat of vaporization of the blends which caused LTC, eventually decreasing the NO_x emission. The NO_x emission is found to be less for all the pentanol blends (from DBOP10 to DBOP40) compared to that of B100 (neat biodiesel—refer Fig. 5.5). However, increasing the pentanol concentration increased the NO_x emission while it decreased hydrocarbon, carbon monoxide, and smoke emissions. In another experimental investigation (Yesilyurt et al. 2020), the various fuel blends such as binary (diesel and biodiesel), ternary (diesel,

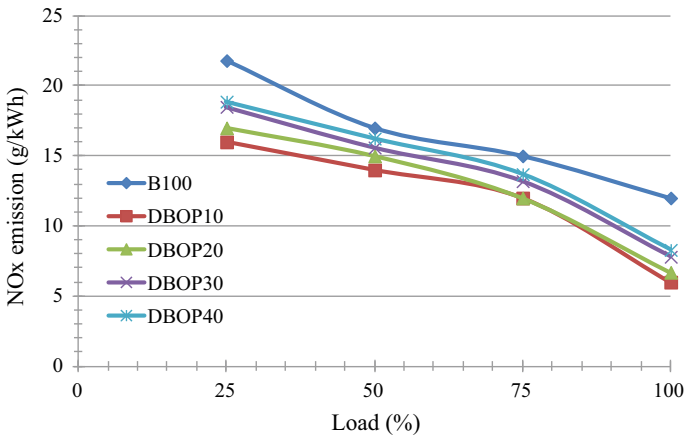

Fig. 5.5 NO_x emission variation for various tested fuels (Appavu et al. 2019)

biodiesel and vegetable oil) and quaternary blends (diesel, biodiesel, vegetable oil and isopentanol/isopropanol/n-butanol) are considered for the study.

The brake thermal efficiency of all quaternary blends is observed to be higher than B100, which increases with increasing the pentanol concentration. Increasing the concentration of pentanol in blend increased NO_x emission and reduced CO, HC, and smoke emissions vis-à-vis diesel fuel. It is also observed that diesel–gasoline–n-butanol blends increased the brake-specific fuel consumption, CO and HC emissions and reduced NO_x and soot emissions (Huang et al. 2016). In RCCI mode, diesel–biodiesel–ethanol–gasoline blends increased the peak pressure at higher loads, decreased both the NO_x (below EURO VI) and smoke emissions and increased CO and HC emissions (Benajes et al. 2015). The effect of alcohol blends on LTC engines is summarized and shown in Table 5.3.

Table 5.3 Summary of the effect of alcohol fuel on LTC engines

Blend types	Key inferences
Binary blends	• Decrease in peak cylinder pressure and heat release for lean mixture (Maurya and Agarwal 2014) • *n*-butanol gasoline blends shortens the combustion duration (less than 15° CA) and advances the auto-ignition • Decrease in NO_x and increase in CO and HC emission are observed • Increase in combustion efficiency (8.3%) and decrease in NO_x (26%), soot (71%), CO and HC emissions (~one third) in RCCI mode (Pedrozo et al. 2016) • Gasoline-n-butanol blends decrease NO_x, smoke, CO, HC emissions (Huang et al. 2016)
Ternary blends	• Ethanol–diesel–biodiesel (waste cooking oil) blends result in a decrease in BSFC and similar brake thermal efficiency • A decrease in NO_x and soot emission and an increase in CO (maximum of 100%) and HC (by 600 ppm) emission • Ethanol RCCI reduced engine knocking (Işık and Aydın 2016) • Increase in fuel consumption, BTE, peak cylinder pressure, and peak heat release rate in RCCI mode (Işık and Aydın 2016) • Shorter combustion duration and ignition delay, however, combustion duration increases with increase in premixed ratio • It is possible to decrease CO and HC emission by increasing alcohol content
Quaternary blends	• Higher brake thermal efficiency can be obtained • In RCCI mode, it is possible to achieve NO_x emission comply EURO VI norms • It is possible to decrease CO and HC emission by optimizing the alcohol content

5.4 Summary

The detailed discussion on alcohol fuels reveals that the alcohol fuels are capable of achieving low-temperate combustion by utilizing the entire advantages of this combustion concept. The oxygen content of alcohol fuel helps solve one of the major drawbacks of LTC such as higher CO and HC emissions. The alcohol fuels are reported to widen the operating load range of LTC. Thus, the various alcohol fuels become more suitable for LTC, and the conclusion of the chapter is presented in the next section.

5.5 Conclusions

This chapter provided the essential details of the alcohol fuel as alternate fuels for internal combustion engines. Alcohol fuels are characterized by their renewability, closer to the properties of gasoline, better adaptability with diesel and advantages of emission reduction. This chapter explained the potential of various alcohol fuels in terms of emission reduction when it is adapted to low-temperature combustion techniques. The alcohol fuel is found to be suitable for any mode of LTC such as HCCI, PCCI, PPC, and RCCI. The fuels are used without major or no modification of the existing engines. Moreover, alcohol fuels are one of the appropriate alternate fuels for the HCCI engine which effectively utilizes the full merits of LTC. The higher octane number, oxygen content, and lower latent heat of evaporation of alcohol fuels suit the requirement of reactivity stratification in RCCI engines. Alcohol fuels are capable of overcoming the major drawback of extending the operational range of LTC engines. Therefore, it is concluded that the alcohol fuel has the potential as effective alternative fuels and for reducing the harmful emissions from internal combustion engines especially in the LTC mode.

Nomenclature

B20	80% diesel and 20% biodiesel blend
BSNO	Brake-specific nitric oxide
BTE	Brake thermal efficiency
CI	Compression ignition
CO	Carbon monoxide
CO_2	Carbon dioxide
EGR	Exhaust gas recirculation
FFV	Flexible fuelled vehicles
HC	Hydrocarbon
HCCI	Homogeneous charge compression ignition

HRF	High-reactivity fuel
IMEP	Indicated mean effective pressure
ITE	Indicated thermal efficiency
LRF	Low-reactivity fuel
LTC	Low-temperature combustion
MTBE	Methyl tertiary butyl ether
PCCI	Premixed charge compression ignition
PPC	Partially premixed combustion
NO_x	Oxides of nitrogen
RCCI	Reactivity-controlled compression ignition
SI	Spark ignition
WB	Waste cooking biodiesel.

References

Amorim RJ, Novella R, Garcia A, Molina S (2017) Study on LTC for light duty engines—part 2—spray enhancements. Fuel 193:206–219. https://doi.org/10.1016/j.fuel.2016.12.050

Annual Fuel Ethanol Production (2020). https://ethanolrfa.org/statistics/annual-ethanol-production/, last accessed 2020/04/29

Appavu P, Ramanan MV, Venu H (2019) Quaternary blends of diesel/biodiesel/vegetable oil/pentanol as a potential alternative feedstock for existing unmodified diesel engine: performance, combustion and emission characteristics. Energy 186:115856. https://doi.org/10.1016/j.energy.2019.115856

Asad U, Kumar R, Zheng M, Tjong J (2015) Ethanol-fueled low temperature combustion: a pathway to clean and efficient diesel engine cycles. Appl Energy 157:838–850. https://doi.org/10.1016/j.apenergy.2015.01.057

ASTM Standard D5797-18 (2018) Standard specification for methanol fuel blends (M51–M85) for methanol-capable automotive spark-ignition engines. ASTM International, United States

ASTM Standard D7862-19 (2019) Standard specification for butanol for blending with gasoline for use as automotive spark-ignition engine fuel. ASTM International, United States

ASTM Standard D5798-20 (2020) Standard specification for ethanol fuel blends for flexible-fuel automotive spark-ignition engines. ASTM International, United States

Atmanli A, Yilmaz N (2020) An experimental assessment on semi-low temperature combustion using waste oil biodiesel/C3-C5 alcohol blends in a diesel engine. Fuel 116357. https://doi.org/10.1016/j.fuel.2019.116357

Benajes J, Molina S, García A, Monsalve-Serrano J (2015) Effects of direct injection timing and blending ratio on RCCI combustion with different low reactivity fuels. Energy Convers Manage 99:193–209. https://doi.org/10.1016/j.enconman.2015.04.046

Carlucci AP, Laforgia D, Motz S, Saracino R, Wenzel SP (2014) Advanced closed loop combustion control of a LTC diesel engine based on in-cylinder pressure signals. Energy Convers Manage 77:193–207. https://doi.org/10.1016/j.enconman.2013.08.054

Çelebi Y, Aydın H (2019) An overview on the light alcohol fuels in diesel engines. Fuel 890–911. https://doi.org/10.1016/j.fuel.2018.08.138

Clean Cities Alternative Fuel Price Reports (2020). https://afdc.energy.gov/fuels/prices.html, last accessed 2020/04/29

DelVescovo D, Wang H, Wissink M, Reitz RD (2015) Isobutanol as both low reactivity and high reactivity fuels with addition of di-tert butyl peroxide (DTBP) in RCCI combustion. SAE Int J Fuels Lubr 8(2):329–343. https://doi.org/10.4271/2015-01-0839

Dempsey AB, Walker NR, Reitz R (2013) Effect of cetane improvers on gasoline, ethanol, and methanol reactivity and the implications for RCCI combustion. SAE Int J Fuels Lubr 170–187. https://doi.org/10.4271/2013-01-1678

Doğan O (2011) The influence of n-butanol/diesel fuel blends utilization on a small diesel engine performance and emissions. Fuel 2467–2472. https://doi.org/10.1016/j.fuel.2011.02.033

Dou Z, Yao C, Wei H, Wang B, Liu M, Chen C, Gao J, Shi J (2017) Experimental study of the effect of engine parameters on ultrafine particle in dieselmethanol dual fuel engine. Fuel 192:45–52. https://doi.org/10.1016/j.fuel.2016.12.006

El-Asrag HA, Ju Y (2014) Direct numerical simulations of NOx effect on multistage autoignition of DME/air mixture in the negative temperature coefficient regime for stratified HCCI engine conditions. Combust Flame 161(1):256–269. https://doi.org/10.1016/j.combustflame.2013.07.012

Fang C, Yang F, Ouyang M, Gao G, Chen L (2013a) Combustion mode switching control in a HCCI diesel engine. Appl Energy 110:190–200. https://doi.org/10.1016/j.apenergy.2013.04.060

Fang Q, Fang J, Zhuang J, Huang Z (2013b) Effects of ethanol-diesel-biodiesel blends on combustion and emissions in premixed low temperature combustion. Appl Therm Eng 54(2):541–548. https://doi.org/10.1016/j.applthermaleng.2013.01.042

Fernando S, Hanna M (2005) Phase behavior of the ethanol-biodiesel-diesel micro-emulsion system. Trans Am Soc Agric Eng 48(3):903–908. https://doi.org/10.13031/2013.18494

Gallagher PW, Brubaker H, Shapouri H (2005) Plant size: capital cost relationships in the dry mill ethanol industry. Biomass Bioenerg 28(6):565–571. https://doi.org/10.1016/j.biombioe.2005.01.001

Han X, Zheng M, Wang J (2013) Fuel suitability for low temperature combustion in compression ignition engines. Fuel 109:336–349. https://doi.org/10.1016/j.fuel.2013.01.049

He BQ, Liu MB, Zhao H (2015) Comparison of combustion characteristics of n-butanol/ethanol-gasoline blends in a HCCI engine. Energy Convers Manag 95:101–109. https://doi.org/10.1016/j.enconman.2015.02.019

Huang H, Zhou C, Liu Q, Wang Q, Wang X (2016) An experimental study on the combustion and emission characteristics of a diesel engine under low temperature combustion of diesel/gasoline/n-butanol blends. Appl Energy 170:219–231. https://doi.org/10.1016/j.apenergy.2016.02.126

Ickes AM, Assanis DN, Bohac SV (2009) Load limits with fuel effects of a premixed diesel combustion mode. SAE Technical Paper, 4970. https://doi.org/10.4271/2009-01-1972

Işık MZ, Aydın H (2016) Analysis of ethanol RCCI application with safflower biodiesel blends in a high load diesel power generator. Fuel 184:248–260. https://doi.org/10.1016/j.fuel.2016.07.017

Jamrozik A (2017) The effect of the alcohol content in the fuel mixture on the performance and emissions of a direct injection diesel engine fueled with diesel-methanol and diesel-ethanol blends. Energy Convers Manage 148:461–476. https://doi.org/10.1016/j.enconman.2017.06.030

Kumar P, Rehman A (2017) Homogeneous charge compression ignition (HCCI) engines: a review. IOSR J Mech Civ Eng 11(6):47–67

Kwanchareon P, Luengnaruemitchai A, Jai-In S (2007) Solubility of a diesel-biodiesel-ethanol blend, its fuel properties, and its emission characteristics from diesel engine. Fuel 86(7–8):1053–1061. https://doi.org/10.1016/j.fuel.2006.09.034

Lapuerta M, García-Contreras R, Campos-Fernández J, Dorado MP (2010) Stability, lubricity, viscosity, and cold-flow properties of alcohol-diesel blends. Energy Fuels 24(8):4497–4502. https://doi.org/10.1021/ef100498u

Leermakers CAJ, Musculus MPB (2015) In-cylinder soot precursor growth in a low-temperature combustion diesel engine: laser-induced fluorescence of polycyclic aromatic hydrocarbons. Proc Combust Inst 35(3):3079–3086. https://doi.org/10.1016/j.proci.2014.06.101

Li Y, Jia M, Chang Y, Xie M, Reitz RD (2016) Towards a comprehensive understanding of the influence of fuel properties on the combustion characteristics of a RCCI (reactivity controlled compression ignition) engine. Energy 99(x):69–82. https://doi.org/10.1016/j.energy.2016.01.056

Lin J, Gaustad G, Trabold TA (2013) Profit and policy implications of producing biodiesel-ethanol-diesel fuel blends to specification. Appl Energy 104:936–944. https://doi.org/10.1016/j.apenergy.2012.11.049

Liu H, Ma G, Hu B, Zheng Z, Yao M (2018) Effects of port injection of hydrous ethanol on combustion and emission characteristics in dual-fuel reactivity controlled compression ignition (RCCI) mode. Energy 145:592–602. https://doi.org/10.1016/j.energy.2017.12.089

Mancaruso E, Vaglieco BM (2015) Spectroscopic analysis of the phases of premixed combustion in a compression ignition engine fuelled with diesel and ethanol. Appl Energy 143:164–75. https://doi.org/10.1016/j.apenergy.2015.01.031

Maurya RK, Agarwal AK (2011) Experimental study of combustion and emission characteristics of ethanol fuelled port injected homogeneous charge compression ignition (HCCI) combustion engine. Appl Energy 88(4):1169–1180. https://doi.org/10.1016/j.apenergy.2010.09.015

Maurya RK, Agarwal AK (2014) Experimental investigations of performance, combustion and emission characteristics of ethanol and methanol fueled HCCI engine. Fuel Process Technol 126:30–48. https://doi.org/10.1016/j.fuproc.2014.03.031

Merola SS, Tornatore C, Iannuzzi SE, Marchitto L, Valentino G (2014) Combustion process investigation in a high speed diesel engine fuelled with n-butanol diesel blend by conventional methods and optical diagnostics. Renew Energy 64:225–237. https://doi.org/10.1016/j.renene.2013.11.017

Niemeyer KE, Daly SR, Cannella WJ, Hagen CL (2015) Investigation of the LTC fuel performance index for oxygenated reference fuel blends. Fuel 155(x):14–24. https://doi.org/10.1016/j.fuel.2015.04.010

Ning L, Duan Q, Chen Z, Kou H, Liu B, Yang B, Zeng K (2020) A comparative study on the combustion and emissions of a non-road common rail diesel engine fueled with primary alcohol fuels (methanol, ethanol, and n-butanol)/diesel dual fuel. Fuel 117034. https://doi.org/10.1016/j.fuel.2020.117034

No SY (2016) Application of biobutanol in advanced CI engines—a review. Fuel 183:641–658. https://doi.org/10.1016/j.fuel.2016.06.121

Nour M, Attia AMA, Nada SA (2019) Combustion, performance and emission analysis of diesel engine fuelled by higher alcohols (butanol, octanol and heptanol)/diesel blends. Energy Convers Manag 313–329. https://doi.org/10.1016/j.enconman.2019.01.105

Pachiannan T, Zhong W, Rajkumar S, He Z, Leng X, Wang Q (2019) A literature review of fuel effects on performance and emission characteristics of low-temperature combustion strategies. Appl Energy 251(301):113380. https://doi.org/10.1016/j.apenergy.2019.113380

Pan S, Li X, Han W, Huang Y (2017) An experimental investigation on multi-cylinder RCCI engine fueled with 2-butanol/diesel. Energy Convers Manag 92–101. https://doi.org/10.1016/j.enconman.2017.10.047

Pan S, Liu X, Cai K, Li X, Han W, Li B (2020) Experimental study on combustion and emission characteristics of iso-butanol/diesel and gasoline/diesel RCCI in a heavy-duty engine under low loads. Fuel 116434. https://doi.org/10.1016/j.fuel.2019.116434

Pedrozo VB, May I, Lanzanova TDM, Zhao H (2016) Potential of internal EGR and throttled operation for low load extension of ethanol-diesel dual-fuel reactivity controlled compression ignition combustion on a heavy-duty engine. Fuel. https://doi.org/10.1016/j.fuel.2016.03.090

Pidol L, Lecointe B, Starck L, Jeuland N (2012) Ethanol-biodiesel-diesel fuel blends: performances and emissions in conventional diesel and advanced low temperature combustions. Fuel 93(x):329–338. https://doi.org/10.1016/j.fuel.2011.09.008

Pimentel D, Patzek TW (2005) Ethanol production using corn, switchgrass, and wood; biodiesel production using soybean and sunflower. Nat Resour Res 14(1):65–76. https://doi.org/10.1007/s11053-005-4679-8

Qian Y, Ouyang L, Wang X, Zhu L, Lu X (2015) Experimental studies on combustion and emissions of RCCI fueled with n-heptane/alcohols fuels. Fuel. https://doi.org/10.1016/j.fuel.2015.09.022

Rajesh Kumar B, Saravanan S (2016) Effects of iso-butanol/diesel and n-pentanol/diesel blends on performance and emissions of a di diesel engine under premixed LTC (low temperature combustion) mode. Fuel 170:49–59. https://doi.org/10.1016/j.fuel.2015.12.029

Rakopoulos CD, Dimaratos AM, Giakoumis EG, Rakopoulos DC (2010) Investigating the emissions during acceleration of a turbocharged diesel engine operating with bio-diesel or n-butanol diesel fuel blends. Energy 35(12):5173–5184. https://doi.org/10.1016/j.energy.2010.07.049

Reang NM, Dey S, Debbarma B, Deb M, Debbarma J (2020) Experimental investigation on combustion, performance and emission analysis of 4-stroke single cylinder diesel engine fuelled with neem methyl ester-rice wine alcohol-diesel blend. Fuel 117602. https://doi.org/10.1016/j.fuel.2020.117602

Satgé De Caro P, Mouloungui Z, Vaitilingom G, Berge JC (2001) Interest of combining an additive with diesel-ethanol blends for use in diesel engines. Fuel 565–574. https://doi.org/10.1016/S0016-2361(00)00117-4

Shirazi SA, Abdollahipoor B, Windom B, Reardon KF, Foust TD (2019) Effects of blending C3-C4 alcohols on motor gasoline properties and performance of spark ignition engines: a review. Fuel Process Technol 106194. https://doi.org/10.1016/j.fuproc.2019.106194

Soloiu V, Duggan M, Harp S, Vlcek B, Williams D (2013) PFI (port fuel injection) of n-butanol and direct injection of biodiesel to attain LTC (low-temperature combustion) for low-emissions idling in a compression engine. Energy 52:143–154. https://doi.org/10.1016/j.energy.2013.01.023

Splitter DA, Reitz RD (2014) Fuel reactivity effects on the efficiency and operational window of dual-fuel compression ignition engines. Fuel 118:163–175. https://doi.org/10.1016/j.fuel.2013.10.045

Srihari S, Thirumalini S (2017) Investigation on reduction of emission in PCCI-DI engine with biofuel blends. Renew Energy 114:1232–1237. https://doi.org/10.1016/j.renene.2017.08.008

Su J, Zhu H, Bohac SV (2013) Particulate matter emission comparison from conventional and premixed low temperature combustion with diesel, biodiesel and biodiesel-ethanol fuels. Fuel 113:221–227. https://doi.org/10.1016/j.fuel.2013.05.068

Thangaraja J, Srinivasan V (2019) Techno-economic assessment of coconut biodiesel as a potential alternative fuel for compression ignition engines. Environ Sci Pollut Res 26(9):8650–8664. https://doi.org/10.1007/s11356-018-04096-9

Turkcan A, Ozsezen AN, Canakci M (2014) Experimental investigation of the effects of different injection parameters on a direct injection HCCI engine fueled with alcohol-gasoline fuel blends. Fuel Process Technol 126:487–496. https://doi.org/10.1016/j.fuproc.2014.05.023

Tutak W (2014) Bioethanol E85 as a fuel for dual fuel diesel engine. Energy Convers Manage 86:39–48. https://doi.org/10.1016/j.enconman.2014.05.016

Xing-Cai L, Jian-Guang Y, Wu-Gao Z, Zhen H (2004) Effect of cetane number improver on heat release rate and emissions of high speed diesel engine fueled with ethanol-diesel blend fuel. Fuel 83:14–15. https://doi.org/10.1016/j.fuel.2004.05.003

Xue J, Grift TE, Hansen AC (2011) Effect of biodiesel on engine performances and emissions. Renew Sustain Energy Rev 15(2):1098–1116. https://doi.org/10.1016/j.rser.2010.11.016

Yesilyurt MK, Aydin M, Yilbasi Z, Arslan M (2020) Investigation on the structural effects of the addition of alcohols having various chain lengths into the vegetable oil-biodiesel-diesel fuel blends: an attempt for improving the performance, combustion, and exhaust emission characteristics of a compression ignition engine. Fuel 117455. https://doi.org/10.1016/j.fuel.2020.117455

Yousefi A, Guo H, Birouk M (2018) An experimental and numerical study on diesel injection split of a natural gas/diesel dual-fuel engine at a low engine load. Fuel 332–346. https://doi.org/10.1016/j.fuel.2017.10.053

Yusri IM, Mamat R, Najafi G, Razman A, Awad OI, Azmi WH, Ishak WFW, Shaiful AIM (2017) Alcohol based automotive fuels from first four alcohol family in compression and spark ignition engine: a review on engine performance and exhaust emissions. Renew Sustain Energy Rev 169–181. https://doi.org/10.1016/j.rser.2017.03.080

Zhang Q, Yao M, Zheng Z, Liu H, Xu J (2012) Experimental study of n-butanol addition on performance and emissions with diesel low temperature combustion. Energy 47(1):515–521. https://doi.org/10.1016/j.energy.2012.09.020

Zheng Z, Xia M, Liu H, Shang R, Ma G, Yao M (2018) Experimental study on combustion and emissions of n-butanol/biodiesel under both blended fuel mode and dual fuel RCCI mode. Fuel 226:240–251. https://doi.org/10.1016/j.fuel.2018.03.151

Zhu L, Cheung CS, Zhang WG, Huang Z (2011) Combustion, performance and emission characteristics of a di diesel engine fueled with ethanol-biodiesel blends. Fuel 90(5):1743–1750. https://doi.org/10.1016/j.fuel.2011.01.024

Zhu L, Qian Y, Wang X, Lu X (2015) Effects of direct injection timing and premixed ratio on combustion and emissions characteristics of RCCI (reactivity controlled compression ignition) with N-heptane/gasoline-like fuels. Energy 93:383–392. https://doi.org/10.1016/j.energy.2015.09.069

Chapter 6
Challenges in Blending the Diesel–Ethanol Blends Using Butanol as Co-solvent Along with Diesel for Replacing the Neat Diesel to Fuel Compression Ignition Engines Suitable for Low-Temperature Application

B. Prabakaran

6.1 Introduction

Renewable energy resources are the major available resources to replace diesel fuel and reduce the dependency of diesel fuel to fuel compression ignition (CI) engines. This is the reason for the researchers to find out a renewable source such as alcohols or biodiesels from various edible or non-edible oils to reduce the consumption of diesel by blending to fuel CI engines. Alcohols are better than biodiesels in terms of combustion efficiency and emissions when fueled in compression ignition engines. Utilization of biodiesel from edible resources as fuel will lead to lack of resource for food. Ethanol (Han et al. 2020) can be blended into diesel for fueling in diesel engine which can be manufactured from biomass. The author utilized ethanol into diesel engine in a dual-fuel mode up to 80% and tested for performance. Author concluded that although 80% blending of ethanol is possible for blending, the increase in the ethanol content increased the ignition delay and decreased the thermal efficiency. It was also reported that misfire occurred by fueling blends containing higher volume of ethanol (higher than 30%) into diesel engine. The limitations in using biodiesel (Shamun et al. 2018; Belgiorno et al. 2018; Mamat et al. 2019) as fuel were stated by the author and recommended for low volume of biodiesel (up to 20%) along with diesel in diesel engine. The author also stated that there was a significant decrease in power by the utilization of biodiesel into CI engine. This motivated the researchers to increase the focus on fueling the CI engines with alcohol-blended diesel instead of

B. Prabakaran (✉)
Department of Automobile Engineering, Hindustan Institute of Technology and Science, Chennai, Tamil Nadu, India
e-mail: b7prabakaran@gmail.com

P. C. Shukla et al. (eds.), *Alcohol as an Alternative Fuel for Internal Combustion Engines*, Energy, Environment, and Sustainability,
https://doi.org/10.1007/978-981-16-0931-2_7

Table 6.1 Properties of fuels standard

S. No.	Property	Diesel	Ethanol	Butanol
1	Density (kg/m^3)	829	785	809
2	Kinematic viscosity (mm^2/s)	4.04	1.07	2.6
3	Calorific value (MJ/kg)	42.8	26.9	33.1
4	Heat of vaporization (MJ/kg)	0.84	0.92	0.43
5	Flammability limits, volume (%)	0.6	19	11.2
6	Flashpoint (°C)	74	13	35
7	Cetane number	50	8	25
8	Research octane number	15–25	129	96
9	Energy density (MJ/L)	45.5	19.6	29

biodiesel-blended diesel. The utilization of methanol is not found attractive as this is meant as poisonous. This paved a way to progress to the next lower alcohol ethanol and its blend with diesel to fuel CI engine. Ethanol started its attempt as fuel for CI engines from 1980s onward. Compilation of previous researches for the utilization of diesel–methanol and diesel–ethanol blends (Kumar et al. 2013) into diesel engine was reported. The author conducted a study on the solubility, properties, and performance of these blends by fueling into CI engine. Table 6.1 shows the standard properties of diesel, ethanol, and butanol (Gao et al. 2019). From the table, the research octane number of ethanol is very much higher, this will lead to higher rate of combustion, and hence, ethanol has been chosen.

The author concluded that further research on the utilization of higher volume of ethanol in ethanol–diesel and higher volume of butanol in butanol–diesel blends can be further progressed in low-temperature analysis. Flame spread characteristics (Singh and Bharj 2019) of ethanol–diesel (containing 5% ethanol) in a CI engine have been compared with that of diesel. The author stated that the flame spread speed was found decreased at the initial phase and remains unchanged after certain height of ullage. This was due to the increase in the combustion efficiency and the rate of oxidation due to the higher oxygen content in the ethanol–diesel blends compared to that of diesel. A study was conducted by fueling 20% of ethanol along with Jatropha methyl ester and diesel blends on the evaporation characteristics in CI engine. It was reported that the liquid penetration and vapor penetration of the ethanol-blended biodiesel–diesel blends were found matching with that of diesel. The improvement in the evaporation rate of the fuel blend was due to the higher heat of vaporization of ethanol in the blend and the higher boiling point of the biodiesel in the blend. Ethanol was blended with diesel up to 19% and studied (Rakopoulos et al. 2019) for the essential properties such as cetane number, calorific value, sulfur content, and flashpoint. The author reported that the properties are found to be closer with respect to that of diesel fuel and suitable to fuel CI engine. The author also studied the performance and emissions characteristics of ethanol–diesel blends when fueled in CI engine. The report indicated that there was a significant increase in brake

thermal efficiency, decrease in the emissions and exhaust temperature by utilizing ethanol–diesel blend in CI engine. Cyclic irregularities of diesel–ethanol (Yu 2019) and diesel–butanol blends were compared when fueled in CI engine as fuel to replace diesel. The author stated that the cyclic variations produced by diesel–ethanol blends were found to be a bit stronger compared to those produced by diesel–butanol blends. The author stated that the reason for this activity was due to the fuel-bound oxygen possessed by ethanol in the blend. Most researchers attempted diesel–ethanol blends as fuel; however, attempts are limited for the fuel blend (Woo et al. 2016; Verma et al. 2018; Ribeiro et al. 2007; Hafid et al. 2017) possessing higher volume of ethanol and for low temperatures. Hence, this experimental study considers the objective as utilizing higher volume of ethanol under low temperature up to 5 °C with the assistance of n-butanol as co-solvent.

6.2 Materials and Methods

6.2.1 Fuels Used and Preparation of Blends

Diesel used in this study is Bharat Stage VI of low-sulfur diesel procured from market. Ethanol is procured from bioethanol producer who produces bioethanol (Stoeberl et al. 2011) from waste cut vegetables. These wastes are generally not utilized properly and thrown into garbage and causing land pollution to a greater extent. Biobutanol is procured from a bulk manufacturer who produces butanol from food (Hansen et al. 2005) wastages. **This is the novelty in this study**. To start with, biobutanol has been blended in proportions (Table 6.2) ranging from 0 to 10% in increments of 1% and kept separately. Table 6.2 lists the different proportions of diesel, ethanol, and butanol.

These biobutanol–diesel blends were taken in a beaker for blending of bioethanol. Bioethanol was filled in burette and slowly added into biobutanol–diesel blends in the proportions ranging from 0–50% in increments of 5% of bioethanol assisted with magnetic stirring. This was carefully handled such that bioethanol will not evaporate during the process of blending. The magnetic stirrer (Fig. 6.1) was operated at a speed of 1500 rpm and for a set cycle of 2 min.

Each blend has been stirred for three to five times, and the prepared blends were kept in a temperature-controlled box (Fig. 6.2) for five different temperatures 5, 10, 15, 20, and 25 °C. This temperature range has been chosen by considering the climatic conditions of India. In India, most part of the country (Prabakaran and Vijayabalan 2016) will attain 5 °C during the winter season. The fuel blend found by this study has to be suitable to fuel CI engine for most places in our country.

Fuel blends after the temperature stability tests are presented in Fig. 6.3. Figure 6.3 shows three representative samples kept at 5 (Fig. 6.5), 15 (Fig. 6.4), and 25 °C (Fig. 6.3) for a period of 20 days. Periodical monitoring has been performed, and the statuses of the blends were recorded. This is to find out the homogeneity of the fuel

Table 6.2 Various proportions of diesel–ethanol blends by varying butanol from 0–10%

Percentage of butanol	Fuels in percentage by volume										
1	D	94	89	84	79	74	69	64	59	54	49
	E	5	10	15	20	25	30	35	40	45	50
2	D	93	88	83	78	73	68	63	58	53	48
	E	5	10	15	20	25	30	35	40	45	50
3	D	92	87	82	77	72	67	62	57	52	47
	E	5	10	15	20	25	30	35	40	45	50
4	D	91	86	81	76	71	66	61	56	51	46
	E	5	10	15	20	25	30	35	40	45	50
5	D	90	85	80	75	70	65	60	55	50	45
	E	5	10	15	20	25	30	35	40	45	50
6	D	89	84	79	74	69	64	59	54	49	44
	E	5	10	15	20	25	30	35	40	45	50
7	D	88	83	78	73	68	63	58	53	48	43
	E	5	10	15	20	25	30	35	40	45	50
8	D	87	82	77	72	67	62	57	52	47	42
	E	5	10	15	20	25	30	35	40	45	50
9	D	86	81	76	71	66	61	56	51	46	41
	E	5	10	15	20	25	30	35	40	45	50
10	D	85	80	75	70	65	60	55	50	45	40
	E	5	10	15	20	25	30	35	40	45	50

D—Diesel, *E*—Bioethanol, *B*—Biobutanol

blend and to ensure that there is no phase separation between diesel and alcohols. The blends were also kept under 30 and 35 °C for 20 day. The blends are in the single liquid phase and no separation has been observe.

6.2.2 Testing the Properties of Fuel Blends

Prepared fuel blends (100 blends) were tested for the essential properties required as per the ASTM standards, and the properties were compared (Prabakaran et al. 2017) with respect to the diesel fuel as base. The instruments used for the properties along with the accuracy and ASTM standards are listed in Table 6.3. Table 6.4 lists the properties of five representative fuel blends (Prabakaran et al. 2019) containing 15, 25, 35, 45 and 50% of ethanol in comparison with that of diesel.

Fig. 6.1 Magnetic stirrer used for the blend preparation

Fig. 6.2 Temperature control box for storing the prepared blend in various temperatures

Fig. 6.3 Representative blends of diesel–ethanol with 10% *n*-butanol kept at 25 °C after 20 days

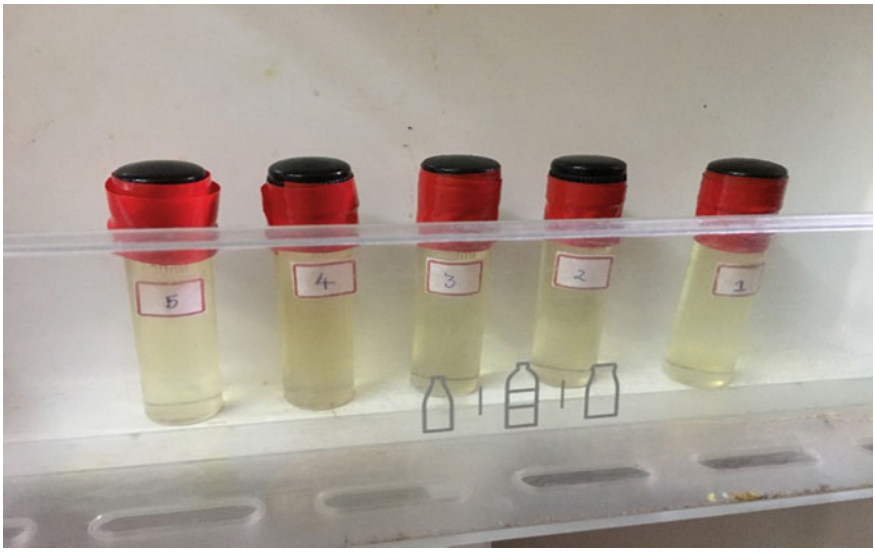

Fig. 6.4 Representative blends of diesel–ethanol with 10% *n*-butanol kept at 15 °C after 20 days

Fig. 6.5 Representative blends of diesel–ethanol with 10% *n*-butanol kept at 5 °C after 20 days

Table 6.3 List of instrument used for property testing

S. No.	Property	Unit	Instrument used	Accuracy	Percentage of uncertainty	ASTM standard
1	Flashpoint	℃	Pensky–Martens Closed cup	±0.1℃	±0.05%	ASTMD 93-16a
2	Kinematic viscosity	mm^2/s	Red wood viscometer	0.01 Centi Stokes	±0.02%	ASTMD445/446
3	Calorific value	kJ/kg	Bomb calorimeter	1 J/grams	±0.1%	ASTMD 4868
3	Cetane Number	No unit	Ignition delay	±0.1	±0.07%	ASTMD976/ASTMD4737

6.2.3 Experiment Setup

A single cylinder, four-stroke, water-cooled, direct injection, Kirloskar make diesel engine (Holman and Gajda 2001) of 4.4 kW capacity at the rated speed 1500 rpm was used for testing the fuel blends. The engine (Fig. 6.6) is coupled with eddy current dynamometer with electrical loading.

Fuel flow was measured with the help of burette and digital stop watch. Intake air flow was monitored by manometer and orifice plate. The displacement volume of the engine used was 661.5 cc, with a compression ratio of 17.5:1, and nozzle opening pressure was set at 200–205 bar. A provision was made for mounting the

Table 6.4 Properties of diesel–ethanol–butanol blends

Blend	Flashpoint	Energy content	Density	Kinematic viscosity	Oxygen content	Cetane number
Units	°C	MJ/kg	kg/m^3	mm^2/s	%	
Diesel	74	42.8	829	4.04	0	50
Ethanol	13	26.9	790	1.37	34.8	8
n-butanol	35	33.1	809	3.2	21.58	25
D75E15B10	64	40.24	823	3.7	5.64	43.3
D65E25B10	57.9	38.65	818	3.45	9.12	39.1
D55E35B10	51.8	37.06	813	3.19	12.59	34.9
D45E45B10	47.5	37.13	807	2.94	17.16	30.7
D40E50B10	39.6	33.88	805	2.62	19.6	26.5

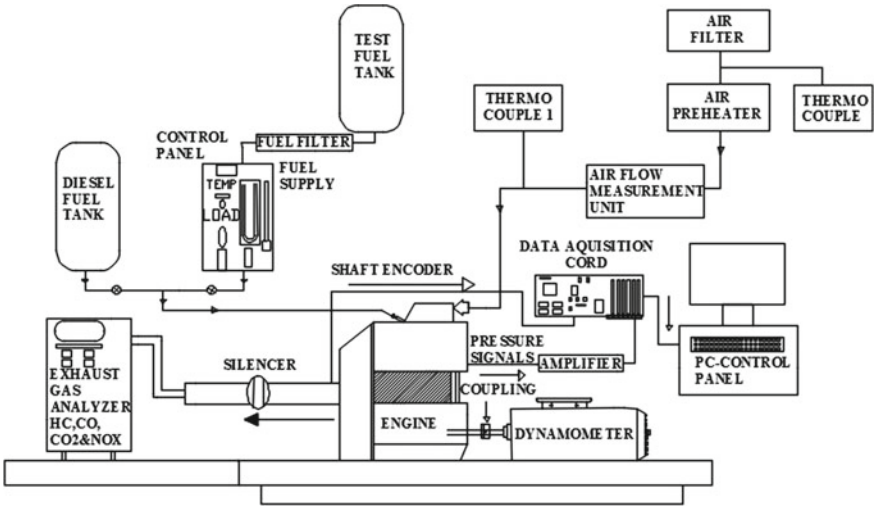

Fig. 6.6 Schematic layout of experimental setup

pressure transducer to capture the in-cylinder pressure signals during combustion and to feed the captured signals to the data acquisition device. The injection system of the experimental setup was mechanically controlled type, and this was periodically cleaned and calibrated as per the recommendations of the manufacturers. Air preheater is used to preheat the incoming air, and it is fixed in the suction side of the engine. In the present study, a heater of coil type of 1.0 kVA capacity is used for heating the incoming air. The temperature of the coil can be varied by varying the input electrical supply by a power regulator installed with the heater. The temperature of the incoming air to the air preheater and outgoing air from the air preheater has been measured by two separate thermocouple enabled with electronic readout. In the present study, a single, three-hole jet injector is deployed assisted by the mechanical

Fig. 6.7 Pressure calibration gage for fuel injector

centrifugal-type governor for injecting the fuel into the cylinder. The nozzle opening pressure is maintained at 200 bar. Variation of injection pressure was done by placing a washer of 0.20 mm for every 10 bar variation in between the nozzle and injector spring. The nozzle opening pressure was measured by calibrated gage with dial. The injector was clamped in the arms of the gage (Fig. 6.7), and the tripping fuel pressure was measured and indicted in the dial. This ensured the proper setting of the nozzle opening pressure. Normal injection timing is maintained at 23 °bTDC. Variation of injection timing was done by placing a shim of 0.25 mm (to attain 3° advance) between engine and fuel pump. The shim used has been calibrated and supplied by the manufacturer to attain the specified angle. Data acquisition system used for the present study consists of a computer, programmed with AVL 621 Indi-Modul system, which is receiving the signals amplified by a charge amplifier from a water-cooled pressure transducer of KISTLER piezoelectric transducer. This system was controlled by IndiCom software. Specifications of the pressure transducer are given in Appendix 4. This device was programmed for generating the combustion data according to the pressure input. Crank angle encoder captures the position of the crank angle of the respective pressure signal and was duly connected to the engine.

Hundred consecutive cycles of pressure data were captured and recorded for the analysis of combustion characteristics in the data acquisition system. This data acquisition system is programmed for combustion parameters calculation from the input received from the pressure transducer, crank angle encoder, and intake air measurement. This also receives the input from the thermocouples for the temperature of the intake air, exhaust gases, and in-cylinder. AVL-444 Di-Gas analyzer is used in this study for capturing the emissions from the test engine fuelled by the blends during the experiment. This measures CO, HC, NO_x, and CO_2 and oxygen concentration. It uses non-dispersive infrared (NDIR) sensor for measuring CO, CO_2, and HC.

Also, it measures NO_x and oxygen concentrations by electrochemical sensors. All the emissions are recorded and converted to g/kWh for further analysis. This device is auto-calibrated periodically as per the manufacturer advice. The measured values from the exhaust gas analyzer are in ppm (Gnanamoorthi and Devaradjane 2015), and the following conversion equations depict the conversion of ppm to g/kWhr which are standard equations (assuming 5% residual oxygen).

1000 ppm of NO_x corresponds to 6.60 g/kWh
100 ppm of HC corresponds to 0.20 g/kWh
100 ppm of CO corresponds to 0.36 g/kWh.

6.2.4 Experimental Uncertainty

Any experiment has its own uncertainty, and the overall uncertainty depends on the uncertainties of the various instruments used in the study and environment. In the present study, various instruments have been used, and each one has different level of uncertainty. This affects the final result. Hence, a detailed uncertainty analysis was carried out by the method of (Kuszewski 2018). The method implemented is recording five consecutive readings for each setting, and the average of these five readings was considered. The error included in these readings was found by using root mean square method. The maximum uncertainty of the experiment was arrived as ±1.3%. The uncertainty in any measured parameter was estimated based on Gaussian distribution method with confidence limits of $\pm 2\sigma$ (95% of measured data lie within the limits of 2σ of mean). Thus, the uncertainty (Eq. (6.1)) was estimated using the following equation:

$$\text{Uncertainty of any measured parameter } (\Delta x_i) = \left(2\sigma_i / \overline{X_i}\right) * 100 \tag{6.1}$$

Experiments were conducted to obtain the mean $(\overline{X_i})$ and standard deviation (σ_i) of any measured parameter (X_i) for a number of readings. Engine was allowed to operate at a typical operating condition. The number of readings (minimum five readings) was taken for speed, load, temperature, pressure, exhaust gas emissions, and time taken for a specified volume of diesel consumption. Some of the measuring instruments and its ranges, accuracy, and the percentage of uncertainties are given at the end of this explanation. From the uncertainties of the measured parameters, the uncertainties in computed parameters are evaluated by using an expression, which is derived as follows. If an estimated quantity R depends on independent variable like $(x_1, x_2, x_3, \ldots, x_n)$, then the error in the value of "*R*" is given by equation

$$R = f(x_1, x_2, \ldots, x_n) \tag{6.2}$$

with "*R*" as the computed result function of the independent measured variables x_1, x_2, x_3, …, x_n, as per the relation equation $x_1 \pm \Delta x_1$, $x_2 \pm \Delta x_2$, …, $x_n \pm \Delta x_n$ as

the uncertainty limits for the measured variables or parameters and the error limits for the computed result as $R \pm \Delta R$. To get the realistic uncertainty limits for the computed result, the principle of root mean square method (Eq. (6.3)) was used to get the magnitude of error given by Holman et al.

$$\Delta R = \left[\left(\frac{\partial R}{\partial x_1} \Delta x_1 \right)^2 + \left(\frac{\partial R}{\partial x_2} \Delta x_2 \right)^2 + \cdots + \left(\frac{\partial R}{\partial x_n} \Delta x_n \right)^2 \right]^{1/2} \tag{6.3}$$

Using equation, the uncertainties in the computed values such as brake power, brake thermal efficiency, and fuel flow measurements were estimated. The measured values such as speed, load, fuel time, voltage, and current were estimated from their respective uncertainties based on the Gaussian distribution.

The estimated uncertainty values at a typical operating condition are given below:

Speed: ±0.12%	Load: ±0.49%
Mass flow rate of air: ±0.62%	Mass flow rate of diesel: ±0.87%
Brake power: ±0.25%	Brake thermal efficiency: ±0.27%
NO_x: ±1.1%	Hydrocarbon: ±0.01%
CO ±0.8%	Smoke: ±1.3%

There are various methods available to reduce the errors observed in the instruments such as selecting the instruments according to the measurement level required (range of measurement), accuracy of the instrument used, and sensitivity, and this experiment was conducted by deploying the appropriate instruments within the range of measurement, accuracy, and sensitivity requirement.

6.3 Results and Discussion

Cylinder pressure diagram with respect to crank angle is the indication of effect of in-cylinder combustion in an engine. Generally, cylinder pressure of any engine depends on the volatility of the fuel used, time duration of combustion, rate of heat release, and energy content of the fuel. It is seen from Fig. 6.8 that higher in-cylinder pressure is produced by blends D75E15B10 and D65E25B10 compared to diesel.

This is due to the improved complete combustion of the blends by the addition of ethanol to a certain extent. However, fuel blends D55E35B10 and D45E45B10 produce lesser in-cylinder pressure compared to diesel (Pinzi et al. 2018). This is due to the suppression of combustion by the higher volume of ethanol in the blends, which is due to higher heat of vaporization. It can also be observed from figure that the peak pressure from D75E15B10 and D65E25B10 is found to be higher by 6.4% and 15.2% compared to diesel. Figure 6.9 shows the variation of in-cylinder peak pressure versus brake power for the blends. It is seen that the addition of ethanol (up

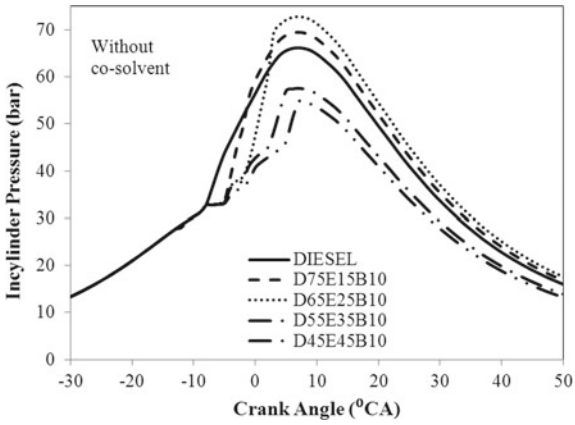

Fig. 6.8 Variation of in-cylinder pressure versus crank angle

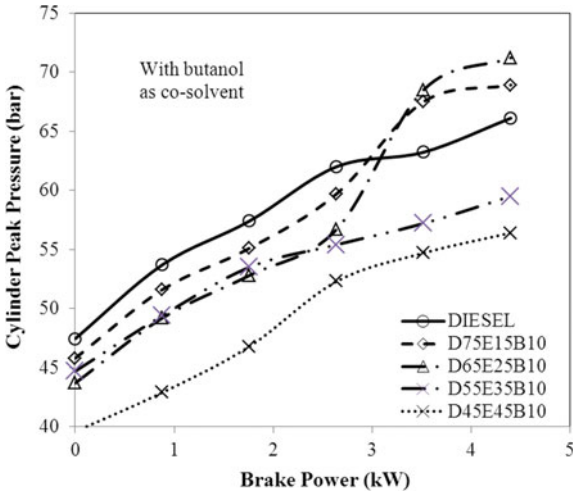

Fig. 6.9 Variation of in-cylinder peak pressures of diesel–ethanol–butanol blends

to a volume of 25%) into diesel increases the in-cylinder peak pressure significantly. Also, the increase in the in-cylinder peak pressure is found proportional to the increase in brake power. This is due to the improvement in the physico-chemical properties of the blends by the addition of ethanol. The improvement in kinematic viscosity (Yilmaz 2012) and density results in better atomization which leads to the more complete combustion.

It is also seen that the addition of ethanol into diesel (higher than 25% by vol.) reduces the in-cylinder peak pressure significantly. This is due to the dominance of heat of vaporization of the blends with the increase in the volume of ethanol (higher than 25% by vol.) in the blend. This produces a cooling effect which results in poor atomization and low rate of oxidation which results in lower in-cylinder peak pressure. The increases in in-cylinder peak pressure of D75E15B10 and D65E25B10

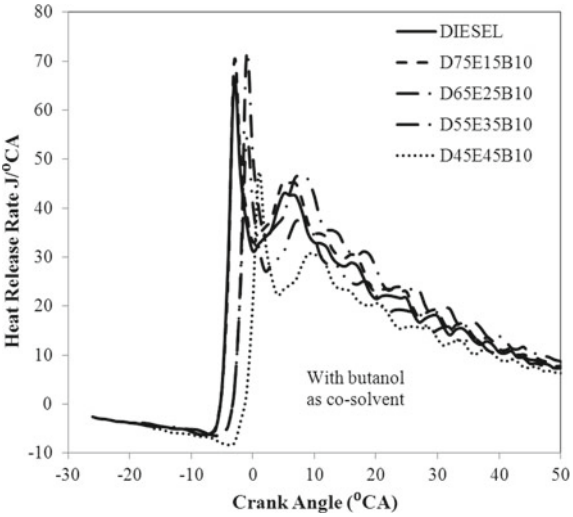

Fig. 6.10 Variation of HRR of fuel blends with crank angle at rated power

significantly. Also, the increase in the in-cylinder peak pressure is found proportional to the increase in brake power. This is due to the improvement in the physico-chemical properties of the blends by the addition of ethanol. Heat release rate is an indicator of combustion efficiency, and these parameters is helping for explaining the brake thermal efficiency (BTE), exhaust gas temperature, rate of pressure rise, emission parameters, and cylinder pressure.

Figure 6.10 shows the variation of HRR of fuel blends with 10% butanol as co-solvent without any modification under full load condition. HRR graphs are generated at all loads, and for representation HRR at full load condition is presented. It can be seen from figure that ethanol addition up to 25% increases the HRR to a greater extent due to the enhanced combustion behavior resulted from better atomization. However, the increase in ethanol content beyond 25% decreases HRR of the blends due to poor atomization which result in lower heat release rate. From figure, it is also seen that the blends containing lower ethanol offer higher HRR and blends containing higher ethanol offer lower HRR. The peak HRR of the blends occurs an angle away from that of diesel with respect to top dead center. The combustion duration of the blends containing lower ethanol is shorter than that of blends containing higher ethanol content.

The increases of HRR of D65E15B10 and D55E25B10 are found to be 8.8 and 12.9% higher compared to diesel (Verma et al. 2018). It can be observed from Fig. 6.11 that two (Ghadikolaei et al. 2018) blends D75E15B10 and D65E25B10 offered higher BTE compared to diesel at all load conditions. This is due to an increase in volatility and an improvement in spray characteristics of the fuel blends till the addition of 25% of ethanol into diesel. This results in higher BTE. However, for the two blends D55E35B10 and D45E45B10 produced lower BTE compared to diesel. This is mainly due to the decrease in self-ignition property of the final blend by the presence of higher volume of ethanol due to this increase in the heat

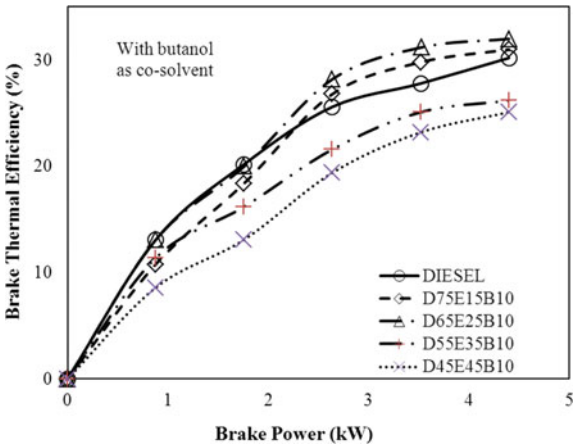

Fig. 6.11 Variation of brake thermal efficiency versus brake power

of vaporization. This increase in heat of vaporization produces cooling effect in the in-cylinder thereby reducing the temperature which in turn reduces the reactivity of oxygen with the fuel. The increases of BTE for D75E15B10 and D65E25B10 are found to be 4.1 and 9.2% higher compared to diesel at full load condition (Kuszewski 2018).

Also, the decreases of BTE for the blends D55E25B10 and D45E45B10 are found to be 1.9 and 2.6% lower than diesel. Variations of EGT versus brake power for the blends are presented in Fig. 6.12. It is seen that the EGT of the blends containing higher volume of ethanol produced a cooling effect by the dominance of heat of vaporization of the final blends. This produces a cooling effect in the in-cylinder

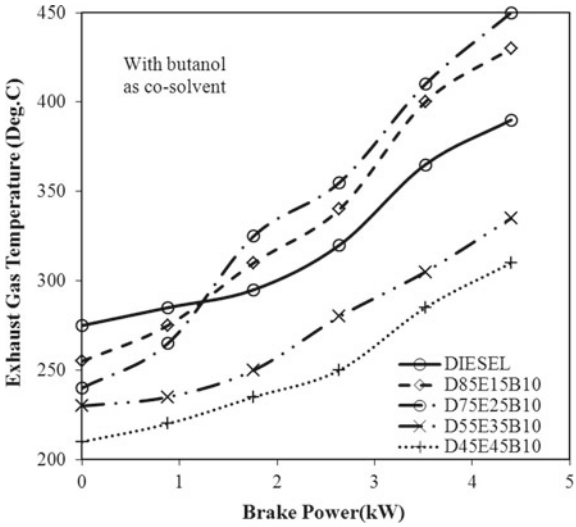

Fig. 6.12 Variations of exhaust gas temperature versus brake power

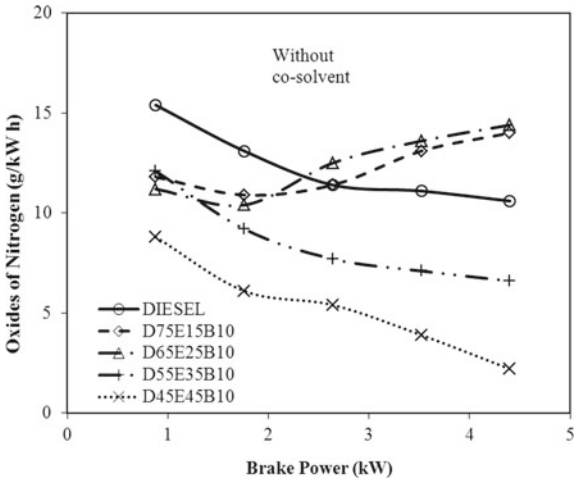

Fig. 6.13 Variation of NO_x emissions of fuel blends versus brake power

which reduces the rate of reaction of fuel particles with oxygen available in the in-cylinder and results in lower BTE and lower EGT. This is the main reason for the decrease in EGT of D55E35B10 and D45E45B10 (Rakopoulos et al. 2014). The increases of EGT for the blends D75E15B10 and D65E25B10 are found to be higher by 16.9% and 22.6%, respectively, compared to diesel at rated power. The decreases of EGT for the blends D55E35B10 and D45E45B10 are found to be 13.6% and 20.4%, respectively, compared to diesel at rated power. This emission from a CI engine is an indication of degree of complete combustion and higher temperature of the in-cylinder (as the formation of oxides of nitrogen is a higher-temperature reaction). From Fig. 6.13, it can be seen that the blends containing lower volume of ethanol (less than 25%) produce higher NO_x emissions and the blends containing higher volume of ethanol (more than 25%) produce lower NO_x emissions compared to diesel. This is mainly due to the higher temperature has been offered by the blends of lower ethanol content and lower temperature offered by the blends containing higher ethanol content. Also, the addition of ethanol up to 25% by volume improves the volatility, atomization of the fuel blends in the in-cylinder, and self-ignition property of the final blend. This is due the higher heat of vaporization of ethanol which suppresses the combustion temperature to a greater extent. D75E15B10 and D65E15B10 offer higher NO_x emissions and are found to be 2.6% and 7.6% higher compared to diesel. However, D55E35B10 and D45E45B10 offer significantly lower NO_x emissions compared to diesel (Rakopoulos et al. 2008). Smoke emissions from a CI engine are also an indication of low temperature of in-cylinder during combustion and the availability of oxygen for combustion of fuel. Figure 6.14 indicates the smoke emissions of blends containing 15, 25, 35, and 45% of ethanol with 10% butanol as co-solvent. From the figure, it is observed that D65E25B10 offers the lowest smoke emissions compared to those produced by other blends. This is due to the improved combustion characteristics of the final blend containing ethanol up to 25% by volume. More specifically, the addition of ethanol up to 25% by volume

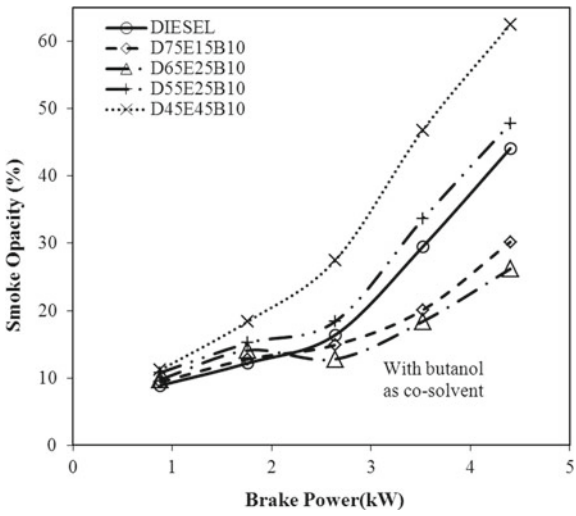

Fig. 6.14 Variation of smoke emissions versus brake power

improves the evaporation rate of the final blend, which leads to a shorter duration for combustion, thereby offering higher temperature.

This enhances the fuel blend to produce lesser smoke emissions compared to diesel and other blends. However, addition of ethanol higher 25% increases the heat of vaporization of the final blend which suppresses the combustion temperature and hence offers lower in-cylinder temperature. This lower temperature reduces the reactivity of oxygen in the in-cylinder, which results in higher smoke emissions. This is the main reason for the higher smoke emissions from D55E35B10 and D45E45B10 compared to diesel. Carbon monoxide emissions from any CI engine are an indication of efficiency of combustion, degree of temperature of the in-cylinder during combustion, availability of oxygen for combustion, and self-ignition property of the fuel utilized in the engine. The present work utilized 15, 25, 35, and 45% of ethanol which possesses higher heat of vaporization.

Hence, this volume of ethanol offers lower temperature in the in-cylinder resulting in higher CO emissions from the blends containing higher volume of ethanol compared to diesel. From Fig. 6.15, it can be seen that blends containing lower volume of ethanol produce lower CO emissions and blends containing high volume of ethanol produce higher CO emissions. This is mainly due to the improvement in the physical and chemical properties of the blend containing lower volume of ethanol (up to 25%) which reduces the CO emissions to a greater extent. Lower volume of ethanol improves the volatility and better atomization of the final blend, which enhances complete combustion and gives out lesser CO emissions compared to diesel. However, addition of ethanol higher than 25% to diesel increases the heat of vaporization to a greater extent which produces a cooling effect in the in-cylinder and hence produces higher CO emissions. This is also due to the slow rate of reactivity of oxygen with fuel during the combustion D75E15B10 and D65E25B10 produce lower CO emissions and D55E35B10 and D45E45B10 produce higher CO

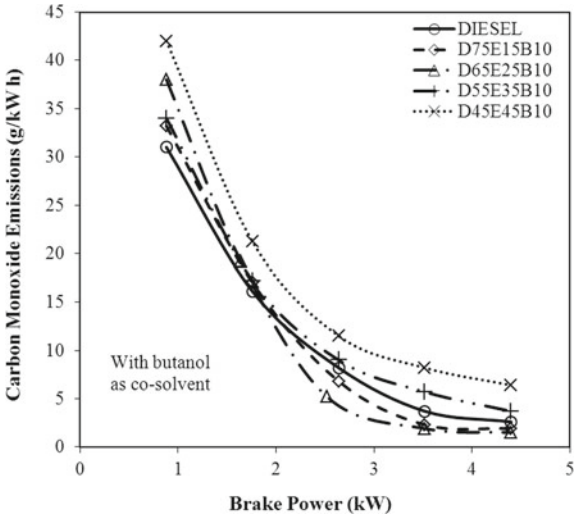

Fig. 6.15 Variation of CO emissions versus brake power

emissions compared to diesel. The decreases of CO emissions from D75E15B10 and D65E25B10 are found to be lower by 27% and 46.1%, respectively, at rated power in comparison with diesel. The increases in CO emissions from D55E35B10 and D45E45B10 are found to be 37.2% and 58.2%, respectively, at rated power in comparison with diesel. This emission from any CI engine is also an indication of incomplete combustion, as the combustion is the one converting the available hydrocarbon in the fuel to carbon dioxide and water as products of complete combustion in the in-cylinder. From Fig. 6.16, it can be seen that containing 15% of ethanol offers lower HC emissions compared to diesel. This is mainly due to the increase in

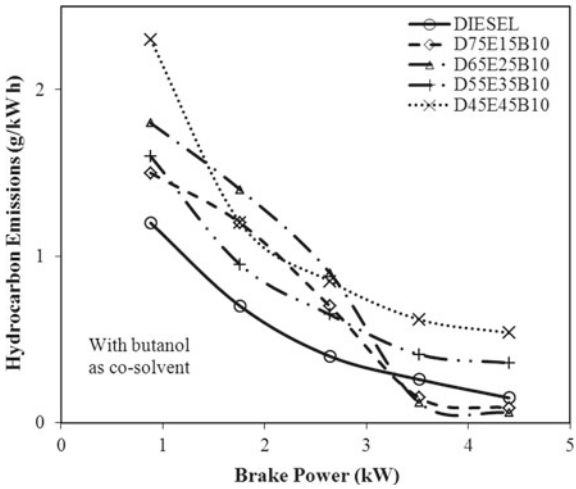

Fig. 6.16 Variations of HC emissions of fuel blends

physico-chemical properties of the blends containing lower volume of ethanol and decrease in combustion characteristics of the blends containing higher volume of ethanol. The flame quenching at the vicinity of the cylinder walls and poor penetration at the crevice volume and the cylinder corners are the reasons for the higher HC emissions. Figure 6.16 shows that D75E15B10 and D65E25B10 produce 28 and 7.6% lower than diesel. The blend containing 45% of ethanol offers higher HC emissions compared to those produced by other blends. However, D55E35B10 and D45E45B10 produce significantly higher emissions compared to diesel at load conditions. However, D55E35B10 and D45E45B10 offer 8.2 and 12.6% lower in-cylinder pressure compared to diesel at full load compared to those produced at low load conditions. Also it can be observed that the start of pressure rise of all fuel blends is away from that of diesel. This is due to low cetane number of the final blend compared to diesel with respect to top dead center. The previous phase of the present study indicated that D45E45B10 blend is the possible volume of ethanol which has failed to produce better performance and emission characteristics. As the blends are producing comparatively low performance the option available to is modify the existing engine operating parameters to fuel the fuel blend in the existing engine. Also in the first phase, this blend has not suffered phase separation which is the major limitation of utilizing ethanol diesel blends in CI engine up to a lower temperature of 5 °C. The suitable parameters for fuelling CI engine by D45E45B10 have been determined by Taguchi method on ANOM approach (analysis of mean). This part of the work used Taguchi method for designing experimental layout and rank matrix to attain optimum level of parameters. The steps involved in the optimization process are as follows: (1) selection of operating parameters and their levels (2) selection of orthogonal array by Taguchi method (3) preparation of experimental layout (4) conducting the experiments using the experimental layout (5) observation of response parameters (6) listing the results and formation of rank matrix (7) suggesting optimal level of parameters, and (8) conducting engine experiment using optimal parameters.

Present investigation has considered four operating parameters, viz. injection pressure (IP), injection timing (IT), compression ratio (CR), and intake air temperature (IAT) for optimization. The range and level of parameters are decided with literature support and preliminary engine experiments. Table 6.6 shows the level of operating parameters. Using these parameters and their levels, a suitable orthogonal array, experimental layout, and number trials of the experiments have been arrived from Taguchi method of optimization.

Taguchi method of optimization offers a systematic approach to arrive at the level of performance parameters involved in the response parameters. The Taguchi method uses an orthogonal array for designing the experimental layout. The selection of orthogonal array is arrived from the degrees of freedom of the parameters involved (Rakopoulos et al. 2008). The minimum number of experiments (trials) for selecting the optimum level of parameters can be determined using the relation:

$$N = (L - 1) * P + 1 \tag{6.4}$$

Table 6.5 Instruments used with accuracies and uncertainties

S. No.	Instruments	Range	Accuracy	Percentage of uncertainties
1	Smoke level measuring instrument	BSU 0–10	+ 0.1 to −0.1	±1
2	Exhaust gas temperature indicator	0–900 °C	+1 to −1 °C	±0.15
3	Speed measuring unit	0–10,000 rpm	+10 to −10 rpm	±0.1
4	Burette for fuel measurement		+0.1 to −0.1 cc	±1
5	Digital stopwatch		+0.6 to − 0.6 s	±0.2
6	Manometer		+1 to −1 mm	±1
7	Pressure pickup	0–110 bar	+ 0.1 to −0.1 kg	±0.1
8	Crank angle encoder		+1° to −1°	±0.2

where N = total number of test runs, L = number of levels of parameters, and P = number of control parameters.

The present study uses (Table 6.5) four parameters and three levels, and hence, the total degrees of freedom of control parameters are 8. Therefore, L_9 is suitable OA for the total degrees of freedom of involved parameters.

Analysis of Mean (ANOM) This is used after attaining the experimental results as per the L_9 orthogonal array of nine experiments containing three sets of reading in each setting. A rank matrix table is utilized for the analysis of captured data. A rank matrix Table 6.8 has been constructed to arrive at the optimal level of parameters. Average of the sum of the each level outcome has been obtained, and the rank is tabulated for the maximum of the outcome.

Assuming that Y as output parameter and the level summation has been obtained as follows:

$$A_1 = Y_1 + Y_2 + Y_3 (\text{in which the level 1 is denoted in the orthogonal array}) \quad (6.5)$$

Similar calculation has been done for three levels and for four parameters, from which the rank matrix table has been constructed.

Table 6.6 Parameters involved in the optimization and their levels

S. No.	Symbol	Parameters	Level 1	Level 2	Level 3
1	A	Injection pressure (IP) (bar)	190	200	210
2	B	Injection timing (IT) (°BTDC)	26	29	32
3	C	Compression ratio (CR)	17.5	19	21
4	D	Intake air temperature(IAT) (°C)	50	75	100

Table 6.7 L_9 orthogonal array

Trial No.	Column No.			
	A	*B*	*C*	*D*
1	1	1	1	1
2	1	2	2	2
3	1	3	3	3
4	2	1	2	3
5	2	2	3	1
6	2	3	1	2
7	3	1	3	2
8	3	2	1	3
9	3	3	2	1

Table 6.8 Rank matrix (for BTE)

Rank	A_1 (Level 1)	B_2 (Level 3)	C_3 (Level 3)	D_4 (Level 3)
Level/Parameter	*A*	*B*	*C*	*D*
1	31.3	31.6	30.6	30
2	31.05	29.86	31.36	31.6
3	31.1	31.96	31.66	31.7

From Table 6.7, it can be concluded that IP 190 bar (LEVEL1), IT 29 °bTDC (LEVEL3), CR 19 (LEVEL3), and IAT 100 (LEVEL3) are the optimal parameters by comparing the rank.

The same sets of readings are captured for NO_x to match with the brake thermal efficiency. The optimized levels of operating parameters are as shown in Table 6.7. Blend D45E45B10 has been tested under the modified operating parameters, and the results are compared with diesel and D45E45B10 under normal operating parameters. The same engine has been used for the testing of the blends under modified operating parameters. The results of the experiment are presented in graphical form. The variations of cylinder pressure with crank angle at rated power for the blend D45E45B10 under standard operating parameters and modified operating parameters are presented in Fig. 6.17, and it is seen that the modified engine operating parameters increased the cylinder pressure significantly compared to diesel. This is due to the increased heat energy release in the combustion chamber with increase in compression ratio and intake air temperature.

Also, the advancement in the injection timing improves the pre-combustion phase and results in more complete combustion. This shows the suitability of the modified engine operating parameters for the blend D45E45B10. The increase in pressure of D45E45B10MOP is found as 7.1% higher than diesel at rated power. However, the cylinder pressure is found lesser than diesel. This is due to the lesser essential properties of D45E45B10 in comparison with diesel. Variation of in-cylinder

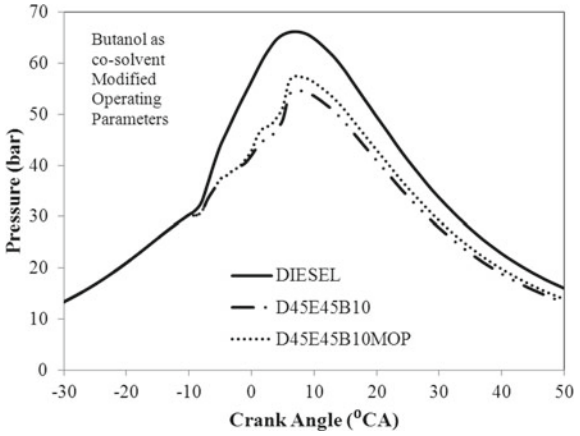

Fig. 6.17 Variation of cylinder pressure with crank angle at rated power

peak pressure versus brake power for D45E45B10 under modified engine operating parameters is shown in Fig. 6.18. It is seen that the in-cylinder peak pressure increases by fuelling D45E45B10 under modified operating parameters compared to that of normal operating parameters. This is due to the suitability of the modified operating parameters for the blend D45E45B10. Also, the increase in the in-cylinder peak pressure is found proportional to the increase in brake power. This increase is due to the improved rate of combustion by the increase in compression ratio and intake air temperature. Also, the advancement of injection timing improved the pre-combustion phase which suppresses the dominance of heat of vaporization of the blend. However, the in-cylinder peak pressure of D45E45B10MOP is found lesser than diesel at all load conditions. This is due to the lesser energy content of D45E45B10 in comparison with diesel. The increase in the in-cylinder peak pressure of D45E45B10MOP is

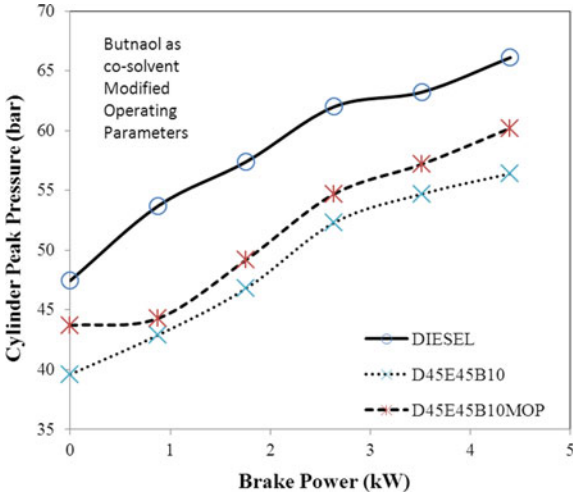

Fig. 6.18 Variation of in-cylinder peak pressure versus brake power

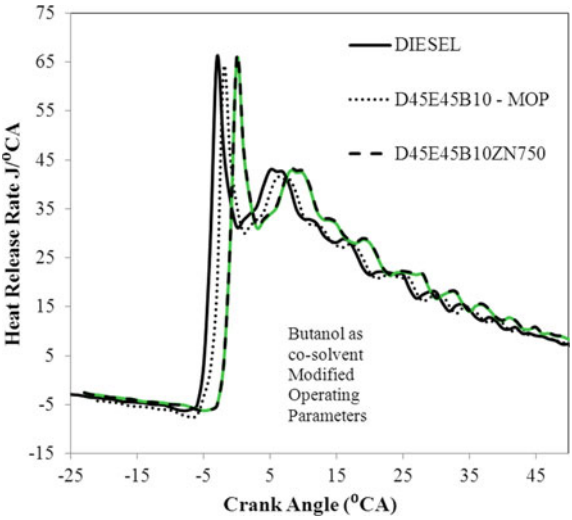

Fig. 6.19 Variation of HRR with crank angle at rated power

found as 6.3% higher than D45E45B10. Heat release rate is an indicator of combustion efficiency, and these parameters are helping for explaining the BTE, exhaust gas temperature, rate of pressure rise, emission parameters, and cylinder pressure.

Figure 6.19 shows the variation of HRR of fuel blends with 10% butanol as co-solvent without any modification under full load condition. HRR graphs are generated at all loads, and for representation HRR at full load condition is presented. It can be seen from figure that ethanol addition up to 25% increases the HRR to a greater extent due to the enhanced combustion behavior resulted from better atomization. However, the increase in ethanol content beyond 25% decreases HRR of the blends as poor atomization resulting in lesser heat release rate. From Fig. 6.19, it is also seen that the blends containing lower ethanol offer higher HRR and blends containing higher ethanol offer lower HRR. The peak HRR of the blends occur an angle away from that of diesel. The combustion duration of the blends containing lower ethanol is shorter than that of blends containing higher ethanol content.

The increases of HRR of D65E15B10 and D55E25B10 are 8.8% and 12.9% higher than diesel. From Fig. 6.20, it is observed that the target blend D45E45B10 offers higher BTE with modified operating parameters compared to that of BTE with normal operating parameters. However, this blend offers lesser BTE compared to that of diesel. The reason for the increase in BTE is due to the increase in heat content of the combustion chamber resulted from the enhanced combustion triggered by the modified operating parameters. Ignition quality decreases the combustion temperature and thereby lesser BTE compared to diesel. Similar observation was presented by previous researchers (Verma et al. 2018) (Fig. 6.20).

The increase in BTE by the modification of operating parameters is 6.7% compared to those in normal operating parameters, which indicates the suitability of the parameters for the target blend. The decrease in BTE of the target blend at modified operating parameters is only 2.1% compared to diesel. Variation of EGT with

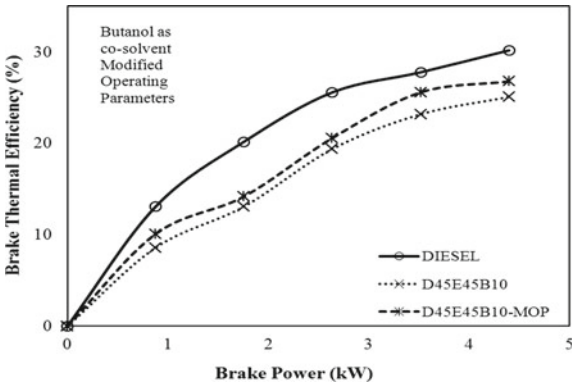

Fig. 6.20 Variation of brake thermal efficiency versus brake power

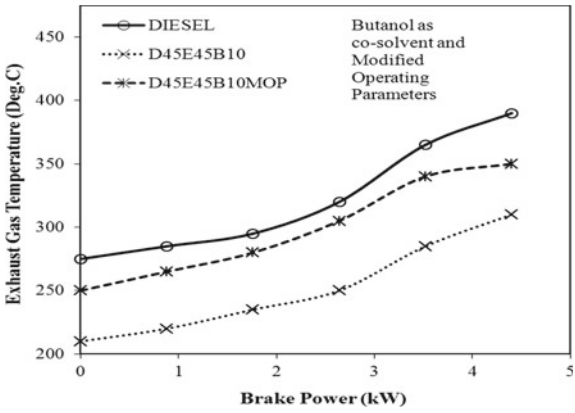

Fig. 6.21 Variation of EGT versus brake power

respect to brake power is as shown in Fig. 6.21. The quantity of ethanol in the blend determines the performance of the blend as the increase in ethanol volume results in poor to brake power for the blend D45E45B10 operated under normal operating parameters and modified operating parameters in comparison with diesel. It is seen that there is a significant increase in EGT of D45E45B10MOP in all load conditions compared to those under normal operating parameters. This is due to the higher heat energy release by the blend operated under modified operating parameters. This is due to the suppression of the dominance created by the heat of vaporization of the higher volume of ethanol by the modified parameters to a certain extent. However, the EGT of D45E45B10MOP is found lesser than diesel. The increase of EGT of D45E45B10MOP is found 13.1% higher than D45E45B10 at rated power. This is due to the increase in heat content of the target blend operating with modified operating parameter and compressed air, which helps to combust the fuel by reducing the ignition delay. However, the emissions of NO_x are lesser than diesel as the higher volume of ethanol suppresses the temperature of the in-cylinder. The increase in NO_x

emissions due to the modification of operating parameters is 100% (approximately double) compared to that of operating under normal operating parameters.

The decrease in NO_x emissions of D45E45B10 –MOP is 40.5% compared to that of diesel at full load condition. Figure 6.23 shows the smoke opacity of the target blend under modified operating parameters at all load conditions. It can be observed that there is a significant reduction in smoke emissions from the target blend under modified operating parameters compared to that under normal operating parameters.

This is due to the reason of increased temperature of the in-cylinder by the modified operating parameters which enhances higher heat release resulted from compressed

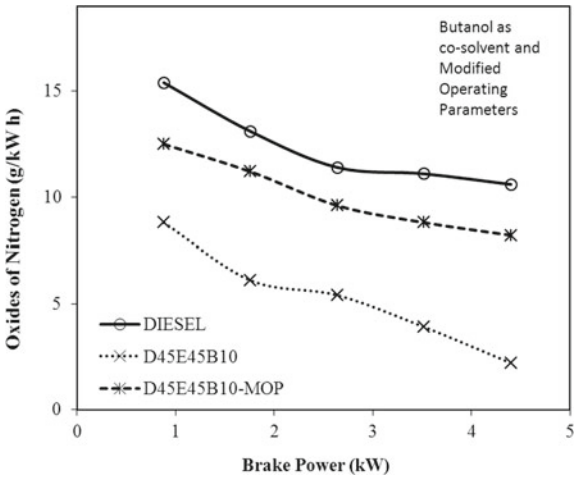

Fig. 6.22 Variation of NO_x emissions versus brake power

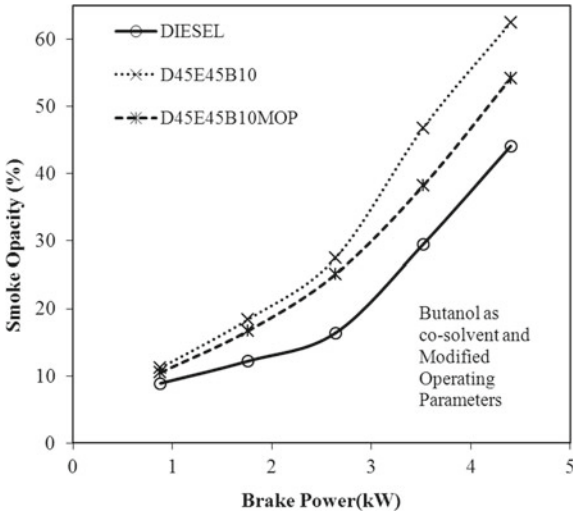

Fig. 6.23 Variation of smoke opacity versus brake power

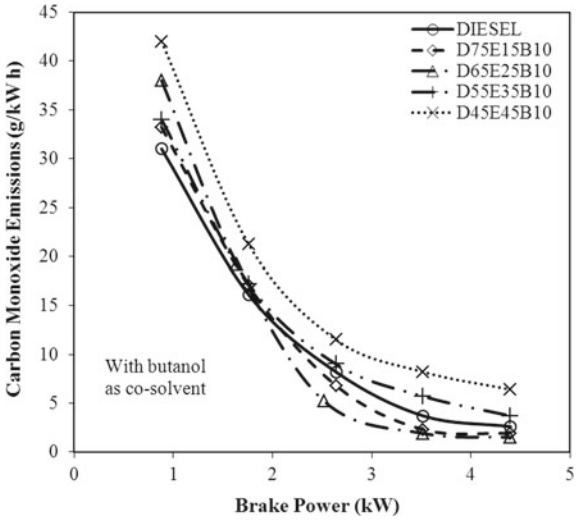

Fig. 6.24 Variations of CO emissions versus brake power

air. However, the higher heat of vaporization of the blend still suppresses the temperature, and hence, there is an increase in smoke emissions compared to that of diesel. The decrease in smoke emissions is 21.2% compared to D45E45B10 operated under normal operating parameters. The increase in smoke emissions of D45E45B10-MOP is 16.5% higher than diesel at full load condition. Similar results were observed by previous researchers (Ghadikolaei et al. 2018). From Fig. 6.24, it can be seen that there is a significant reduction of CO emissions due to the modification of operating parameters to the target blend.

This is due to impact of the modified parameters on the combustion characteristics to a certain extent. However, the higher ethanol content increases the heat of vaporization of the final blend, which results in poor ignition quality which results in lesser temperature of the in-cylinder shows the variation of CO emissions of D45E45B10 fuelled in the test engine under modified operating parameters compared to that of diesel. This reduces the BTE of the blend lesser than diesel. The increase in BTE of the blend at modified operating parameters is 29.6% compared to that operated under normal operating parameters. However, the increase in CO of the blend is 19.3% higher than diesel. Higher ethanol content affects the self-ignition property; hence, it reduces reaction rate, combustion temperature, and heat release rate (Rakopoulos et al. 2008). Figure 6.25 presents the HC emissions of D45E45B10 under modified operating parameters along with diesel for comparison. It is seen that there is a significant reduction in HC emissions from the target blend. This is due to the increase heat content of the combustion chamber and compressed air by the modified parameters which results in better reactivity of the available oxygen with fuel.

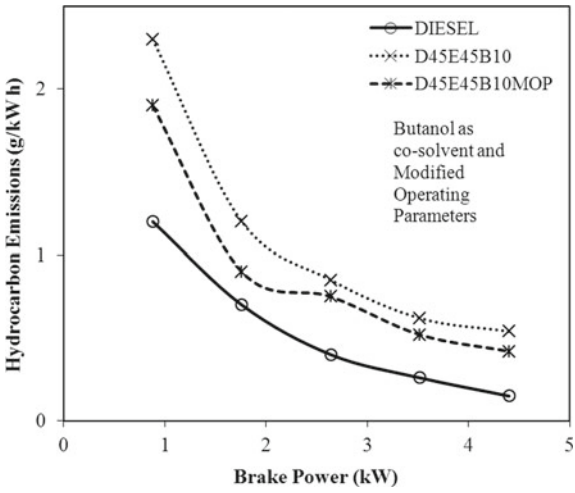

Fig. 6.25 Variation of HC emissions versus brake power

6.4 Conclusion

Different phases of study have been followed to utilize diesel ethanol blends as fuel in compression ignition (CI) engine in this study. Experiments have been conducted with diesel ethanol without co-solvent and with butanol as co-solvent. The effects of engine operating parameters such as injection pressure (IP), injection timing (IT), compression ratio (CR), and intake air temperature (IAT) on engine performance, combustion, and emission were studied.

- Results of the solubility test indicate that ethanol can be blended with diesel up to a volume of 50% with 10% butanol as co-solvent. This blend is found as stable up to a lower temperature of 5 °C for 20 days.
- Results of property testing show those properties of the blend containing 45% of ethanol and 10% butanol as co-solvent are found suitable for replacing diesel to fuel CI engine. However, blend containing 50% ethanol and 10% butanol is found not suitable as the cetane number is less than 30 which is a minimum requirement as per ASTM standards.
- The D80E20 shows higher peak pressure of 72.2 bar compared to D90E10l and diesel showing 68 bar and 66.4 bar, respectively, at rated power due to improved physico-chemical properties, better ignition quality, improved air–fuel mixing, and higher oxygen content. D80E20 shows higher HRR of 71.2 J/^{o} CA compared to diesel and D90E10 at rated power. The brake thermal efficiency of D80E10 (31.8%) is higher than that of diesel (30.2%). Increase the NO_x emission by 13.2% in the case of D80E20, whereas 2.9% increase is observed for D90E10 compared with diesel.
- The lower cetane number of D45E45B10 retards the combustion by 4 ºCA compared to diesel operation. The peak pressure is lower for D45E45B10 in the entire load range when compared to diesel operation. This blend shows a

significantly lower brake thermal efficiency compared to diesel operation and is found 16.8% lesser than diesel at rated power.

- The NO_x emission for D45E45B10 is 22.5% lesser, and the increase in smoke emission is about 49.2% compared to diesel. HC is increased by 6.7% in the case of D45E45B10 operation compared to diesel operation. The CO emission follows the same trend as that of HC emission. Although this phase gave adverse effects in performance and emissions, higher volume of ethanol is utilized without any phase separation.
- D45E45B10MOP operation advances the combustion and improves premixed combustion compared to D45E45B10 under normal operating parameters. However, D45E45B10 shows lower peak heat release rate and peak pressure at rated power compared to diesel operation. This blend produced an increase in BTE at rated power is 6.8% higher than D45E45B10 fuelled under normal operating parameters. However, BTE of D45E45B10MOP is found lesser than diesel at rated power. An increase in NO_x emission by fueling D45E45B10MOP operation is found compared to D45E45B10. The increase in NO_x emissions of D45E45B10MOP is found thrice that of NO_x emissions from D45E45B10 fuelled under normal operating parameters. However, NO_x emissions of D45E45B10MOP are found lesser than diesel at rated power.
- The smoke emission is reduced by 15.4% in fueling D45E45B10MOP compared to D45E45B10 fuelled under normal operating parameters. The HC and CO emissions are reduced by 22.5% and 9.2%, respectively, in fuelling D45E45B10MOP compared to D45E45B10 fuelled under normal operating parameters.

As a sum up, although the efficiency produced by D45E45B10 is found to be marginally lower and the emissions of smoke, and HC and CO produced are found to be marginally higher compared to that of diesel. The utilized ethanol and butanol are manufactured from waste products, and the emissions of oxides of nitrogen produced are found to be significantly lower compared to that of diesel. Hence, higher volume of ethanol can be utilized and a saving of 55% of diesel fuel can be achieved by the implementation of this modification in fuel and in engine. This in turn reduces the dependency of other countries for import of crude oil.

References

Belgiorno G, Di Blasio G, Shamun S, Beatrice C, Tunestål P, Tunér M (2018) Performance and emissions of diesel-gasoline-ethanol blends in a light duty compression ignition engine. Fuel 217:78–90

Gao Z, Lin S, Ji J, Li M (2019) An experimental study on combustion performance and flame spread characteristics over liquid diesel and ethanol-diesel blended fuel. Energy 170:349–355

Ghadikolaei MA, Cheung CS, Yung KF, (2018) Study of combustion, performance and emissions of diesel engine fueled with diesel/biodiesel/alcohol blends having the same oxygen concentration. Energy

Gnanamoorthi V, Devaradjane G (2015) Effect of compression ratio on the performance, combustion and emission of DI diesel engine fueled with ethanol–diesel blend. J Energy Inst 88(1):19–26

Hafid HS, Shah UKM, Baharuddin AS, Ariff AB (2017) Feasibility of using kitchen waste as future substrate for bioethanol production: a review. Renew Sustain Energy Rev 74:671–686
Han J, Somers LMT, Cracknell R, Joedicke A, Wardle R, Mohan VRR (2020) Experimental investigation of ethanol/diesel dual-fuel combustion in a heavy-duty diesel engine. Fuel 275:117867
Hansen AC, Zhang Q, Lyne PW (2005) Ethanol–diesel fuel blends—A review. Biores Technol 96(3):277–285
Holman JP, Gajda WJ (2001) Experimental methods for engineers, vol 2. McGraw-Hill, New York
Kumar S, Cho JH, Park J, Moon I (2013) Advances in diesel–alcohol blends and their effects on the performance and emissions of diesel engines. Renew Sustain Energy Rev 22:46–72
Kuszewski H (2018) Experimental investigation of the effect of ambient gas temperature on the autoignition properties of ethanol–diesel fuel blends. Fuel 214:26–38
Mamat R, Sani MSM, Sudhakar K, Kadarohman A, Sardjono RE (2019) An overview of Higher alcohol and biodiesel as alternative fuels in engines. Energy Rep 5:467–479
Pinzi S, López I, Leiva-Candia DE, Redel-Macías MD, Herreros JM, Cubero-Atienza A, Dorado MP (2018) Castor oil enhanced effect on fuel ethanol-diesel fuel blend properties. Appl Energy 224:409–416
Prabakaran B, Vijayabalan P (2016) Evaluation of the performance of n-butanol-ethanol-diesel blends in a diesel engine. Int J Energy Clean Environ 17:81–97
Prabakaran B, Vijayabalan P, Balachandar M. (2017) Experimental Investigation of ethanol-diesel-butanol blends in a compression ignition engine by modifying the operating parameters. SAE Int J Eng 11(03-11-05-0037)
Prabakaran B, Vijayabalan P, Balachandar M (2019) An assessment of diesel ethanol blend fueled diesel engine characteristics using butanol as cosolvent for optimum operating parameters. Energy Sources Part A-Recov Util Environ Effects
Rakopoulos DC, Antonopoulos KA, Rakopoulos DC, Hountalas DT (2008) Multi-zone modeling of combustion and emissions formation in DI diesel engine operating on ethanol–diesel fuel blends. Energy Convers Manage 49(4):625–643
Rakopoulos DC, Rakopoulos CD, Giakoumis EG, Papagiannakis RG, Kyritsis DC (2014) Influence of properties of various common bio-fuels on the combustion and emission characteristics of high-speed DI (direct injection) diesel engine: vegetable oil, bio-diesel, ethanol, *n*-butanol, diethyl ether. Energy 73:354–366
Rakopoulos CD, Rakopoulos DC, Kosmadakis GM, Papagiannakis RG (2019) Experimental comparative assessment of butanol or ethanol diesel-fuel extenders impact on combustion features, cyclic irregularity, and regulated emissions balance in heavy-duty diesel engine. Energy 174:1145–1157
Ribeiro NM, Pinto AC, Quintella CM, da Rocha GO, Teixeira LS, Guarieiro LL, do Carmo Rangel M, Veloso MC, Rezende MJ, Serpa da Cruz R, de Oliveira AM (2007) The role of additives for diesel and diesel blended (ethanol or biodiesel) fuels: a review. Energy Fuels 21(4):2433–2445
Shamun S, Belgiorno G, Di Blasio G, Beatrice C, Tunér M, Tunestål P (2018) Performance and emissions of diesel-biodiesel-ethanol blends in a light duty compression ignition engine. Appl Thermal Eng 145:444–452
Singh GN, Bharj RS (2019) Study of physical-chemical properties for 2nd generation ethanol-blended diesel fuel in India. Sustain Chem Pharm 12:100130
Stoeberl M, Werkmeister R, Faulstich M, Russ W (2011) Biobutanol from food wastes–fermentative production, use as biofuel an the influence on the emissions. Procedia Food Sci 1:1867–1874
Verma S, Sharma B, Ahmad J, Dwivedi G, Nandan G (2018) Impact assessment of ethanol as fuel for engine operation. Mater Today: Proceed 5(2):6115–6120
Woo C, Kook S, Hawkes ER (2016) Effect of intake air temperature and common-rail pressure on ethanol combustion in a single-cylinder light-duty diesel engine. Fuel 180:9–19

Yilmaz N (2012) Comparative analysis of biodiesel–ethanol–diesel and biodiesel–methanol–diesel blends in a diesel engine. Energy 40(1):210–213
Yu Y (2019) Experimental study on effects of ethanol-diesel fuel blended on spray characteristics under ultra-high injection pressure up to 350 MPa. Energy 186:115768

Chapter 7
Recent Development for Use of Alcohol-Based Renewable Fuels in Compression Ignition Engine

Nikhil Sharma

7.1 Introduction

Energy crisis and growing environmental concerns have given importance to renewable fuels. Beyond the problems of energy crises, renewable fuel provides advantage to overcome harmful emissions with fossil fuels. Petroleum reserves are limited and may vanish in future if they are consumed continuously. Due to limited fossil fuel availability, dependence of the global transportation sector (94%) is estimated to decrease to 89% by 2030 (Petroleum 2012). Securities of energy supply and climate change are the principal factors encouraging use of alternative fuels in transport sector. Due to limited resources and increasing demand for energy, numerous alternative transport fuels are being considered. Alternative fuel candidates, which are expected to displace petroleum fuels in the transport sector, have to perform nearly similar to conventional fuels. Cost competitiveness, infrastructure development, toxicity, emissions, and contribution to greenhouse gas (GHG) emissions could be fair criteria to judge those alternative fuel candidates. Fuels other than diesel and gasoline are considered as alternative fuels. These comprise electricity, liquefied petroleum gas (LPG), unconventional fossil oils, natural gas, hydrogen, Fischer–Tropsch liquids, ethers, alcohols, biodiesels, gasohol, etc. Market developments and government policies for implementation of appropriate alternative fuels will play a significant role in their implementation and acceptance. The aim in near future should be to diversify energy resources portfolio in order to meet future transport sector demands. Dr Rudolf Diesel demonstrated that a fuel–air mixture in engine combustion chamber can be ignited by compression ignition. The engine was successfully operated in

N. Sharma (✉)
Department of Mechanical Engineering, Malaviya National Institute of Technology Jaipur, Jaipur, Rajasthan 302017, India
e-mail: nikhil.mech@mnit.ac.in

P. C. Shukla et al. (eds.), *Alcohol as an Alternative Fuel for Internal Combustion Engines*, Energy, Environment, and Sustainability,
https://doi.org/10.1007/978-981-16-0931-2_8

compression ignition mode in 1897 (Debnath et al. 2013). Since 1897, compression ignition engine is preferred to be used in applications of power generation, transportation, agriculture, offshore drilling, military, marine, telecommunication, and generator. With growing population, energy security is becoming an important concern for government worldwide. Due to this reason, scientists are exploring for renewable environmentally friendly fuels which can be blended with conventional gasoline or diesel fuel to reduce carbon footprint.

In general, alcohols are usually considered as a spark-ignition engine fuel. Few decades back, in 1970 and 1980, it was emphasized and shown that it is likely to use alcohols as diesel engine fuel with addition of fuel additive and ignition aids. Sometimes, tertiary butyl alcohol (TBA) is considered as an additive, extender, and co-solvent when mixing methanol and ethanol. Dimethyl ether (DME) is considered as a clean fuel because of no carbon bound present in DME structure and therefore produces less emission and is excellent fuel to be used with diesel. However, DME has limitation in terms of production, handling of fuel, and availability. Therefore, alcohols are considered as a fuel because it has combustion properties similar to diesel and gasoline. Alcohols have relatively lower energy density; they produce formaldehyde and acetaldehyde combustion by-products.

Fuel properties: Alcohols consist of hydroxyl groups fixed to a carbon atom. Molecular structures of primary alcohols vis-à-vis gasoline are shown in Table 7.1.

Alcohols are oxygenated fuel and when blended with diesel results in complete combustion due to inherent oxygen content of fuel. Figure 7.1 shows various oxygenates as a replacement for conventional fuel. Figure 7.2 shows diesel engine emission and its cause. Figure 7.3 shows possible emission reduction techniques once the emission is formed in tail pipe. Once they are formed in the tail pipe, diesohol results in efficient combustion efficiency and reduces the engine-out gaseous and particulate emissions. The most popular oxygenated fuels are methanol, ethanol, and butanol, and the physical and chemical properties allow them to be used in compression ignition engine. Pentanols are less used as a commercial fuel because of high cost of production. There are two popular methodologies of alcohol diesel

Table 7.1 Molecular structures of primary alcohols vis-à-vis gasoline

Test fuel	Molecular structure
Methanol	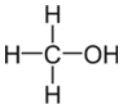
Ethanol	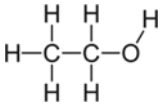
Butanol	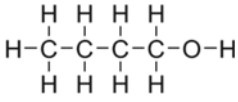

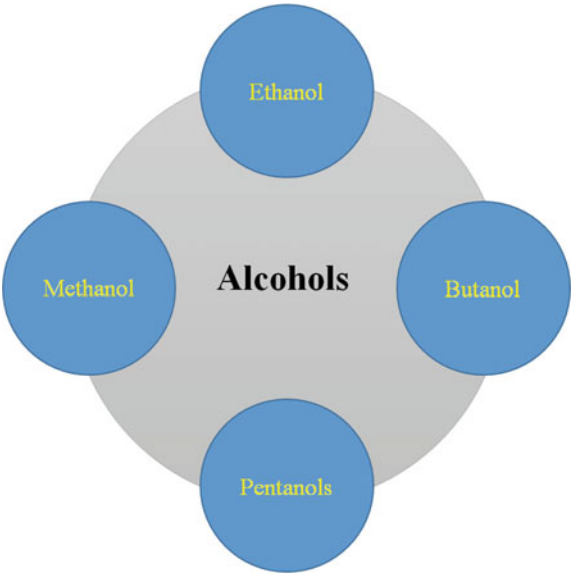

Fig. 7.1 Flowchart of oxygenates as an additive for automotive application

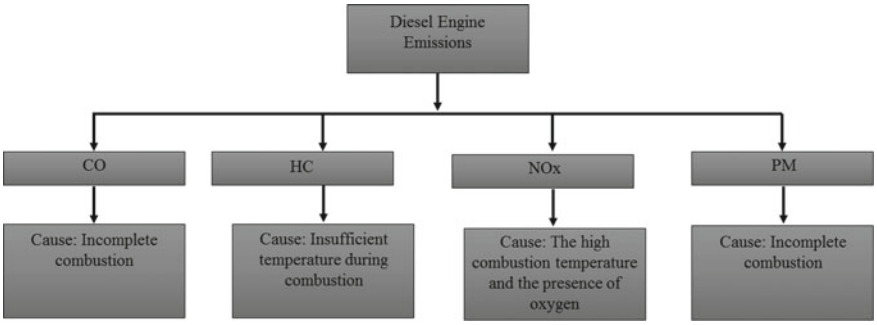

Fig. 7.2 Diesel engine emission and cause

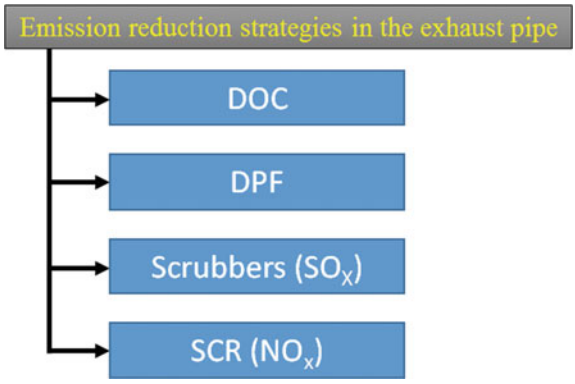

Fig. 7.3 Diesel engine after-treatment emission reduction strategies

combustion in automotive sector among many other available alternatives. The first method is the use of diesel–alcohol-blended externally for direct injection combustion. In the second method, mineral diesel is injected in cylinder as high-reactivity fuel (HRF), and alcohol is injected in port as low-reactivity fuel (LRF). This is called reactivity-controlled compression ignition (RCCI) combustion. Blending relatively higher percentage of alcohol with diesel sometimes does not offer an ignition in an un-modified engine with compression and therefore is a major issue. Therefore, a high cetane number and low auto-ignition temperature are possible compression ignition engine fuel. This is possible in dual-fuel engine. Liao et al. (2007) and Zhang et al. (2008) investigated the laminar flame speed for mixtures of methanol and air at relatively elevated temperatures. Authors stated that laminar burning velocity was related to initial temperature and equivalence ratio. A notably large size of research has been published on using alcohol with diesel in a compression ignition engine. The present chapter reviews these to provide insightful views. This chapter addresses several critical areas and future research scope.

7.2 Economic Aspect

It is important to discuss economic aspect of fuel because people's decision to buy biofuel is based on price. People will buy cars with biofuels if price of biofuel is attractive and competitive compared to other biofuels and conventional fuels such as diesel and gasoline. Some of the biofuels are being mass produced, and the technology has been developed over the past few decades. Nevertheless, some of the biofuels are still in laboratory scale because of the higher price compared to conventional fuels. Cost of biofuel varies from country to country because of variation in feedstock prices. Government in different countries also encourages the industries to produce biofuels and provide subsidy from year to year. This subsidy stimulates industries to establish themself in due course of time and makes the price competitive in marketplace and develop infrastructure. Another aspect is taxes implemented by government on fuels which makes a lot of difference in end user price.

Figure 7.4 shows the projected price of ethanol and butanol. Different biofuels have different costs. For example, butanol is extensively investigated by researchers, but the production of butanol is still limited to laboratory scale. The innovative biotechnological production of biofuels from non-edible feedstocks results in decrease of prices, and limited petroleum reserves may encourage people to use biofuels.

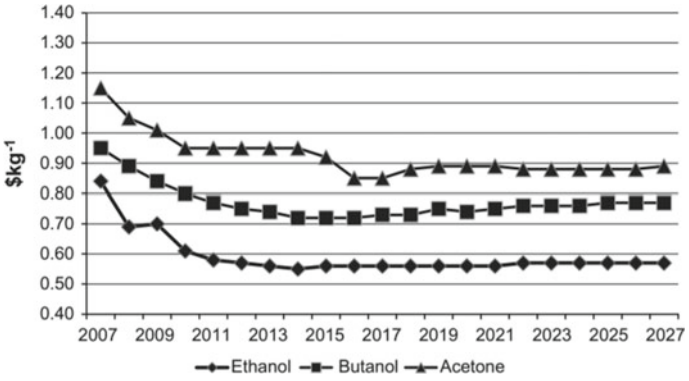

Fig. 7.4 Projected prices of ethanol, butanol, and acetone (Pfromm et al. 2010)

7.3 Properties of Alcohol Relevant to Engines and Its Material Compatibility

As discussed earlier, alcohols are fuels of the family of oxygenate, and generally speaking, all alcohols can combust. Figure 7.5 shows structure of monohydric alcohols. In organic compounds, one hydroxyl (−OH) group is replaced for one hydrogen atom. Thus, methane becomes methyl alcohol, CH_30H; ethane becomes ethyl alcohol, C_2H0H (ethanol). As of today, only ethanol and methanol are economically suitable as fuels for internal combustion engines. Biobutanol is also gaining an interest, and process is being found out by scientists to make it an economical fuel for internal combustion engine. Alcohols have relatively higher flame speeds and slightly longer flammability limits compared to its counterpart hydrocarbons. A limitation of oxygenated fuel is that it reduces the heating value of the fuel when compared to hydrocarbon fuels. Methanol has relatively higher oxygen present in it compared to butanol and can be commercially produced. As an internal combustion engine fuel, methanol has physical and chemical fuel properties similar to ethanol. Also,

Fig. 7.5 Structure of monohydric alcohols

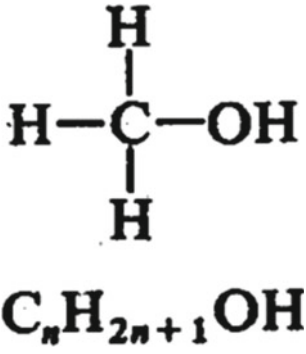

Table 7.2 Properties of alcohol fuels (Awad et al. 2017; Campos-Fernández et al. 2012; Chen et al. 2010; Chen et al. 2013; Chen et al. 2014; Giakoumis et al. 2013; Kumar and Saravanan 2016; Kumar et al. 2013; Shahir et al. 2014; Zhang et al. 2006)

Property	Diesel	Gasoline	Methanol	Ethanol	Propanol	Butanol
Boiling point (°C)	180–370	27–225	65	78	97.1	117–118
RON	20–30	80–99	136	129	112	96
CN	40–55	0–10	3.8	5–8	12	25
Low heating value (MJ/kg)	42.5	42.7	20.1	26.9	30.6	33.1
Heat of vaporization (kJ/kg)	243	349	1162.64	918.42	727.88	585.40
Flashpoint (°C)	65–88	−13 to 45	12	13	22	35
Auto ignition temperature (°C) (Kumar and Saravanan 2016)	∼300	257	463	420	350	345
Stoichiometric air/fuel ratio (Lapuerta et al. 2010)	14.3	14.7	6.47	9.01	10.35	11.19

methanol has relatively lower risk of flammability compared to gasoline. Ethanol is a colorless and renewable fuel in nature because it is made from biomass by distillation fermentation. Ethanol can be produced from many different feedstokes but tend to have same chemical formula irrespective to its production methodology. Octane number of ethanol is relatively higher and therefore gives a premium blending properties. Propanol is relatively expensive and difficult to produce and therefore is a less researched fuel among scientists. The energy content of propanol is nearly similar to ethanol, and therefore, ethanol is preferred because of less cost of production. Butanol is another promising renewable internal combustion fuel. Butanol has relatively higher heat of evaporation than its counterpart ethanol and results in reduced combustion temperature and therefore results in reduced formation of NO_x (Cucchi and Samuel 2015). Table 7.2 shows properties of alcohols adapted from the literature for different investigations.

In the next section, alcohol-based fuel compatibility issues in IC engine will be discussed. Thereafter, effect of specific alcohol on material compatibility issues in IC engine will be discussed. Figure 7.6 shows alcohol-based material compatibility issues.

Friction, wear, corrosion, and lubricant issues are related to fuel physical and chemical properties. Viscosity, density, and oxidation stability are the fuel properties among many others which cause such issues. High value of viscosity results in poor atomization. Biodiesel has three OH groups attached on the glycerol molecules that are esterified with the same fatty acid. Therefore, it is called simple triglyceride. Figure 7.7 shows a simple triglyceride molecule structure.

- **Wear and friction**: Wear is common in internal combustion engine because of the several rotating parts such as crankshaft, piston, and connecting rod and valves. In addition to rotating parts, wear also depends on engine load, engine rpm, temperature of the engine, type of lubricant used, and additives present in lubricant. This

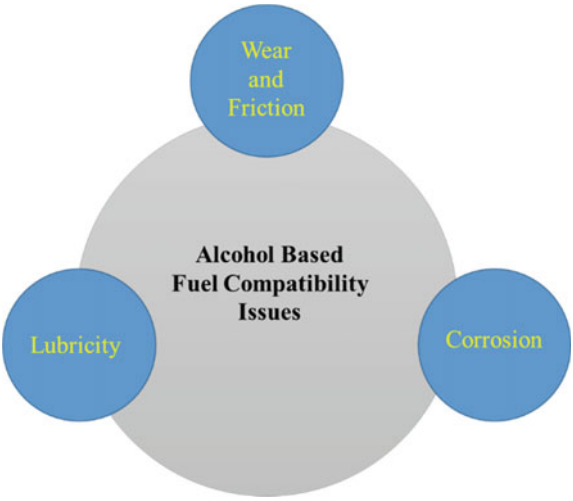

Fig. 7.6 Compatibility of alcohol fuels for IC engine

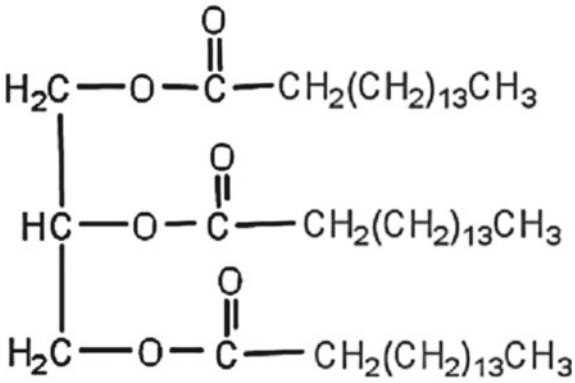

Fig. 7.7 Simple triglyceride molecule

wear due to rotating parts is dependent on lubricating property of fuel as well and reduces the life engine components.

- **Corrosion**: Engine parts/components can become corrosive with time if fueled with oxygenated fuel or if conventional fuel is blended with oxygenated fuel. This is because alcohols may absorb water and in turn accelerates the rate of corrosion. Corrosive rate of biofuels is also dependent on method of preparation and from bacterial contamination during the fermentation process. Corrosion is undesirable because it damages the metal surface of engine, in particular fuel injection system. It is believed that anti-corrosion components added in fuel may reduce the corrosion rate but with a plenty of new and more harmful emissions products. Each alcohol fuel (ethanol, methanol, butanol, or propanol) has different responses to corrosion because of its inherent properties.

- **Lubricity**: Lubricity of fuel is vital property because it reduces wear and friction of fuel injection component (injection pumps and fuel injectors) and other engine rotating component. Lurbicating oil changes its property with time because it gets contaminated from soot, metals, water, and other hydrocarbons produced with combustion of fuel.

Apart from the above three alcohol-based fuel compatibility issues in IC engine, different alcohols also have specific effect on material of IC engine. In the next section, material compatibility issues by the use of specific alcohol fuel will be discussed.

- **Methanol**: Among alcohols, methanol is more violent in terms of materials compatibility, and it can affect both metals and elastomers. Magnesium has poor reaction when it comes in contact with metals. Therefore, the use of magnesium is usually probated. Moreover, aluminum is also corroded when it comes in contact with methanol, but the reactions in comparison with magnesium are slow. Once corrosion of methanol occurs with aluminum, aluminum hydroxide and gelatinous precipitates are produced. These can plug filters and generally result in wear of fuel injectors and results in increase of engine wear. Normal carbon steel and stainless steel do not result in aggressive corrosion and are relatively less affected by methanol in dry form. The reason is that it does not have large amount of dissolved water and therefore has less foreign impurities. On the other hand, metals such as brass, bronze, and die cast zinc can corrode quickly when methanol is blended with gasoline. Fuel hoses are more prone to damage (crack upon hardening), and the life span of hoses is also less if they come in contact with methanol. Therefore, hoses made of cross-linked polyethylene are compatible methanol fuel material
- **Ethanol**: Compared to methanol, ethanol is relatively less violent in terms of materials compatibility toward both metals and elastomers. A corrosion potential is water present in methanol which results from art effect of production. The amount of water is more compared to methanol and therefore more prone to corrosion. Carbon steel, stainless steel, and bronze are the metals which can be considered when using ethanol as a fuel. Metals such as magnesium, zinc, cast iron, brass, and copper are not recommended. Aluminum is coated with cadmium, hard chromium, nickel, or anodized aluminum to make them compatible. Ethanol is less violent to elastomers compared to methanol. Buna-N, Viton, Teflon fluorosilicones, neoprene, and natural rubber are some of the compatible elastomers.

7.4 Cold Start

A cold start is a condition attained in vehicle when a vehicle is at low temperature, relative to its normal operating temperature due to cold weather condition. Cold-start emissions are unavoidable while driving a vehicle. In colder countries, low ambient temperature results in increase in oil viscosity and also reduces the in-cylinder gas

temperature up to few initial seconds of start of engine (An et al. 2016; Armas et al. 2012). This low in-cylinder gas temperature makes the fuel droplets difficult to atomize. Since droplets are less atomized, they evaporate relatively less, and they mix lesser with the air. An ambient temperature of 20 degree C was considered to be cold-start condition by Armas et al. (2012) investigate the effect of different alcohol engine characteristics. In addition, cetane number of the blends during cold start was adjusted so that blended fuel acts as an ignition improver in the existing un-modified diesel engine. Moreover, alcohol may result in increase in emission at cold-start conditions. In a study (Zhang et al. 2016), hot- and cold-start particulate emissions were investigated by author. They found that cold start (120 s of idling) resulted in increase in nucleation mode particles significantly compared to hot-start emission. Another investigation (Iodice and Senatore 2014) found that higher blends of ethanol with gasoline resulted in relatively higher engine-out emission in cold-start condition.

7.5 Combustion Characteristics

Ning et al. investigated diesel fuel and its blend with methanol, ethanol, and butanol for combustion characteristics. Figure 7.8 shows combustion characteristics of diesel with alcohol.

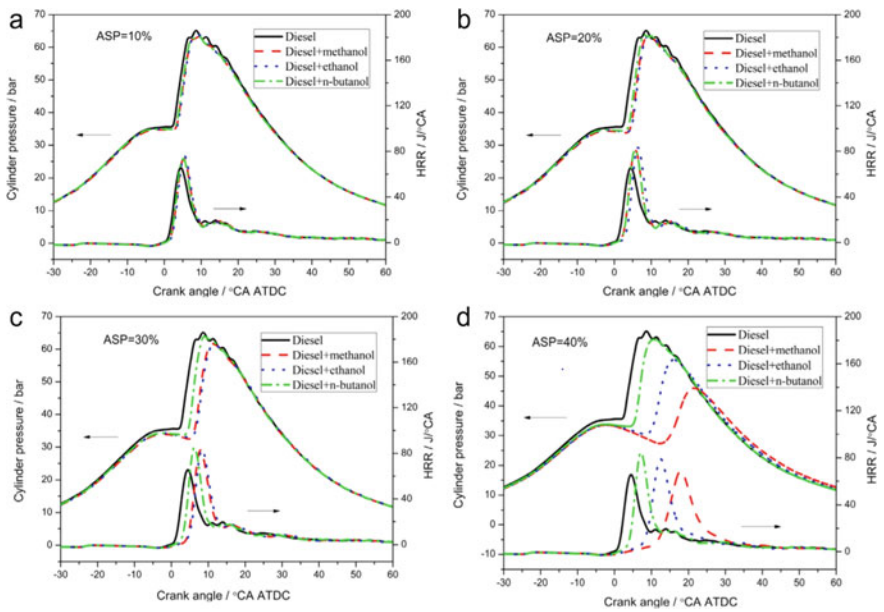

Fig. 7.8 Effects of alcohol additions on cylinder pressure (Ning et al. 2020)

In this experimental investigation, a relative study of the consequences of addition of alcohols such as methanol, ethanol, and n-butanol on the combustion characteristics was achieved. P_{max} in case of alcohol was found to be lower in comparison with diesel. As seen in the figure, diesel and the n-butanol/diesel mixture resulted in relatively higher P_{max} value. Similarly, HRR_{max} was relatively higher for alcohol fuels.

Yusri et al. (2019) investigated the effect of different fuel properties on combustion characteristics. In this experimental investigation, n-butanol was blended with diesel in volumes of 5, 10, and 15% in diesel fuel, and engine was operated at an engine speed of 2500 rpm with load of 15 Nm. Figure 7.9 shows distribution of the maximum engine in-cylinder pressure (P_{max}) at 15 Nm load for an average of 1000 consecutive engine cycles. It was observed that the P_{max} decreases with more butanol in the diesel-blended fuels. Authors plotted the graph with the help of wavelet transform analysis. By this innovative technique, the frequency of cyclic variation can be investigated with the help of time series and frequency. As seen in the above graph, the engine cycle-to-cycle distribution has significant effects on P_{max}.

Similar to the above authors, Jamrozik et al. (2018) investigated the effect of addition of alcohol fuel to diesel fuel in a compression ignition engine. Their experimental investigation explores the results of blending alcohol to diesel fuel on the basis of same energy content of fuel injected per cycle. Figure 7.10a represents the blending of diesel fuel with ethanol, Fig. 7.10b represents blending of diesel fuel with ethanol, Fig. 7.10c represents the blending of diesel fuel with 2-propanol, and the last Fig. 7.10d represents blending of diesel fuel with 1-butanol.

In this paper, authors made a comparison based on the same energy content of the diesel fuel replaced by different types of alcohol fuels. As seen in figure above, 15, 30, 45, 55, and 70% of total energy supplied with diesel fuel to the combustion chamber was replaced by alcohol. The results were compared with reference fuel diesel.

Consider the last case in Fig. 7.10 wherein 70% energy was provided by alcohol fuel. The aim was to achieve 1100 J/cycle of energy by different test fuels. It can be seen that in order to reach the goal of 1100 J/cycle, nearly 8 mg of diesel fuel and 39 mg of methanol, 30 mg of ethanol, 27 mg of 2-propanol, or 23 mg of 1-butanol were needed to reach required energy content of fuel. It can be inferred from the experiments that increasing percentage of alcohols in diesel fuel increase oxygen content in the fuel–air mixture. This in turn affects stoichiometric fuel–air ratio and thus changes the individual phases of the combustion process during a cycle.

Many researchers have blended kerosene with diesel to investigate emission characteristics. In a similar experiment by Agarwal et al. (2019), authors experimentally investigated diesel fuel blended with kerosene and gasoline. Authors implemented advanced endoscopy visualization technique to find out soot distribution in the images of combustion of compression ignition engine. Authors made a comparative analysis K20 (20% kerosene (v/v) blended with mineral diesel) and G20 (20% gasoline (v/v) blended with mineral diesel) with diesel.

Figure 7.11 shows combustion images acquired from endoscope and its spatial soot distribution with respect to in-cylinder pressure and HRR curve. As seen in the

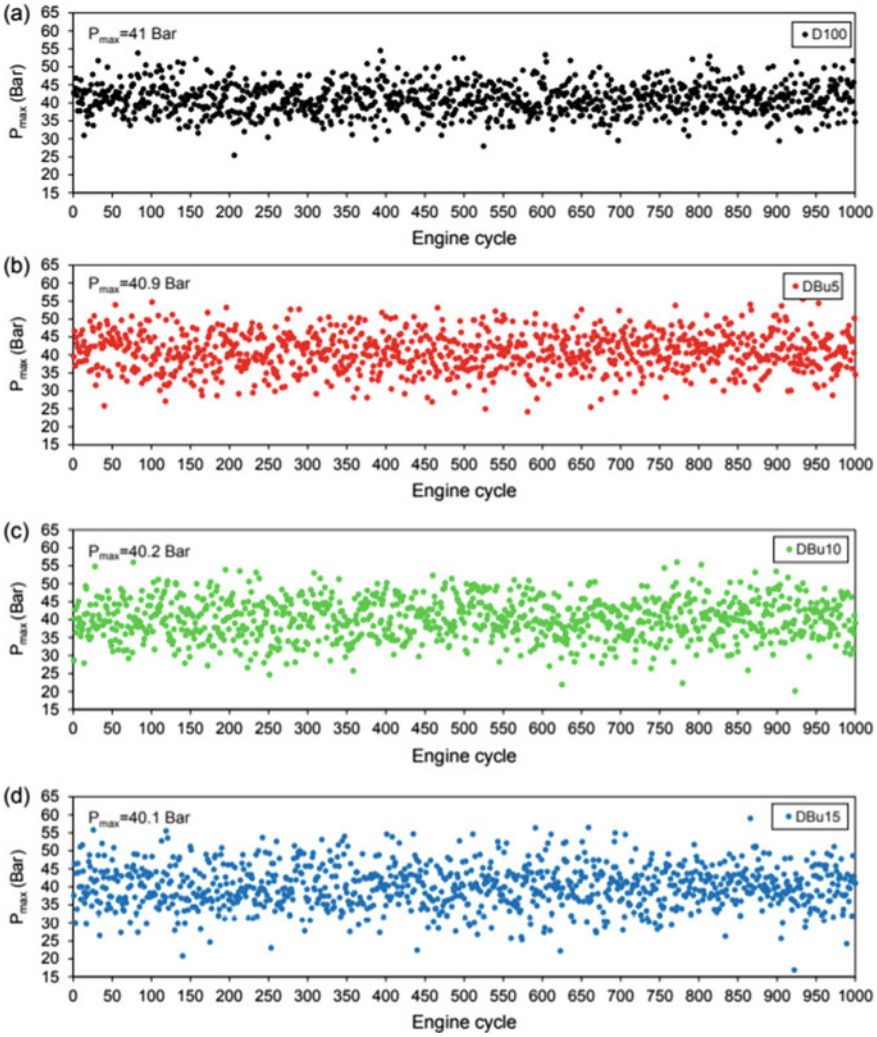

Fig. 7.9 Pmax for different tested fuels (Yusri et al. 2019)

images, authors have attempted to correlate the results from combustion images to in-cylinder data. The pressure crank angle curve showed superior combustion characteristics compared to diesel and K20. In the results from pressure transducer data, G20 exhibited better combustion characteristics when compared with diesel and K20. As expected, Pmax, Rmax, and combustion duration were more for G20 test fuel. As far as endoscopy images are concerned, G20 and K20 exhibited relatively lowest R intensity values for G20 test fuel. This designated lower soot concentration for G20 test fuel. Overall, authors made an experimental investigation using endoscopy

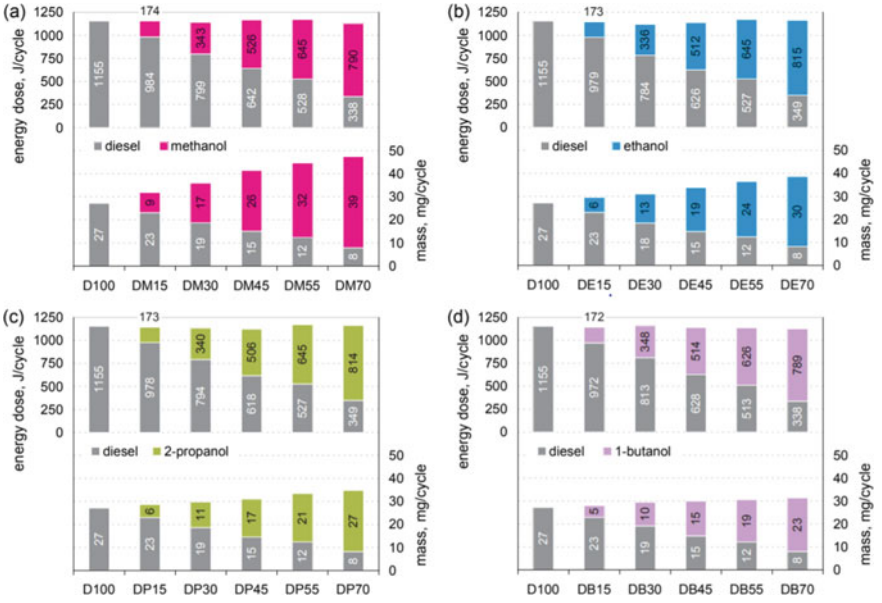

Fig. 7.10 Effect of the addition of alcohol to diesel (Jamrozik et al. 2018)

technique and showed that it is a useful technique for characterization of in-cylinder combustion process and detect soot distribution.

7.6 Conclusions, Outlook, and Recommendations

The literature review shows that blending of diesel with alcohol fuels can increase combustion efficiency of engine. As expected from the calorific value, brake power is relatively lower of alcohol-blended diesel fuel. Brake power also depends on cetane number of blended fuel. Properties such as lower density, viscosity, and calorific value of the alcohol fuels compared to mineral diesel result in increasing fuel consumption. Many research laboratories are working on application of methanol, ethanol, propanol, and butanol in the compression ignition engine like dual fuel, RCCI, and PCCI because of the potential to decrease emissions. Higher vaporization and higher oxygen content of fuel result in complete combustion and reduced emission. The present review shows that alcohol is a promising fuel to be blended with diesel; however, material compatibility and combustion process have to be optimized to take the advantage of oxygen present in fuel to reduce emission.

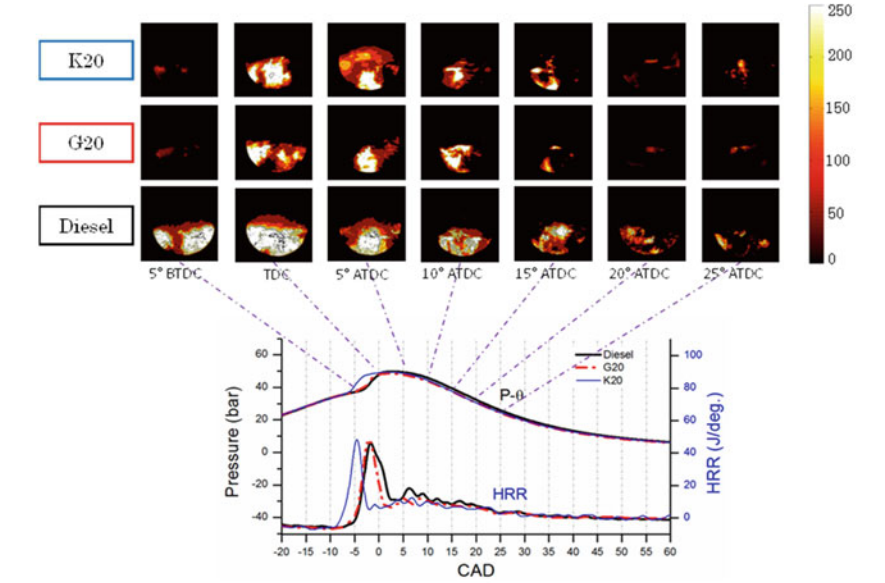

(a) No load

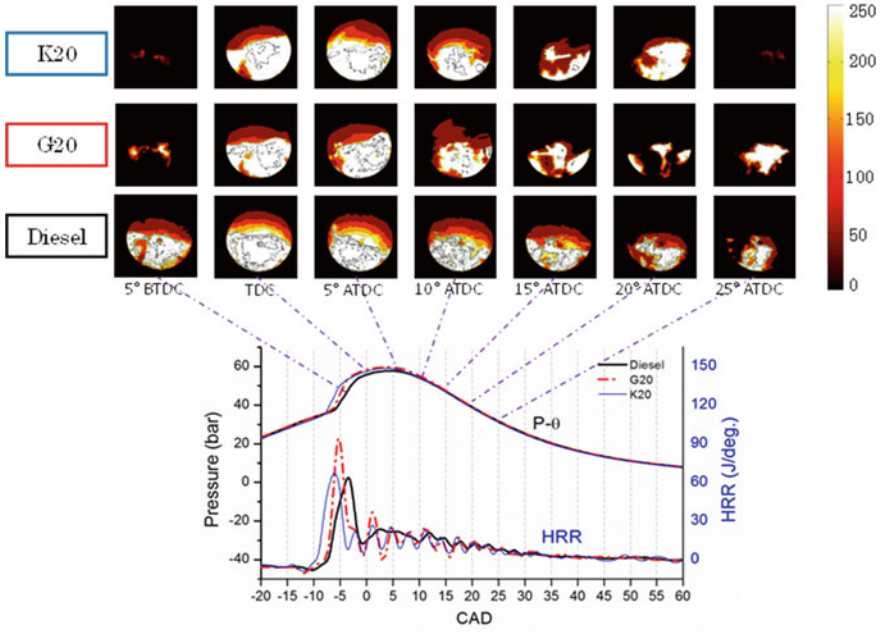

(b) 3.0 kW

Fig. 7.11 Soot contours, cylinder pressure, and HRR (Agarwal et al. 2019)

References

Agarwal AK, Jiotode Y, Sharma N (2019) Endoscopic visualization of engine combustion chamber using diesoline, diesosene and mineral diesel for comparative spatial soot and temperature distributions. Fuel 241:901–913

An Y-Z, Teng S-P, Pei Y-Q et al (2016) An experimental study of polycyclic aromatic hydrocarbons and soot emissions from a GDI engine fueled with commercial gasoline. Fuel 164:160–171

Armas O, García-Contreras R, Ramos Á (2012) Pollutant emissions from engine starting with ethanol and butanol diesel blends. Fuel Process Technol 100:63–72

Awad OI, Ali OM, Mamat R et al (2017) Using fusel oil as a blend in gasoline to improve SI engine efficiencies: a comprehensive review. Renew Sustain Energy Rev 69:1232–1242

Campos-Fernández J, Arnal JM, Gómez J et al (2012) A comparison of performance of higher alcohols/diesel fuel blends in a diesel engine. Appl Energy 95:267–275

Chen C-C, Liaw H-J, Shu C-M et al (2010) Autoignition temperature data for methanol, ethanol, propanol, 2-butanol, 1-butanol, and 2-methyl-2, 4-pentanediol. J Chem Eng Data 55:5059–5064

Chen G, Shen Y, Zhang Q et al (2013) Experimental study on combustion and emission characteristics of a diesel engine fueled with 2, 5-dimethylfuran–diesel, n-butanol–diesel and gasoline–diesel blends. Energy 54:333–342

Chen Z, Wu Z, Liu J et al (2014) Combustion and emissions characteristics of high n-butanol/diesel ratio blend in a heavy-duty diesel engine and EGR impact. Energy Convers Manag 78:787–795

Cucchi M, Samuel S (2015) Influence of the exhaust gas turbocharger on nano-scale particulate matter emissions from a GDI spark ignition engine. Appl Therm Eng 76:167–174

Debnath BK, Saha UK, Sahoo N (2013) Effect of compression ratio and injection timing on the performance characteristics of a diesel engine running on palm oil methyl ester. Proc. Instit. Mechan. Eng. J. Power Energy 227:368–382

Giakoumis EG, Rakopoulos CD, Dimaratos AM et al (2013) Exhaust emissions with ethanol or n-butanol diesel fuel blends during transient operation: a review. Renew Sustain Energy Rev 17:170–190

Iodice P, Senatore A (2014) Cold start emissions of a motorcycle using ethanol-gasoline blended fuels. Energy Procedia 45:809–818

Jamrozik A, Tutak W, Pyrc M, Gruca M, Kočiško M (2018) Study on co- combustion of diesel fuel with oxygenated alcohols in a compression ignition dual-fuel engine. Fuel 221:29–345

Kumar BR, Saravanan S (2016) Use of higher alcohol biofuels in diesel engines: a review. Renew Sustain Energy Rev 60:84–115

Kumar S, Cho JH, Park J et al (2013) Advances in diesel–alcohol blends and their effects on the performance and emissions of diesel engines. Renew Sustain Energy Rev 22:46–72

Lapuerta M, García-Contreras R, Campos-Fernández J et al (2010) Stability, lubricity, viscosity, and cold-flow properties of alcohol − diesel blends. Energy Fuels 24:4497–4502

Liao S, Jiang D, Huang Z et al (2007) Laminar burning velocities for mixtures of methanol and air at elevated temperatures. Energy Convers Manag 48:857–863

Ning L, Duan Q, Chen Z, Kou H, Liu B, Yang B, Zeng K (2020) A comparative study on the combustion and emissions of a non-road common rail diesel engine fueled with primary alcohol fuels (methanol, ethanol, and n- butanol)/diesel dual fuel. Fuel

Petroleum B (2012) BP statistical review of world energy. British Petroleum, London

Pfromm PH, Boadu VA, NelsonR, Vadlani P, Madl R (2010) Bio-butanol vs. bio- ethanol: a technical and economic assessment for corn and switchgrass fermented by yeas tor Clostrididium ccetobutylicum. Biomass Bioenergy 34:515–24

Shahir S, Masjuki H, Kalam M et al (2014) Feasibility of diesel–biodiesel–ethanol/bioethanol blend as existing CI engine fuel: an assessment of properties, material compatibility, safety and combustion. Renew Sustain Energy Rev 32:379–395

Yusri IM, Mamat R, Akasyah MK, Jamlos MF, Yusop AF (2019) Evaluation of engine combustion and exhaust emissions characteristics using diesel/butanol blended fuel. Appl Therm Eng 25(156):209–19

Zhang S, Chen R, Wu H et al (2006) Ginsenoside extraction from Panax quinquefolium L. (American ginseng) root by using ultrahigh pressure. J Pharm Biomed Anal 41:57–63

Zhang Z, Huang Z, Wang X et al (2008) Measurements of laminar burning velocities and Markstein lengths for methanol–air–nitrogen mixtures at elevated pressures and temperatures. Combust Flame 155:358–368

Zhang T, Nilsson LJ, Björkholtz C et al (2016) Effect of using butanol and octanol isomers on engine performance of steady state and cold start ability in different types of diesel engines. Fuel 184:708–717

Chapter 8
Alcohol Fuels in Low-Temperature Combustion Engines

Ayat Gharehghani and Alireza Kakoee

8.1 Introduction

In comparison with conventional compression ignition engines, low-temperature combustion (LTC) operates in lower combustion temperature due to excess air to fuel ratio (QUOTE), usually higher than 1, or usage exhaust gas recirculation (EGR), Salahi and Gharehghani (2019). In fact, in stoichiometric condition, fuel–air oxidation results in higher in-cylinder reaction temperature which producing high level of NO_x emissions; moreover, reduction of oxygen in the area of spray injecting in conventional diesel combustion (CDC) engines leads to produce higher amounts of soot emissions, Scott Goldsborough et al. (2017). Usually, high injection pressure is needed to overcome fuel evaporation and mixing air–fuel issues to reduce soot emissions, but high injection pressure increased wall impingement due to spray tip penetration (STP) effects, Wu et al. (2017). Providing more ignition delay using various techniques, such as variable valve timing control, high level of cooled EGR, and low compression ratio, allows more time to air–fuel mixing process to have more homogenous air–fuel mixture. Although EGR reduced in-cylinder peak temperature, it limits engine operational range and deteriorates engine combustion process which results in decrease of indicated thermal efficiency; in this case, higher amounts of air needed to overcome deficiency of in-cylinder combustion, Imtenan et al. (2014), Thangaraja and Kannan (2016). Recently, modern diesel engines are designed with expensive strategies related to enhancing premixed charge and promote desire in-cylinder peak temperature, such as dual-fuel injection, multiple injection strategies, and negative valve overlapping technology to provide a low-temperature combustion, Harari (2018) and Bhiogade et al. (2017). High swirl ratio and high fuel injection

A. Gharehghani (✉) · A. Kakoee
School of Mechanical Engineering, Iran University of Science and Technology, Tehran, Iran
e-mail: ayat_gharehghani@iust.ac.ir

P. C. Shukla et al. (eds.), *Alcohol as an Alternative Fuel for Internal Combustion Engines*, Energy, Environment, and Sustainability,
https://doi.org/10.1007/978-981-16-0931-2_9

pressure achieved higher level of premixed air–fuel where EGR rate is used to control and obtain desire start of combustion, Gharehghani et al. (2012).

Among all methods to control combustion emissions, advanced combustion technology which controls maximum in-cylinder temperature and equivalence ratio cause to achieve cleaner combustion, especially lower NO_x emissions and near-zero exhaust particle matter (PM), homogenous charge compression ignition (HCCI), premixed charge compression ignition (PCCI), and reactivity-controlled compression ignition (RCCI) engines categorized in low-temperature strategies, was investigated and studied by various researchers, Kakoee and Gharehghani (2019). These investigations encountered with various advanced combustion control techniques such as injection timing strategies, EGR usage, and variable valve actuations (VVAs). Moreover, many investigations suggested that a modification of fuel or combination of fuels and fuel blending provides easier way to control in-cylinder combustion, Gharehghani and Pourrahmani (2019). Generally, in low-temperature combustion strategies, higher volubility and lower reactive fuel or fuel blends are preferable to conventional fuels, like diesel or biodiesel, but various fuels beneficially influence the combustion and emissions characteristics and detreated some other properties Taghavi et al. (2019).

Alcohol fuels were used widely as alternative fuels in spark-ignition and compression ignition engines. Ethanol, methanol, and *n*-butanol show many advantages in diesel and spark-ignition engines. Colorless, high purity, and productibility from many resources such as natural gas, coal, and biomass make alcohols attractive to replace with conventional fuels such as diesel and gasoline, Zhen and Wang (2015). Furthermore, primary alcohol contains higher oxygen content, and also, hydroxyl group (OH) results to have more clean combustion, especially in soot emissions due to more late combustion phase and low temperature; in fact, cooling effects of alcohol fuels provide lower temperature in-cylinder ambient in all loads that cause more late combustion start that this engine specification is also influenced from lower cetane number of alcohol fuels Nour et al. (2019), Hao Chen et al. (2018). According to high octane number of alcohols, they can be used directly in spark-ignition (SI) engines as single-fuel mode or with gasoline as dual-fuel SI mode, Gong et al. (2019,2020). Lower cetane number and viscosity of alcohols make some obstacles in diesel engines without ignition assistance; hence, alcohol fuels are usually used in dual-fuel mode in diesel engines such as alcohol/diesel blends or in high loads in HCCI engines directly, Çelebi and Aydın (2019).

In this chapter, application of alcohol fuels was discussed in various types of low-temperature combustion (LTC) strategies, HCCI, PCCI, and RCCI. Three various main alcohol types are investigated which are ethanol, methanol, and butanol isomers. Operational conditions effects, optimizing operational range, fuel properties, ringing intensity(RI), and emission characteristics were investigated as the main topics in this chapter. In this comparison study, each type of low-temperature combustion strategies was discussed separately with three different alcohol fuel influences. Table 8.1 illustrates various alcohol fuel properties beside common commercial fuels (https://en.wikipedia.org/wiki/Alcohol_fuel).

Table 8.1 Alcohol fuel properties beside gasoline and diesel (https://en.wikipedia.org/wiki/Alcohol_fuel)

Specification	Diesel	Gasoline	Methanol	Ethanol
Molecular formulae	C12–C25	C4–C12	CH_3OH	C_2H_5OH
Cetane number	48	10	03–05	8
Octane number	20–30	97	106–115	110
Oxygen content	***	***	49.9	34.8
Density (g/cm^3)	0.8179	0.7371	0.793	0.7893
LHV (MJ/kg)	42.8	43.5	19.916	26.778
Boiling point	180–370	25–215	64.7	78
Latent heat (kJ/kg)	270	380–500	1167	904

*** means to Zero

8.2 Low-Temperature Combustion Strategies

Numerous advanced combustion strategies have been proposed in recent years to meet the current and future emission requirements. Many of the current strategies fall into the category of premixed low-temperature combustion (LTC). Lower combustion temperatures have the following benefits: reduction in nitrogen oxide contaminants due to high activation energy of nitrogen oxide reactions (energy that needs to produce nitrogen oxides), and the heat transfer losses are reduced, and the higher proportion of special heaters (QUOTE) leads to more efficient work access, Kakoee et al. (2018). In addition, with long ignition delay times, sufficient mixing time is created before combustion begins, so rich areas are reduced and soot formation is prevented. As it was mentioned, there are three general low-temperature strategies available in the literature: homogeneous charge compression ignition (HCCI), premixed charge compression ignition (PCCI) or partial premix combustion (PPC), and reactivity-controlled compression ignition (RCCI) strategies. The relationship between different pollutants for different values of local equivalence ratio and temperature in the combustion strategies of CDC, HCCI, PCCI, and RCCI is shown in Fig. 8.1. Although the boundaries shown in Fig. 8.1 are somewhat optional, the form is useful for understanding different combustion properties Agarwal et al. (2017).

According to this figure, conventional diesel combustion (CDC) comprises areas with high local equivalence ratios and high local temperatures, but low-temperature strategies tend to operate in poor equivalence ratios with lower maximum temperatures than the formation of nitrogen oxides (NO_x) and soot emissions prevented. However, low-temperature zones are those where the least oxidation of unburned hydrocarbons and carbon monoxide occurs. Although low-temperature strategies can reduce the emissions of nitrogen oxides and soot while maintaining diesel performance with higher efficiencies, they often increase the emissions of unburned hydrocarbons, carbon monoxide, and sometimes more difficult combustion controls. These strategies also increase the maximum pressure rise rate (PPRR), Kim et al. (2009). In

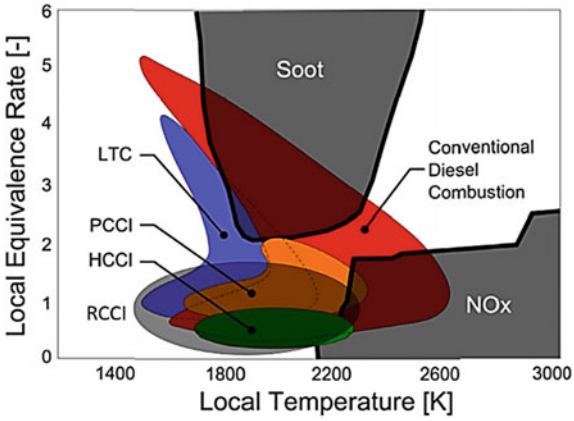

Fig. 8.1 Temperature and equivalence ratio changes in operational regimes of CDC, HCCI, PCCI, and RCCI (Agarwal et al. 2017)

addition to these low combustion temperatures, they often reduce the temperatures of the exhaust gases and therefore require highly efficient tools to recover the energy output such as advanced turbochargers (Kim et al. 2009).

8.2.1 Homogenous Charge Compression Ignition (HCCI) and Alcohol Fuels

Ethanol was used in various investigations related to HCCI engines due to its desire effects on combustion and emissions where wet ethanol that was produced cheaper than dry ethanol, (which is shown in Fig. 8.2), was used directly in HCCI engines (Fig. 8.3), Mack et al. (2009).

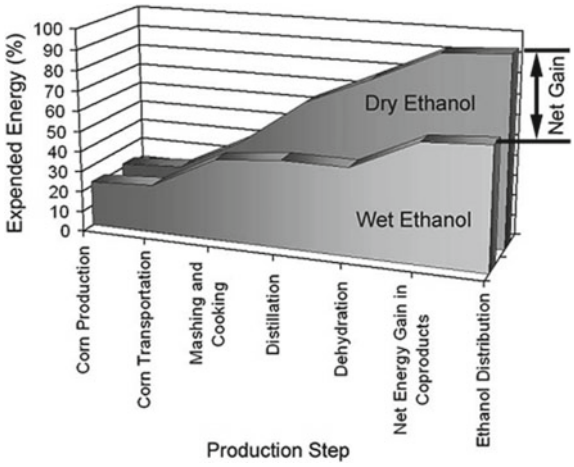

Fig. 8.2 Comparison between expended energy of ethanol and wet ethanol, 35% ethanol in water (Mack et al. 2009)

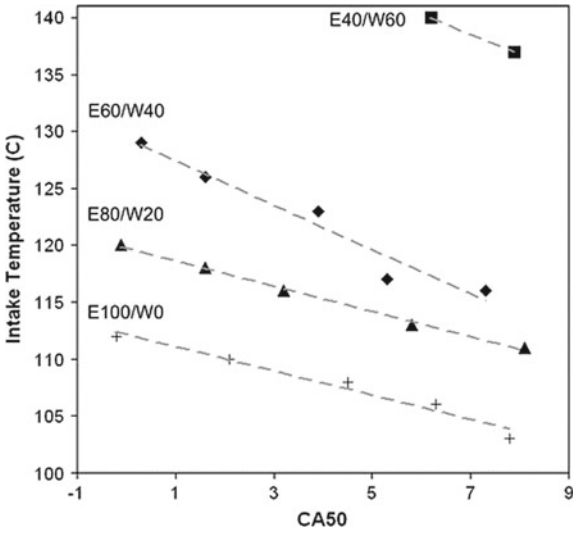

Fig. 8.3 Intake temperature for various ethanol percentages (Mack et al. 2009)

Based on Fig. 8.3, as it was expected, lower cumulative heat release was observed in higher percentages of water that results to lower in-cylinder temperature caused to increase carbon monoxide (CO) and hydrocarbon (HC) and reduced NO_x and soot as engine pollutant. But according to production energy consumption of ethanol in comparison with wet ethanol, overlay, wet ethanol was suggested as suitable fuel in HCCI engines (Mack et al. 2009).

According to restriction of air–fuel ratio in HCCI engines, a suitable air–fuel (ethanol) ratio in various intake temperatures is reported in Fig. 8.4. According to this figure, restricted air–fuel ratios are achieved with applying misfiring condition and engine knocking limitation. More equivalence ratio of ethanol is required for higher intake temperature Kumar et al. (2011).

Power boosting, downsizing, swirl motion, and thermo-physical properties of an ethanol HCCI are illustrated in Fig. 8.5; according to this figure, reduction in displace-

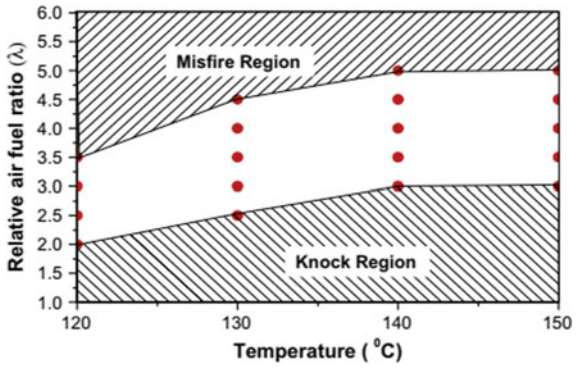

Fig. 8.4 HCCI stable operating range of ethanol (Maurya and Agarwal 2011)

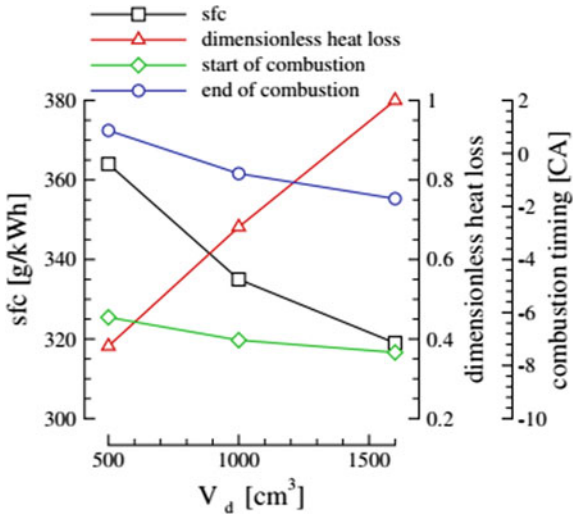

Fig. 8.5 Specific fuel consumption against displacement volume (Viggiano and Magi 2012)

ment volume (V_d) in a dimensionless heat loss, increased specific fuel consumption; in this condition, there were higher amount of HC and CO and lower NO_x as emissions, Viggiano and Magi (2012).

Experimental analysis shows that ethanol HCCI engine produced higher ringing intensity in higher charge temperature and more engine loads. Higher combustion duration in diesel engines in comparison with ethanol ones increases the heat transfer loses. More brake thermal efficiency occurred in ethanol case. In all loads, lower HC and CO emissions were found for diesel HCCI case Bendu and Sivalingam (2016).

Ethanol and *n*-heptane were used also as a fuel mixture in HCCI engines. Higher indicated mean effective pressure was observed in higher ethanol percentages in high loads. Due to higher octane number of ethanol than *n*-heptane increasing ethanol percentage delayed start of ignition and reduced low-temperature heat released peak point where misfiring was occurred at conditions above 50% of ethanol, Lü et al. (2006). It should be explained that octane number is a factor to categorizing fuels in direction of auto-ignition capability; fuels with high octane number and low cetane number are weak in auto-ignition such as gasoline and alcohol fuels which cause to use this type of fuels in CI engines with a high cetane number fuel such as diesel or DME. Experimental analysis shows that although increasing *n*-heptane percentages reduced in-cylinder pressure and temperature, sensitivity of these parameters was negligible, approximately, Vuilleumier et al. (2014). Investigations on emissions show higher amounts of HC and CO in higher ethanol where release of NO_x emissions reported lower in higher ethanol, Wu et al. (2011). Gasoline/ethanol as port fuel was investigated in a partial homogenous charge compression ignition engine in an experimental and numerical research with diesel direct injection fuel. According to the results in the same injection timing, ethanol produced lower engine emissions, CO, HC, NO_x, and soot (Wu et al. 2011).

Comparative studies between ethanol and other fuels in HCCI engines were performed by various researchers; for example, Zou et al. (2016) (https://en.wikipedia.org/wiki/Alcohol_fuel) compared alcohol fuels and diesel in a numerical study. Ethanol, methanol, and gasoline were used as alternative fuels also, and comparing results are reported by (Maurya and Agarwal 2014). Figure 8.6 depicts optimization of operating range of various fuels in constant IMEPs. According to this figure, intake temperature did not influence effectively on IMEP, but equivalence ratio QUOTE shows significant effects on it; in Fig. 8.6, *y*-axis represented equivalence ratio QUOTE and *x*-axis indicated intake temperature. From this figure, HCCI engines have vast range of operational condition in lower engine speed where ethanol HCCI engine operated in more region than two other fuels (methanol, gasoline).Ethanol indicated that thermal efficiency was higher than methanol where ethanol ringing intensity was lower than methanol in the same temperature and equivalence ratio (ER) (Maurya and Agarwal 2014). A comparison with natural gas during an experimental HCCI engine showed higher operational range and combustion efficiency beside high level of HC emission for ethanol and methanol than natural gas, Gharehghani (2019).

Methanol was used as port fuel injection with different high-reactivity fuels such as DME and diesel and also with gasoline which is a low-reactivity fuel. Experimental investigation on methanol in HCCI engines shows delaying in start of combustion where also higher charge temperature has the same effect. Higher equivalence ratio increased thermal efficiency in low charge temperature where in higher charge temperature higher ER reduced it, Zhang and Wu (2016).

Methanol with DME as fuel mixture was used widely in HCCI engines due to its production from biomasses (hydrated type), Huisman et al. (2011); experimental investigation on this type of fuel mixture shows that DME was affected on HCCI methanol engine where its concentration advanced start of combustion and boosted indicated thermal efficiency where EGR also shows same effects in this type of engine. Although methanol shows higher amounts of CO and HC in exhaust emissions due to lower temperature, using DME and EGR with methanol reduced it in HCCI engines. Yao et al. (2006), Pedersen et al. (2010). Numerical studies on methanol and also ethanol show that blending with another fuels such as DME or DEE (diethyl ether), higher equivalence ratio of these types of alcohols increased in-cylinder temperature and pressure which increases engine knocking Zhou et al. (2018). Computational control study in HCCI engine of methanol in combination with DME shows that higher amounts of methanol increased the pressure rise rate and reduced the cumulative heat release, Lee and Lim (2016).

Both gasoline and methanol were categorized in low-reactivity fuels with low cetane number; as a result, combination of these fuels shows different behaviors than methanol and gasoline alone or with other high-reactivity fuels such as DME and diesel. According to experimental studies in a mixture of ethanol and gasoline, advanced start of combustion occurred in comparison with gasoline alone in HCCI engines, Turkcan et al. (2018) where higher amounts of ethanol or methanol in mixture retarded start of combustion and CA50 (crank angle degree where 50% of fuel burned). In a mixture of 10% of ethanol and gasoline (E10), higher amounts of

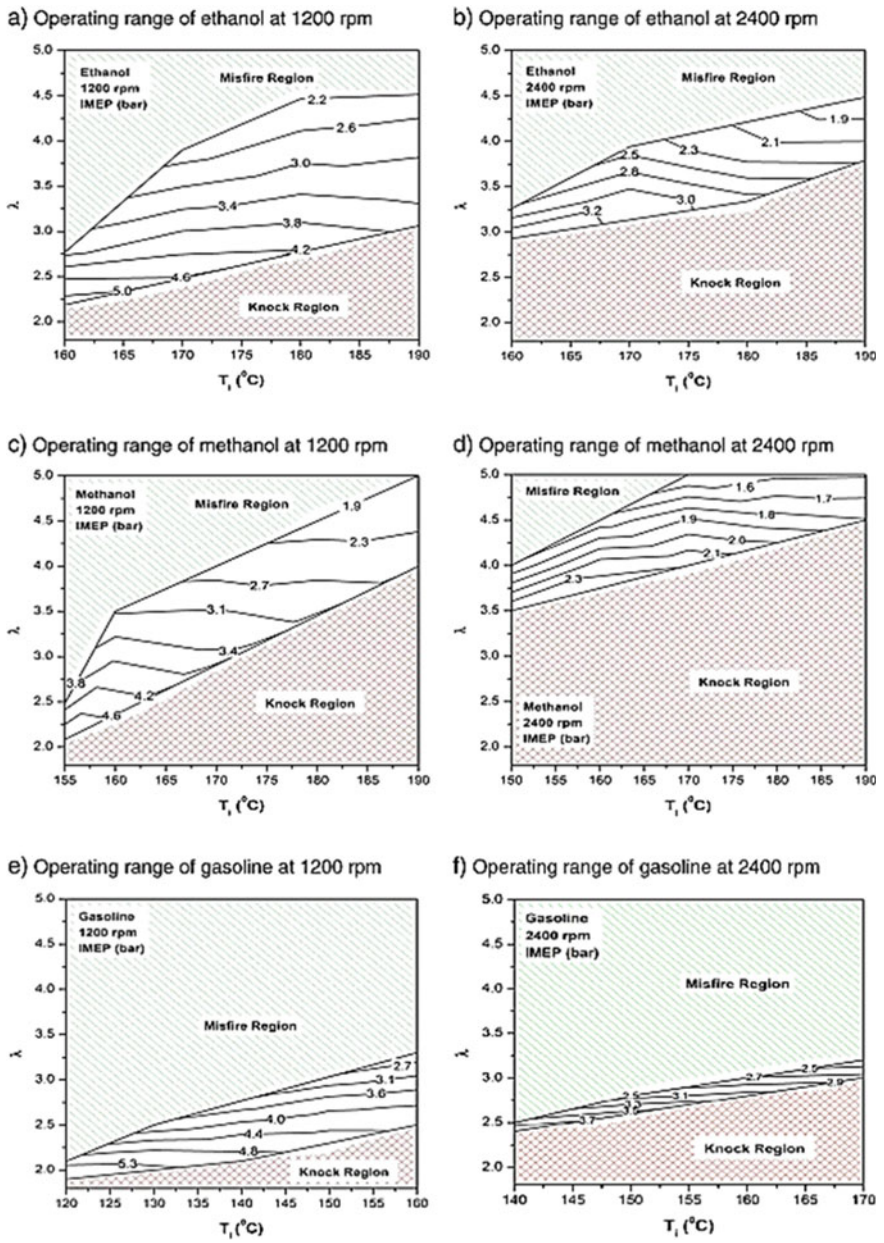

Fig. 8.6 HCCI operation range for various cases studied in constant IMEPs, (Maurya and Agarwal 2014)

pressure rise rate and rate of heat release were reported where M10 (methanol 10% and gasoline) shows higher rate of heat release rate (ROHR) than E10 and gasoline (Turkcan et al. 2018).Methanol also was used as cooling and anti-detonate fuel with *n*-heptane in a HCCI engine, Thanapiyawanit et al. (2012). Comparison between methanol, ethanol, gasoline, and natural gas shows that methanol has vaster operation conditions than gasoline and natural gas, but it has lower area of operation than ethanol as alcohol fuels in HCCI engines, and it should be noted at operational range restricted with knocking area and misfiring limits, Kumar et al. (2014), Gharehghani (2019).

Variation of fuel octane number can be performed with fuel blending. Methanol and ethanol as alcohol fuels in HCCI engines were used in various researches as discussed in the previous sections. Butanol isomers (1-butanol, 2-butanol and *n*-butanol) and their properties are given in Table 8.2 and also investigated in several studies. Butanol has higher cetane number than other alcohol that makes this fuel attractive to use in HCCI engines. Experimental studies show than such as other alcohol fuels *n*-butanol comparison with diesel fuel postponed start of combustion with lower in-cylinder temperature cause to increased HC and CO_2 and reduced NO_x emissions, Zheng et al. (2015). Cooling effects of alcohols result in controlling in-cylinder temperature and pressure with boosting intake pressure and temperature that cause to advancing combustion phasing and ROHR (rate of heat release) in comparison with diesel HCCI case, Xie et al. (2016), and this property also results to use this fuel with *n*-heptane which is a high-reactivity fuel in HCCI engines. Studies show that *n*-butanol reduced maximum pressure rise rate blended with *n*-heptane in comparison with ethanol/*n*-heptane fuel in HCCI mode, where higher hydroxyl radicals of *n*-butanol show better condition than ethanol and isopropanol blend cases in combustion quality and output emissions Saisirirat et al. (2011).

Advanced combustion phasing and higher rate of heat release (ROHR) are reported in *n*-butanol/gasoline HCCI engine in comparison with a gasoline HCCI engines. Figure 8.7 shows experimental investigation results which indicate mean effective pressure (IMEP) coefficient of variation as a factor of ringing intensity for various *n*-butanol/gasoline compared also with ethanol/gasoline blends, Uyumaz (2015),

Table 8.2 Butanol isomers thermos chemical properties (He et al. 2015b; https://en.wikipedia.org/wiki/Alcohol_fuel)

Specification	*n*-butanol	2-butanol	Isobutanol
Molecule formula	C_4H_9OH	C_4H_9OH	C_4H_9OH
Cetane number	12	*	*
RON	96	101	113
Oxygen content	21.6	21.62	21.6
Density (g/cm^3)	0.81	0.806	0.802
LHV (MJ/kg)	35.1	32.74	32.96
Boiling point	117.7	99.5	107.89
Latent heat (kJ/kg)	430	671	579.9

* means to Not defined

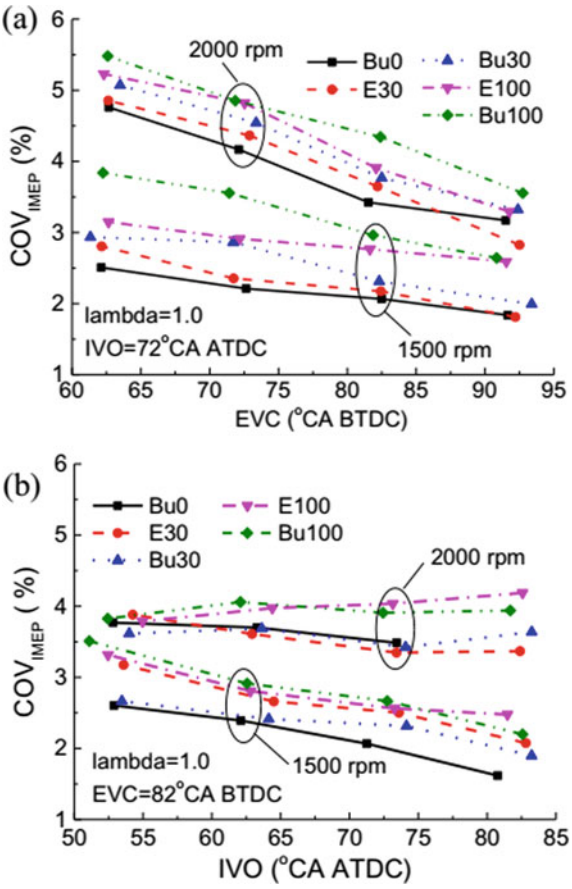

Fig. 8.7 Coefficient of variation of various fuels (He et al. 2015a)

He et al. (2015a). According to Fig. 8.7, two various engine speeds B100 (100% butanol) produced higher coefficient of variation (COV) of IMEP in various intake temperatures (He et al. 2015a).

Comparative studies also reported that *n*-butanol and isobutanol required lower intake temperature to achieve desire combustion phasing compared to ethanol and gasoline where this temperature is reduced against boosting pressure, (He et al. 2015b). Due to suffering HCCI engine from engine knocking, it should be noted that butanol 25% in butanol/*n*-heptane blends needs higher equivalence ratio to avoiding misfiring and engine knocking compared with E25 and M25 which results in higher specific fuel consumption, (Mack et al. 2016). In this case, butanol blends produced moderate indicated thermal efficiency (ITE) and IMEP compared with ethanol and methanol in HCCI engines, Calam et al. (2020).

8.2.2 *Premixed Charge Compression Ignition (PCCI) and Alcohol Fuels*

Premixed charge compression ignition (PCCI), categorized in low-temperature combustion strategies, is first used by Aoyama et al. (1996).In PCCI strategies, fuel is injected into the port fuel early to provide high premixed quality of fuel and air, and PCCI abbreviation is used for early in-cylinder injection also. In this strategy, the fuel, for example, diesel, is usually injected into the cylinder at crank angle degree of 30 to 160 degree bTDC. Mohammadi et al. (2005). In this case, similar to other low-temperature strategies, various control methods were studied such as multi-fuel injection strategies, EGR usage, and alternative fuel use. In PCCI engine, using ethanol in combination with diesel reduced NO_x emissions beside delayed combustion start (Mohammadi et al. 2005). In comparison with gasoline, ethanol/diesel blends produced higher break thermal efficiency, and as the nature of LTC strategies, higher hydrocarbons were observed in PCCI engine Saravanan et al. (2015).It should be noted that ethanol/diesel blends produced lower amounts of HC and CO compared to ethanol/gasoline mixture. Saravanan et al. (2015). Experimental and numerical studies showed that in PCCI engines higher ethanol percentages reduced pressure rise rate and heat release rate (HRR) where these changes increased HC and CO emissions Natarajan et al. (2017), Elzahaby et al. (2018).

Methanol (alcohols) properties such as high mixing rate and octane number cause to difficult cold start and crudely operation of diesel engine Li et al. (2014). Complementary physico-chemical properties of methanol and DME make it attractive for researcher in PCCI engines due to its perfect stratification combustion (Li et al. 2014). Experimental investigations revealed that in methanol direct injection (DI) and DME port fuel injection (PFI), too early injection of methanol results in low in-cylinder temperature that cause a long ignition delay for formation of a high premixed ratio. This low-temperature ignition delay produced higher amounts of CO and HC. On the contrary, very late injection timing dropped in-cylinder temperature, and as a result, combustion process of DME will end sooner than usual and results to remained unburned methanol cause to excessive amount of HC, especially CO. In moderate injection timing, in-cylinder temperature is high enough, and ignition delay is short; as a result, combustion of methanol occurred at high speed which results in minimum release of HC and CO (Yan and Zhang 2014). Higher DME provides higher in-cylinder temperature that produced lower engine-out emissions (Yan and Zhang 2014).

Butanol usage with diesel (blend injecting) decreased the net heating value of fuel mixture which increased brake-specific fuel consumption (BSFC). This influence is also observed in addition to EGR to fuel mixture. In the same injection timing, especially earlier start of injection (SOI), higher injection pressure increased BSFC. Earlier start of injection of butanol produced higher in-cylinder pressure, and more advanced start of combustion results in advance combustion phasing. Earlier start of injection (SOI) also resulted in fast heat release rate and strong premixed combustion, Valentino et al. (2012).

A premixed charge compression ignition engine fueled with ultra-low-sulfur diesel (ULSD#2) and *n*-butanol was compared with direct binary mixture of the same fuel mixture by Soloiu et al. (2015). It was reported that butanol percentages were more effective in direct injection of binary mixture fuels where there was about 12 CAD change in delaying of start of combustion from zero to 65% butanol addition. In-cylinder pressure was higher in port fuel injection (PFI) of butanol, and this is because of effects of fuel cetane number. In PFI strategy, due to lower homogeneity of diesel and *n*-butanol, combustion occurred first in ULSD#2, so butanol burning will be started after ULSD#2 which denoted more effectiveness of ULSD#2 cetane number on combustion start, and this phenomenon is different in *n*-butanol and ULSD#2 binary mixture.

In fact, ULSD#2roles as semi-one fuels with lower cetane number that postponed start of combustion (Soloiu et al. 2015). In PFI strategy, ringing intensity reduced against increasing butanol percentages; in the contrary, higher amounts of butanol in direct injection increased ringing intensity. Apparent heat release rate (APHRR) influences greatly on engine ringing intensity which is higher in direct injection (DI) strategies. Moreover, lower semi-one fuel cetane number is effective on RI also. Lower amounts of engine-out emissions were observed in direct fuel blend injection also (Soloiu et al. 2015). It should be noted that due to lower viscosity of Bu65-DI than ULSD#2, opening of injector delayed a bit and lower LHV of Bu65-DI causes to increase injection duration 2 CAD more than ULSD#2 (Soloiu et al. 2015).

8.2.3 Reactivity-Controlled Compression Ignition (RCCI) and Alcohol Fuels

One of the low-temperature combustion strategies is reactivity-controlled compression ignition (RCCI) which is interested by researchers as a way to have high efficient and clean combustion. In this strategy, low-reactivity fuel such as gasoline or alcohol fuels or blend of alcohol fuels and gasoline or diesel were imported to the cylinder via intake port that is known as port fuel injection (PFI), and high-reactivity fuel like diesel, *n*-heptane, dimethyl ether (DME), etc., is injected directly into the cylinder which is known as DI fuel; in other words, this strategy provides a lean mixture which cause to have low-temperature combustion that results to have more clean combustion beside high engine efficiency Kakoee et al. (2019).

Various experimental and computational researches have been done on ethanol as low-reactivity fuel beside a high-reactivity fuel with single direct injection. A multidimensional computational research with Kiva-3v coupling with chemistry solver (CHEMKIN) on early diesel injection into provided in-cylinder E85 (85% hydrous ethanol) and air mixture as a PCCI dual-fuel strategy was done which was later called RCCI, (Splitter et al. 2011). RCCI mode (E85 + diesel) shows smoother operation where burn duration takes 3.5 ms and PCCI diesel takes 2.5 ms of burn duration (Splitter et al. 2011). RCCI mode of operation cause to delay start of combustion

(SOC) in comparison with diesel PCCI which is because of fuel mixture reduced cetane number, but ethanol PCCI has more delayed SOC in comparison with two other investigated studies (RCCI diesel and PCCI diesel), and this phenomenon is due to lower cetane number of fuel–air mixture of ethanol and then ethanol/diesel and diesel, Splitter et al. (2010). Comparison between gasoline and ethanol in three different premixed ratios (0.47, 0.57, and 0.67) shows that ethanol postponed the start of combustion because of higher octane number than gasoline, and this property also causes to lower in-cylinder peak pressure; ethanol/*n*-heptane blends produced lower amounts of NO_x in comparison with gasoline/*n*-heptane RCCI engine cases, Qian et al. (2015). Studies also show that in the same case of engine load, ethanol produced higher in-cylinder temperature and pressure beside more delayed start of combustion and lower burn duration (Qian et al. 2015). In the same ethanol percentage, SOC was delayed, and burn duration decreased in higher engine loads which cause to reduce thermal loses and higher thermal efficiency beside higher ringing intensity, Dempsey et al. (2012). It should be noted that octane number in RCCI engines influenced from both LRF and HRF where in PCCI engine that usually used a single-fuel affected from PFI fuel, the main difference between effects of octane number in RCCI and PCCI engines is related to circumstances of start of combustion; in RCCI engines, combustion will start due to HRF and penetrated to fuel–air mixture, but in PCCI engine, even in two or one fuel due to premixed fuel–air, the combustion start due to PFI air–fuel (fuels) mixture cetane number or on the other words in PCCI premixed fuels roles as a unic fuel with fuel mixture cetane number.

Single-injection strategy in CDC engines and RCCI strategy usually produce high in-cylinder pressure rise rate that cause to knocking in internal combustion engines, as a way to overcome this problem, double-injection strategy is used and has been investigated numerically and experimentally by many researchers with various fuel blends and engine characteristics. Investigating the main SOI changes shows that delaying in main SOI descends ringing intensity and rate of heat release (ROHR) in medium load of operation for various ethanol-gasoline (E10-95, E10-98, E20-95, and E85, port fuel injected)and B7 (biodiesel/diesel) blends; in this case, CA50 increased and start of combustion delayed Benajes et al. (2015). A double-injection strategy with 75% hydrous ethanol and diesel RCCI engine shows that the second injection timing had no effect on HC and CO emissions in all engine load cases where NO_x emission in low loads increased with delaying SOI2 Fang et al. (2015).

Experimental studies on methanol low-reactivity port fuel injection in combination with diesel DI as high-reactivity fuel show that RCCI mode of operation with methanol produced lower in-cylinder pressure and temperature with SOC delaying, Jia and Denbratt et al. (2018). Delayed diesel injection postponed start of combustion which reduced brake thermal efficiency (BTE) and engine output power (Wei et al. 2016). Increasing methanol mass fraction (methanol mass to total mass) from zero to moderate amounts (40 and 60) ascended in-cylinder pressure and temperature, and methanol boiling point is lower than diesel, wherein moderate amounts of methanol/diesel blends a better combustion occurred due to moderate cetane number, but in higher amount of methanol, octane number increased which causes to lower combustion quality. In higher amount of methanol, 80%, for example, misfiring was

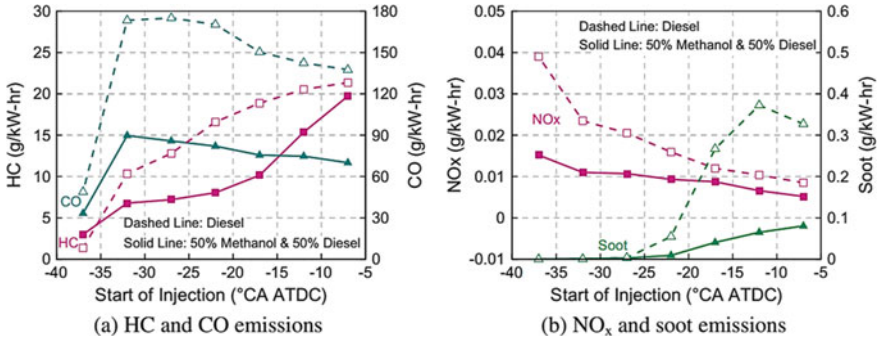

Fig. 8.8 Injection timing effect on emissions (Li et al. 2013)

occurred. Ringing intensity was decreased during increasing methanol mass fraction. Li et al. (2013). Figure 8.8 illustrates emissions of two different fuels in various start of injection; according to this picture, NO_x and soot emissions of methanol/diesel fuel mixture were lower than diesel conventional; moreover, HC and CO as emissions also had better condition in methanol/diesel fuel (Li et al. 2013).

RCCI numerical modeling of methanol/biodiesel with various parameters showed that increasing EGR rate in both high and medium load decreased knocking intensity, and this property ascended in higher methanol mass fraction but decreased against SOI delaying. CO production against MF was increasing in medium loads where soot emissions in all loads decreased. NO_x emission decreased against methanol mass fraction in low and medium loads, where ascending of NO_x emissions in high loads occurred till 20% mass fraction of methanol Zhou et al. (2015a; b).

Comparison between RCCI and direct dual-fuel stratification (DDFS) of methanol/diesel illustrated that DDFS mode released higher thermal efficiency and achieved higher potential of energy recovery beside lower emissions and needs lower demand in-cylinder initial temperature, Li et al. (2020).

Butanol isomers given in Table 8.2 were used also as LRF with various high-reactivity fuels. Comparing conventional diesel combustion, 2-butanol/diesel RCCI engine shows higher in-cylinder peak pressure and maximum heat release and also smaller burn duration. RCCI mode produced lower brake thermal efficiency where it was higher than CDC in high loads (Pan et al. 2017). Experiments on isobutanol depicted that higher injection pressure effects on air–fuel mixture process that cause to advance in ignition and produced lower NO_x as pollutant, Pan et al. (2017).

Blended fuel mode and dual-fuel *n*-butanol/diesel RCCI mode of operation in an experimental engine showed that ignition delay (ID) in RCCI mode did not affect from *n*-butanol ratio in low and medium engine loads, where in high loads, higher ratio of *n*-butanol reduced the ignition delay. Combustion duration of RCCI mode was greater than blended fuel mode of operation in low and medium load, but in high loads, blended fuel mode combustions take longer times (Mobasheri and Seddiq 2018). Investigation on emission characteristics shows that in all loads and *n*-butanol percentages, blended fuel mode released lower amount of soot, HC, and CO where

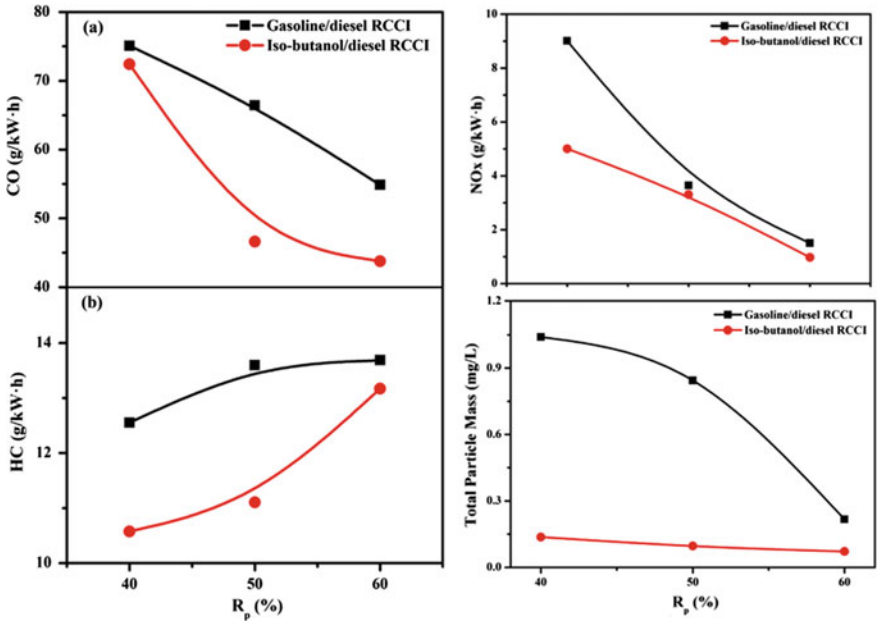

Fig. 8.9 Emission characteristics of various case studies (Zheng et al. 2018)

NO_x emissions in this mode of operation was illustrated higher than RCCI mode, Mobasheri et al. (2018).

Experimental study on isobutanol/diesel and gasoline/diesel in an RCCI engine revealed that higher ignition delay (ID), combustion duration (CD), and CA50 are allocated to isobutanol/diesel in each premixed fuel ratio (PFR) as shown in Fig. 8.9. According to this figure, gasoline/diesel produced higher emissions; those are CO, HC, NO_x, and particle matter, (Zheng et al. 2018).

Ethanol, methanol, and butanol as low-reactivity fuel with diesel in RCCI engine in comparison with gasoline as LRF showed that to obtain a fixed combustion phasing, more diesel quality is needed in the cases of alcohols as LRFs. Methanol/diesel (MD) and ethanol/diesel (ED) released lower combustion duration and pressure rise rate in comparison with gasoline/diesel where these characteristics were higher than *n*-butanol/diesel (nBD) cases. MD and ED fuel mixtures were less sensitive to single-injection strategy compared to gasoline/diesel (GD) and nBD and showed higher sensitivity to PFI premixed ratio. It was concluded that GD and nBD behavior against SOI changes is close to each other, and MD and ED have the same condition. Delayed SOI increased NO_x and decreased soot in low loads that these trends are vice versa in high loads. GD and nBD depicted better condition in NO_x and soot emissions in low loads where in high loads, ED and MD fuel mixture released lower NO_x and emissionsXiang Zhou et al. (2016).

8.3 Conclusions

Various investigations of alcohol fuel application in advanced combustion technologies (ACT), especially low-temperature combustion (LTC) strategies, were reviewed and discussed in this chapter. Effects of fuels mass fraction, injection timing, EGR effects, various engine loads, intake temperature, fuel import strategies, etc., have been explained and discussed. According to the literature review, the main conclusions were listed as follows:

- High octane number of alcohol fuels, greater than gasoline and diesel, makes some difficulty of using them in compression ignition engines. As a result, these fuels were widely used in combination with other fuels, especially high cetane number fuels such as diesel, biodiesel, and dimethyl ether.
- Cooling effects and higher octane number of alcohols make them as a controller fuel for in-cylinder temperature, ringing intensity, and engine knocking.
- Alcohols mentioned properties usually increased unburned hydrocarbons (UHC) and carbon monoxides beside decreasing nitrogen oxides. Undesired UHC and CO can eliminate using exhaust gas recirculation's effects.
- Combination of alcohol fuels with high-reactivity fuels was used to adjust ignition delay, CA50, and engine-out emissions which obtain a desire fuel mixture cetane number.
- Lower density beside LHV increased indicated specific fuel consumption where, in this case, butanol isomers have better condition than ethanol and methanol.
- Among three most used alcohols as fuels (ethanol, methanol, and butanol), ethanol shows vaster rage of operation after methanol and butanol which also have better condition than gasoline and natural gas in HCCI engines.
- Higher hydroxyl content of alcohols in comparison with gasoline produced higher amount of UHC and CO with drastically lower amounts of NO_x.
- In comparison with methanol and butanol, ethanol produced lower coefficient of variable of indicated mean effective pressure which is a factor of ringing intensity.
- Overall, the main limitation of using alcohol fuels in IC engines related to these fuel cooling effects and lower cetane number that cause to weak auto-ignition beside lower heating values and density which results in higher fuel consumption; moreover, hardware fuel delivery system also can be a negative point in using alcohol fuels.

Alcohol fuel application in various countries is dependent on the countries geographical situation and their policies; Brazil, China, USA, European Union, and Japan are the most areas of using alcohol fuels. In this way, government policies were effective on people demands of this type of fuels with providing special vehicles; for example, using flexible-fuel engines in Brazil could increase alcohol fuel demand, especially ethanol up to 88%, and a flexible-fuel engine is a dual-fuel engine with separated fuel tank. Fuel alternative providing in USA also is one of the effectiveness

government policies which deliver E10 and E85 as gasohol fuels. Overall, accessibility of fuels and vehicles were two most influenced government policies in using alcohols as fuels (Moradi et al. 2020).

References

Agarwal AK, Singh AP, Maurya RK (2017) Evolution, challenges and path forward for low temperature combustion engines. Progr Energy Combust Sci 61:1–56. ISSN 0360-1285. https://doi.org/https://doi.org/10.1016/j.pecs.2017.02.001

Aoyama T, Hattori Y, Mizuta JI, Sato Y (1996) An experimental study on premixed-charge compression ignition gasoline engine (No. 960081). SAE technical paper, https://doi.org/https://doi.org/10.4271/960081

Benajes J, Molina S, García A, Monsalve-Serrano J (2015) Effects of low reactivity fuel characteristics and blending ratio on low load RCCI (reactivity controlled compression ignition) performance and emissions in a heavy-duty diesel engine. Energy 90:1261–1271. ISSN 0360-5442. https://doi.org/https://doi.org/10.1016/j.energy.2015.06.088

Bendu H, Sivalingam M (2016) Experimental investigation on the effect of charge temperature on ethanol fueled HCCI combustion engine. J Mech Sci Technol 30(10):4791–4799. https://doi.org/10.1007/s12206-016-0951-6

Bhiogade GE, Sunheriya N, Suryawanshi JG (2017) Investigations on premixed charge compression ignition (PCCI) engines: a review. In: Fluid mechanics and fluid power–contemporary research. Springer, New Delhi, pp 1455–1463. https://doi.org/https://doi.org/10.1007/978-81-322-2743-4_139

Calam A, Aydoğan B, Halis S (2020) The comparison of combustion, engine performance and emission characteristics of ethanol, methanol, fusel oil, butanol, isopropanol and naphtha with n-heptane blends on HCCI engine. Fuel 266:117071. ISSN 0016-2361. https://doi.org/https://doi.org/10.1016/j.fuel.2020.117071

Çelebi Y, Aydın H (2019) An overview on the light alcohol fuels in diesel engines. Fuel 236:890–911. ISSN 0016-2361. https://doi.org/https://doi.org/10.1016/j.fuel.2018.08.138

Chen H, Zhang P, Liu Y (2018). Investigation on combustion and emission performance of a common rail diesel engine fueled with diesel-ethylene glycol dual fuel. Appl Thermal Eng 142:43–55. ISSN 1359-4311. https://doi.org/https://doi.org/10.1016/j.applthermaleng.2018.06.073

Dempsey AB, Das Adhikary B, Viswanathan S, Reitz RD (2012) Reactivity controlled compression ignition using premixed hydrated ethanol and direct injection diesel. J Eng Gas Turbines Power 134(8). https://doi.org/https://doi.org/10.1115/1.4006703

Elzahaby AM, Elkelawy M, Bastawissi HAE, El_Malla SM, Naceb AMM (2018) Kinetic modeling and experimental study on the combustion, performance and emission characteristics of a PCCI engine fueled with ethanol-diesel blends. Egypt J Petrol 27(4):927–937. ISSN 1110-0621. https://doi.org/https://doi.org/10.1016/j.ejpe.2018.02.003

Fang W, Fang J, Kittelson DB, Northrop WF (2015) An experimental investigation of reactivity-controlled compression ignition combustion in a single-cylinder diesel engine using hydrous ethanol. J Energy Resour Technol 137(3). https://doi.org/https://doi.org/10.1115/1.4028771

Gharehghani A (2019) Load limits of an HCCI engine fueled with natural gas, ethanol, and methanol. Fuel 239:1001–1014. ISSN 0016-2361. https://doi.org/https://doi.org/10.1016/j.fuel.2018.11.066

Gharehghani A, Pourrahmani H (2019) Performance evaluation of diesel engines (PEDE) for a diesel-biodiesel fueled CI engine using nano-particles additive. Energy Convers Manag 198:111921. ISSN 0196-8904. https://doi.org/https://doi.org/10.1016/j.enconman.2019.111921

Gharehghani A, Mirsalim SM, Jazayeri SA (2012) Numerical and experimental investigation of combustion and knock in a dual fuel gas/diesel compression ignition engine. J Combust. https://doi.org/https://doi.org/10.1155/2012/504590

Goldsborough SS, Hochgreb S, Vanhove G, Wooldridge MS, Curran HJ, Sung CJ (2017) Advances in rapid compression machine studies of low-and intermediate-temperature autoignition phenomena. Progr Energy Combust Sci 63:1–78. ISSN 0360-1285. https://doi.org/https://doi.org/10.1016/j.pecs.2017.05.002

Gong C, Li Z, Yi L, Liu F (2019) Comparative study on combustion and emissions between methanol port-injection engine and methanol direct-injection engine with H2-enriched port-injection under lean-burn conditions. Energy Convers Manage 200:112096. ISSN 0196-8904. https://doi.org/https://doi.org/10.1016/j.enconman.2019.112096

Gong C, Li Z, Huang K, Liu F (2020) Research on the performance of a hydrogen/methanol dual-injection assisted spark-ignition engine using late-injection strategy for methanol. Fuel 260:116403. ISSN 0016-2361. https://doi.org/https://doi.org/10.1016/j.fuel.2019.116403

Harari PA (2018) Comprehensive review on enabling reactivity controlled compression ignition (RCCI) in diesel engines. Integr Res Adv 5(1):5–19. https://www.pubs.iscience.in/journal/index.php/ira/article/view/758

He B-Q, Liu M-B, Zhao H (2015) Comparison of combustion characteristics of n-butanol/ethanol–gasoline blends in a HCCI engine, Energy Conversion and Management, Volume 95, 2015, Pages 101–109, ISSN 0196-8904. https://doi.org/https://doi.org/10.1016/j.enconman.2015.02.019

He BQ, Liu MB, Zhao H (2015) Comparison of combustion characteristics of n-butanol/ethanol–gasoline blends in a HCCI engine. Energy Convers Manag 95:101–109. ISSN 0196-8904. https://doi.org/https://doi.org/10.1016/j.enconman.2015.02.019

https://en.wikipedia.org/wiki/Alcohol_fuel

Huisman GH, Van Rens GLMA, De Lathouder H, Cornelissen RL (2011) Cost estimation of biomass-to-fuel plants producing methanol, dimethylether or hydrogen. Biomass Bioenergy 35:S155–S166. ISSN 0961-9534. https://doi.org/https://doi.org/10.1016/j.biombioe.2011.04.038

Imtenan S, Varman M, Masjuki HH, Kalam MA, Sajjad H, Arbab MI, Fattah IR (2014) Impact of low temperature combustion attaining strategies on diesel engine emissions for diesel and biodiesels: a review. Energy Convers Manage 80:329–356. https://doi.org/10.1016/j.enconman.2014.0

Jia Z, Denbratt I (2018) Experimental investigation into the combustion characteristics of a Methanol-Diesel heavy duty engine operated in RCCI mode. Fuel 226:745–753. ISSN 0016-2361. https://doi.org/https://doi.org/10.1016/j.fuel.2018.03.088

Kakoee A, Gharehghani A (2019) Comparative study of hydrogen addition effects on the natural-gas/diesel and natural-gas/dimethyl-ether reactivity controlled compression ignition mode of operation. Energy Convers Manage 196:92–104. https://doi.org/10.1016/j.enconman.2019.05.113

Kakoee A, Bakhshan Y, Aval SM, Gharehghani A (2018) An improvement of a lean burning condition of natural gas/diesel RCCI engine with a pre-chamber by using hydrogen. Energy Convers Manag 166:489–499. ISSN 0196-8904. https://doi.org/https://doi.org/10.1016/j.enconman.2018.04.063

Kakoee A, Bakhshan Y, Gharehghani A, Salahi MM (2019) Numerical comparative study of hydrogen addition on combustion and emission characteristics of a natural-gas/dimethyl-ether RCCI engine with pre-chamber. Energy 186:115878. ISSN 0360-5442. https://doi.org/https://doi.org/10.1016/j.energy.2019.115878

Kim D, Ekoto I, Colban WF, Miles PC (2009) In-cylinder CO and UHC imaging in a light-duty diesel engine during PPCI low-temperature combustion. SAE Int J Fuels Lubricants 1(1):933–956. www.jstor.org/stable/26272062

Lee H, Lim O (2016) A computational study of DME-methanol fractions with controlling several factors on HCCI combustion. J Mech Sci Technol 30(4):1931–1941. https://doi.org/10.1007/s12206-016-0352-x

Li Y, Jia M, Liu Y, Xie M (2013) Numerical study on the combustion and emission characteristics of a methanol/diesel reactivity controlled compression ignition (RCCI) engine. Appl Energy 106:184–197. ISSN 0306-2619. https://doi.org/https://doi.org/10.1016/j.apenergy.2013.01.058

Li W, Xu YK, Wang W (2014) Experimental study on emission characteristics of the PCCI-DI Combustion with DME and methanol. In: Applied mechanics and materials, vol. 521, pp 633–637. Trans Tech Publications Ltd. https://doi.org/https://doi.org/10.4028/www.scientific.net/amm.521.633

Li Y, Jia M, Xu L, Bai XS (2020) Multiple-objective optimization of methanol/diesel dual-fuel engine at low loads: a comparison of reactivity controlled compression ignition (RCCI) and direct dual fuel stratification (DDFS) strategies. Fuel 262:116673. ISSN 0016-2361. https://doi.org/https://doi.org/10.1016/j.fuel.2019.116673

Lü X, Hou Y, Zu L, Huang Z (2006) Experimental study on the auto-ignition and combustion characteristics in the homogeneous charge compression ignition (HCCI) combustion operation with ethanol/n-heptane blend fuels by port injection. Fuel 85(17–18):2622–2631. ISSN 0016-2361. https://doi.org/https://doi.org/10.1016/j.fuel.2006.05.003

Mack JH, Aceves SM, Dibble RW (2009) Demonstrating direct use of wet ethanol in a homogeneous charge compression ignition (HCCI) engine. Energy 34(6):782–787. ISSN 0360-5442. https://doi.org/https://doi.org/10.1016/j.energy.2009.02.010

Mack JH, Schuler D, Butt RH, Dibble RW (2016) Experimental investigation of butanol isomer combustion in homogeneous charge compression ignition (HCCI) engines. Appl Energy 165:612–626. ISSN 0306-2619. https://doi.org/https://doi.org/10.1016/j.apenergy.2015.12.105

Maurya RK, Agarwal AK (2011) Experimental study of combustion and emission characteristics of ethanol fuelled port injected homogeneous charge compression ignition (HCCI) combustion engine. Appl Energy 88(4):1169–1180. ISSN 0306-2619. https://doi.org/https://doi.org/10.1016/j.apenergy.2010.09.015

Maurya RK, Agarwal AK (2014) Experimental investigations of performance, combustion and emission characteristics of ethanol and methanol fueled HCCI engine. Fuel Process Technol 126:30–48. ISSN 0378-3820. https://doi.org/https://doi.org/10.1016/j.fuproc.2014.03.031

Mobasheri R, Seddiq M (2018) Effects of diesel injection parameters in a heavy duty iso-butanol/diesel reactivity controlled compression ignition (RCCI) engine (No. 2018-01-0197). SAE technical paper. https://doi.org/https://doi.org/10.4271/2018-01-0197

Mohammadi A, Kee SS, Ishiyama T, Kakuta T, Matsumoto T (2005) Implementation of ethanol diesel blend fuels in PCCI combustion (No. 2005–01–3712). SAE technical paper. https://doi.org/https://doi.org/10.4271/2005-01-3712

Moradi J, Gharehghani A, Mirsalim M (2020) Numerical investigation on the effect of oxygen in combustion characteristics and to extend low load operating range of a natural-gas HCCI engine. Appl Energy 276:115516. https://doi.org/10.1016/j.apenergy.2020.115516

Natarajan S, Shankar SA, Sundareswaran AM (2017) Early injected PCCI engine fuelled with bio ethanol and diesel blends–an experimental investigation. Energy Procedia 105:358–366. ISSN 1876-6102. https://doi.org/https://doi.org/10.1016/j.egypro.2017.03.326

Nour M, Attia AM, Nada SA (2019) Combustion, performance and emission analysis of diesel engine fuelled by higher alcohols (butanol, octanol and heptanol)/diesel blends. Energy Convers Manag 185:313–329. ISSN 0196-8904. https://doi.org/https://doi.org/10.1016/j.enconman.2019.01.105.

Pan S, Li X, Han W, Huang Y (2017) An experimental investigation on multi-cylinder RCCI engine fueled with 2-butanol/diesel. Energy Convers Manag 154:92–101. ISSN 0196-8904, https://doi.org/https://doi.org/10.1016/j.enconman.2017.10.047

Pedersen TD, Schramm J, Yanai T, Sato Y (2010) Controlling the heat release in HCCI combustion of DME with methanol and EGR (No. 2010–01–1489). SAE technical paper. https://doi.org/https://doi.org/10.4271/2010-01-1489

Qian Y, Wang X, Zhu L, Lu X (2015) Experimental studies on combustion and emissions of RCCI (reactivity controlled compression ignition) with gasoline/n-heptane and ethanol/n-heptane as fuels. Energy 88:584–594. https://doi.org/10.1016/j.energy.2015.05.083

Saisirirat P, Togbé C, Chanchaona S, Foucher F, Mounaïm-Rousselle C, Dagaut P (2011) Auto-ignition and combustion characteristics in HCCI and JSR using 1-butanol/n-heptane and ethanol/n-heptane blends. Proc Combust Inst 33(2):3007–3014. ISSN 1540-7489. https://doi.org/https://doi.org/10.1016/j.proci.2010.07.016

Salahi MM, Gharehghani A (2019) Control of combustion phasing and operating range extension of natural gas PCCI engines using ozone species. Energy Convers Manage 199:112000. ISSN 196-8904. https://doi.org/https://doi.org/10.1016/j.enconman.2019.112000

Saravanan S, Pitchandi K, Suresh G (2015) An experimental study on premixed charge compression ignition-direct ignition engine fueled with ethanol and gasohol. Alexandria Eng J 54(4):897–904. ISSN 1110-0168. https://doi.org/https://doi.org/10.1016/j.aej.2015.07.010

Soloiu V, Muinos M, Harp S (2015) Investigation of dual fuel PCCI (PFI of n-Butanol and DI-ULSD) compared with DI of binary mixtures of the same fuels in an omnivorous diesel engine (No. 2015-01-0857). SAE technical paper. https://doi.org/https://doi.org/10.4271/2015-01-0857

Splitter D, Kokjohn S, Rein K, Hanson R, Sanders S, Reitz R (2010) An optical investigation of ignition processes in fuel reactivity controlled PCCI combustion. SAE Int J Engines 3(1):142–162. www.jstor.org/stable/26275475

Splitter DA, Hanson RM, Reitz RD, Manente V, Johansson B (2011) Modeling charge preparation and combustion in diesel fuel, ethanol, and dual-fuel PCCI engines. Atomization Sprays 21(2). https://doi.org/https://doi.org/10.1615/AtomizSpr.2011002836

Taghavi M, Gharehghani A, Nejad FB, Mirsalim M (2019) Developing a model to predict the start of combustion in HCCI engine using ANN-GA approach. Energy Convers Manag 195:57–69. ISSN 0196-8904. https://doi.org/https://doi.org/10.1016/j.enconman.2019.05.015

Thanapiyawanit B, Lu JH (2012) Cooling effect of methanol on an n-heptane HCCI engine using a dual fuel system. Int J Automot Technol 13(7):1013–1021. https://doi.org/10.1007/s12239-012-0104-6

Thangaraja J, Kannan C (2016) Effect of exhaust gas recirculation on advanced diesel combustion and alternate fuels-a review. Appl Energy 180:169–184. https://doi.org/10.1016/j.apenergy.2016.07.096

Turkcan A, Altinkurt MD, Coskun G, Canakci M (2018) Numerical and experimental investigations of the effects of the second injection timing and alcohol-gasoline fuel blends on combustion and emissions of an HCCI-DI engine. Fuel 219:50–61. ISSN 0016-2361. https://doi.org/https://doi.org/10.1016/j.fuel.2018.01.061

Uyumaz A (2015) An experimental investigation into combustion and performance characteristics of an HCCI gasoline engine fueled with n-heptane, isopropanol and n-butanol fuel blends at different inlet air temperatures. Energy Convers Manag 98:199–207. ISSN 0196-8904. https://doi.org/https://doi.org/10.1016/j.enconman.2015.03.043

Valentino G, Corcione FE, Iannuzzi SE, Serra S (2012) Experimental study on performance and emissions of a high speed diesel engine fuelled with n-butanol diesel blends under premixed low temperature combustion. Fuel 92(1):295–307. ISSN 0016-2361. https://doi.org/https://doi.org/10.1016/j.fuel.2011.07.035

Viggiano A, Magi V (2012) A comprehensive investigation on the emissions of ethanol HCCI engines. Appl Energy 93:277–287. ISSN 0306-2619. https://doi.org/https://doi.org/10.1016/j.apenergy.2011.12.063

Vuilleumier D, Kozarac D, Mehl M, Saxena S, Pitz WJ, Dibble RW, Chen JY, Sarathy SM (2014) Intermediate temperature heat release in an HCCI engine fueled by ethanol/n-heptane mixtures: An experimental and modeling study. Combust Flame 161(3):680–695. ISSN 0010-2180. https://doi.org/https://doi.org/10.1016/j.combustflame.2013.10.008

Wei L, Yao C, Han G, Pan W (2016) Effects of methanol to diesel ratio and diesel injection timing on combustion, performance and emissions of a methanol port premixed diesel engine. Energy 95:223–232. ISSN 0360-5442. https://doi.org/https://doi.org/10.1016/j.energy.2015.12.020

Wu HW, Wang RH, Ou DJ, Chen YC, Chen TY (2011) Reduction of smoke and nitrogen oxides of a partial HCCI engine using premixed gasoline and ethanol with air. Appl Energy 88(11):3882–3890. ISSN 0306-2619. https://doi.org/https://doi.org/10.1016/j.apenergy.2011.03.027

Wu B, Zhan Q, Yu X, Lv G, Nie X, Liu S (2017) Effects of Miller cycle and variable geometry turbocharger on combustion and emissions in steady and transient cold process. Appl Therm Eng 118:621–629. https://doi.org/10.1016/j.applthermaleng.2017.02.074

Xie K, Yanai T, Yang Z, Reader G, Zheng M (2016) Emission analysis of HCCI combustion in a diesel engine fueled by butanol (No. 2016–01–0749). SAE technical paper. https://doi.org/https://doi.org/10.4271/2016-01-0749

Yan Y, Zhang YS (2014) The study on PCCI mode of diesel engine fueled with methanol/dimethyl ether. In: Applied mechanics and materials, vol. 607, pp 629–632. Trans Tech Publications Ltd. https://doi.org/https://doi.org/10.4028/www.scientific.net/amm.607.629

Yao M, Chen Z, Zheng Z, Zhang B, Xing Y (2006) Study on the controlling strategies of homogeneous charge compression ignition combustion with fuel of dimethyl ether and methanol. Fuel 85(14–15):2046–2056. ISSN 0016-2361. https://doi.org/https://doi.org/10.1016/j.fuel.2006.03.016

Zhang C, Wu H (2016) Combustion characteristics and performance of a methanol fueled homogenous charge compression ignition (HCCI) engine. J Energy Inst 89(3):346–353. ISSN 1743-9671. https://doi.org/https://doi.org/10.1016/j.joei.2015.03.005

Zhen X, Wang Y (2015) Numerical analysis on original emissions for a spark ignition methanol engine based on detailed chemical kinetics. Renew Energy 81:43–51. ISSN 0960-1481. https://doi.org/https://doi.org/10.1016/j.renene.2015.03.027

Zheng M, Han X, Asad U, Wang J (2015) Investigation of butanol-fuelled HCCI combustion on a high efficiency diesel engine. Energy Convers Manage 98:215–224. ISSN 0196-8904. https://doi.org/https://doi.org/10.1016/j.enconman.2015.03.098

Zheng Z, Xia M, Liu H, Shang R, Ma G, Yao M (2018) Experimental study on combustion and emissions of n-butanol/biodiesel under both blended fuel mode and dual fuel RCCI mode. Fuel 226:240–251. ISSN 0016-2361. https://doi.org/https://doi.org/10.1016/j.fuel.2018.03.151

Zhou DZ, Yang WM, An H, Li J (2015) Application of CFD-chemical kinetics approach in detecting RCCI engine knocking fueled with biodiesel/methanol. Appl Energy 145:255–264. ISSN 0306-2619. https://doi.org/https://doi.org/10.1016/j.apenergy.2015.02.058

Zhou DZ, Yang WM, An H, Li J, Shu C (2015) A numerical study on RCCI engine fueled by biodiesel/methanol. Energy Convers Manag 89:798–807. ISSN 0196-8904. https://doi.org/https://doi.org/10.1016/j.enconman.2014.10.054

Zhou Q, Ali MJM, Mohan B, Lu XC, Im H (2018) A computational study of lean limit extension of alcohol HCCI engines (No. 2018–01–1679). SAE technical paper. https://doi.org/https://doi.org/10.4271/2018-01-1679

Zou X, Wang H, Zheng Z, Reitz R, Yao M (2016) Numerical study of the RCCI combustion processes fuelled with methanol, ethanol, n-butanol and diesel (No. 2016-01-0777). SAE technical paper. https://doi.org/https://doi.org/10.4271/2016-01-0777

Chapter 9
Effect of *n*-Butanol and Gasoline Blends on SI Engine Performance and Emissions

Balendra V. S. Chauhan, M. K. Shukla, and Atul Dhar

Abbreviations

CR	Compression ratio
MEP	Mean effective pressure
MON	Motor octane number
RON	Research octane number
C_f	Calorific value
HP	Horse power
P	In-cylinder pressure
Temp	Temperature
CC	Centimeter cube
RPM	Revolution per minute
N m	Newton meter
s	Second
h	Hour
CO_2	Carbon dioxide
CO	Carbon monoxide
SFC	Specific fuel consumption
g	Gram
T	Torque
IC	Internal combustion
SI	Spark ignition

B. V. S. Chauhan · M. K. Shukla (✉)
Automotive Fuels and Lubricants Application Division, CSIR-Indian Institute of Petroleum, Dehradun, India
e-mail: mshukla@iip.res.in

M. K. Shukla · A. Dhar
School of Engineering, Indian Institute of Technology Mandi, Mandi, India

P. C. Shukla et al. (eds.), *Alcohol as an Alternative Fuel for Internal Combustion Engines*, Energy, Environment, and Sustainability,
https://doi.org/10.1007/978-981-16-0931-2_10

CI	Compression ignition
A/*F*	Air/fuel ratio
MBT	Maximum brake torque
Q	Heat
°C	Degree centigrade
Eth	Ethanol
But	Butanol
M.P.	Melting point
RVP	Reid vapor pressure
IBP	Initial boiling point
FBP	Final boiling point
VLI	Vapor lock index

9.1 Introduction

Biobutanol is considered as next-generation alcoholic fuel having lower volatility and higher energy density as compared to ethanol. Biobutanol alludes to butanol that has been produced through the feedstock based on biomass. Biomass is made by the microbial fermenting alike ethanol and may be produced through a range of starch, sugar, or cellulosic feedstock. For the time being, the production of butanol is too exorbitant than ethanol; hence it has not been scaled up on a mass scale. Despite that, biobutanol exhibits numerous benefits as compared to ethanol, and hence, it is the focal point of significant research and development (Karimi et al. 2015; Pfromm et al. 2010; Puthiyapura et al. 2016; Kumar and Gayen 2011; Wu et al. 2008; Swana et al. 2011; Agathou and Kyritsis 2011; Rakopoulos et al. 2011; Merwe et al. 2013). The butanol is a clear colorless liquid having a stable characteristic order. Butanol is a highly refractive compound, moderately water-soluble (having 63 g/l water solubility), and miscible with most of the solvents (ether, ketones, alcohols, aldehydes, and aromatic and aliphatic hydrocarbons) (Singh et al. 2010; Schoo and Hoxie 2012; Laza and Bereczky 2011; Atmanli 2016; Atmanli et al. 2015; Carvalho et al. 2012; Rakopoulos et al. 2010; Hönig et al. 2014). Butanol is made effectively by starch or sugar through anaerobic fermentation. Biobutanol can be produced from the fermentation of sugar beets, corn, potatoes, agricultural waste, grain, grass, trees, or leaves, etc.

Butanol is a better alcohol-based alternative fuel to ethanol and provides numerous advantages comprising a lower latent heat of vaporization and a higher heating value (Lapuerta et al. 2018; Yusri et al. 2017; Sileghem et al. 2015; Yilmaz et al. 2014; Jin et al. 2011; Moxey et al. 2016). Butanol's octane number is higher than ethanol. Moreover, butanol absorbs lesser water than ethanol, and it is less corrosive than ethanol. Lower corrosiveness of butanol makes its blending and utilization suitable without any significant modification in the current fuel supply infrastructure and engine fuel handling system. Researchers around the globe have done a lot of study

on methanol blended with gasoline, the reported difference of emissions and engine performance is not very prominent (Lapuerta et al. 2017a; Elfasakhany 2018; Varol et al. 2014; Calam et al. 2020; Li et al. 2018; Iliev 2018).

The chapter describes the blending gasoline with butanol in different volume by volume percentages presented as But10G or B10 (10% butanol with 90% gasoline), But30G or B30 (30% butanol with 70% gasoline), But50G or B50 (50% butanol with 50% gasoline), But70G or B70 (70% butanol with 30% gasoline). The properties such as density, calorific value, Reid vapor pressure (RVP), initial boiling point (IBP), final boiling point (FBP), research octane number (RON), vapor lock index (VLI) of the blended butanol with gasoline helped to understand the volatility of the gasoline and blended fuel. RON is determined by operating the fuel under controlled conditions in a test engine with a variable compression ratio, and comparing the results to those for iso-octane and n-heptane mixtures (Sayin et al. 2005; Rankovic et al. 2015; Hsieh et al. 2002). RVP is described as the absolute vapor pressure exerted by the liquid vapor and any dissolved gases/moisture at 37.8 °C (100 °F) as calculated by the ASTM-D-323 test method (Vazquez-Esparragoza et al. 1992; Dudar et al. 2017). The VLI is the test used to regulate the gasoline's propensity to form a vapor lock. Vapor lock arises when the actual pressure of the gasoline falls below the vapor pressure level of the gasoline, somewhere in the fuel supply system. If this occurs, the gasoline vaporizes from a liquid phase to a vapor phase, and insufficient quantity of gasoline enters the combustion chamber to maintain the correct air/fuel (A/F) ratio. Consequently, the engine operation is disturbed (Xu et al. 2008). This chapter describes the engine performances of butanol blend fuelled engine by comparing the maximum torque, maximum power, and BSFC for each blend with gasoline.

9.2 General Characteristics of *n*-Butanol

The general fuel properties of butanol such as heat of vaporization, air/fuel ratio, energy density, specific energy, MON, RON, and kinematic viscosity are compared with some commonly used alcohols used with gasoline as blendes for fueling SI engines in Table 9.1. As compared to other alcohol fuels, the A/F requirement of butanol is closest to gasoline which is the most widely used fuel for SI engines. This ensures that power drop from designed gasoline fuelled engine is small on butanol fuelling when compared to gasoline fuelled operation of the engine.

The *n*-butanol's octane rating is lower than methanol and ethanol, but it's quite comparable with gasoline. The *n*-Butanol has a RON value of 96 and a MON value of 78, whereas *t*-butanol is having the RON of 105 and MON of 89. Moreover, *t*-Butanol is employed in gasoline as an additive; however, its higher M.P. of 25.5 °C makes it inappropriate to be utilized in its pure form, as a higher melting point triggers it to behave like gel at room temperature (Ni et al. 2001; Ku and Wang 2002).

Knocking is less prone in fuel with higher octane rating (extremely spontaneous and rapid combustion by compression) and control system attached with any modern car's engine can easily have an advantage from this by simply making an adjustment

Table 9.1 Fuel properties (Yusri et al. 2017; Kumar et al. 2013; Chen et al. 2010, 2013, 2014; Campos-Fernández et al. 2012; Zhang et al. 2006; Li et al. 2019; Shahir et al. 2014; Giakoumis et al. 2013; Kumar and Saravanan 2016; Awad et al. 2017)

Type of fuel	Energy density (MJ/l)	Heat of vaporization (MJ/kg)	Specific energy (MJ/kg)	*A*/*F* ratio	RON	MON
Ethanol	19.6	0.92	29.99	9.0	129	102
Methanol	16	1.2	19.69	6.5	136	104
Butanol	29.2	0.43	36.60	11.2	96	78
Gasoline	32	0.36	46.40	14.6	91–99	81–89

in the ignition timing (Rashid et al. 2019; Kalghatgi 2001a, b; Stein et al. 2012; Szybist et al. 2010; Mittal and Heywood 2010; Yates et al. 2005; Wei et al. 2016). It will enhance the energy efficiency, which may lead to an improved fuel economy as compared to the energy content shown by different fuels. By raising the CR, further improvement in fuel economy, torque, and power can be attained.

The alcohol fuels, butanol, and ethanol need to run at richer mixtures than gasoline as they are partially oxidized. To accommodate the variations in the fuel, the standard gasoline engines in cars can regulate *A*/*F* ratio in certain limits. The engine will run lean, if it is made to run on a gasoline blend with large percentage of butanol or on pure butanol, and there is a risk that the components may get critically damaged. Moreover, in comparison to ethanol, butanol can be mixed in higher ratios with gasoline to be used in existing cars, and there is no need to retrofit, because of the reason that the energy content remains close to gasoline (Yusri et al. 2019; Xu and Avedisian 2015). The per unit volume and per unit weight energy density of alcohol fuels are lower as compared to gasoline. With the increase in carbon chains, alcohol's viscosity increases. So, whenever a great viscous solvent is wished, butanol is employed as compared to shorter alcohols (Lapuerta et al. 2017b). Butanol's kinematic viscosity 4.1 mm^2/s (Serras-Pereira et al. 2009) is approximately 10 times greater than gasoline, and it is more viscous as compared to diesel fuels. During the cold start and in colder weather, the inadequate vaporization of alcohols is a well-known issue (Yaws and Hopper 1976; Turner et al. 2007; Zhu et al. 2012; Bharathiraja et al. 2017). As compared to the engine running on methanol or ethanol, it is easier to start the engine operating on butanol, as its heat of vaporization is lesser by half of the ethanol.

9.3 Experimental Setup

Important fuel properties were examined according to the standards of ASTM, which are given in Table 9.2. The density of the fuels was assessed by, DMA 4500 M and Anton Paar density meter according to the standards of ASTM 4052. The Research Octane number (RON) is calculated through ERASPEC instrument according to the standards of ASTM D 2699. The Reid vapor pressure (RVP) of blends was

Table 9.2 Blended fuel properties

Characteristics	Gasoline	Eth10G	But10G	But30G	But50G	But70G
Density(g/cc)@15 °C	0.7602	0.7630	0.7655	0.8222	0.7838	0.7958
RVP (kPa)	59.5	52.7	45.5	26	22.8	
IBP	41.5	34.5	32.6	43.2	44.5	50.2
RON	85.9	86	87.5	92.6	98.5	>104
FBP	198.7	199.9	196.6	180.8	173.8	126.1
Calorific value (Cal/g)	11,263.3	10,932.3	10,939.2	10,291.0	9642.8	8994.6

measured by following ASTM D 323 standards by the RVP measuring instrument (ISL Company). The automated distillation instruments ADA-IV, Precision, and CEL|D-86-13 were used to measure the D86 distillation property. The bomb calorimeters (Paar industries instruments 6300 Calorimeter) was used to measure the calorific values.

9.3.1 Distillation Characteristics of the Blends

To get the distillation properties of the various blends, standard ASTM D-86 test method was carried out at atmospheric pressure, and the results are shown in this test is fundamental for the quality control of fuel because it gives a broad data that can be derived from the interpolation of the obtained results. The distillation (volatility) test measures the vaporized fuel's percentage with temperature increment. It additionally characterizes the critical impact on the performance and safety of the fuel. The distillation curve for different butanol, gasoline blends is shown in Fig. 9.1.

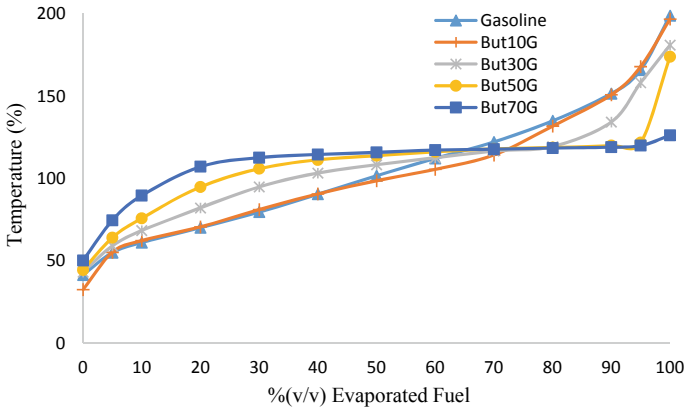

Fig. 9.1 Distillation characteristics of gasoline and butanol blends

Table 9.3 Engine specifications

Engine specifications	
Type of engine	4-Stroke, single-valve engine, forced air-cooled
Stroke × Bore (mm)	61 × 73
Number of cylinders	1
Compression ratio (CR)	5.1:1
Displacement (mm)	256
Capacity of lube oil sump	950 ml
Ignition system	TCI
Rated output (HP/HR)	4.0/3000
Generator specifications	
Frequency	50 Hz
Maximum AC output	2400 V A
Voltage	220 V
Rated AC output	2200 V A
Current	10 A

Temperature for which 50% v/v vaporization of fuel is observed can be called as critical parameter. Too low temperature for 50% vaporization may result in solidification of water vapors present in intake air, which may lead to the development of ice on the elements involved in blend formation. If the temperature value for which 90% v/v vaporization of fuel is observed is too high, then the fuel can survive in liquid form inside the cylinder. This liquid fuel moves the lubricant and triggers the dilution of the oil. In addition, proper combustion may be hindered, resulting in an improper operation of the engine. The 3000 rpm steady speed, forced air-cooled SI engine (single cylinder) with CR 5.1 along with 2.2 KVA AC was utilized for experimental investigations of butanol blends performance and emissions characteristics. The generator and engine's details are depicted in Table 9.3.

The engine was loaded with an electrical generator of frequency 50 Hz, 10 A current and voltage 220 V. Engine load was estimated by measurement of current and voltage out of the electrical generator. The experimental setup is given in Fig. 9.2. For monitoring the exhaust gas and engine oil temperature, *K*-type thermocouples were used. Table 9.3 shows the generator and engine specifications. The engine was stabilized for 15 min to achieve the steady state indicated by constant engine oil temperature of 75 °C, after setting the operating point engine oil reaches. For each of the test fuels, tests were performed for 3 times. The resistive load bank connected with generator was outfitted with a frequency meter, ammeter, and voltmeter for measuring the engine load.

MEXA-584L automotive exhaust analyzer, was used to measure the emissions of the engine's tailpipe. For every test fuel, the emissions during cold start were also measured. The concentration of hydrocarbon (HC), carbon dioxide (CO_2), carbon monoxide (CO), nitrogen monoxide (NO) and specific fuel consumption in the

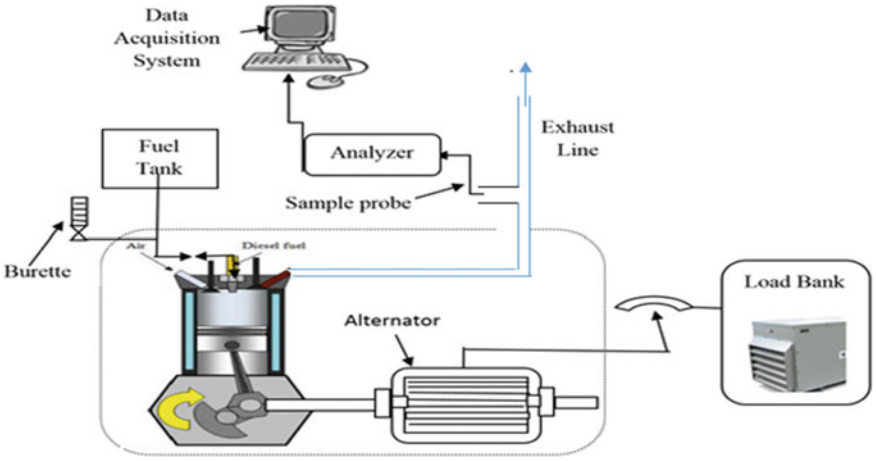

Fig. 9.2 Experimental setup

engine exhaust were measured. The experimental results of these measurements are presented in the next section.

9.4 Results and Discussion

9.4.1 Brake Power and Torque

The torque and maximum brake power at full throttle for all test fuels are shown in Figs. 9.3 and 9.4, respectively. The maximum brake power and torque are achieved by gasoline fuel at full throttle position as expected due to its higher calorific value than gasoline butanol blends.

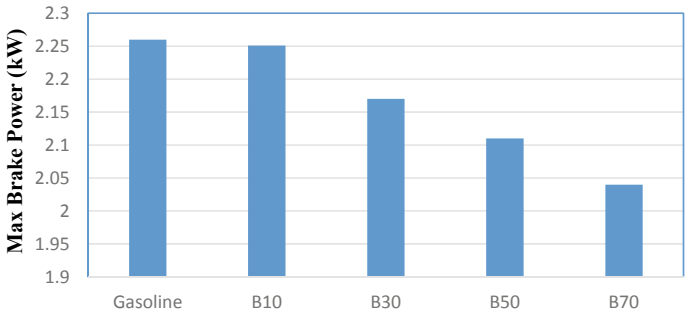

Fig. 9.3 Maximum brake power for various alcohol blends

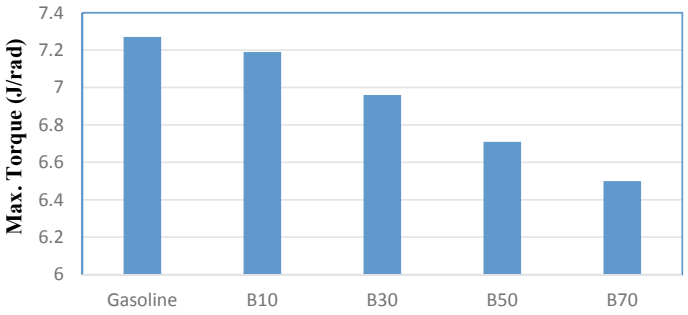

Fig. 9.4 Max torque for various butanol blends

The maximum power output from the engine for But70G (70% butanol with 30% gasoline) fuel was lowest as it has the least calorific value. The maximum torque achieved by the engine gradually reduces as the blending ratio of butanol increases in the fuel.

9.4.2 Brake-Specific Fuel Consumption (BSFC)

Figure 9.5 shows comparative specific fuel consumption for gasoline and butanol–gasoline blends. Here But70G has the least calorific value because butanol has lower energy density than gasoline. For producing 1.935 kW power, gasoline consumes the least amount of fuel. BSFC gradually increases from gasoline to higher blends of butanol.

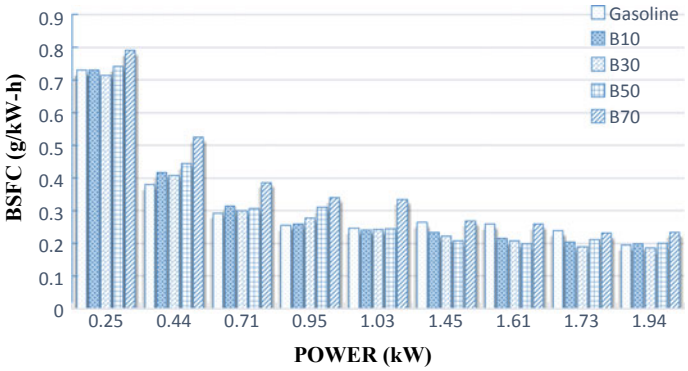

Fig. 9.5 BSFC for various butanol blends

9.4.3 Engine Emissions

Figure 9.6 shows the comparative CO emission for gasoline and butanol blends. CO is a toxic gas which is formed due to incomplete combustion in the short supply of oxygen. Whenever the oxygen-containing butanol is blended with gasoline, it improves the combustion resulting into lower carbon monoxide emissions. At around 1 kW load, the engine CO emission shows maximum in case of gasoline fuel. Due to the presence of more oxygen in oxygenated fuels, CO formed during the combustion process gets oxidized into CO_2. Thus, the amount of CO in the exhaust increased drastically for But70G due to deficiency of air supply since the stoichiometric air requirement of butanol is higher than gasoline. It indicates that butanol blending with gasoline at higher butanol concentrations is not feasible in unmodified SI engines designed for gasoline.

The various fuels' effect on HC emission is shown in Fig. 9.7. As the load increases, the HC concentration in tailpipe decreases. Because of oxygen contained

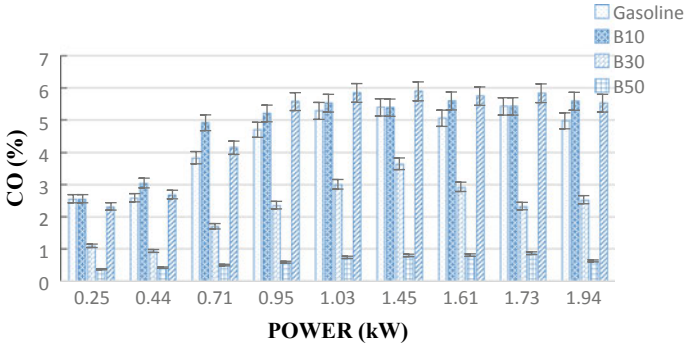

Fig. 9.6 Comparative CO emission for various butanol blends

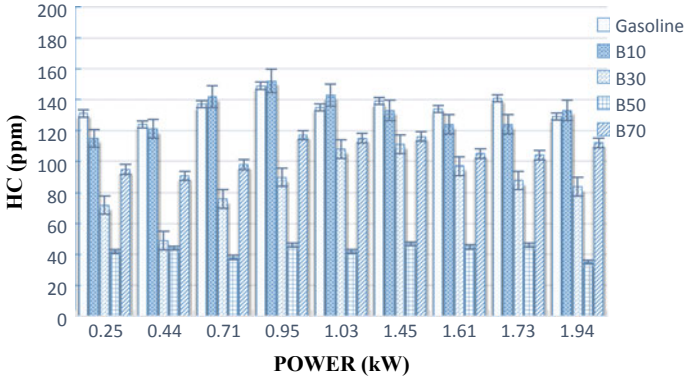

Fig. 9.7 Comparative HC emission for various butanol blends

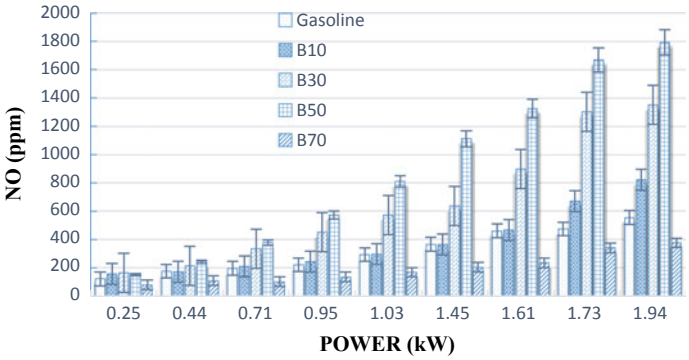

Fig. 9.8 Comparative NO emission for various butanol blends

in But70G fuels, the fuel burns better than in case of gasoline so less HC emission is observed. Least HC concentration is seen at maximum load for But50G. Butanol in gasoline HC emission decreases with a rise in the percentage of oxygenates added to the fuel blend up to 50% butanol blending. The lowest level of HC emission is given by 50% butanol in gasoline as compared to other butanol–gasoline blends. This is because of efficient combustion taking place in the presence of more oxygenated fuel, but a higher blending percentage of butanol results into oxygen deficiency due to the requirement of more oxygen for producing the same energy from the combustion of butanol in comparison to gasoline. Also, butanol has higher flame speed than gasoline so for the same amount of time more fuel is getting burned to leave less HC in the exhaust pipe.

The effect of various engine loads on NO emissions is given in Fig. 9.8. Due to the reaction of oxygen and nitrogen under high pressure and temperature in the engine cylinder, NO is formed. As shown in Fig. 9.8, at 1935 W engine loads, 50% butanol–gasoline blend has the highest NO emission. For butanol–gasoline blends as the engine load increases, NO emissions also increase. At maximum load, maximum concentration of NO is seen in all the fuels out of which But50G has the highest value. Due to the efficient burning of fuel with 50% butanol, the temperature of exhaust gases rises and this increases NO concentration. Therefore, according to this, the highest concentration is found in 50% butanol. This proves that efficient combustion, on one hand, reduces HC emissions but on the other hand, increases NO emissions.

9.4.4 Cold Emissions

When the gasoline-fuelled vehicle starts at low ambient temperatures, then excessive emissions are produced (Yusuf and Inambao 2018, 2019). Researchers have reported that the majority of CO and HC total emissions in average real world are because

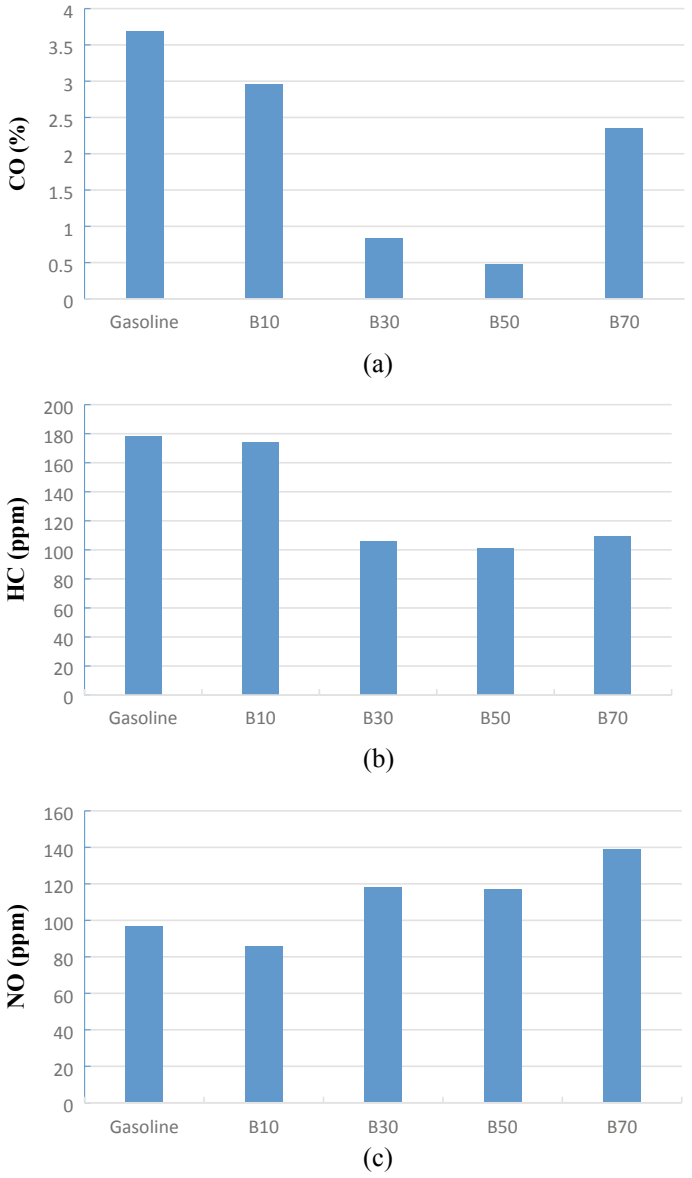

Fig. 9.9 Cold. **a** CO, **b** HC, and **c** NO emissions for different blends

of extra emissions seen during cold start (Yusuf and Inambao 2018). There is less available data, for newer vehicles to reveal the impact of butanol–gasoline blends on the exhaust emissions, mainly related to warm and cold start processes.

Cold start emissions for all fuel blends are plotted in Fig. 9.9 with gasoline emissions. But50G was observed to have lowest CO, HC emissions than others as butanol has higher flame speed than gasoline. As the percentage of butanol in the gasoline blends increases (up to 50%), combustion improves and less CO and HC emissions are observed. Further increase in butanol percentage in the blends may result in poor fuel vaporization and air/fuel mixing. This poor mixture quality results into higher CO and HC emission for B70 in comparison to B50.

The exhaust emissions may be high during first 2 min, if car's engine has been idle for many hours. This takes place due to following reasons:

Rich A/F ratio requirement in cold engines: The fuel does not vaporize totally when cold engine is made to start that results in higher CO and HC emissions. CO and HC emissions lower when engine attains normal operating temperature. There are many techniques practiced to reduce the start-up phase duration, some of them are material and technology advancement such as fuel injection controlled by computer, deduction in intake lengths, and fuel preheating. Catalytic converter's inefficiency in cold operating conditions: An inefficiency is seen in catalytic converters until they are warmed up to their ideal operating temperature. The techniques practiced to resolve this includes placing the catalytic converter nearer to the exhaust manifold, and installing a quick-to-heat-up small-sized catalytic converter right at exhaust manifold. This is done in order to allow the bigger main catalytic converter to take its time in warming up and reaching the operating temperature. More techniques are being developed such as chemical reaction preheating, electric heating, flame heating and thermal battery for improving the light-off duration of the catalytic convertor systems.

Blending of butanol into the gasoline up to 50% can be one possible strategy for reducing the cold start HC and CO emissions.

9.5 Conclusions

The engine test results of butanol blends with gasoline are comparable to that of baseline gasoline. Some major deductions that can be made are as follows:

- The maximum torque achieved by the engine gradually reduces as the blending ratio of butanol increase in the fuel.
- BSFC gradually increases from gasoline to higher blends of butanol.
- The CO emissions increased drastically for But70G due to the deficiency of air supply as the stoichiometric air requirement of butanol is higher than gasoline.
- As the load increases, the HC concentration in tailpipe decreases, but NO emissions increase.

In most of the cases, butanol blends are a better choice over gasoline in terms of emissions and performance. Being an oxygenated fuel, butanol gives better combustion efficiency and reduces most of the emissions except NO, which can be taken care of by the means of after treatments. Results of this study indicate that butanol blending with gasoline at higher butanol concentrations (>50%) is not feasible in unmodified SI engines designed for gasoline. Production and consumption cycle of biobutanol, as a whole, results in smaller emission than the conventional fuels of fossil origins as it is a biofuel. However, further study of these blends, as well as butanol production process, needs to be conducted to further reduce its market cost and make the commercial use of this fuel possible.

References

Agathou MS, Kyritsis DC (2011) An experimental comparison of non-premixed bio-butanol flames with the corresponding flames of ethanol and methane. Fuel 90(1):255–262

Atmanli A (2016) Comparative analyses of diesel–waste oil biodiesel and propanol, n-butanol or 1-pentanol blends in a diesel engine. Fuel 176:209–215

Atmanli A, Ileri E, Yuksel B, Yilmaz N (2015) Extensive analyses of diesel–vegetable oil–n-butanol ternary blends in a diesel engine. Appl Energy 145:155–162

Awad OI, Ali OM, Mamat R, Abdullah AA, Najafi G, Kamarulzaman MK, Yusri IM, Noor MM (2017) Using fusel oil as a blend in gasoline to improve SI engine efficiencies: a comprehensive review. Renew Sustain Energy Rev 69:1232–1242

Bharathiraja M, Venkatachalam R, Murugesan A, Tiruvenkadam N (2017) Experimental investigation of a novel alcohol fumigation in a single-cylinder constant speed diesel engine. Int J Amb Energy 38(8):794–802

Calam A, Aydoğan B, Halis S (2020) The comparison of combustion, engine performance and emission characteristics of ethanol, methanol, fusel oil, butanol, isopropanol and naphtha with n-heptane blends on HCCI engine. Fuel 266:117071

Campos-Fernández J, Arnal JM, Gómez J, Dorado MP (2012) A comparison of performance of higher alcohols/diesel fuel blends in a diesel engine. Appl Energy 95:267–275

Carvalho DL, de Avillez RR, Rodrigues MT, Borges LE, Appel LG (2012) Mg and Al mixed oxides and the synthesis of n-butanol from ethanol. Appl Catal A 415:96–100

Chen CC, Liaw HJ, Shu CM, Hsieh YC (2010) Autoignition temperature data for methanol, ethanol, propanol, 2-butanol, 1-butanol, and 2-methyl-2, 4-pentanediol. J Chem Eng Data 55(11):5059–5064

Chen G, Shen Y, Zhang Q, Yao M, Zheng Z, Liu H (2013) Experimental study on combustion and emission characteristics of a diesel engine fueled with 2, 5-dimethylfuran–diesel, n-butanol–diesel and gasoline–diesel blends. Energy 54:333–342

Chen Z, Wu Z, Liu J, Lee C (2014) Combustion and emissions characteristics of high n-butanol/diesel ratio blend in a heavy-duty diesel engine and EGR impact. Energy Convers Manage 78:787–795

Dudar AM, Jentz RR (2017) Ford global technologies LLC, 2017. Estimating vehicle fuel Reid vapour pressure. U.S. Patent 9,850,853

Elfasakhany A (2018) Exhaust emissions and performance of ternary iso-butanol–bio-methanol–gasoline and n-butanol–bio-ethanol–gasoline fuel blends in spark-ignition engines: Assessment and comparison. Energy 158:830–844

Giakoumis EG, Rakopoulos CD, Dimaratos AM, Rakopoulos DC (2013) Exhaust emissions with ethanol or n-butanol diesel fuel blends during transient operation: a review. Renew Sustain Energy Rev 17:170–190

Hönig V, Kotek M, Mařík J (2014) Use of butanol as a fuel for internal combustion engines. Agron Res 12(2):333–340
Hsieh WD, Chen RH, Wu TL, Lin TH (2002) Engine performance and pollutant emission of an SI engine using ethanol–gasoline blended fuels. Atmos Environ 36(3):403–410
Iliev S (2018) Comparison of ethanol, methanol and butanol blending with gasoline and relationship with engine performances and emissions. Ann DAAAM Proc 29
Jin C, Yao M, Liu H, Chia-fon FL, Ji J (2011) Progress in the production and application of n-butanol as a biofuel. Renew Sustain Energy Rev 15(8):4080–4106
Kalghatgi GT (2001) Fuel anti-knock quality-Part I. Engine studies. SAE Trans 1993–2004
Kalghatgi GT (2001) Fuel anti-knock quality-Part II. Vehicle studies-how relevant is motor octane number (MON) in modern engines? SAE Trans 2005–2015
Karimi K, Tabatabaei M, Sárvári Horváth I, Kumar R (2015) Recent trends in acetone, butanol, and ethanol (ABE) production. Biofuel Res J 2(4):301–308
Ku, Y. and Wang, L.K., 2002. Decomposition of 2-chlorophenol in aqueous solutions by ozone and UV/ozone processes in the presence of t-butanol. Ozone Sci Eng 24(2):133–144
Kumar M, Gayen K (2011) Developments in biobutanol production: new insights. Appl Energy 88(6):1999–2012
Kumar BR, Saravanan S (2016) Use of higher alcohol biofuels in diesel engines: a review. Renew Sustain Energy Rev 60:84–115
Kumar S, Cho JH, Park J, Moon I (2013) Advances in diesel–alcohol blends and their effects on the performance and emissions of diesel engines. Renew Sustain Energy Rev 22:46–72
Lapuerta M, Ballesteros R, Barba J (2017a) Strategies to introduce n-butanol in gasoline blends. Sustainability 9(4):589
Lapuerta M, Rodríguez-Fernández J, Fernández-Rodríguez D, Patiño-Camino R (2017b) Modeling viscosity of butanol and ethanol blends with diesel and biodiesel fuels. Fuel 199:332–338
Lapuerta M, Hernández JJ, Rodríguez-Fernández J, Barba J, Ramos A, Fernández-Rodríguez D (2018) Emission benefits from the use of n-butanol blends in a Euro 6 diesel engine. Int J Engine Res 19(10):1099–1112
Laza T, Bereczky Á (2011) Basic fuel properties of rapeseed oil-higher alcohols blends. Fuel 90(2):803–810
Li Y, Chen Y, Wu G, Chia-fon FL, Liu J (2018) Experimental comparison of acetone-n-butanol-ethanol (ABE) and isopropanol-n-butanol-ethanol (IBE) as fuel candidate in spark-ignition engine. Appl Therm Eng 133:179–187
Li S, Liu J, Wang F, Wang J, Wei M, Yang S (2019) Experimental study on combustion and emission characteristics of a diesel engine fueled with diesel-gasoline-iso-butanol blends. Fuel 255:115761
Mittal V, Heywood JB (2010) The shift in relevance of fuel RON and MON to knock onset in modern SI engines over the last 70 years. SAE Int J Engines 2(2):1–10
Moxey BG, Cairns A, Zhao H (2016) A comparison of butanol and ethanol flame development in an optical spark ignition engine. Fuel 170:27–38
Ni N, Tesconi M, Tabibi SE, Gupta S, Yalkowsky SH (2001) Use of pure t-butanol as a solvent for freeze-drying: a case study. Int J Pharm 226(1–2):39–46
Pfromm PH, Amanor-Boadu V, Nelson R, Vadlani P, Madl R (2010) Bio-butanol vs. bio-ethanol: a technical and economic assessment for corn and switchgrass fermented by yeast or Clostridium acetobutylicum. Biomass Bioenergy 34(4):515–524
Puthiyapura VK, Brett DJ, Russell AE, Lin WF, Hardacre C (2016) Biobutanol as fuel for direct alcohol fuel cells, investigation of Sn-modified pt catalyst for butanol electro-oxidation. ACS Appl Mater Interfaces 8(20):12859–12870
Rakopoulos DC, Rakopoulos CD, Giakoumis EG, Dimaratos AM, Kyritsis DC (2010) Effects of butanol–diesel fuel blends on the performance and emissions of a high-speed DI diesel engine. Energy Convers Manage 51(10):1989–1997
Rakopoulos CD, Dimaratos AM, Giakoumis EG, Rakopoulos DC (2011) Study of turbocharged diesel engine operation, pollutant emissions and combustion noise radiation during starting with bio-diesel or n-butanol diesel fuel blends. Appl Energy 88(11):3905–3916

Rankovic N, Bourhis G, Loos M, Dauphin R (2015) Understanding octane number evolution for enabling alternative low RON refinery streams and octane boosters as transportation fuels. Fuel 150:41–47

Rashid AK, Mansor MRA, Racovitza A, Chiriac R (2019) Combustion characteristics of various octane rating fuels for automotive thermal engines efficiency requirements. Energy Procedia 157:763–772

Sayin C, Kilicaslan I, Canakci M, Ozsezen N (2005) An experimental study of the effect of octane number higher than engine requirement on the engine performance and emissions. Appl Therm Eng 25(8–9):1315–1324

Schoo R, Hoxie A (2012) Basic properties of refined, bleached and deodorized soybean oil–butanol blends. Fuel 102:701–708

Serras-Pereira J, Aleiferis PG, Richardson D, Wallace S (2009) Characteristics of ethanol, butanol, iso-octane and gasoline sprays and combustion from a multi-hole injector in a DISI engine. SAE Int J Fuels Lubr 1(1):893–909

Shahir SA, Masjuki HH, Kalam MA, Imran A, Fattah IR, Sanjid A (2014) Feasibility of diesel–biodiesel–ethanol/bioethanol blend as existing CI engine fuel: an assessment of properties, material compatibility, safety and combustion. Renew Sustain Energy Rev 32:379–395

Sileghem L, Ickes A, Wallner T, Verhelst S (2015) Experimental investigation of a DISI production engine fuelled with methanol, ethanol, butanol, and iso-stoichiometric alcohol blends. Argonne National Laboratory (ANL), Argonne, IL (United States)

Singh KP, Agarwal H, Shukla VK, Vibhu I, Gupta M, Shuka JP (2010) Ultrasonic velocities, densities, and refractive indices of binary mixtures of polyethylene glycol 250 dimethyl ether with 1-propanol and with 1-butanol. J Solution Chem 39(11):1749–1762

Stein RA, Polovina D, Roth K, Foster M, Lynskey M, Whiting T, Anderson JE, Shelby MH, Leone TG, VanderGriend S (2012) Effect of heat of Vapourization, chemical octane, and sensitivity on knock limit for ethanol-gasoline blends. SAE Int J Fuels Lubr 5(2):823–843

Swana J, Yang Y, Behnam M, Thompson R (2011) An analysis of net energy production and feedstock availability for biobutanol and bioethanol. Biores Technol 102(2):2112–2117

Szybist J, Foster M, Moore WR, Confer K, Youngquist A, Wagner R (2010) Investigation of knock limited compression ratio of ethanol gasoline blends (No. 2010-01-0619). SAE Technical Paper

Turner JWG, Pearson RJ, Holland B, Peck R (2007) Alcohol-based fuels in high performance engines. SAE Trans 55–69

Van der Merwe AB, Cheng H, Görgens JF, Knoetze JH (2013) Comparison of energy efficiency and economics of process designs for biobutanol production from sugarcane molasses. Fuel 105:451–458

Varol Y, Öner C, Öztop HF, Altun Ş (2014) Comparison of methanol, ethanol, or n-butanol blending with unleaded gasoline on exhaust emissions of an SI engine. Energy Sour Part A Recov Util Environ Effects 36(9):938–948

Vazquez-Esparragoza JJ, Iglesias-Silva GA, Hlavinka MW, Bullin JA (1992) How to estimate Reid vapour pressure (RVP) of blends. Bryan Research & Engineering, Inc. Encycl Chem Proc Des 47:415–424

Wei H, Feng D, Pan M, Pan J, Rao X, Gao D (2016) Experimental investigation on the knocking combustion characteristics of n-butanol gasoline blends in a DISI engine. Appl Energy 175:346–355

Wu M, Wang M, Liu J, Huo H (2008) Assessment of potential life-cycle energy and greenhouse gas emission effects from using corn-based butanol as a transportation fuel. Biotechnol Prog 24(6):1204–1214

Xu Y, Avedisian CT (2015) Combustion of n-butanol, gasoline, and n-butanol/gasoline mixture droplets. Energy Fuels 29(5):3467–3475

Xu SH, Liu X, Qin M (2008) Study on the evapouration property and gas block tendency of methanol-gasoline. Veh Engine 3

Yates AD, Swarts A, Viljoen CL (2005) Correlating auto-ignition delays and knock-limited spark-advance data for different types of fuel. SAE Trans 735–747

Yaws CL, Hopper JR (1976) Physical and thermodynamic properties. 20. Methanol, ethanol, propanol, and butanol. Chem Eng 83(12):119–127

Yilmaz N, Vigil FM, Benalil K, Davis SM, Calva A (2014) Effect of biodiesel–butanol fuel blends on emissions and performance characteristics of a diesel engine. Fuel 135:46–50

Yusri IM, Mamat R, Najafi G, Razman A, Awad OI, Azmi WH, Ishak WFW, Shaiful AIM (2017) Alcohol based automotive fuels from first four alcohol family in compression and spark ignition engine: A review on engine performance and exhaust emissions. Renew Sustain Energy Rev 77:169–181

Yusri IM, Mamat R, Akasyah MK, Jamlos MF, Yusop AF (2019) Evaluation of engine combustion and exhaust emissions characteristics using diesel/butanol blended fuel. Appl Therm Eng 156:209–219

Yusuf AA, Inambao FL (2018) Progress in alcohol-gasoline blends and their effects on the performance and emissions in SI engines under different operating conditions. Int J Amb Energy 1–17

Yusuf AA, Inambao FL (2019) Effect of cold start emissions from gasoline-fueled engines of light-duty vehicles at low and high ambient temperatures: recent trends. Case Stud Thermal Eng 14:100417

Zhang S, Chen R, Wu H, Wang C (2006) Ginsenoside extraction from *Panax quinquefolium* L. (American ginseng) root by using ultrahigh pressure. J Pharm Biomed Anal 41(1):57–63

Zhu H, Kee RJ, Chen L, Cao J, Xu M, Zhang Y (2012) Vaporisation characteristics of methanol, ethanol and heptane droplets in opposed stagnation flow at low temperature and pressure. Combust Theor Model 16(4):715–735

Chapter 10
Ethanol Fumigation and Engine Performance in a Diesel Engine

Ali Zare, Richard J. Brown, and Timothy Bodisco

Abbreviations and Symbols

E00	Neat diesel
E10	10% ethanol substitution
E20	20% ethanol substitution
E30	30% ethanol substitution
E40	40% ethanol substitution
BSFC	Brake-specific fuel consumption
BMEP	Brake mean effective pressure
CoV	Coefficient of variation
FMEP	Friction mean effective pressure
IMEP	Indicated mean effective pressure.

10.1 Introduction

The negative aspects of fossil fuels (e.g., environmental degradation, adverse health effects and global warming) have directed the world toward renewable alternatives such as biofuels (Directive 2009/28/EC). For example, the EU issued EC Directive 2003/30 to increase the share of biofuel to 2% by 2005 and to 5.75% by 2010. Directive 2009/28/EC was also issued to increase the share of biofuel to 10% by

A. Zare · T. Bodisco (✉)
School of Engineering, Deakin University, Waurn Ponds, Geelong, VIC 3216, Australia
e-mail: t.bodisco@deakin.edu.au

R. J. Brown
Biofuel Engine Research Facility, Queensland University of Technology, Brisbane, QLD 4001, Australia

P. C. Shukla et al. (eds.), *Alcohol as an Alternative Fuel for Internal Combustion Engines*, Energy, Environment, and Sustainability,
https://doi.org/10.1007/978-981-16-0931-2_11

2020. Therefore, researchers around the world are investigating various types of biofuels conducting different studies to evaluate the feasibility of using them for different applications.

Between biofuels, alcohol fuels became of great interest and promise owing to their availability, storage and handling—there are some issues and difficulties with some other biofuels (Imran et al. 2013). For example, biogas needs to be used at high pressure and biodiesels from edible oils have the potential to lead to food shortages, even biodiesels derived from non-edible oil require cultivation at a large scale (Ghadikolaei 2016). Alcohol can be produced from locally grown crops, agricultural feedstock which are carbon-based, or even from waste materials such as waste paper, grass, and tree trimmings (Ghadikolaei 2016). Recently, the production of alcohol fuels from renewable resources has increased globally (Imran et al. 2013); however, it is not something new to use alcohol as a fuel in combustion. For example, Ford Motor Company used corn alcohol in Henry Ford's Model T in 1908 (Ghosh and Prelas (2011)).

Established in the 1970s as an alternative to conventional fossil fuels due to the oil crisis, ethanol is an alcohol biofuel widely used in the transportation sector (Popa et al. 2001). This could be because using ethanol as a fuel mixture was feasible in conventional vehicles without modification. A famous story of turning to ethanol is related to Brazil. This country has a high capacity for growing sugarcane, and their response to oil price increase was promoting the indigenous ethanol production from sugarcane and mandating the mixture of ethanol with gasoline in 1976. In the Euro regulation (Technologies 2019), the use of ethanol (commonly denoted as E10, which is a blend of 90% petrol and 10% ethanol by volume) became mandated by March 2016 for new types and August 2018 for all types of petrol vehicles. In EPA regulation, after 2020, E15 (15% ethanol by volume) will be the certification fuel for all petrol vehicles (Technologies 2019).

Ethanol can be produced from sugarcane, potato, sugar beets and a number of other starch-containing plants (Imran et al. 2013). Ethanol, which is known to have a hydroxyl group (–OH) attached to one of the carbon atoms (Ghadikolaei 2016), has a low viscosity compared to diesel, thereby making injection easier and also it can better atomize and mix with air. It also has high oxygen content, no sulfur, and a high hydrogen-to-carbon ratio; it therefore has some advantages in terms of emissions, such as particulate matter (Imran et al. 2013).

In positive-ignition engines, alcohol fuels such as ethanol can be used directly as a blend with petrol (E5 and E10), or directly as a pure fuel (in some cases, engine modifications are required), due to the fact that ethanol has a high octane number and similar physical properties to petrol (Imran et al. 2013; Ghadikolaei 2016). While, in compression ignition engines, alcohol fuels such as ethanol cannot be used as a pure fuel owing to different factors such as its low cetane number (Kuszewski et al. 2017).

In compression ignition engines, alcohol fuels such as ethanol can be used via blending or fumigation (Ghadikolaei 2016). In the blending method, alcohol gets mixed with diesel before fuel injection. However, this method typically requires fuel additives to avoid miscibility issues, consequently there are some limitations in

terms of the blending ratio and potential cost issues with the additives (Lapuerta et al. 2009). The alternative to the blending method is fumigation. During fumigation, the fuel is introduced into the intake air via carburetion, spray, or injection. This method can be advantageous as it premixes a portion of the fuel (in this case alcohol fuel) with the intake air outside the combustion chamber and then diesel fuel gets injected directly into the cylinder and the combined mixture of the air, alcohol, and diesel combusts; therefore, a part of the required energy will be provided by the alcohol energy. However, the fumigation method requires some minor modification to the engine, which can be done by adding a separate fuel tank, fuel line and controlling system in addition to a low-pressure fuel injector. Through this method, a large portion of the alcohol fuel can be introduced without the miscibility issues inherent with blending (Udayakumar et al. 2004). Abu-Qudais et al. (2000) used a single-cylinder diesel engine and compared the effect of ethanol fumigation and ethanol–diesel blend on engine performance and emission parameters, and reported that the engine performed better via the fumigation method. Other studies have also shown that fumigation has a more positive effect on thermal efficiency than blending (Imran et al. 2013; Ghadikolaei 2016).

Using ethanol fumigation can affect the engine performance parameters. Zhang et al. (2011) investigated the effect of ethanol fumigation (at 10 and 20% substitution) on engine performance parameters using a direct-injection diesel engine and reported a decrease in thermal efficiency at low load and an increase at high loads. Tsang et al. (2010) used a four-cylinder diesel engine with a direct-injection system and investigated the effect of ethanol fumigation (up to 20%) on different engine performance parameters and reported that using ethanol fumigation decreased the thermal efficiency at low and medium loads and increased the peak in-cylinder pressure and heat release rate. Morsy (2015) performed an experimental investigation on a single-cylinder direct-injection diesel engine using different ethanol–water mixture fumigations and reported an improvement in exergy and energy efficiencies. Abu-Qudais et al. (2000) used a single-cylinder direct-injection diesel engine and studied the effect of ethanol fumigation and reported that the thermal efficiency was improved using ethanol fumigation. Studies by Heisey et al. (1981) and Hansdah et al. (2014) reported an increase in thermal efficiency as well. Ekholm et al. (2009) used a heavy-duty six-cylinder turbocharged diesel engine and reported that ethanol fumigation resulted in higher thermal efficiency. Reduced exhaust temperature, improvement in thermal efficiency, and increased heat release rate were also reported by another study (Goldsworthy 2013) which investigated the influence of ethanol–water mixture fumigation on a heavy-duty engine at a constant speed under two engine loads (17 and 20 bar, BMEP).

There are some studies in the literature evaluating the influence of ethanol fumigation (mostly by up to 20% by substitution) on some engine performance parameters. However, given that using ethanol in the transportation sector is increasing, there is a need in the literature for a comprehensive study on engine performance

aspects of using this fuel. Therefore, this study aims to address this by fundamentally investigating the effect of ethanol fumigation on a wide range of engine performance and combustion parameters using 0, 10, 20, 30, and 40% ethanol substitutions (by energy) at 1500 rpm (speed at which peak torque occurs) and 2000 rpm (rated speed). The parameters discussed in this study are ethanol energy, mass ratio, FMEP, BSFC, mechanical efficiency, thermal efficiency, in-cylinder pressure and volume, maximum in-cylinder pressure, maximum rate of pressure rise, combustion instability, and heat release rate.

10.2 Methodology

This study used a Cummins diesel engine coupled to an electronically controlled hydraulic dynamometer which can control the engine speed/load. Table 10.1 shows the engine specification.

Figure 10.1 shows the test setup schematic diagram to feature the ethanol fumigation system and in-cylinder data acquisition. In the fumigation system, ethanol was directly introduced into the intake air at the inlet manifold between the turbocharger and intercooler. Vaporization and mixing with air took place while the charge air flowed through the inlet manifold and through several elbows. In order to ensure the repeatability of the fuel delivery at different engine speeds/loads, the pressure difference between the post turbocharger manifold and the ethanol fuel rail was used as a feedback to the pressure relief valve of ethanol. Using this feedback mechanism and regulating the pressure relief valve ensured the steady supply of ethanol to the cylinder. In the experiment, calibrated flow meters were used to assure the quality of the measurements. Also, to collect the in-cylinder pressure data, a piezoelectric transducer, Kistler (6053CC60), and Data Translation simultaneous A-to-D convertor (DT9832) were connected to a computer using an in-house National Instruments LabView program. Crank angle data was collected by a Kistler-type 2614 sensor.

Table 10.1 Engine specifications

Model	Cummins ISBe220 31
Aspiration	Turbocharged
Maximum power (kW @ rpm)	162 @ 2000
Maximum torque (Nm @ rpm)	820 @ 1500
Capacity (L)	5.9
Cylinders	6 in-line
Bore × stroke (mm × mm)	102 × 120
Compression ratio	17.3:1
Emission standard	Euro III
Dynamometer type	Electronically controlled water brake

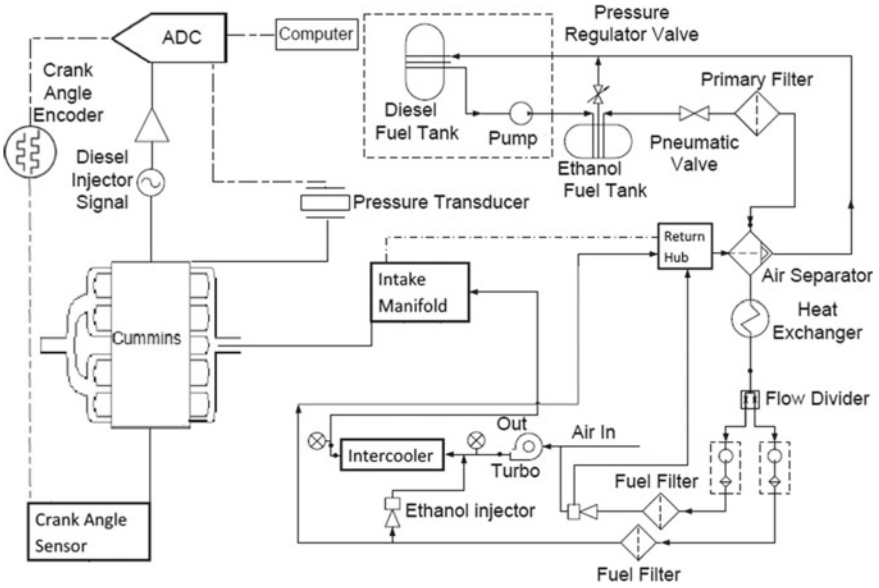

Fig. 10.1 Schematic diagram of test setup (Bodisco and Brown 2013)

More detailed information about the data collection and test facility can be found in reference (Bodisco and Brown (2013); Bodisco et al. 2015).

In this experimental investigation, the engine was run under 25, 50, 75, and 100% engine loads at engine speeds of 1500 rpm (speed at which peak torque occurs) and 2000 rpm (rated speed) using 0–40% ethanol substitutions (by energy) denoted E00 (diesel), E10 (10% ethanol substitution), E20 (20% ethanol substitution), E30 (30% ethanol substitution) and E40 (40% ethanol substitution). To perform the test for each substitution, the engine was run with diesel and stabilized at the required load, then the diesel energy was reduced via reducing the engine load by the substitution percentage, and then, given that during fumigation the fuel is introduced into the intake air via carburetion, spray or injection, the fumigated ethanol was introduced to the system to achieve the original engine load. The engine was left to stabilize again before data collection.

10.3 Results and Discussion

This section discusses engine performance parameters, such as ethanol energy, mass ratio, FMEP, BSFC, mechanical efficiency and thermal efficiency. The analysis of combustion parameters such as in-cylinder pressure, maximum in-cylinder pressure, pressure rise maximum rate, combustion instability, pressure–volume diagram, and heat release rate is also discussed.

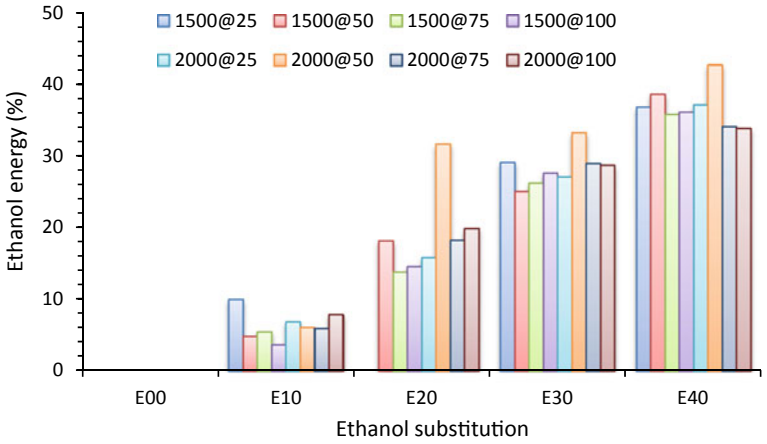

Fig. 10.2 Ethanol energy at different engine operating conditions with 0–40% ethanol substitutions

10.3.1 Engine Performance Parameters

10.3.1.1 Energy by Ethanol and Mass Ratio

As the 10, 20, 30, and 40% substitution values are nominal, Fig. 10.2 shows the actual energy derived by ethanol at the different engine operating conditions on each of the tests. For each substitution, ethanol energy changes with engine load and speed due to the amount of ethanol during the combustion. This can be shown by the mass ratio, which is the portion of ethanol to diesel by mass. This is because in performing the test for each substitution, the engine ran with diesel at the required load, then the diesel energy was reduced via reducing the engine load by the substitution percentage, and fumigated ethanol was introduced to achieve the original engine load. Figure 10.3 shows that there is a strong correlation with the $R2$ of 0.95 between the ethanol energy and mass ratio. The reason is that increasing the mass ratio means that the amount of ethanol compared to diesel has increased; therefore, the ethanol energy increases.

10.3.1.2 Friction Mean Effective Pressure

FMEP, which is the difference between the brake mean effective pressure (BMEP) and IMEP, is influenced by different factors, such as engine operating condition (Nabi et al. 2016), temperature (Zare et al. 2018, 2020), and fuel properties (Zare et al. 2016). FMEP can be an indicator of friction losses in engines arising from different reasons, such as the mechanical friction between the parts or friction losses from fuel, oil, and water pumps. Figure 10.4 shows the FMEP at different engine operating conditions with 0–40% ethanol substitutions. As seen, FMEP increases

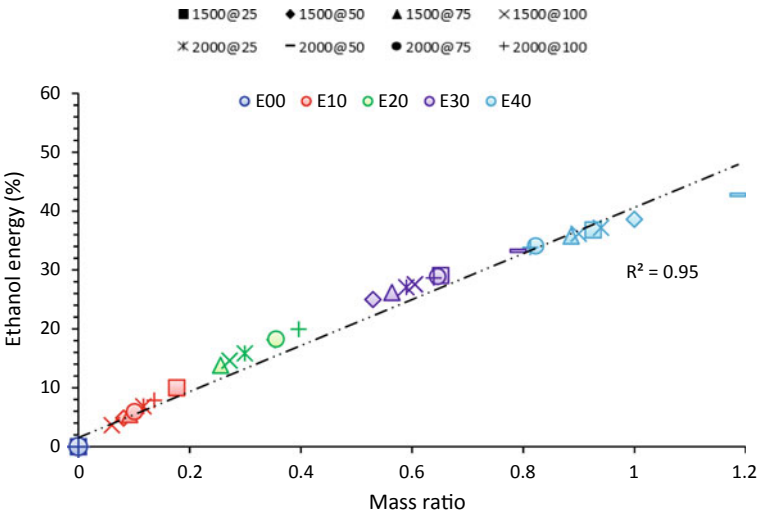

Fig. 10.3 Ethanol energy versus mass ratio at different engine operating conditions with 0–40% ethanol substitutions

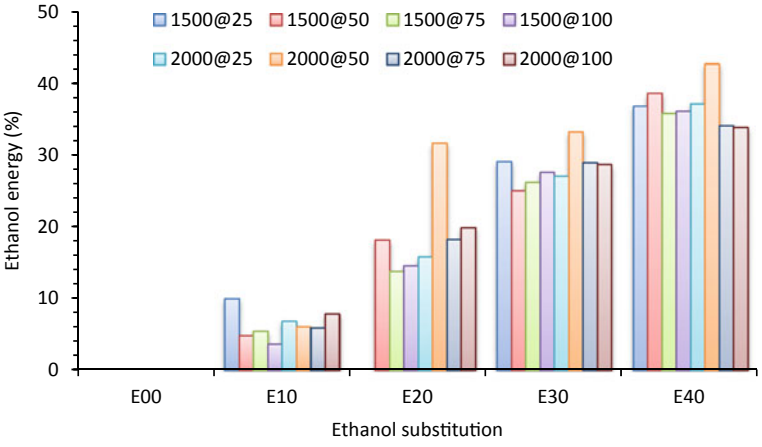

Fig. 10.4 FMEP at different engine operating conditions with 0–40% ethanol substitutions

with the speed and mostly decreased with load. Fuel lubricity can also influence the friction loss, as the lubricity of ethanol is significantly lower than that of diesel. However, the effects of engine speed and load on FMEP change are more dominant.

Figure 10.5 shows how FMEP changes with different ethanol substitutions as compared to E00. Comparing different colors in the graph show that by increasing the ethanol substitution, which increases the mass ratio, FMEP variation tends toward higher values. For example, using E10 and E20 in some of the operating modes can

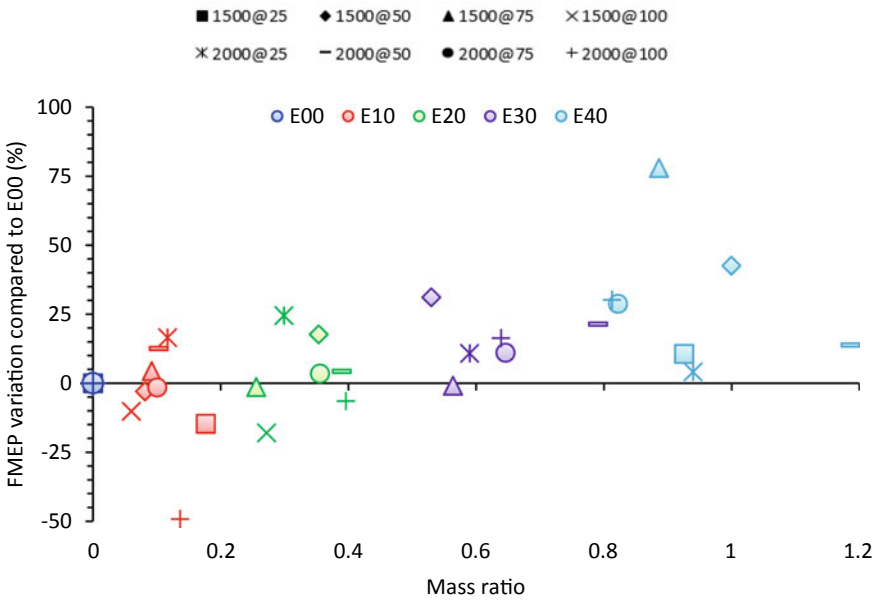

Fig. 10.5 FMEP variation compared to E00 versus mass ratio at different engine operating conditions with 0–40% ethanol substitutions

decrease FMEP by 14 and 17%, respectively; while, using E30 and E40 increases FMEP in almost all of the operating conditions. Also, the range of FMEP change by using E10 and E20 is much lower when compared to E30 and E40. This shows that E10 and E20 perform better when compared to E30 and E40.

10.3.1.3 Brake-Specific Fuel Consumption

BSFC can be defined as the portion of fuel consumed to the produce a unit of power by the engine, as shown in Eq. 10.1 (John 1988).

$$\mathrm{BSFC} = \frac{\dot{m}_{\mathrm{fuel}}}{\mathrm{BP}} (\mathrm{kg/kWh}) \tag{10.1}$$

Fuel consumption depends on the engine operating condition and fuel properties (Nabi et al. 2017a, b). Figure 10.6 shows how the BSFC changes with different ethanol substitutions as compared to E00. In general, it can be seen that using ethanol substitutions (except E10) increased the fuel consumption in most of the operating modes, which shows that diesel engines with fumigation consume a larger quantity of fuel to maintain power, compared to diesel. The primary reason for this is that alcohol fuels have significantly lower calorific values than diesel, alcohol fuels also have a higher heat of evaporation; therefore, the amount of extracted heat during the

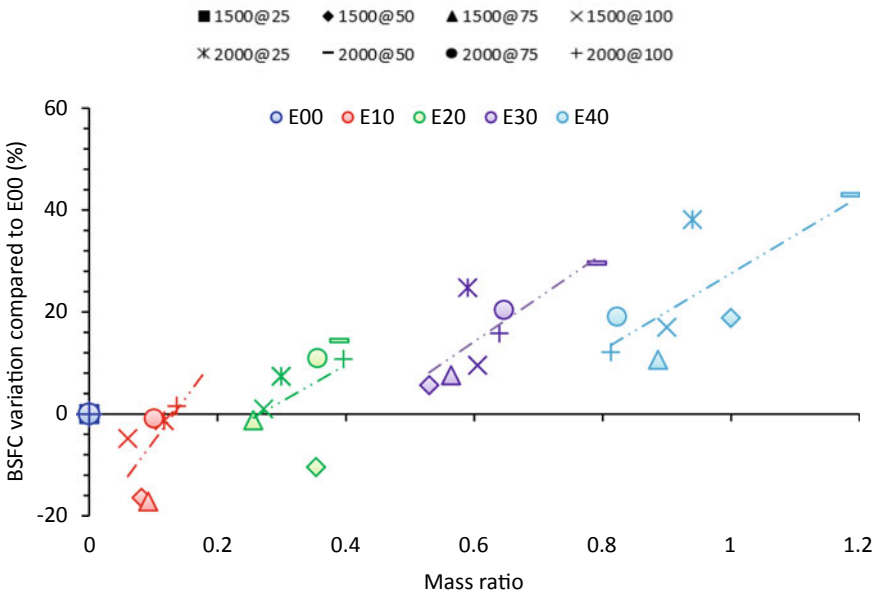

Fig. 10.6 BSFC variation compared to E00 versus mass ratio at different engine operating conditions with 0–40% ethanol substitutions

combustion process is less, so more fuel is required to produce the same power output (Imran et al. 2013; Jafari et al. 2019). Comparing different colors in the graph shows that by increasing the ethanol substitution, which increases the mass ratio, BSFC increases. For example, using E10 in some of the operating modes can decrease BSFC by 16 and 17% when compared to E00; while, using E30 or E40 instead of E00 increases BSFC in all of the operating modes, the increase can be up to 40%. This could be due to the fact that increasing the ethanol substitution decreases the combined calorific value of the fuels. Also, the range of BSFC values systematically increases across the operating modes. E10, and some E20 points, shows an improvement in BSFC compared to neat diesel. Given the lower calorific value of ethanol, compared to diesel, this shows that E10 performs very well, especially when compared to other higher substitutions, E30 and E40.

10.3.1.4 Mechanical Efficiency

Mechanical efficiency is the ratio of indicated power divided by the brake power (John 1988). Figure 10.7 shows the variation in mechanical efficiency compared to E00 at different engine operating conditions with 0–40% ethanol substitutions. Comparing different colors in the graph shows that by increasing the ethanol substitution, which increases the ethanol–diesel mass ratio, the mechanical efficiency decreases. For example, using E10 instead of E00 increases the efficiency in half of the operating

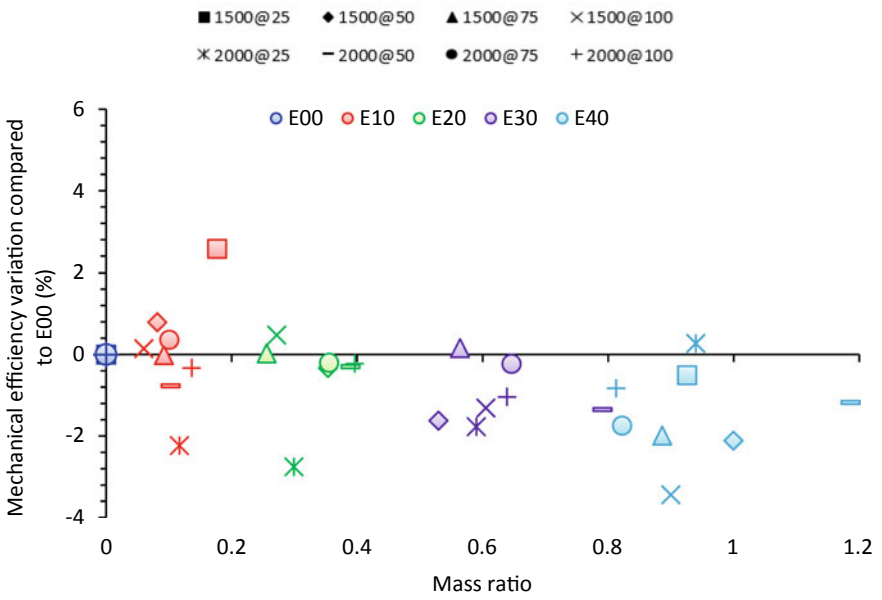

Fig. 10.7 Mechanical efficiency variation compared to E00 versus mass ratio at different engine operating conditions with 0–40% ethanol substitutions

modes; however, the changes were mostly within ±1%. While using E30 and E40 decreases the mechanical efficiency in almost all of the operating conditions. Also, the range of mechanical efficiency change by using E10 and E20 is much smaller when compared to E30 and E40. This shows that E10 and E20 perform better when compared to E30 and E40. Further analysis showed that this parameter increased with engine load and decreased with engine speed.

10.3.1.5 Thermal Efficiency

Thermal efficiency is the ratio of actual work divided by the chemical energy of the fuel released through combustion. Figure 10.8 shows how thermal efficiency changes with different ethanol substitutions as compared to E00. In general, it can be seen that using ethanol substitutions instead of E00 increased the thermal efficiency in most of the engine operating modes. The reason for this could be that alcohol fuels have a high laminar flame propagation speed, which can lead to the completion of the combustion process earlier and an improvement in thermal efficiency (Ghadikolaei 2016; Adelman 1979). Comparing different colors in the graph shows that by increasing the ethanol substitution, which increases the mass ratio, thermal efficiency decreases. This could be due to the leaner mixture and cooling effect of higher ethanol substitutions. A study by Huang et al. (2015) reported that the cooling

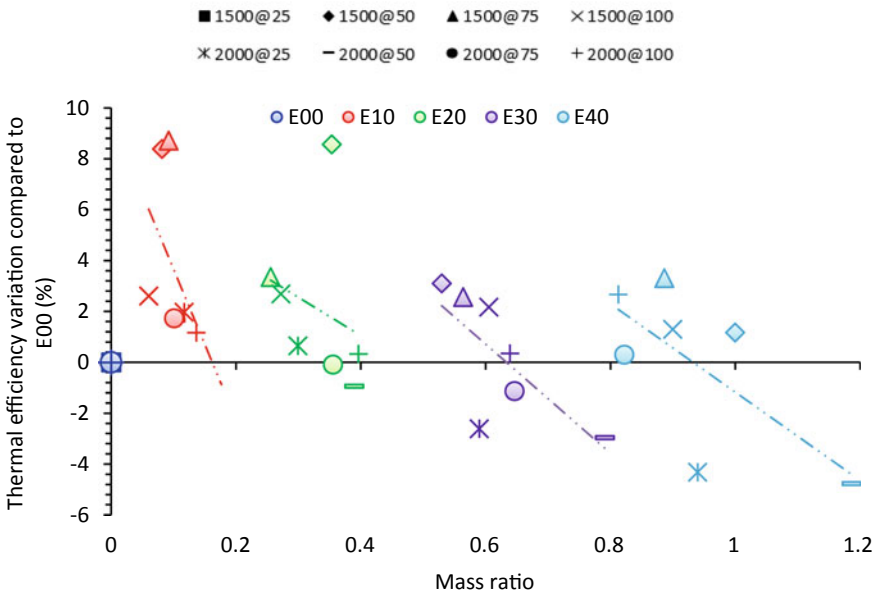

Fig. 10.8 Thermal efficiency variation compared to E00 versus mass ratio at different engine operating conditions with 0–40% ethanol substitutions

effect increased with increasing the ethanol ratio. Increasing the ethanol substitution needs a higher latent heat for ethanol evaporation. And the cooling potential will be limited by the evaporation rate of ethanol. Increased ethanol substitution requires more time and energy for evaporation, and this may lead to an incomplete evaporation which causes an incomplete combustion negatively impacting the thermal efficiency.

Using E10 increases the efficiency at all the operating modes and the increase can be up to 9%; while, using E30 or E40 instead of E00 can decrease the efficiency at lower loads. This shows that E10 performs better than diesel at all loads, E20 is typically performing better or at least close to neutral and E30 and E40 perform better at the higher loads only. The lower loads, particularly at E30 and E40 (but also evident at E20), are particularly degraded by increasing the ethanol substitution, compared to neat diesel operation.

Figure 10.8 shows that the thermal efficiency was higher at 1500 rpm than 2000. It also shows that in most of the cases, increasing the ethanol substitution decreases the thermal efficiency at lower loads (25 and 50%). However, at higher loads (75 and 100%), thermal efficiency increased when higher ethanol substitutions were used. A similar trend has been reported in the literature (Zhang et al. 2011; Tsang et al. 2010; Cheng et al. 2008). The reason could be that at lower engine loads, lower combustion temperature, lean mixture, and the cooling effect of higher ethanol substitutions can result in a poorer combustion causing an inefficient burn of the ethanol. While at higher engine loads, the richer mixture and higher combustion temperature can

possibly reduce the cooling effect of the higher ethanol substitutions leading to a more efficient combustion. The figure also shows that the thermal efficiency was higher at 1500 rpm than 2000. The reason could be that the lower engine speed allows a more complete combustion, therefore a higher efficiency.

10.3.2 Combustion Analysis

10.3.2.1 In-Cylinder Pressure

Figure 10.9 shows the in-cylinder pressure at 2000 rpm under 100% engine load for all of the ethanol substitutions. It can be seen that by increasing the ethanol substitution the maximum in-cylinder pressure increases and its location moves toward the right. For example, with E10 the maximum pressure is 12.8 MPa and it occurs at 363.3°; while, with E40 the maximum pressure is 15.1 MPa occurring at 364.4°. The reason for selecting this graph was that at each speed, the difference between the in-cylinder pressure behaviors of ethanol substitutions is more visually evident at higher loads. In-cylinder pressure behavior of all the operating modes is further analyzed to investigate maximum in-cylinder pressure, maximum rate of pressure rise and cyclic variability, which will be discussed in the next sections.

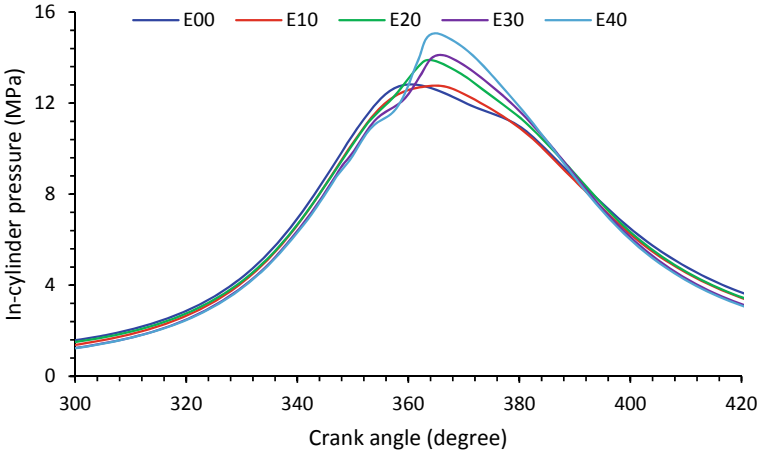

Fig. 10.9 In-cylinder pressure at 2000 rpm under 100% engine load with 0–40% ethanol substitutions

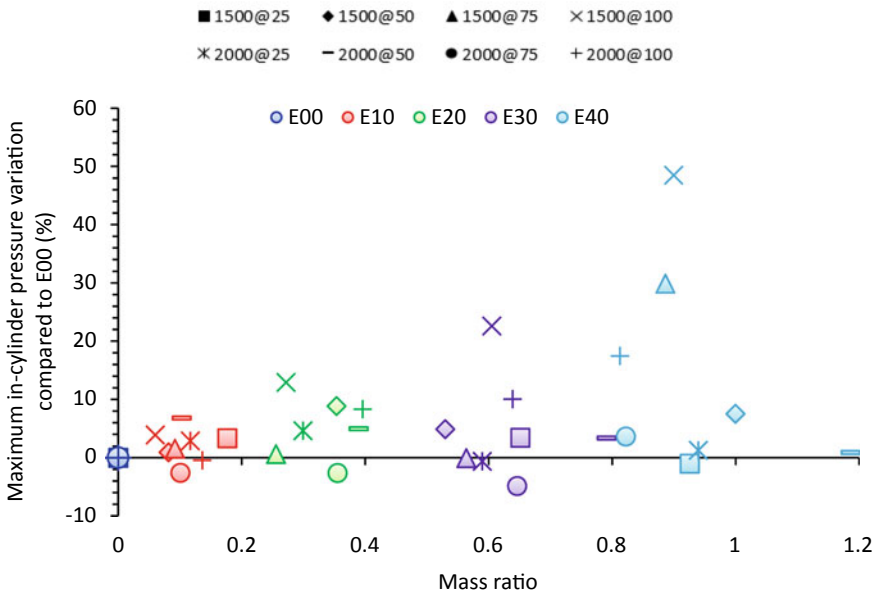

Fig. 10.10 Maximum in-cylinder pressure variation compared to E00 versus mass ratio at different engine operating conditions with 0–40% ethanol substitutions

10.3.2.2 Maximum In-Cylinder Pressure

Figure 10.10 illustrates how the maximum in-cylinder pressure changes with different ethanol substitutions as compared to E00. Comparing different colors in the graph shows that by increasing the ethanol substitution, which increases the mass ratio, the maximum in-cylinder pressure increases. For example, at 1500 rpm under 100% engine load, using E10, E20, E30, and E40 instead of E00 increases the maximum in-cylinder pressure by 4, 13, 23, and 49%, respectively. The figure also shows that the range of change increases with mass ratio. For example, the range of change by using E10 is much lower (between −3 and 7%) when compared to E40 (between −1 and 49%). The maximum in-cylinder pressure depends on the fuel consumption within the premixed combustion phase which characterizes the fuel ability to mix with the air and burn. Further analysis showed that this parameter increased with engine load and speed.

10.3.2.3 Maximum Rate of Pressure Rise

The maximum rate of pressure rise, which is related to engine noise and vibration, can indicate how fast the in-cylinder pressure can increase, impacting the cylinder wall/head and piston crown (Barik and Murugan 2016). This parameter

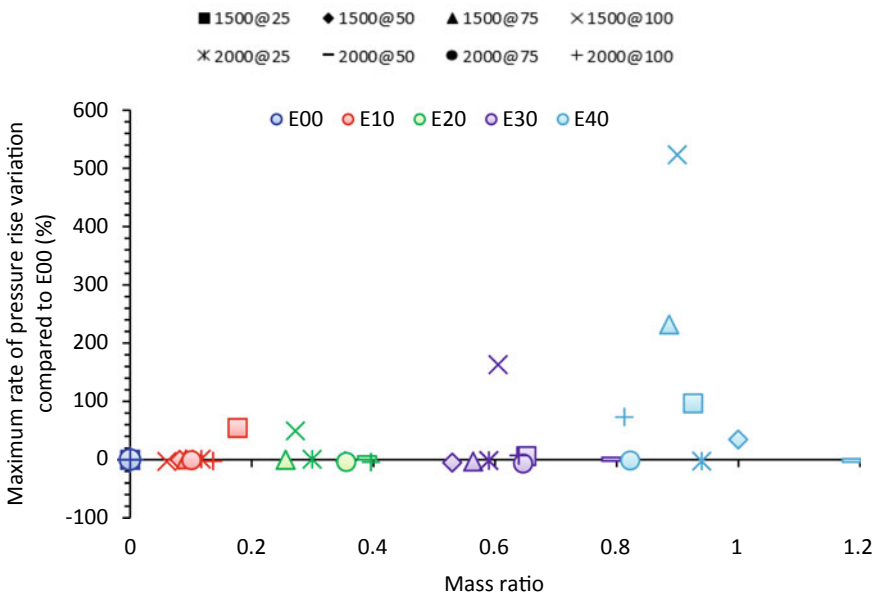

Fig. 10.11 Maximum rate of pressure rise variation compared to E00 versus mass ratio at different engine operating conditions with 0–40% ethanol substitutions

which depends on fuel consumption within the premixed combustion phase can be influenced by the fuel type (Zare et al. 2017). Figure 10.11 shows how maximum rate of pressure rise changes with different ethanol substitutions as compared to E00. It shows that except for one operating mode, using low ethanol substitutions such as E10 and E20 instead of E00 slightly changes the maximum rate of pressure rise (mostly by up to 4%); this change can be significant with E40, where the engine also had audible knock. This significant increase in maximum rate of pressure rise could lead to significant wear issues owing the piston ring being pushed against the cylinder wall and a decrease in lubricating oil between the piston and the cylinder wall. The lubricity of ethanol is significantly lower than that of diesel which can also adversely affect the piston ring/cylinder wall lubrication regime. High pressure rise rate will adversely impact on the big end and gudgeon pin bearings, and such high substitution as E40 may not be sustainable over long periods of engine operation.

10.3.2.4 Combustion Instability

Combustion instability can negatively impact the exhaust emissions and performance parameters and also cause unwanted vibrations and noise which can harm vehicle parts and impact passenger comfort. There can be different reasons for these phenomena, such as injection parameters, engine operating conditions, engine

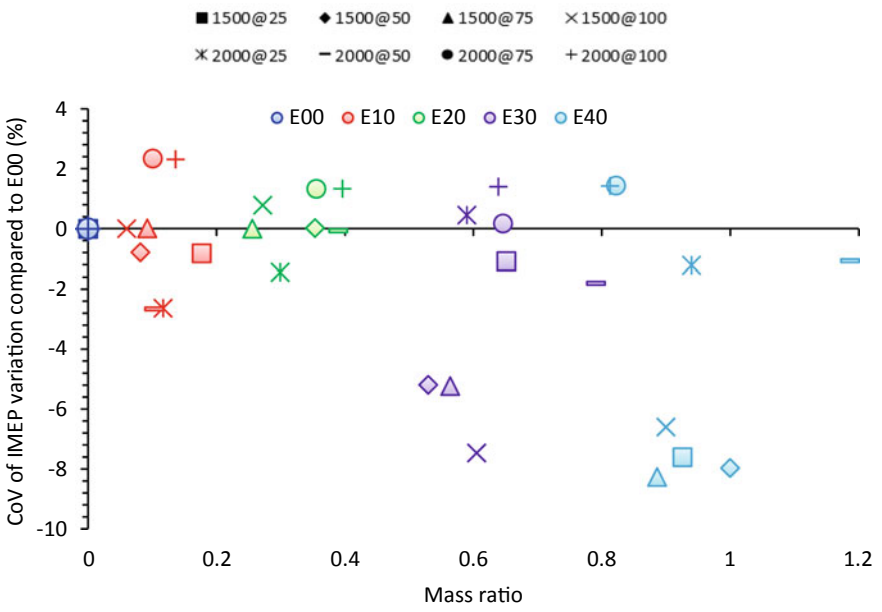

Fig. 10.12 CoV of IMEP variation compared to E00 versus mass ratio at different engine operating conditions with 0–40% ethanol substitutions

temperature, air-to-fuel ratio, and fuel properties. Combustion instability can be evaluated by investigating the cyclic variability in combustion using parameters such as CoV of IMEP which is the standard deviation divided by the average of IMEP.

Figure 10.12 shows that at 1500 rpm, using higher substitutions can decrease the CoV of IMEP at all of the engine loads. For example, the decrease with E40 is between 6.6 and 8.3% at all the loads while that for E30 was also down to 7.5%. However, with lower substitutions, E10 and E20, the change was within ±1%. Comparing to 1500 rpm, the change at 2000 rpm in most of the engine loads using ethanol substitutions instead of diesel (E00) increased the CoV of IMEP; however, the change was within ±2.7%. This is similar to the thermal efficiency trend in which using higher ethanol substitutions at 1500 rpm showed greater improvements compared to 2000 rpm. The reason could be that the lower engine speed allows a more complete combustion, therefore a higher efficiency.

10.3.2.5 In-Cylinder Pressure Versus Volume

Figure 10.13 shows a P–V indicator diagram at 1500 and 2000 rpm under 100% engine load for all of the ethanol substitutions. The graph clearly shows that for both of the engine speeds, increasing the ethanol substitution increases the maximum pressure at the end of compression stroke and the start of the power stroke. At

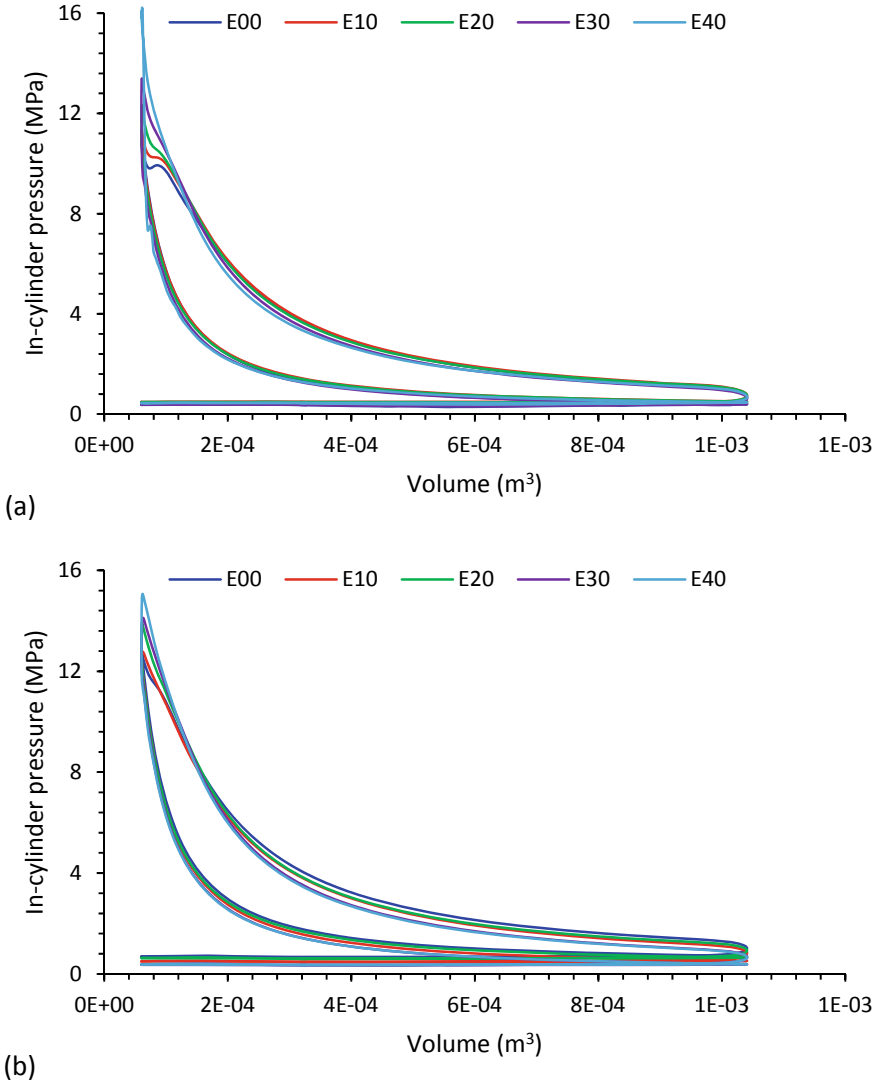

Fig. 10.13 In-cylinder pressure versus volume at **a** 1500 and **b** 2000 rpm under 100% engine load with 0–40% ethanol substitutions

this part of the graph, it can also be seen that the maximum pressure is higher at 2000 rpm compared to 1500 rpm (except for E40). The figure also shows that during the compression stroke, E00 has the highest pressure and increasing the ethanol substitution decreases the pressure (E40 has the lowest). The reason could be the higher heat of vaporization of the ethanol which results in a so-called cooling effect in the intake process and compression stroke, and it increases the volumetric efficiency of the engine and therefore less work is required (Ghadikolaei 2016). It can also be

seen that the difference between the substitutions during the compression stroke is smaller at 1500 rpm than 2000 rpm, and this could be due to the lower cooling effect at lower engine speeds.

10.3.2.6 Heat Release Rate

Heat release analysis, which involves the first law of the thermodynamics, can determine a number of important combustion related parameters. There are four stages during combustion which can be seen in a heat release diagram (John 1988). The first stage is during the ignition delay period, between the start of injection and the start of combustion. In this short preparatory phase, fuel is added but not ignited. The heat release rate during this period is negative as the energy is absorbed by the injected fuel owing to both the relatively cooler fuel (compared to the in-cylinder environment) and the energy required to undergo vaporization and chemical changes (Bodisco et al. 2015). The second stage is the pre-mixed combustion phase, which can be seen where the heat release rate increases from zero at the start of combustion to a maximum value and decreases to an intermediate minimum value after the peak. This stage is related to the initial combustion of the air and fuel mixture. A high proportion of heat release (typically one-third) happens during this phase. In the third phase, which is called mixing-controlled combustion phase or diffusion burning, the burning rate is controlled by the combustion of the available air/mixture. Therefore, the burning rate highly depends on the fuel vapor and air mixing process. In heat release diagram, this phase starts from the intermediate minimum value at the end of the pre-mixed combustion phase and reaches to a lower peak and then decreases. The end of injection mostly occurs within this phase. The last phase is called the late combustion phase in which the heat releases due to some possible energy release from the unburned fuel, soot and fuel-rich combustion products, but at a lower rate as the cylinder temperature decreases significantly during the expansion stroke.

This study uses the apparent heat release rate, which is the difference between the released energy from the combustion of the fuel and the lost energy by the transferred heat to the walls (Goldsworthy 2013). The apparent heat release rate can better and more directly indicate the effect of the fuel on combustion. Figure 10.14 shows the apparent heat release rate for all of the ethanol substitutions at different engine operating conditions. Figure 10.14a shows the heat release diagram for all of the crank angles in a cycle at 1500 rpm under 25% load as an example of a full diagram and magnifies the combustion phase of the diagram to facilitate the analysis. All the other subfigures, (b–f), show the combustion phase of the diagram only for clearer observation and analysis.

At 1500 rpm, under 25% load, the peak value of the apparent heat release rate with E00, E10, E20, E30, and E40 are 88, 118, 125, 51, and 150 J/° occurring at 371.6°, 372.2°, 372.3°, 372.7°, and 374.6°, respectively. This means that increasing the ethanol substitution increases the maximum apparent heat release rate (except for E30) and its location. Also, the onset of the heat release rate occurs slightly later. At 2000 rpm, E10 showed a closer behavior to E00 with 8% higher value and using

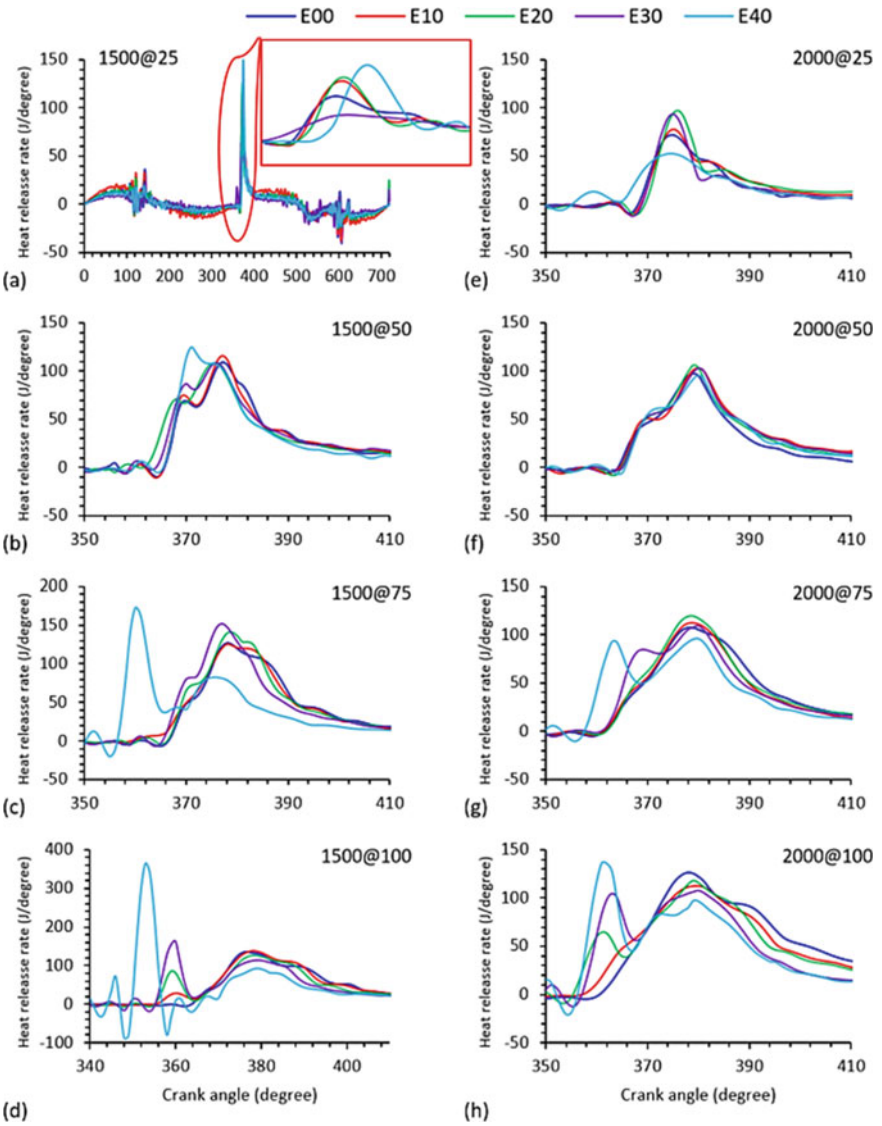

Fig. 10.14 Heat release rate at different engine operating conditions with 0–40% ethanol substitutions

E20 and E30 increased the peak value by up to 36% moving it slightly toward higher crank angles. However, E40 had a different behavior. Under 25% engine load, the heat release pattern is dominated by the liquid fuel injection, especially with low ethanol substitutions.

Under 50% engine load at both speeds, the heat release diagram shows a double peak and a distinct minimum between the two peaks (at 1500 rpm) and increasing

the ethanol substitution, increases the first peak value and retards its location. There is also a slight increase in the second peak value. Under 50% load, it can be seen that E10 has a similar trend as E00 with up to 6% higher peak values occurring at a similar crank angle. This is more evident at 75% engine load.

Under 75% engine load at both the engine speeds, it can be seen that by increasing the ethanol substitution, there is a tendency toward having double peaks and the first peak value increases (which will be more visible in the graph). Also, similar to 50% load, the second peak value increases as the ethanol substitution rate increases. E10 has a similar value to E00 with a small change. Also, under this load, the E40 diagram moves toward left with a significant increase in the first peak and decrease in the second peak. E40 shows a similar trend under 100% load.

At 1500 and 2000 rpm under full load, by increasing the ethanol substitution, the double peak and a distinct minimum between them become more evident. The first peak increases and the second peak diminishes as the ethanol rate increases. Under 100% load, E10 behavior is close to E00, particularly when compared to other substitutions.

The tendency of having two peaks by increasing the ethanol substitution can be analyzed using the flammability concept. The mixture of ethanol and air, even with high substitutions such as E40, is not flammable in atmospheric pressure and temperature. However, given that the high pressure and temperature can increase the flammability, at the end of compression stroke, the ethanol–air mixture with high substitutions such as E40 can be flammable. Therefore, at the end of the compression stroke at which the pressure and temperature increase significantly the flammability increases. There is, therefore, the potential for the mixture of ethanol and air, after being ignited by pre-injection, to burn independently of the injected diesel within the premixed combustion phase. In that case, the first peak on heat release rate occurs before the end of fuel injection and the second peak occurs after the end of fuel injection, and the minimum points between the peaks occur nearly at the end of fuel injection. This is more obvious at high ethanol substitutions under high engine load, in which the cylinder temperature and pressure are relatively high.

In general, alcohol fuels have a high laminar flame propagation speed, which can be a reason for completing the combustion process earlier (Ghadikolaei 2016). The different behavior of E40 under 75 and 100% engine loads at 1500 rpm, compared to other fuels can be due to auto-ignition, which occurs when the mixture is too lean to support a flame front, and the mixture temperature is high enough for a sufficient time. Given that the auto-ignition temperature can decrease if the pressure increases, near the end of the compression stroke at high engine load using high ethanol substitution can lead to auto-ignition given that the substitution will expose to elevated temperature through the compression stroke. This can be a reason for the early combustion of E40 shown in heat release diagrams.

10.4 Summary

This study investigated the effect of ethanol fumigation on engine performance parameters using a modern turbocharged diesel engine. Ethanol substitutions of 10, 20, 30, and 40 were tested under 25, 50, 75, and 100% engine load at 1500 and 2000 rpm, and different engine performance was investigated and following conclusions were drawn:

- Using E10 and E20 in some of the operating modes decreased FMEP by 14 and 17%, respectively. However, there was an increasing trend in FMEP associated with increasing the ethanol substitution.
- Using E10 in some of the operating modes decreased BSFC by ~17%; while, using E30 or E40 increased BSFC in all the operating modes (up to 40%).
- Using E10 slightly increased the mechanical efficiency in half of the operating modes; while there was a decreasing trend in mechanical efficiency associated with increasing the ethanol substitution.
- Using E10 increased the thermal efficiency. By increasing the ethanol substitution, the thermal efficiency decreased at lower loads and increased at higher loads.

This study also analyzed in-cylinder data and some relevant parameters, and the following conclusions were drawn:

- Increasing the ethanol substitution increased the maximum in-cylinder pressure.
- The maximum rate of pressure rise changed slightly with low ethanol substitutions (up to 4%) and significantly changed with high ethanol substitution (up to 5 times).
- At 1500 rpm, using high ethanol substitutions decreased the CoV of IMEP significantly (6.6–8.3%). At 2000 rpm using ethanol substitutions instead of diesel increased the CoV of IMEP at some of the engine loads, however, the change was within ±3%.
- Under 25% engine load, increasing the ethanol substitution increased the maximum apparent heat release rate.
- Under 50 and 75% engine loads at both the engine speeds, by increasing the ethanol substitution there was a tendency toward having double peaks in the heat release diagram.
- Under full load, by increasing the ethanol substitution, the double peak and a distinct minimum between them became more evident in heat release diagram.

Given that the share of ethanol in the transportation sector is increasing, there is a need for further research on the effect of using high ethanol substitutions not only on engine performance and combustion parameters, but also on exhaust emissions such as particle number and NO_x.

Acknowledgements The authors would like to acknowledge the excellent work by the technical staff at the Biofuel Engine Research Facility at QUT for facilitating this work and maintaining the equipment, with particular mention to Anthony Morris and Noel Hartnett. Special thanks are also owed to Andrew Elder of Dynolog Pty. Ltd. for his work in supporting the functioning of

the research engine and dynamometer. Lastly, the authors would like to acknowledge the financial support of this work provided by the Australian Research Council (ARC) grant LP0775178.

References

Abu-Qudais M, Haddad O, Qudaisat M (2000) The effect of alcohol fumigation on diesel engine performance and emissions. Energy Convers Manag 41(4):389–399. https://doi.org/10.1016/S0196-8904(99)00099-0

Adelman H (1979) Alcohols in diesel engines-a review. SAE Technical Paper, 0148-7191. https://doi.org/10.4271/790956

Barik D, Murugan S (2016) Effects of diethyl ether (DEE) injection on combustion performance and emission characteristics of Karanja methyl ester (KME)–biogas fueled dual fuel diesel engine. Fuel 164:286–296. https://doi.org/10.1016/j.fuel.2015.09.094

Bodisco T, Brown RJ (2013) Inter-cycle variability of in-cylinder pressure parameters in an ethanol fumigated common rail diesel engine. Energy 52:55–65. https://doi.org/10.1016/j.energy.2012.12.032

Bodisco T, Tröndle P, Brown RJ (2015) Inter-cycle variability of ignition delay in an ethanol fumigated common rail diesel engine. Energy 84:186–195. https://doi.org/10.1016/j.energy.2015.02.107

Cheng CH, Cheung CS, Chan TL, Lee SC, Yao CD, Tsang KS (2008) Comparison of emissions of a direct injection diesel engine operating on biodiesel with emulsified and fumigated methanol. Fuel 87(10):1870–1879. https://doi.org/10.1016/j.fuel.2008.01.002

Delphi Technologies (2019) Worldwide emissions standards-passenger cars and light duty vehicles. https://www.delphi.com/innovations

Ekholm K, Karlsson M, Tunestål P, Johansson R, Johansson B, Strandh P (2009) Ethanol-diesel fumigation in a multi-cylinder engine. SAE Int J Fuels Lubr 1(1):26–36

Ghadikolaei MA (2016) Effect of alcohol blend and fumigation on regulated and unregulated emissions of IC engines—a review. Renew Sustain Energy Rev 57:1440–1495. https://doi.org/10.1016/j.rser.2015.12.128

Ghosh TK, Prelas MA (2011) Ethanol. In: Energy resources and systems. Springer, Berlin, pp 419–493. https://doi.org/10.1007/978-94-007-1402-1

Goldsworthy L (2013) Fumigation of a heavy duty common rail marine diesel engine with ethanol–water mixtures. Exp Thermal Fluid Sci 47:48–59. https://doi.org/10.1016/j.expthermflusci.2012.12.018

Hansdah D, Murugan S (2014) Bioethanol fumigation in a DI diesel engine. Fuel 130:324–333. https://doi.org/10.1016/j.fuel.2014.04.047

Heisey J, Lestz S (1981) Aqueous alcohol fumigation of a single-cylinder DI diesel engine. SAE Technical Paper, 0148-7191. https://doi.org/10.4271/811208

Huang Y, Hong G, Huang R (2015) Investigation to charge cooling effect and combustion characteristics of ethanol direct injection in a gasoline port injection engine. Appl Energy 160:244–254

Imran A, Varman M, Masjuki HH, Kalam MA (2013) Review on alcohol fumigation on diesel engine: a viable alternative dual fuel technology for satisfactory engine performance and reduction of environment concerning emission. Renew Sustain Energy Rev 26:739–751. https://doi.org/10.1016/j.rser.2013.05.070

Jafari M, Verma P, Bodisco TA, Zare A, Surawski NC, Borghesani P, Stevanovic S, Guo Y, Alroe J, Osuagwu C (2019) Multivariate analysis of performance and emission parameters in a diesel engine using biodiesel and oxygenated additive. Energy Convers Manag 201:112183. https://doi.org/10.1016/j.enconman.2019.112183

John B (1988) Heywood, internal combustion engine fundamentals. McGraw Hill International Editions

Kuszewski H, Jaworski A, Ustrzycki A (2017) Lubricity of ethanol–diesel blends–study with the HFRR method. Fuel 208:491–498. https://doi.org/10.1016/j.fuel.2017.07.046

Lapuerta M, Armas O, Garcia-Contreras R (2009) Effect of ethanol on blending stability and diesel engine emissions. Energy Fuels 23(9):4343–4354. https://doi.org/10.1021/ef900448m

Morsy MH (2015) Assessment of a direct injection diesel engine fumigated with ethanol/water mixtures. Energy Convers Manag 94:406–414. https://doi.org/10.1016/j.enconman.2015.01.086

Nabi MN, Zare A, Hossain FM, Rahman MM, Bodisco TA, Ristovski ZD, Brown RJ (2016) Influence of fuel-borne oxygen on European stationary cycle: diesel engine performance and emissions with a special emphasis on particulate and NO emissions. Energy Convers Manag 127:187–198. https://doi.org/10.1016/j.enconman.2016.09.010

Nabi MN, Zare A, Hossain FM, Bodisco TA, Ristovski ZD, Brown RJ (2017a) A parametric study on engine performance and emissions with neat diesel and diesel-butanol blends in the 13-mode European stationary cycle. Energy Convers Manag 148:251–259. https://doi.org/10.1016/j.enconman.2017.06.001

Nabi MN, Zare A, Hossain FM, Ristovski ZD, Brown RJ (2017b) Reductions in diesel emissions including PM and PN emissions with diesel-biodiesel blends. J Clean Prod 166:860–868. https://doi.org/10.1016/j.jclepro.2017.08.096

Popa MG, Negurescu N, Pana C, Racovitza A (2001) Results obtained by methanol fuelling diesel engine. SAE Technical Paper 0148-7191. https://doi.org/10.4271/2001-01-3748

Tsang K, Zhang Z, Cheung C, Chan T (2010) Reducing emissions of a diesel engine using fumigation ethanol and a diesel oxidation catalyst. Energy Fuels 24(11):6156–6165. https://doi.org/10.1021/ef100899z

Udayakumar R, Sundaram S, Sivakumar K (2004) Engine performance and exhaust characteristics of dual fuel operation in DI diesel engine with methanol. SAE Technical Paper, 0148-7191. https://doi.org/10.4271/2004-01-0096

Zare A, Nabi MN, Bodisco TA, Hossain FM, Rahman MM, Ristovski ZD, Brown RJ (2016) The effect of triacetin as a fuel additive to waste cooking biodiesel on engine performance and exhaust emissions. Fuel 182:640–649. https://doi.org/10.1016/j.fuel.2016.06.039

Zare A, Bodisco TA, Nabi MN, Hossain FM, Ristovski ZD, Brown RJ (2017) Engine performance during transient and steady-state operation with oxygenated fuels. Energy Fuels 31(7):7510–7522. https://doi.org/10.1021/acs.energyfuels.7b00429

Zare A, Bodisco TA, Nabi MN, Hossain FM, Ristovski ZD, Brown RJ (2018) A comparative investigation into cold-start and hot-start operation of diesel engine performance with oxygenated fuels during transient and steady-state operation. Fuel 228:390–404. https://doi.org/10.1016/j.fuel.2018.05.004

Zare A, Bodisco TA, Verma P, Jafari M, Babaie M, Yang L, Rahman MM, Banks A, Ristovski ZD, Brown RJ (2020) Emissions and performance with diesel and waste lubricating oil: a fundamental study into cold start operation with a special focus on particle number size distribution. Energy Convers Manag 209:112604. https://doi.org/10.1016/j.enconman.2020.112604

Zhang ZH, Tsang KS, Cheung CS, Chan TL, Yao CD (2011) Effect of fumigation methanol and ethanol on the gaseous and particulate emissions of a direct-injection diesel engine. Atmos Environ 45(11):2001–2008. https://doi.org/10.1016/j.atmosenv.2010.12.019

Chapter 11
Low and Medium Carbon Alcohol Fueled Dual-Fuel Compression Ignition Engine

Mohit Raj Saxena and Rakesh Kumar Maurya

Abbreviations

CI	Compression ignition
SI	Spark ignition
PFI	Port fuel injection
TDC	Top dead center
bTDC	Before top dead center
aTDC	After top dead center
SOC	Start of combustion
EGR	Exhaust gas temperature
CAD	Crank angle degree
HRR	Heat release rate
PPRR/MPRR	Peak/maximum pressure rise rate
MGT	Mean gas temperature
ITE	Indicated thermal efficiency
BTE	Brake thermal efficiency
BSFC	Brake-specific fuel consumption
DME	Dimethyl ether
CO_2	Carbon dioxide
NO_x	Oxides of nitrogen
CO	Carbon monoxide
CA_{50}	Combustion phasing corresponding to 50% heat release
HC	Hydrocarbon
PSD	Particle size distribution

M. R. Saxena · R. K. Maurya (✉)
Department of Mechanical Engineering, Indian Institute of Technology Ropar, Rupnagar 140001, India
e-mail: rakesh.maurya@iitrpr.ac.in

P. C. Shukla et al. (eds.), *Alcohol as an Alternative Fuel for Internal Combustion Engines*, Energy, Environment, and Sustainability,
https://doi.org/10.1007/978-981-16-0931-2_12

AMP	Accumulation mode particle
NMP	Nucleation mode particle
CNG	Compressed natural gas
UV–VIS	Ultraviolet visible
HCHO	Formaldehyde
CH_3OH	Unburned methanol
HCOOH	Formic acid
C_6H_6	Benzene
1,3-C_4H_6	1,3-Butadiene
C_7H_8	Toluene

11.1 Introduction

Compression ignition (CI) engines are widely used in agricultural applications, transportation, and industrial sectors because of their better power-torque characteristics and fuel conversion efficiencies. At present, fossil diesel mainly used as a fuel in CI-engines, and its utilization increased significantly with urbanization. The combustion of fossil diesel in CI-engine has a negative effect on humans and the environment (OECD/International Transport Forum 2013; WHO 2014; McClellan 1987; Krahl et al. 2003; Ris 2007; Austin et al. 2019; Weitekamp et al. 2020). The drastic increase in fossil fuel prices, rigorous emission norms, and an increasing share of global greenhouse gas emissions from transportation are major challenges for engine research. The development of cleaner alternative fuels and combustion strategy is getting more attention for engine research to reduce the pollutants emitted from the engine and decrease the dependency over fossil fuel (Datta and Mandal 2016; Park and Lee 2014; Yao et al. 2017; Niculescu et al. 2019). The European Parliament gave Directive 2009/28/EC on the promotion of the usage of renewable energy sources (Directive 2009/28/EC 2009; Tutak et al. 2015). This provision requires EU member states to use 10% of renewable fuels in transport by 2020 (Directive 2009/28/EC 2009; Tutak et al. 2015). The Energy Outlook, 2019, depicts that presently the usage of oil in the transportation sector is 94%, which is expected to be reduced to approximately 85% by 2040, and 60 million tons of biofuels could be used in the transport sector (BP Statistical Review of World Energy 2019; Hariharan et al. 2020). The use of oxygenated fuel along with fossil diesel has a great potential to improve the performance and emissions from CI-engine. Biofuels can be easily produced from agricultural biomass, and it can reduce the dependency on petroleum products. Fuel production from biomass could also support the income of the farmers and farming industries. Additionally, biofuel has the potential to reduce emissions such as unburnt hydrocarbon, carbon dioxide, particulate matter (Hariharan et al. 2020).

The combustion of biofuel caused lower carbon emissions in comparison with conventional fuels (Hariharan et al. 2020; Panithasan et al. 2019). Alcohols such as ethanol, methanol, and butanol are considered as a promising alternative fuel

for the combustion engine and can be produced from various biomass feedstocks. The methodology typically used for the production of alcohol is discussed briefly in Sect. 11.2. Ethanol as an alternative fuel has been used in Brazil for more than the past 35 years. Methanol was used as an alternative fuel during the oil crisis in 1970. In primary alcohols, OH (hydroxyl) radical is connected to a primary carbon (Ning et al. 2020). Several benefits of using alcohol as an alternative fuel in the automotive engines are (i) lower cost, (ii) higher oxygen contents, (iii) lower greenhouse gas emissions, (iv) higher octane number, (v) wider flammability limits, and (vi) improvement of overall efficiency. The higher oxygen content of alcohol and OH group in alcohol fuel improved the soot oxidation during mixing-controlled and late combustion phase (Ning et al. 2020; Chen et al. 2018; Nour et al. 2019). The alcohol fuels have a higher octane number, which means it is resistant to the auto-ignition. Due to the higher octane number and heat of vaporization, alcohol, such as ethanol, can be used directly in spark-ignition engines (up to certain blending ratio with gasoline) (Gong et al. 2020, 2019). The direct use of alcohol in CI-engine is difficult due to its ignition characteristics (i.e., higher auto-ignition temperature, lower cetane number, and viscosity). These fuels can be used in CI-engine either in blending mode or in dual-fuel combustion mode. An extra additive such as dodecanol, dimethyl ether (DME), acetone is required to mix during the blending of ethanol–methanol and diesel to avoid the layer separation before injecting it into the cylinder (Szulczyk 2010). However, butanol has no miscibility issue with diesel, thus can be used in blended fuel (butanol–diesel blend) (Saxena and Maurya 2018). In dual-fuel combustion mode, alcohol fuel is separately injected through the port fuel injection (PFI) technique, whereas diesel is directly injected into the cylinder using a direct injection strategy (common rail direct injection) (Blasio et al. 2013, 2017, 2014). The dual-fuel combustion mode has similar or higher thermal efficiency than conventional diesel combustion depending on the operating conditions. However, it has significantly higher HC and CO emissions in comparison with neat diesel operation (Blasio et al. 2017). Dual-fuel operation is fuel flexible; thus, various alcohols and other low-reactivity fuels, along with other high-reactivity fuel such as diesel or various biodiesels, can be used.

Additionally, dual-fuel combustion in CI-engine is capable of simultaneous in-cylinder reduction of NO_x and PM emissions, which is one of the major challenges in conventional diesel combustion due to the trade-off between NO_x and PM species. That means when an engine operating parameter is adjusted to reduce the combustion temperature for reducing the NO_x emission, smoke, and particulate emissions increase and vice versa. In dual-fuel combustion mode, the alcohol–diesel premixing ratio can be varied and instantaneously controlled online, based on the engine demand under a wider engine operating map (Ning et al. 2020). The detail about the concept of dual-fuel combustion mode in CI-engine is discussed in Sect. 11.3. This chapter describes the application of low and medium carbon alcohol fuels (i.e., methanol, ethanol, and butanol) in dual-fuel CI-engine. In this chapter, firstly, the production process of methanol, ethanol, and butanol are discussed briefly. Secondly, the concept of the dual-fuel combustion process in CI-engine is discussed in detail. Later on, the effect of various engine operating parameters on the combustion and performance

characteristics of dual-fuel CI-engine is explained. Additionally, the regulated and unregulated emission along with particle number characteristics dual-fuel CI-engine has been discussed.

11.2 Production of Alcohol Fuels and Their Properties

The alcohol fuels such as methanol, ethanol, and butanol are produced from various resources. Methanol and ethanol are low-carbon fuels having single and double carbon, respectively. *Methanol* is a simple molecule (CH_3OH), and ethanol (C_2H_5OH) can be derived from methanol. Methanol and ethanol can be produced from variable renewable sources such as agricultural biomass [i.e., sweet sorghum, maize, cassava, sugarcane, and other high starch crops (Sharma and Ogbeide 1982)], waste biomass and wood. However, in the present scenario, the primary feedstock for methanol production remains non-renewable natural gas (Thring 1983; Chmielniak and Sciazko 2003). Methanol can be derived from biomass via gasification process to yield syngas, which later reacts to form renewable methanol in the presence of a catalyst. Methanol can also be produced from coal and heavy crude oil via the synthesis gas process (Sayin and Uslu 2008). The method of formation of methanol from methane gas via the synthesis process is briefly discussed below.

Methanol production from methane gas consists of three processes, i.e., steam reforming, water gas shift reaction, and methanol synthesis process (Üçtuğ et al. 2014). In the steam reforming process, the methane gas reacts with steam at very high pressure and temperature (2–3 MPa and 800–1000 °C) in the presence of nickel (act as a catalyst) to form H_2 and CO (Üçtuğ et al. 2014). In the water gas shift reaction, the CO formed in the previous process continues to react with steam and form to H_2 and CO_2. The resultant mixture of CO_2, H_2, and CO is typically known as syngas. The mixture of gases exit from the furnace above 800 °C and cooled down to 32 °C when passes through tubes. The extracted heat from cooling is used to produce compressed steam (to heat water from boiler feed), some fraction of heat is carried to the distillation branch, and rest is lost in the air. At the end of cooling, some fraction of unreacted steam is condensed and recycled to water treatment (Üçtuğ et al. 2014). In the methanol synthesis process, produced syngas in the previous method is supplied to methanol converter under high pressure, where syngas is converted into gaseous methanol in the presence of a zinc–copper catalyst. Under high pressure and temperature, the H_2 and CO combine to form methanol. The gaseous mixture is supplied through the cooling area, where methanol condensed and stored for the further refining process. The unconsumed mixture of gases returned to further mixing with synthesis gas (Üçtuğ et al. 2014). More details about the production of methanol via the synthesis process are given in the study (Üçtuğ et al. 2014). The schematic of methanol synthesis via the reforming process is shown in Fig. 11.1.

$$CH_4 + H_2O \leftrightarrow CO + 3H_2 \quad \Delta H_r = 206 \text{ kJ/mol}$$

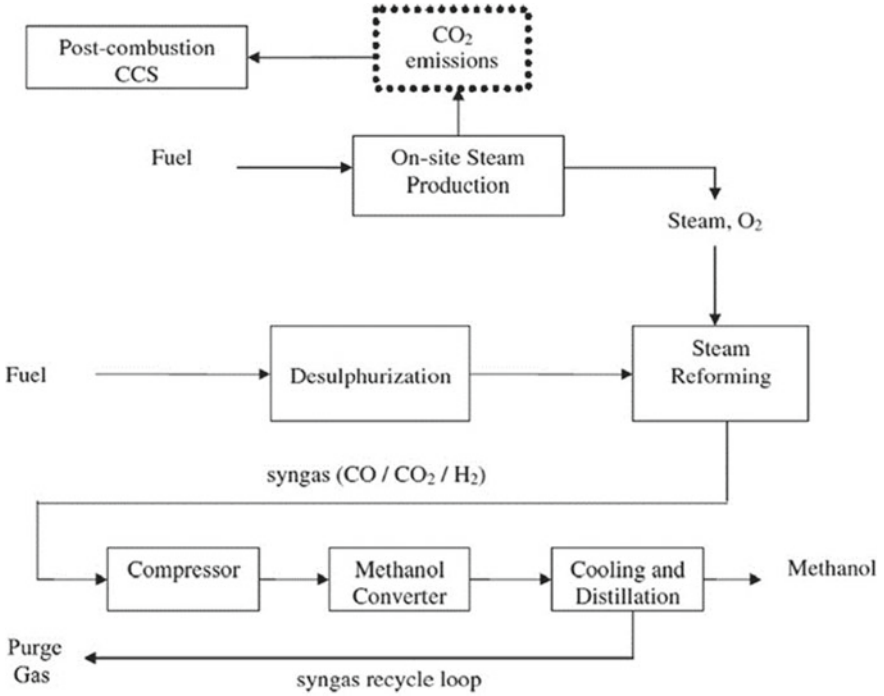

Fig. 11.1 Schematic diagram of methanol synthesis via reforming (Üçtuğ et al. 2014)

$$CO + H_2O \leftrightarrow CO_2 + H_2 \quad \Delta H_r = 206 \text{ kJ/mol}$$

$$2H_2 + CO \leftrightarrow CH_3OH \quad \Delta H_r = -90.7 \text{ kJ/mol}$$

$$H_2 + CO_2 \leftrightarrow CO + H_2O \quad \Delta H_r = 49.8 \text{ kJ/mol}$$

$$3H_2 + CO_2 \leftrightarrow CH_3OH + H_2O \quad \Delta H_r = 49.8 \text{ kJ/mol}$$

Ethanol can be derived from agricultural products, which can be fermented to yield ethanol. Ethanol can also be obtained by acid hydrolysis of lignocellulosic materials (Sharma and Ogbeide 1982; Sayin and Uslu 2008; Tillman 1978; Tsao et al. 1978). The ethanol production via fermentation process consists of yeast fermentation, distillation, and dehydration processes. Before fermentation, hydrolysis of carbohydrates like cellulose and starch into sugar is required for some crops. During hydrolysis, enzymes are used. Presently, sugarcane and corn are mainly used for the production of ethanol. Ethanol can be derived by microbial fermentation of sugar. Cellulose and starch are the main components of the plants made of sugars, which can

be easily transformed into sugar for fermentation. The water fraction and yeast solids are removed for the utilization of ethanol as fuel. Thus, distillation is performed to get ethanol after the fermentation process. However, the purity of the separated ethanol is limited to approximately 96%. The prepared ethanol is hydrous ethanol, which can be used as fuel (up to a very limited blending ratio with gasoline). Therefore, water contents further need to be removed to utilize in combustion engines (Filho and Orlando 2008). The dehydration process is used to remove the water content from hydrous ethanol. In the dehydration process, benzene/cyclohexane is mixed to azeotropic ethanol/water mixture. The mixing of benzene/cyclohexane resulted in the formation of a heterogeneous mixture. Distillation of this mixture produces a vapor mixture of ethanol, water, and benzene/cyclohexane and anhydrous ethanol. The more details about the production of ethanol is available in the study (Bergmann et al. 2018). The flow diagram of ethanol production from sugarcane is shown in Fig. 11.2.

Butanol is a medium carbon fuel, having four carbons, and can also be produced via fermentation of sugar and from similar feedstocks. The fermentation process of butanol production is the same as that for ethanol. The stoichiometric conversion of butanol from glucose depicts a lower theoretical maximum yield compared to ethanol produced per unit glucose (Blasio et al. 2014; Hoogewind 2014). The stoichiometric

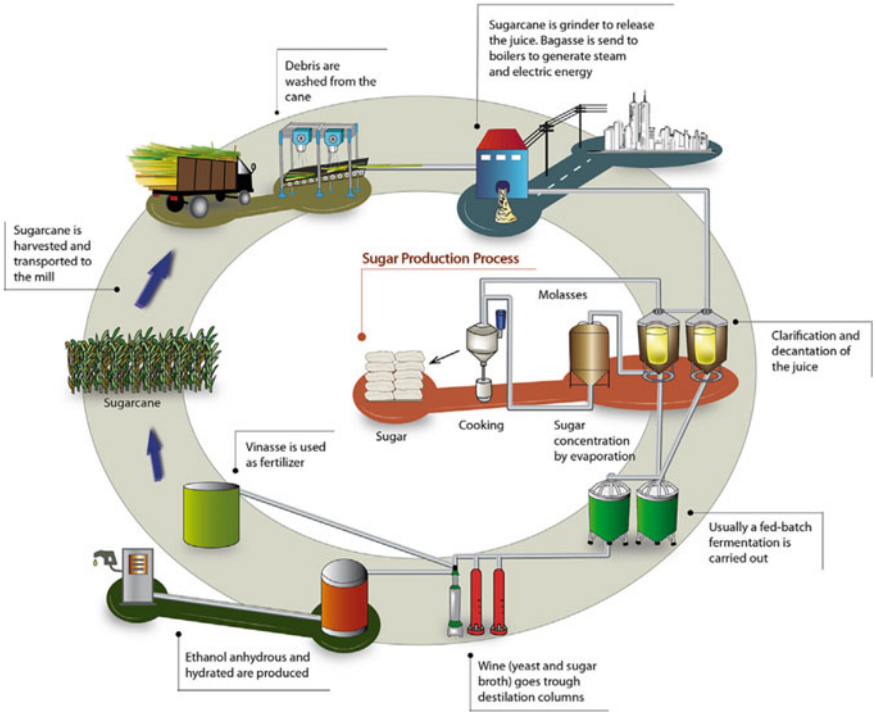

Fig. 11.2 Schematic of ethanol production from sugarcane (Bergmann et al. 2018)

conversion of glucose ethanol and butanol can be written as

$$\begin{array}{l} C_6H_{12}O_6 \rightarrow 2C_2H_5OH + 2CO_2 \\ 180.16\,\text{kg} \quad 92.14\,\text{kg} \quad 88.02\,\text{kg} \\ C_6H_{12}O_6 \rightarrow C_4H_9OH + 2CO_2 + H_2O \\ 180.16\,\text{kg} \quad 74.12\,\text{kg} \quad 88.02\,\text{kg} \quad 18.02\,\text{kg} \end{array}$$

The butanol fermentation by solventogenic strains of Clostridium species produces a mixture of solvents (acetone, ethanol, and some strains produce 2-propanol) rather than pure *n*-butanol (Hoogewind 2014).

Butanol has superior fuel-related properties in comparison with low-carbon alcohols. Butanol has a higher air–fuel ratio and energy content and air–fuel ratio in comparison with methanol and ethanol. Butanol is relatively less toxic and has lower volatility in comparison with methanol and ethanol. Lower volatility of butanol leads to reduce the chances of cavitation and vapor lock problem. The calorific value of butanol is higher in comparison with ethanol and methanol. Butanol has a lower vapor pressure point and higher flashpoint temperature, which makes it safer in comparison with methanol and ethanol. Additionally, the cetane number of the butanol is higher in comparison with ethanol and diesel; therefore, butanol can be easily auto-ignites than methanol and ethanol (Chen et al. 2018; Nour et al. 2019). Thus, based on the butanol benefits, it could be said that butanol is better fuel for CI-engine in comparison with methanol and ethanol. The properties of fossil diesel, methanol, ethanol, and butanol are presented in Table 11.1.

Table 11.1 Fuel properties of ethanol, methanol, butanol, and diesel (Jin et al. 2011)

Property	Diesel	Ethanol	Methanol	*n*-butanol
Molecular formula	C_{12}–C_{25}	C_2H_5OH	CH_3OH	C_4H_9OH
Cetane number	40–55	8	3	25
Octane number	20–30	108	111	96
Oxygen content (% weight)	–	34.8	50	21.6
Density (g/ml) at 20 °C	0.82–0.86	0.790	0.796	0.808
Auto-ignition temperature (°C)	210	434	470	385
Flash point (°C) at closed cup	65–88	9	12	35
Lower heating value (MJ/kg)	42.5	26.8	19.9	33.1
Boiling point (°C)	180–370	78.4	64.5	117.7
Latent heating (kJ/kg) at 25 °C	270	904	11.09	582
Viscosity (mm^2/s) at 40 °C	1.9–4.1	1.08	0.59	2.63

11.3 Dual-Fuel Combustion

In dual-fuel CI-engine, in-cylinder fuel blending of a low-reactivity fuel and high-reactivity fuel is used in the same combustion cycle. Typically, high octane fuel (i.e., low reactivity) is injected in the intake manifold through the port fuel injection strategy (PFI) (similar to SI-engines), and high cetane fuel (i.e., high-reactivity) is directly injected in the cylinder through direct injection system (similar to CI-engine). The dual-fuel combustion regime is an intermediate combustion mode between the conventional SI and CI-engine. Gasoline-like fuel is typically injected in the intake manifold during the intake stroke with air. In contrast, diesel-like fuel is injected into the cylinder during the end of the compression stroke (near TDC position). The schematic diagram of the dual-fuel CI-engine experimental test setup is shown in Fig. 11.3. The auto-ignition temperature of low-reactivity fuels is higher. Therefore, the compressed premixed charge of low-reactivity fuel and air does not auto-ignite at the end of the compression stroke. The auto-ignition of a premixed charge in the dual-fuel CI-engine initiates with the auto-ignition of injected diesel near TDC. The injection of diesel near the TDC position acts as an ignition source in dual-fuel CI-engine. In conventional dual-fuel CI-engine, the charge burns in the premixed and diffusion combustion phase (similar to conventional CI-engine), as well as flame, propagates similar to SI-engine (Maurya 2018). However, in the later stages, flame propagates similarly to the SI-engine. A study optically diagnoses the burning dynamics of ethanol/*n*-heptane dual-fuel CI-engine (Fraioli et al. 2014).

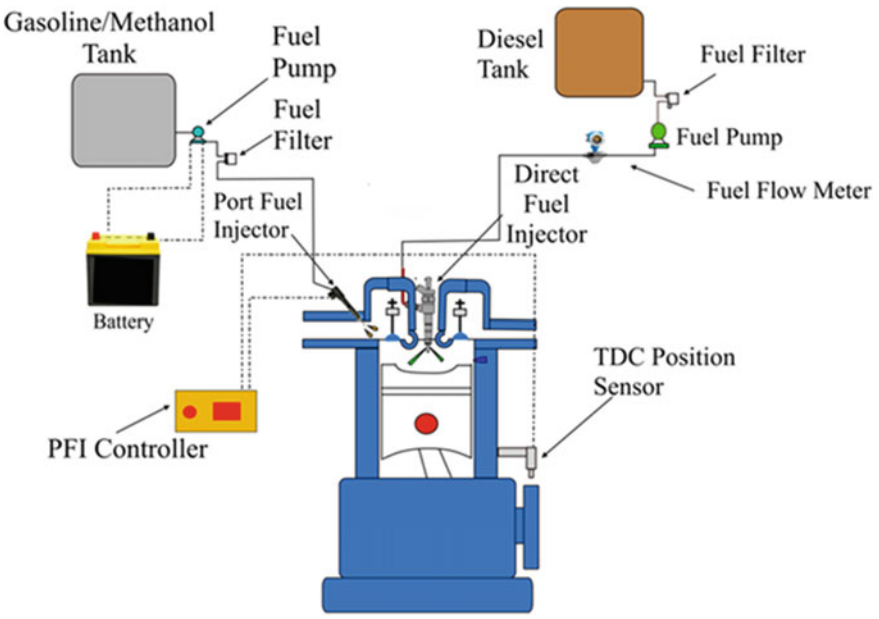

Fig. 11.3 Schematic diagram showing the concept of dual-fuel CI-engine

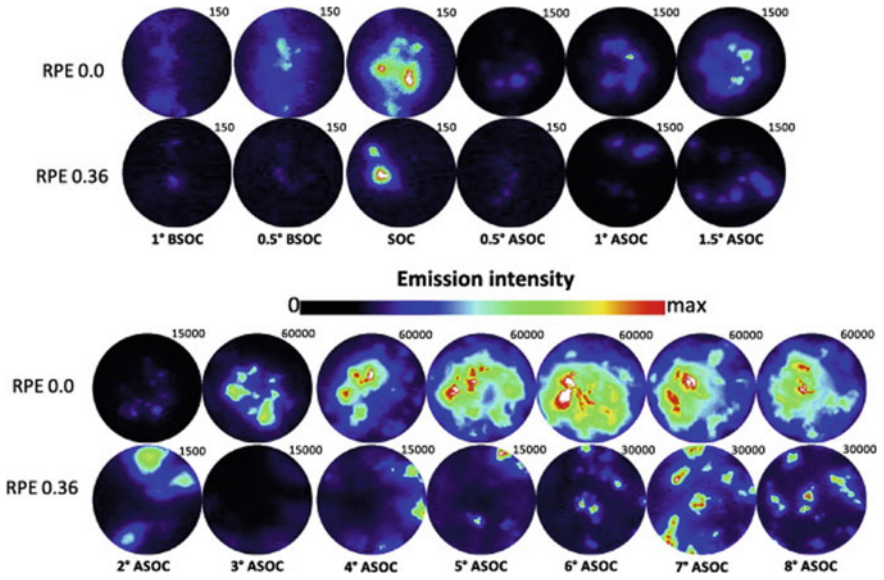

Fig. 11.4 UV–VIS images detected in the optical engine for neat *n*-heptane and ethanol/*n*-heptane dual-fuel CI-engine (Fraioli et al. 2014)

Figure 11.4 presents the UV–VIS (ultraviolet–visible) images of the optical engine at a premixing ratio of 0 and 36% with color scale and maximum intensity of each frame (can be depicted on the upper right side). This imaging strategy was used in the optical engine to determine the intermediate chemical species such as OH, HCO, and CO in terms of their spatial distribution and temporal evolution. This technique allows us to identify the in-cylinder cores with high reactivity of mixed fuels. Additionally, the influence of available low-reactivity fuel on the burning dynamics of the directly injected fuel can be investigated. The figure depicts the strong activity in the mixing process for both the operations (i.e., *n*-heptane (0% premixing ratio) and ethanol/*n*-heptane dual-fuel (36% premixing ratio)). Figure 11.4 shows that in the case of neat *n*-heptane operation, the highest intensity was observed in the center of the piston bowl from the start of combustion (SOC) up to 80 after SOC. Figure 11.4 illustrates that flame is mainly observed under the nozzle area and started from 10 after SOC, while the highest intensity and white-colored zone was observed at 60 after SOC. This indicates strong chemical reactions are occurring in this area, and the flames are producing the soot (Fraioli et al. 2014).

However, in the case of ethanol/*n*-heptane dual-fuel operation, the combustion behavior is significantly different as compared to neat diesel operation. In dual-fuel operation, mainly the chemical activities were occurring close to the piston bowl walls, which started from SOC while the larger area remains blue (Fraioli et al. 2014). The flame with a relatively higher intensity was observed in the bowl after 40 SOC (even have a lower intensity as compared to neat diesel operation) (Fraioli et al. 2014). In another optical study, the authors reported that during the cool flame stage,

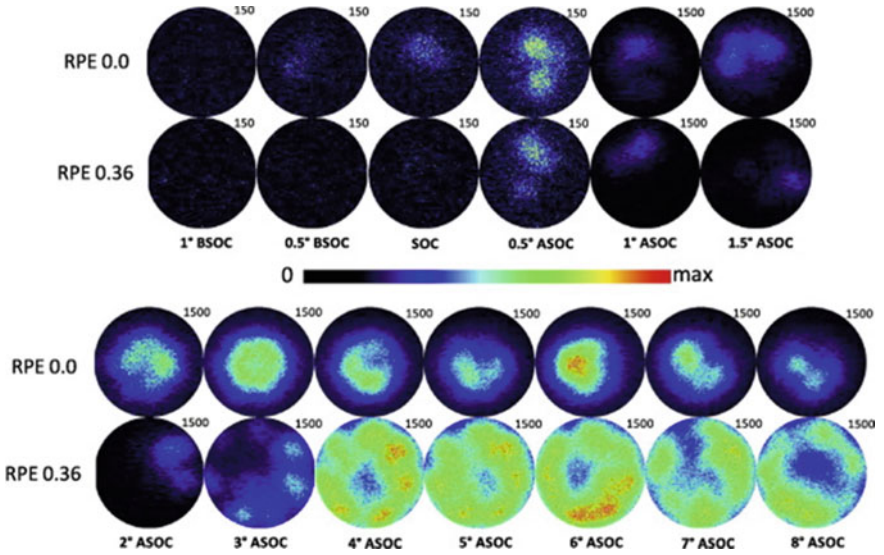

Fig. 11.5 Spatial distribution of OH radical (Fraioli et al. 2014)

CH, HCOH, HCO, CN, C_2 were present (Mancaruso and Vaglieco 2011). They had reported all the spectra presented a background due to HCOH, HCO radicals, and various peaks because of other species and radicals that superimposed it (Mancaruso and Vaglieco 2011). Additionally, during the second stage of ignition, CH and OH radicals were found in the significant concentration (Mancaruso and Vaglieco 2011). Again, they superimposed the background due to HCO, HCOH, which start to turn into CO–O (Mancaruso and Vaglieco 2011).

Figure 11.5 illustrates the spatial distribution of OH radical detection for an optical engine for *n*-heptane and ethanol/*n*-heptane dual-fuel CI-engine. Figure 11.5 depicts that in the case of neat *n*-heptane operation, the intensity of OH radicals is higher close to the nozzle tip. In contrast, in the case of ethanol–diesel dual-fuel operation, the OH radicals are homogeneously distributed throughout the combustion chamber with lower intensity near the injector nozzle tip. This reveals more fraction of premixed combustion occurs in the case of dual-fuel combustion (Fraioli et al. 2014). Additionally, study reported that in the case of neat *n*-heptane operation, *n*-heptane impinges on the wall surface and creates reactivity stratification in the charge (Fraioli et al. 2014). On the contrary, HCO is consumed during the first stage of combustion and converted into CO–O (Fraioli et al. 2014). The dual-fuel CI-engine is fuel flexible, and various low-reactivity fuels such as alcohols and gaseous fuels (such as CNG, H_2) can be utilized. Premixing of high octane fuel leads to a reduction in the mean gas temperature, which results in lower NO_x formation during combustion. Additionally, the premixing of high octane fuel (similar to SI-engine) leads to reduce local fuel-rich region formation, which lowers the soot formation during combustion. A study optically investigated the nitrogen oxide and

particle formation in methane–diesel dual-fuel CI-engine (Iorio et al. 2017). Their result indicates that methane–diesel dual-fuel combustion is characterized by lower extended flame area and soot concentration in comparison with a conventional diesel engine. This leads to a decrease in the total particle number concentration in dual-fuel CI-engine, which was mainly due to the lower carbon atom in methane (Iorio et al. 2017). The formation of soot particles depends on the locally rich fuel–air charge. The premixing of methane leads to a decrease in the locally rich fuel–air zone in the combustion chamber. Additionally, the lower carbon atom of methane causes to decrease the formation of soot precursors, which results in lower particle emissions in methane/diesel dual-fuel operation. Furthermore, dual-fuel operation has a lower flame temperature, which leads to a decrease in the NO emission in comparison with neat diesel operation. However, NO_2 emissions are higher in dual-fuel CI-engine in comparison with diesel combustion (Iorio et al. 2017).

Performance Characteristics

The performance characteristics of dual-fuel CI-engine is discussed in this section. Various studies have been found which investigated the different aspects of performance characteristics of alcohol–diesel dual-fuel CI-engine (Meng et al. 2016; Britto and Martins 2014; Yousefi et al. 2015; Jamuwa et al. 2016; Song et al. 2008). In dual-fuel CI-engine, an increase in engine load resulted in higher brake thermal efficiency (BTE) and lower brake-specific fuel consumption (BSFC) for all the fuel premixing ratios (Saxena et al. 2018). Decreased ratio of friction to brake power is responsible for increased BTE with engine load. Additionally, earlier combustion phasing at higher load causes to increase the expansion ratio, which results in improved efficiency. Reduced BSFC is because of the interaction between these parameters (Saxena et al. 2018). The influence of injection timing on BTE at different air intake temperatures for fumigated methanol–diesel dual-fuel operation is presented in Fig. 11.6. The dashed line in the figure indicates the BTE of a baseline diesel engine at a fixed intake air temperature of 35 °C. The figure indicates that the BTE is lower in dual-fuel combustion in comparison with neat diesel operation at 35 °C air intake temperature for both the methanol–diesel premixing ratios. However, significant improvement in BTE is observed for higher intake air temperature (i.e., 75 and 115 °C), when diesel injection timing is 7.4° bTDC. The maximum BTE is obtained for 60% methanol–diesel premixing ratio and 115 °C intake air temperature. The latent heat of vaporization of methanol is higher in comparison with diesel. Methanol premixing–substitution causes to reduce the local charge temperature at the end of the compression stroke. At 35 °C, the reduction in BTE is attributed to the charge cooling effect of methanol, which caused to decrease in the average combustion temperature in the combustion chamber (Wang et al. 2015a).

An increase in intake air temperature improves the evaporation of methanol, which enhances the rate of auto-ignition reaction of charge and broadens flammability limits. Thus, flame propagates in a comparatively leaner charge. This caused to improve combustion efficiency and BTE (Wang et al. 2015a). No significant variations in BTE are observed for earlier injection timing from 7.4° bTDC, whereas BTE significantly decreased when injection timing retarded from 7° bTDC (Fig. 11.6).

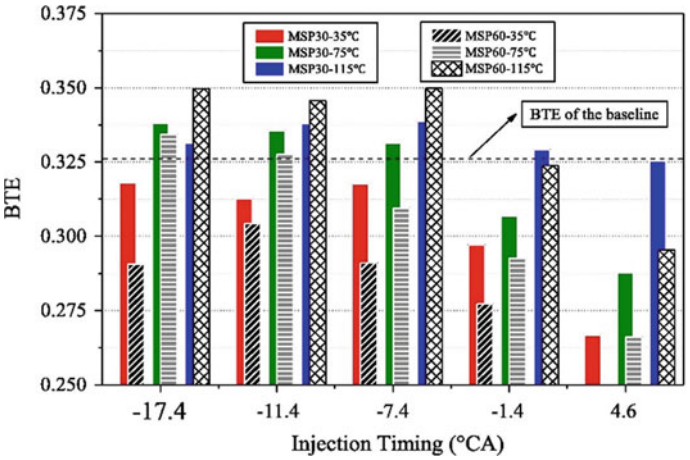

Fig. 11.6 Variation of BTE with injection timing for different intake temperatures and the methanol–diesel premixing ratio (Wang et al. 2015a)

Advanced diesel injection timing leads to longer ignition delay, and more energy from diesel injection contributes to the onset of multiple propagation flames. On the other hand retarded diesel injection leads to delayed combustion, which caused to incomplete combustion of methanol (since more amount of mixture combust when piston moving away from TDC), resulted in decreased BTE (Wang et al. 2015a). However, no significant reduction in BTE with retard injection timing is observed in the case of a 30% methanol–diesel premixing ratio at 115 °C intake air temperature. It is attributed to the auto-ignition of methanol prior to diesel injection, which caused a relatively earlier start of combustion and resulted in higher BTE (Wang et al. 2015a). Another study also investigates the influence of air intake temperature and methanol–diesel premixing ratio on the indicated thermal efficiency (ITE) (Pan et al. 2015). ITE decreases with an increase in air intake temperature for neat diesel operation, whereas increases for methanol–diesel dual-fuel operation (for most of the test conditions) (Pan et al. 2015). The ITE increases with an increase in methanol premixing (up to 30%) for 20 and 40 °C air intake temperature. However, a further rise in methanol premixing resulted in worsening combustion and reduced efficiency (Pan et al. 2015). For higher intake air temperature from 40 °C, the ITE increases with methanol premixing. The study reported that for higher air intake temperature than 70 °C, an increase in methanol premixing is restricted by higher peak combustion pressure (Pan et al. 2015).

The influence of gasoline and butanol premixing on ITE (indicated thermal efficiency) and BTE is shown in Fig. 11.7. The figure indicates a slight increase in efficiency for a 20% fuel premixing ratio for both the operations; however, a further increase in gasoline and butanol substitution leads to reduce BTE and ITE. A decrease in BTE–ITE, with an increase in premixing, is attributed to the higher heat of vaporization of gasoline and butanol (Saxena and Maurya 2020).

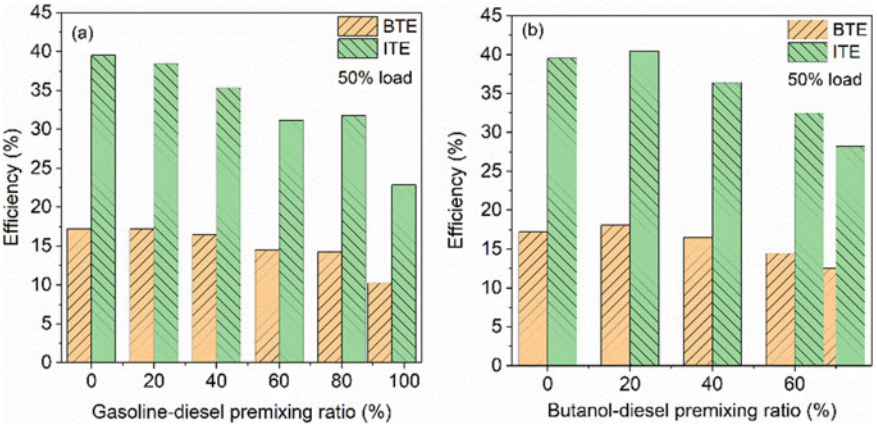

Fig. 11.7 Variation of ITE and BTE with gasoline–butanol premixing

Higher heat of vaporization of butanol and gasoline decreases the temperature of the compressed mixture, which causes longer ignition delay and retard the ignition timing and combustion phasing (CA_{50}). Therefore, more fraction of mixture combusts when the piston starts moving away from the TDC, thus results in reduced thermal efficiency. The thermal efficiency is comparatively higher for the 20% butanol–diesel premixing ratio (Fig. 11.7). Higher fuel bound oxygen content of butanol leads to improve the combustion process. Additionally, higher auto-ignition temperature of butanol (as compared to gasoline) caused to longer ignition delay, thus more fraction of mixture burned in the premixed combustion phase and resulted in improved thermal efficiency. Further increase in butanol premixing resulted in decreased BTE. In the case, when the butanol–diesel premixing ratio is higher than 60%, BTE is lower in comparison with gasoline–diesel dual-fuel operation. Higher latent heat of vaporization of butanol as compared to gasoline also caused delayed ignition timing and CA_{50}, which reduces the in-cylinder mean gas temperature and resulted in decreased thermal efficiency. Thus, the efficiency of dual-fuel CI-engine depends on the dominating factor (Saxena and Maurya 2020).

An increase in the butanol–soyabean biodiesel premixing ratio resulted in decreased combustion efficiency and ITE as well (Liu et al. 2014). For higher premixing ratio, more fraction of butanol may be trapped in crevices, which is difficult to oxidize and resulted in lower combustion efficiency. With retard biodiesel injection timing, firstly, the combustion efficiency and ITE increased and then decreased (Liu et al. 2014). An advanced or retard injection timing caused delayed combustion phasing, decreased mean gas combustion temperature, and lower degree of constant volume combustion, which resulted in lower combustion efficiency and ITE (Liu et al. 2014). Combustion efficiency decreases with an increase in exhaust gas recirculation (Liu et al. 2014). Possibly partial fuel cannot oxidize completely due to reduced combustion temperature with an increase in exhaust gas recirculation (Liu et al. 2014). For higher exhaust gas recirculation (45%), the ITE decreased by 1–2%.

Reduction in combustion efficiency resulted in reduced ITE (Liu et al. 2014). On the contrary, for higher exhaust gas recirculation, the combustion duration increases, which caused to decrease in the degree of constant volume combustion (Liu et al. 2014).

The operating load boundary of the fumigated methanol–diesel dual-fuel engine is shown in Fig. 11.8. In the plot, *X*-axis depicts the methanol–diesel premixing ratio, *Y*-axis depicts the engine load, and the contour depicts the BTE. The operating boundary of methanol–diesel dual-fuel operation is restricted by four factors, i.e., partial burn, roar combustion–higher pressure rise rate, misfire, and knock (Fig. 11.8) (Wang et al. 2015b). The lower boundary of dual-fuel operation is restricted by the partial burn, which at lower engine load with higher methanol–diesel premixing ratio. For medium engine load, the methanol premixing is restricted by misfire (on the right side in Fig. 11.8). The figure indicates that when the engine load increased from medium to higher load, the range of methanol premixing starts decreasing. In dual-fuel combustion, excessive fuel premixing at higher engine load resulted in higher pressure rise rate, which restricts the range of methanol premixing. At higher engine load (neat full load), strong acoustic oscillations in pressure traces were observed, which depicts the knock and restrict the range of methanol premixing (Fig. 11.8) (Wang et al. 2015b). With an increase in engine load, the combustion characteristics

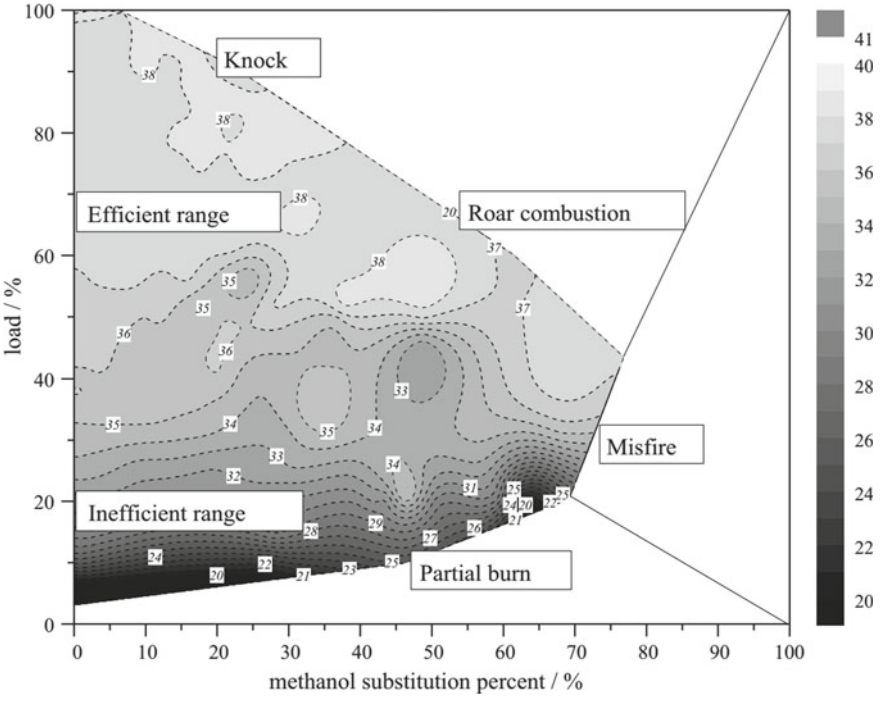

Fig. 11.8 Experimental operating range and BTE contours for the fumigated methanol–diesel dual-fuel engine (Wang et al. 2015b)

changed from partial burn to misfire to roar combustion and to knocking (Wang et al. 2015b).

The contour in the figure depicts the BTE. The figure depicts that BTE increases with engine load for all the premixing ratios. The figure indicates that at a lower engine load, the BTE is decreased as the methanol premixing increases in comparison with neat diesel operation (0% premixing ratio). The possible reason for lower BTE is already discussed in this section. At medium engine load, the BTE initially decreases and then increases with an increase in methanol premixing (Wang et al. 2015b). The homogeneous charge burns with higher rapid heat release, which possibly caused to increase BTE for higher methanol–diesel premixing ratio (Wang et al. 2015b). At higher engine load, the mean gas temperature is higher, and the combustion of richer charge resulted in higher BTE (Wang et al. 2015b).

Combustion Characteristics

The combustion characteristics of dual-fuel CI-engine is discussed in this section. In this section, the influence of engine operating parameters on ignition delay, in-cylinder pressure, heat release rate, combustion phasing (CA_{50}), and duration have been discussed for alcohol–diesel fueled CI-engine.

Ignition Delay

Ignition delay is typically defined as the time delay from the start of fuel injection to the beginning of the combustion. Charge combustion and its phasing strongly depend on the ignition delay. In the dual-fuel CI-engine, the ignition delay has a significant effect on the combustion characteristics of the engine. The effect of the methanol–diesel premixing ratio on ignition delay is shown in Fig. 11.9. The figure indicates that higher engine load has a shorter ignition delay for neat diesel and methanol–diesel dual-fuel as well. Dual-fuel operation has longer ignition delay, which increases with an increase in the methanol premixing. In dual-fuel operation, the ignition delay period is influenced by in-cylinder temperature, pressure, and oxygen concentration at the time of diesel injection. In a study (Prakash et al. 1999), the authors developed the empirical model for the determination of ignition delay for dual-fuel CI-engine, which is given by Eq. (11.1).

$$\tau_i(\mathrm{CA}) = C(O_{df})^k(0.36 + 0.22M_{PS}) \times \exp\left[E_A\left(\frac{1}{RT_m(r_c)^{n-1}} - \frac{1}{17190}\right) + \left(\frac{21.2}{P_m(r_c)^n - 12.4}\right)^{0.63}\right] \quad (11.1)$$

where 'C' denotes the modified coefficient, 'P_m' is the manifold pressure, 'M_{PS}' is the mean piston speed, 'E' is the activation energy as a function of cetane number, 'n' is the polytropic index 'r_c' is the compression ratio, 'k' is the constant, and 'O_{df}' is the oxygen concentration ratio of the dual-fuel engine (Prakash et al. 1999).

$$O_{df} = \frac{(O_f)_{\text{dualfuel}}}{(O_f)_{\text{diesel}}} \quad (11.2)$$

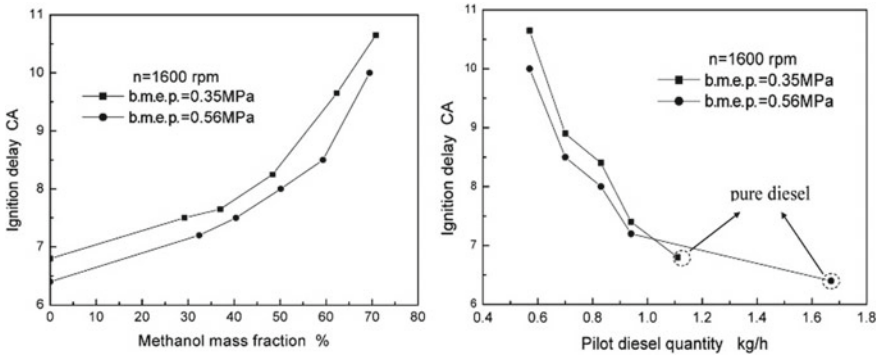

Fig. 11.9 Influence of methanol addition and pilot diesel quantity on ignition delay (Wang et al. 2008)

where 'O_f' denotes the mole fraction of oxygen, (O_f) dual-fuel mole fraction of oxygen in gaseous fuel in dual-fuel mode, and $(O_f)_{\text{diesel}}$ is the mole fraction of oxygen in neat diesel fuel operation. Mole fraction of oxygen can be calculated from Eq. (11.3) (Prakash et al. 1999).

$$O_f = \frac{M_a}{4.76(M_{\text{mixture}})} \tag{11.3}$$

and

$$M_{\text{mixture}} = M_a + M_{\text{methanol}} + M_{\text{exh.gas}} \tag{11.4}$$

where 'M' depicts the mole fractions.

The premixing of low-reactivity fuel leads to a reduction in the temperature and pressure of compressed charge (Lata and Misra 2011). The decrease in the charge temperature mainly depends on the heat of vaporization of fuel and heat transfer through the cylinder wall (Lata and Misra 2011; Verhelst et al. 2009; Lambe and Watson 1992). The concentration of oxygen also decreases with an increase in substitution percentage of low-reactivity fuel in dual-fuel operation as compared to neat diesel operation (Eq. 11.3). It is because of the reduction in the amount of inducted air into the cylinder (during intake stroke) with the addition of high octane fuel during the intake stroke. The reduction in the concentration of oxygen depends on the volumetric density of the inducted fuel. Lower the volumetric density of the inducted fuel, the higher will be the reduction (Lata and Misra 2011). The increase in the percentage of low-reactivity fuel leads to a decrease in the charge temperature at BDC and TDC. Additionally, the polytropic index during the compression stroke is also decreased. This caused to increase in the ignition delay for the same engine operating condition in comparison with the neat diesel case (Wang et al. 2008). Premixing of alcohol (i.e., high octane fuel) also leads to reduced charge temperature at the end of compression stroke because of the higher heat of the vaporization of alcohol. The premixing of

alcohol fuels reduces the rate of pre-ignition chemical processes, which results in higher ignition delay in the dual-fuel CI engine.

A study investigated the influence of exhaust gas recirculation (EGR) rate on the ignition delay for butanol–soyabean biodiesel dual-fuel CI-engine (Liu et al. 2014). Their results indicate that the ignition delay has little effect of exhaust gas recirculation for early injection timings, whereas ignition delay is significantly influencing by exhaust gas recirculation for late injection timings. Higher exhaust gas recirculation resulted in longer ignition delay (Liu et al. 2014).

Heat Release Rate

This section presents the effect of the engine operating parameter on the heat release rate dual-fuel CI-engine. The influence of methanol–diesel and ethanol (E85)–diesel premixing–substitution ratio on heat release rate (HRR) is shown in Fig. 11.10. The first and second peaks of heat release depict the premixed and mixing-controlled combustion, respectively (Tutak et al. 2015). The figure indicates an increase in engine load leads to a higher heat release rate for neat diesel and dual-fuel as well. At higher engine load, more fraction of fuel burns in the engine cycle, which caused to higher heat release rate. The figure also indicates that dual-fuel operation has a relatively lower and slightly retarded peak of heat release rate in comparison with neat diesel operation at 34 and 67% engine load. Methanol and E85 are high octane fuels. Premixing of alcohol fuel (resistant to auto-ignition) caused to longer ignition delay, which leads to delayed ignition timing and CA_{50} as well. Methanol and E85 have a higher heat of vaporization, which caused to reduce the temperature of the compressed mixture due to the charge cooling effect. This leads to reducing the rate of auto-ignition reactions and contributes to retarded ignition timing and combustion. Therefore, more amount of mixture burns when the piston moves in a downward direction (toward BDC) and results in reduced mean gas temperature and combustion pressure. Both these factors are contributing to reduced and retarded heat release, which also depends on the premixing ratio and engine load (Tutak et al. 2015).

At 100% engine load, the peak HRR is 134 J/CAD obtained at 2 CAD aTDC for neat diesel operation. For a 20% methanol–diesel premixing ratio, the peak heat release increased to 166 J/CAD obtained, whereas for 20% E85/diesel premixing ratio, the peak heat released increased to 156 J/CAD obtained at 2 CAD aTDC. However, the trend seems similar for both the dual-fuel operation with a 20% premixing ratio. At higher fuel premixing ratio (50 and 75%), two peaks of HRR are observed for both the dual-fuel operation. The first peak is attributed to the combustion of diesel fuel, and the second peak is due to the combustion of methanol/E85 (Tutak et al. 2015). At a 90% premixing ratio, a single peak of heat release is obtained for both the dual-fuel operation. The absence of diesel HRR is attributed to higher vaporization of methanol/E85 (since injected in a higher concentration for this premixing ratio). Thus, the charge cooling effect on the combustion rate became more significant (Tutak et al. 2015).

A study investigated the influence of diesel injection timing and air intake temperature on the HRR of the methanol–diesel dual-fuel CI-engine (Wang et al. 2015a). They have observed three-stage HRR in methanol–diesel dual-fuel operation, which

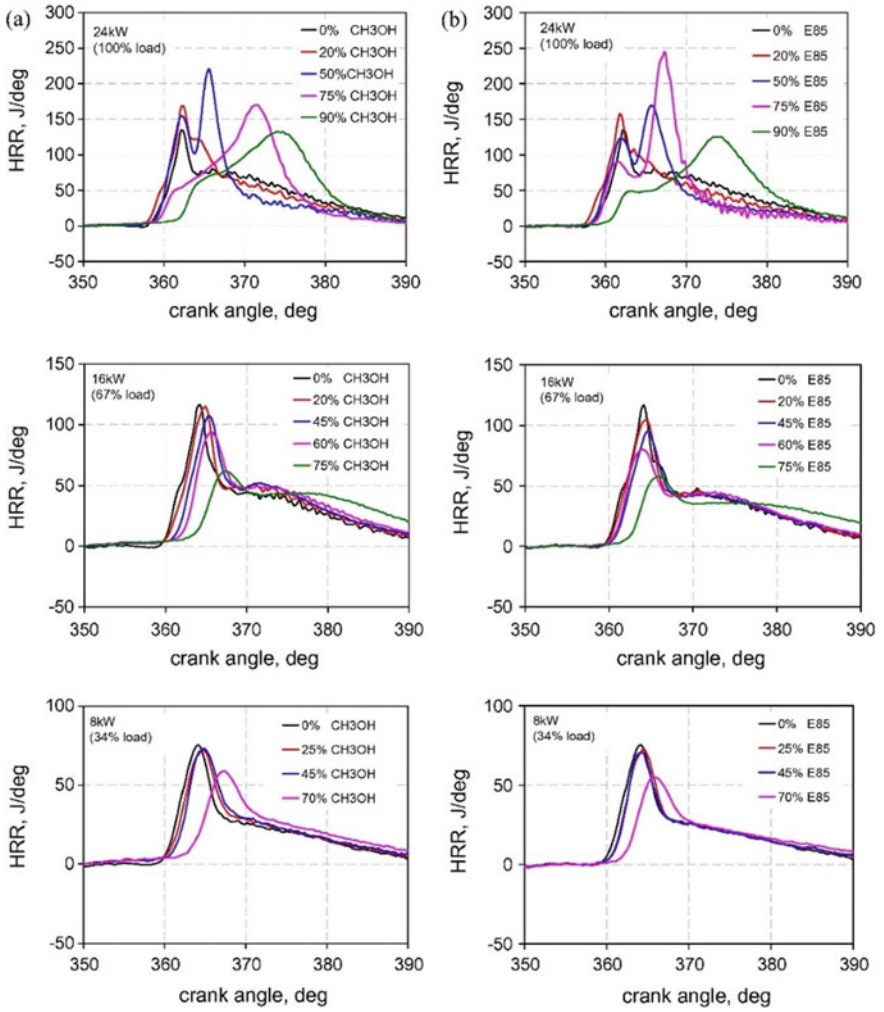

Fig. 11.10 Influence of ethanol and methanol premixing ratio on heat release rate of dual-fuel CI-engine (Tutak et al. 2015)

is more obvious at higher air intake temperature (can be seen in Fig. 11.11). The first-stage heat release is attributed to the premixed combustion of diesel and combustion of a small fraction of methanol entrained in the spray. In the second-stage heat release, the remaining fuel burns in mixing-controlled combustion phase, while the methanol–air charge in the close vicinity of pilot spray is ignited and burned. The combustion of methanol–air charge by flame propagation initiated from the spray zone in the third stage of heat release (Wang et al. 2015a). At lower temperatures (35 °C), combustion occurs with first- and third-stage heat release, whereas second stage is not various

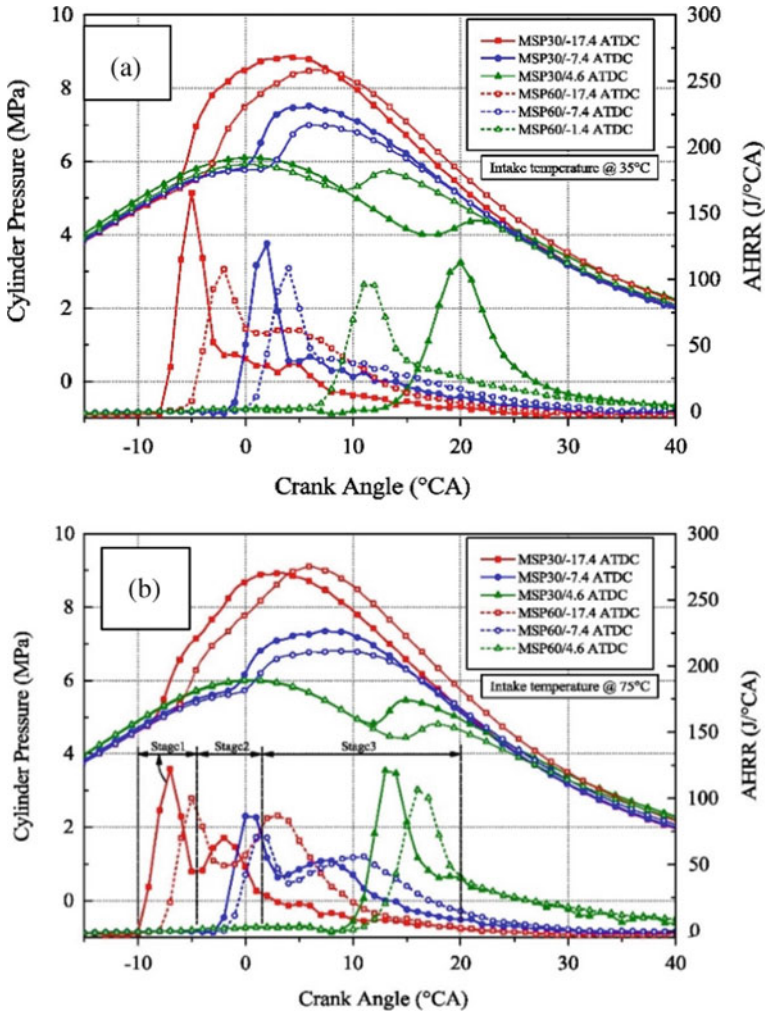

Fig. 11.11 Combustion pressure and HRR for various injection timings (Wang et al. 2015a)

obviously distinct for lower air temperature conditions (Fig. 11.11a) (Wang et al. 2015a).

At lower air intake temperature, the ignition delay is longer; thus, more amount of diesel combusts in the premixed phase of combustion (Wang et al. 2015a). The energy produced from the premixed combustion of diesel is sufficient to multipoint ignition of a premixed mixture of methanol–air and resulted in combined first- and second-stage heat release (Wang et al. 2015a). The remaining lean premixed mixture of methanol–air away from spray combustion burns in the third stage (Wang et al. 2015a). At lower air intake temperature, with an increase in methanol premixing, peak of first-stage heat release slightly decreases and retarded, while the third-stage

heat release increased (Fig. 11.11a). The possible reason for the reduced peak of HRR (first stage) with an increase in methanol premixing is already discussed in this section. The increase in the third stage of heat release is because of enhanced flame propagation speed with an increase in methanol–air ratio (Wang et al. 2015a). Retarded injection timing caused to decrease in the peak in-cylinder combustion pressure and heat release rate with delayed combustion phasing. At lower air intake temperature and higher methanol premixing further, retard diesel injection from 4.6 CAD bTDC leads to misfire (Wang et al. 2015a). Retarded diesel injection timing resulted in decreased and delayed the first peak of HRR. It is possibly due to less amount of diesel combusts in the premixed phase of combustion. Additionally, single-stage heat release observed when injection timing is further retarded after TDC (Wang et al. 2015a).

For higher air intake temperature, the three-stage heat release for dual-fuel CI-engine can be seen in Fig. 11.11b. At higher air intake temperature, the ignition delay is shorter; therefore, less amount of diesel burns in premixed combustion, which resulted in a decreased peak of first-stage heat release in comparison with a lower temperature. At higher air temperature, the premixed mixture of methanol–air burns rapidly in the close vicinity of pilot spray, which results in an increased second-stage heat release rate (Wang et al. 2015a). During this, higher temperature leads to enhance flame propagation; thus, the stage three combustion ends at an earlier crank angle. Therefore, the combustion starts in advance and ends at an earlier crank angle, resulting in improved performance (Wang et al. 2015a). Similar to operation at lower air intake temperature, the peak of first-stage heat release decreases and retarded with an increase in methanol premixing, whereas the second-stage peak increases and retarded. Additionally, retarded injection timing caused to decrease the peak in-cylinder combustion pressure and heat release rate with delayed combustion phasing similar to as that for lower air intake temperature.

The influence of diesel injection pressure on in-cylinder pressure and heat release rate of methanol–diesel dual-fuel CI-engine is investigated in a study (Liu et al. 2015). Higher diesel injection pressure leads to the increased and advanced peak of combustion pressure and heat release rate (Liu et al. 2015). Higher diesel injection pressure causes improved fuel atomization, which enhances the mixing of diesel and a premixed mixture of methanol–air and reduces the ignition delay, thus resulted in advanced ignition timing. Lower diesel injection pressure (leads to relatively poor fuel atomization) and higher heat of vaporization of methanol collectively lead to reduce combustion pressure (Liu et al. 2015). An increase in the injection pressure leads to advanced combustion phasing. The study reported that for the same fuel premixing ratio, lower engine load has advanced combustion phasing in comparison with higher engine load (in dual-fuel operation) (Liu et al. 2015). At higher engine load, for maintaining the same methanol–diesel premixing ratio, a higher amount of methanol needs to be injected. Higher heat of vaporization of methanol caused to reduce the temperature due to the charge cooling effect. This leads to longer ignition delay and resulting in retard ignition timing and CA_{50}. Furthermore, for higher diesel injection pressure (115 MPa), the compression pressure is comparatively higher in comparison with lower diesel injection pressure. An increase in diesel injection

pressure leads to an increase in the peak cylinder pressure, combustion chamber, and cylinder wall temperature, which caused to reduce the cooling effect of methanol with the higher latent heat of vaporization (Liu et al. 2015).

Pressure Rise Rate, Combustion Phasing, and Duration

This section presents the effect of engine operating parameters on the pressure rise rate combustion phasing and duration of alcohol–diesel dual-fuel CI-engine. Typically, the peak pressure rise rate (PPRR) is used to define the upper load boundary of the combustion engine. With an increase in the engine load, the PPRR increases, whereas it reduces with an increase in the low-reactivity fuel premixing (Saxena and Maurya 2017). The decrease in the PPRR with an increase in substitution of low-reactivity fuel is due to the retard combustion phasing (Saxena and Maurya 2017). Typically, the PPRR depends on the charge combust in the premixed phase of combustion. The substitution of high octane fuel increases the ignition delay as compared to neat diesel operation. Prolonged ignition delay leads to burn more amount of fuel in the premixed phase of combustion, which results in higher PPRR. An increase in the premixing of low-reactivity fuel causes to further retard the ignition timing and CA_{50} due to the lower overall reactivity of the charge. Therefore, more amount of mixture will burn when piston moving toward the downward direction, which results in reduced PPRR. The study reported that residual gas fraction has a significant effect on the auto-ignition reactions in the dual-fuel operation (Lata et al. 2011). The effect of methanol substitution ratio on PPRR at different engine loads is shown in Fig. 11.12. The figure indicates that at lower engine load, the PPRR slightly decreases with an increase in methanol substitution ratio, whereas PPRR increases with methanol substitution at higher engine load. The ignition delay, the rapid combustion, and the downward movement of the piston combine to control the change in PPRR (Wang et al. 2008).

Advanced diesel injection (from 20° to 23° bTDC) leads to higher PPRR for all the tested gasoline–diesel premixing ratio. Further advances in diesel injection from 23° bTDC lead to decrease PPRR because of the delayed start of ignition (Saxena and Maurya 2017). However, for methanol–diesel dual-fuel operation, 23° bTDC diesel injection timing seems optimal, advance/retard diesel injection results in higher PPRR. A study investigates the effect of injection timing on butanol–soyabean biodiesel dual-fuel CI-engine (Liu et al. 2014). The PPRR restricts the range of injection timing (Liu et al. 2014). In the case of early injection (45°–35° bTDC), the delayed injection timing leads to an increase in the PPRR, which limits the upper limit of PPRR. However, in the case of late injection (10° bTDC), the delayed injection timing leads to a decrease in the PPRR (Liu et al. 2014). The decreased PPRR is possibly due to delayed CA_{50}. During delayed CA_{50}, the more fraction of fuel burns when the piston is moving toward the downward direction, which caused decreased combustion temperature and resulted in slower PPRR (Liu et al. 2014). Even though the delayed CA_{50} results in slower PPRR, however, excessive delayed CA_{50} also results in higher cyclic variations (Liu et al. 2014).

When the engine load increases from medium to higher load, the range of the methanol premixing is limited by higher PPRR (Wang et al. 2015b). At higher

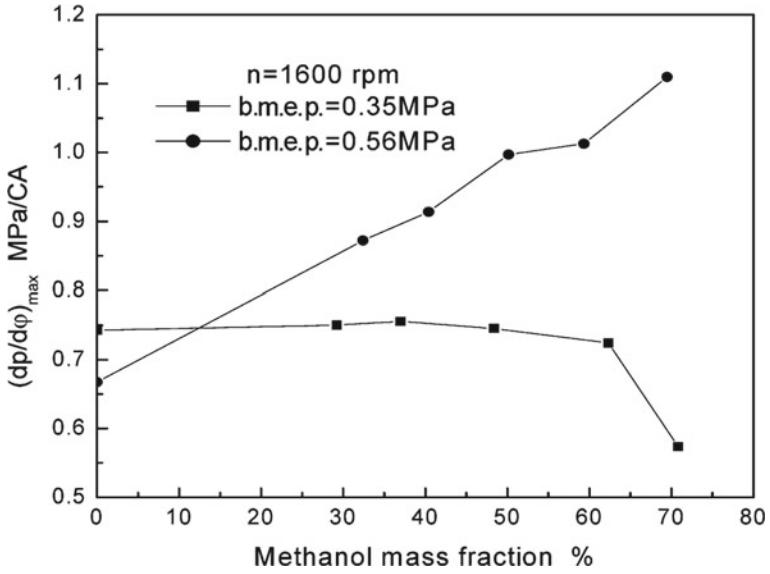

Fig. 11.12 Influence of methanol mass fraction on PPRR (Wang et al. 2008)

combustion noise conditions (i.e., higher premixing ratio and load), the compression pressure in dual-fuel operation is lower in comparison with neat diesel operation, which is because of higher heat of vaporization of methanol. For higher methanol–diesel premixing ratio, the comparatively less amount of diesel is injected into the cylinder (at constant engine speed and load condition). Higher methanol fraction leads to an increase in the ignition delay of pilot diesel, which then auto-ignites and starts burning the premixed methanol fuel at a higher rate of pressure rise (Wang et al. 2015b).

The effect of a single-pulse injection (SPI) and twin-pulse injection (TPI) strategy on PPRR is shown in Fig. 11.13. The figure depicts that at 50% engine load, the PPRR is lower for twin-pulse injection strategy in comparison with single-pulse injection. This is attributed to a shorter ignition delay of main diesel injection because of the burning of pilot diesel injection (Yadav and Ramesh 2018). Additionally, at 50% load, increased premixing of butanol leads to increase PPRR for both the injection strategies. It is attributed to the simultaneous combustion of diesel and methanol because of longer ignition delay (Yadav and Ramesh 2018). In the case of neat diesel operation at 100% engine load, the twin-pulse injection strategy has lower PPRR in comparison with single-pulse injection. When butanol premixing increased, PPRR steeply rises. Except for neat diesel operation, the PPRR is higher for twin-pulse injection strategy, which is because of the pilot diesel in the twin-pulse injection strategy-aided auto-ignition of butanol (Yadav and Ramesh 2018).

Premixing of alcohol fuel in dual-fuel CI-engine resulted in a delayed CA_{10} position. The crank position corresponds to 10% of total heat release which is depicted as CA_{10} position (Saxena and Maurya 2017). The alcohol fuels have a higher heat

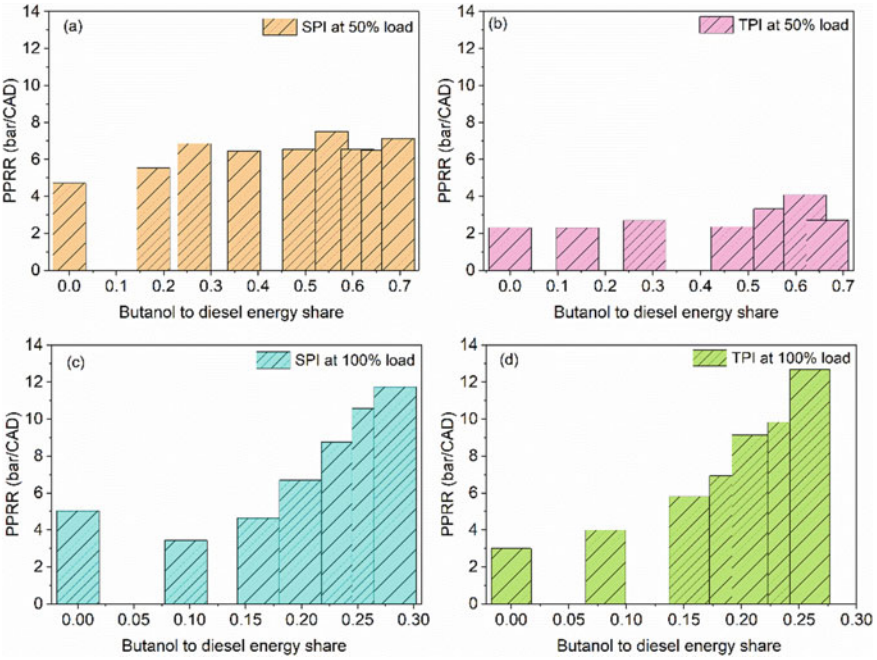

Fig. 11.13 Influence of single- and twin-pulse injection on PPRR/MRPR for butanol–diesel dual-fuel CI-engine. Adapted from Yadav and Ramesh (2018)

of vaporization and auto-ignition temperature. Premixing of alcohol in dual-fuel CI-engine caused to increase in the ignition delay, which results in delayed CA_{10}. Additionally, alcohol fuels having higher heat of vaporization and auto-ignition temperature result in a more retard CA_{10} position. For the delayed CA_{10}, the combustion phasing (CA_{50}) is also retarded with an increase in alcohol premixing. The crank position corresponds to 50% of total heat release is depicted as combustion phasing. The possible reason for retarded CA_{50} with an increase in alcohol premixing is the same as that for CA_{10}.

Additionally, at higher engine load, earlier CA_{10} and CA_{50} position is observed because of higher in-cylinder mean gas temperature due to the burning of a higher amount of fuel in the engine cycle, which leads to an increase in the cylinder wall and residual gas temperature (Saxena and Maurya 2017).

The effect of diesel injection pressure on combustion phasing is illustrated in Fig. 11.14. The study reported that CA_{50} is the crank angle of the combustion center and affects the economy of the combustion process (Swor et al. 2010). The figure depicts that increase in the diesel injection pressure results in advanced combustion phasing. Higher diesel injection leads to better diesel/premixed methanol + air mixing and better fuel atomization, which caused to decrease the ignition delay and resulted in earlier ignition timing and CA_{50}. However, the trend of CA_{50} with engine load is inconsistent with the previous study; i.e., the figure indicates lower engine

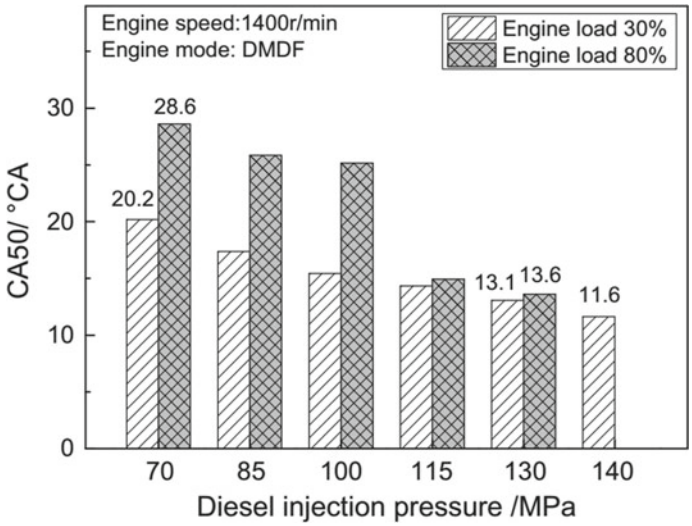

Fig. 11.14 Influence of injection pressure on CA_{50} of methanol–diesel dual-fuel operation (Liu et al. 2015)

load has advanced combustion phasing in comparison with a higher engine load. At higher engine load, more fuel is burnt in the cycle, which coupled with fuel injection pulse-width extended leads to a prolonged combustion duration and a delayed CA_{50} (Liu et al. 2015). A study investigated the influence of diesel injection timing on the CA_{50} of butanol–soyabean biodiesel dual-fuel CI-engine (Liu et al. 2014). They have found that for early injection strategy, the retard injection timing results in advanced combustion phasing, whereas for late-injection strategy, the CA_{50} delayed as the injection timing delayed (Liu et al. 2014).

Combustion duration represents the overall rate of combustion happening in the engine cycle. Combustion duration is typically defined as the difference between the crank angle positions of 90 and 10/5% of the total heat release and is represented as $CA_{90\text{-}10}$. The substitution of methanol fuel in dual-fuel CI-engine leads to an increase in the combustion duration (Masimalai 2014). An increase in the alcohol substitution caused to delayed ignition timing and CA_{10} position. The retarded ignition timing and CA_{10} depict a slower rate of burning, which prolongs with an increase in premixing. Slower burning rate is because of reduced in-cylinder combustion temperature, which further retards the CA_{50}. Thus, more fraction of fuel combusts during the mixing-controlled combustion phase. This caused longer combustion duration with an increase in alcohol premixing.

The effect of diesel injection pressure on combustion duration is shown in Fig. 11.15. The figure indicates that higher diesel injection pressure results in a shorter combustion duration. For higher diesel injection pressure, the diesel injection rate is faster, and the heat release is increased. At constant injection pressure, longer combustion duration obtained for the higher engine load. This is possible

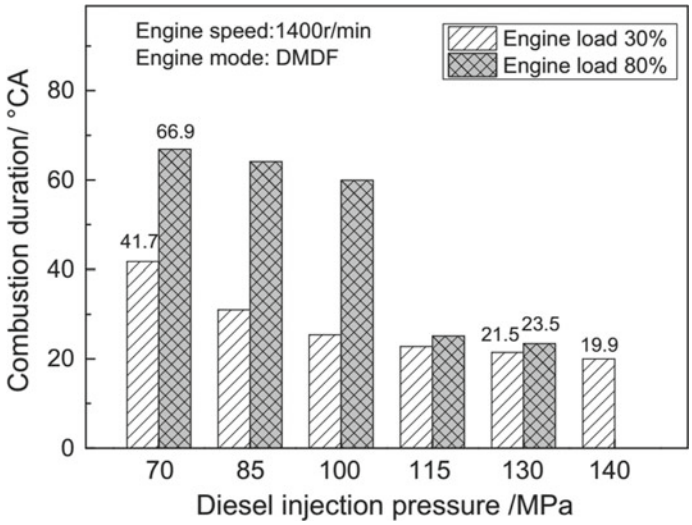

Fig. 11.15 Effect of diesel injection pressure on the combustion duration of methanol–diesel dual-fuel CI-engine (Liu et al. 2015)

because of the increased injection duration and charge preparation (comparatively more amount of fuel is injected at a higher load) (Liu et al. 2015). The combustion duration also depends on the exhaust gas recirculation. With the increase in exhaust gas recirculation rate, the combustion duration increases. Higher exhaust gas recirculation leads to reduce the rate of the combustion reaction and increases the combustion duration (Liu et al. 2014; Lu et al. 2019). The CA_{05} is delayed with an increase in exhaust gas recirculation due to the thermodynamic and chemical function of EGR and a reduction in oxygen concentration (Lu et al. 2019; Maiboom et al. 2008). The availability of longer time for premixing leads to premixed combustion with a higher rate, which increases the mean gas temperature and accelerates the post-combustion of a premixed mixture of diesel and methanol + air, thus resulted into shorter combustion duration (Lu et al. 2019).

The influence of high octane fuel premixing on maximum mean gas temperature (MGT) for dual-fuel CI-engine is illustrated in Fig. 11.16. The figure shows that increasing the fuel premixing results in reduced maximum MGT (at lower and medium engine load). The reduction in maximum MGT is attributed to delayed CA_{50} with an increase in the low-reactivity fuel substitution ratio. At 100% engine load, up to a certain premixing ratio, the maximum MGT increases; further increase in gasoline–diesel premixing ratio leads to a decrease in the maximum MGT. At higher engine load for maintaining the same fuel premixing ratio, more amount of diesel is injected, which leads to advanced ignition timing and combustion phasing and results in higher maximum MGT. Additionally, the figure also depicts that for the same premixing ratio, the butanol–diesel dual-fuel operation has a lower maximum

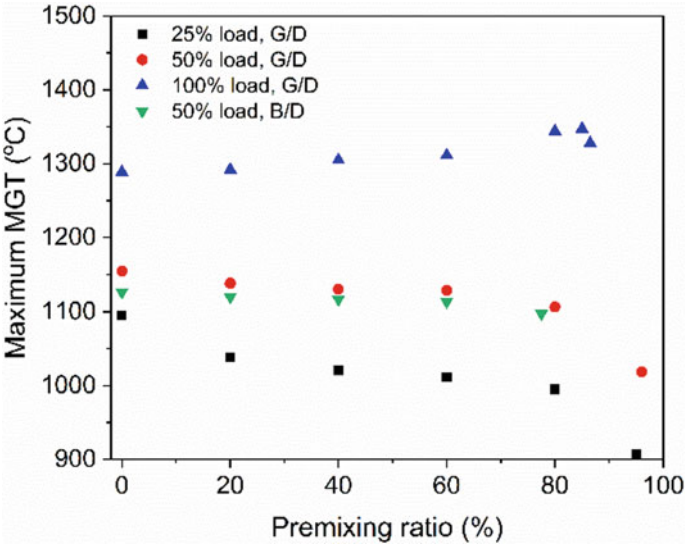

Fig. 11.16 Variation of maximum mean gas temperature of with gasoline–butanol–diesel premixing ratio

MGT. Another study also reported that an increase in the substitution percentage of methanol leads to a decrease in the MGT (Saxena and Maurya 2017).

Emission Characteristics

The regulated and unregulated emission characteristics of dual-fuel CI-engine is presented in this section. The engine operating parameters significantly influence the formation of emissions. Premixing of alcohol in dual-fuel engine leads to decrease the NO_x emission (Britto and Martins 2014; Júnior and Martins 2015). The influence of alcohol substitution ratio, injection timing, and EGR on NO_x, soot, HC, and CO emissions for butanol–soyabean biodiesel dual-fuel CI-engine is shown in Fig. 11.17. Figure 11.17a indicates that an increase in the butanol premixing ratio results in decreased NO_x emission. A similar trend for NO_x emission with the premixing ratio is also observed for methanol–diesel dual-fuel operation (Saxena and Maurya 2017). The formation of NO_x emission strongly depends on the mean gas temperature, and NO_x emission increases with an increase in mean gas temperature. As discussed in the previous section, the premixing of methanol–butanol fuel caused to delayed ignition timing and CA_{50}, thus more amount of mixture combust when the piston moves toward a downward direction (BDC). Combustion of more amount of fuel when the piston moves away from the TDC causes to reduce MGT and results in lower NO_x emissions.

The figure also indicates that, for early injection strategy, the retarded injection timing results in higher NO_x emission. Retarded injection timing caused to increase charge stratification. Burning of a more stratified charge leads to an increase in the combustion temperature and resulting in higher NO_x emission. However, for the

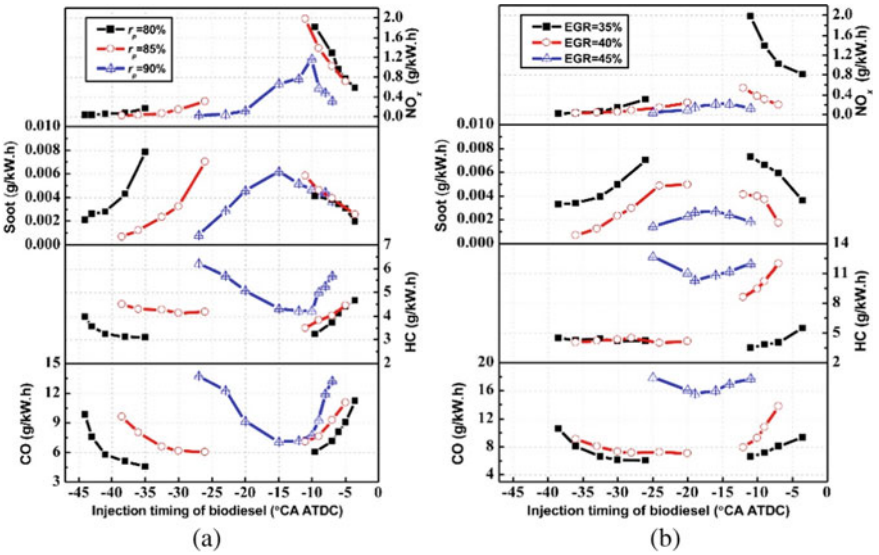

Fig. 11.17 Effect of injection timing, premixing ratio, and exhaust gas recirculation on emission characteristics of butanol–soyabean biodiesel dual-fuel CI-engine (Liu et al. 2014)

case of late-injection strategy, the retarded injection timing results in decreased NO_x emission. It is due to delayed CA_{50} (for these injection timings), which leads to a decrease in the combustion temperature. The possible reason for delayed CA_{50} with retard injection timing for late-injection strategy is discussed in the previous section. It is interesting to note that early injection strategy has significantly lower NO_x emission in comparison with late-injection strategy. This is because of the combustion of more homogeneous charge, form in the early injection strategy, which causes to reduce the local high-temperature zone. The study reported that late-injection strategy has a more high-temperature zone in comparison with early injection strategy, thus results in increased NO_x emission. A study reported that NO_x emission decreases with a decrease in air intake temperature at fixed alcohol–diesel substitution ratio (Pan et al. 2015).

The figure indicates that soot emissions are very low (<0.01 g/kW h) for dual-fuel CI-engine. Premixing of alcohol fuel and diesel (especially in early injection strategy) offers a more homogeneous charge, which caused to reduce the local high-temperature and high equivalence ratio zone. Additionally, the butanol has higher oxygen content, which enhances the soot oxidation. However, for both the injection strategy (early and late injection), the soot emissions are comparable, even though the late-injection strategy leads to charge stratification. The simulation results indicate that the early injection strategy has a lower soot formation because the local equivalence ratio is more homogeneously distributed in the chamber (Liu et al. 2014). Higher soot is formed for late-injection strategy because of a more stratified charge (locally rich charge region). Combustion of a more stratified mixture leads to a rise

in the MGT, which enhances the rate of oxidation of soot and results in lower soot emission. Higher diesel injection pressure results in decreased smoke emission (Liu et al. 2015). An increase in methanol–ethanol–butanol premixing results in higher HC and CO emissions (Liu et al. 2014; Saxena and Maurya 2017; Júnior and Martins 2015). At higher premixing of alcohol fuel, more fraction of low-reactivity fuel may be trapped in crevices, which is difficult to oxidize and results in higher CO and HC emissions. Higher diesel injection pressure causes to reduce the CO and HC emissions in dual-fuel combustion mode (Liu et al. 2015; Júnior and Martins 2015). The figure depicts that with delayed injection timing, the CO and HC emission initially decrease than start increases. With early or late injection timings, the combustion phasing is retarded, and the degree of constant volume combustion is also lower. This caused to decrease in the in-cylinder combustion temperature and results in higher CO and HC emissions because of the lower rate of oxidation. The simulation results indicate that the main CO emissions formed the near-wall region, where the temperature is lower (Liu et al. 2014). Additionally, the late-injection strategy has higher CO emissions in comparison with the early injection strategy (Liu et al. 2014). In the case of late-injection strategy, the biodiesel distribution is concentrated near the center of the combustion chamber. Because of this, the radicals formed from the burning of biodiesel cannot react with butanol completely. Thus, butanol fraction near the wall cannot oxidize and results in higher CO emissions. The study reported that early injection strategy has more benefits in comparison with late-injection strategy because of reduced NO_x emissions and comparably similar or lower CO, HC, and soot emissions (Liu et al. 2014).

Figure 11.17b depicts the influence of exhaust gas recirculation on NO_x, CO, HC, and soot emissions. In the case of late-injection strategy, the NO_x emission decreases with an increase in the fraction of exhaust gas recirculation. The figure indicates a reduction in soot emission with an increase in the fraction of exhaust gas recirculation. It is possibly because of longer ignition delay with an increase in exhaust gas recirculation percentage, which caused to enhance the charge mixing and reduces the local fuel-rich core (Liu et al. 2014). An increase in exhaust gas recirculation fraction leads to an increase in the CO and HC emission (Fig. 11.17b), which is because of the reduced in-cylinder combustion temperature. Higher CO and HC emissions also resulted in decreased combustion efficiency in the case of a higher fraction of exhaust gas recirculation. An increase in air intake temperature results in decreased HC and CO emissions (Pan et al. 2015). Higher air intake temperature caused to increase the in-cylinder gas temperature, which enhances the oxidation of HC and CO emission and also prevents the effect of quenching (Pan et al. 2015).

Along with gaseous emissions, soot particles are also emitted from the CI-engine in significant concentration, which has an adverse effect on the health of human beings (Harrod et al. 2005; McDonald et al. 2007; Peters et al. 2006; Kreyling et al. 2006). Based on the electrical mobility diameter, particles can be categorized in nucleation and accumulation mode particles. Particles having a diameter of less than 50 nm are known as nucleation mode particles (NMP), whereas above 50 nm diameters particles are called accumulation mode particles (AMP) (Kittelson 1998). The effect of the premixing of high octane fuels (gasoline and methanol) on the particle

size and number distribution (PSD) is demonstrated in Fig. 11.18. The distribution follows the bimodal lognormal trend in which the first and second peak specifies the NMP and AMP, respectively. The concentration of particles of any size is proportional to the area under the curve within that range. The figure indicates that for neat diesel operation at lower engine load, the peak of NMP is higher, whereas an increase in engine load results in the increased peak of AMP. The higher combustion temperature at higher engine load caused to enhance the agglomeration rate and reduced the nucleation mode particle formation. Moreover, more percentage of mixture burns in mixing-controlled combustion phase, which caused to enhance the formation of AMP.

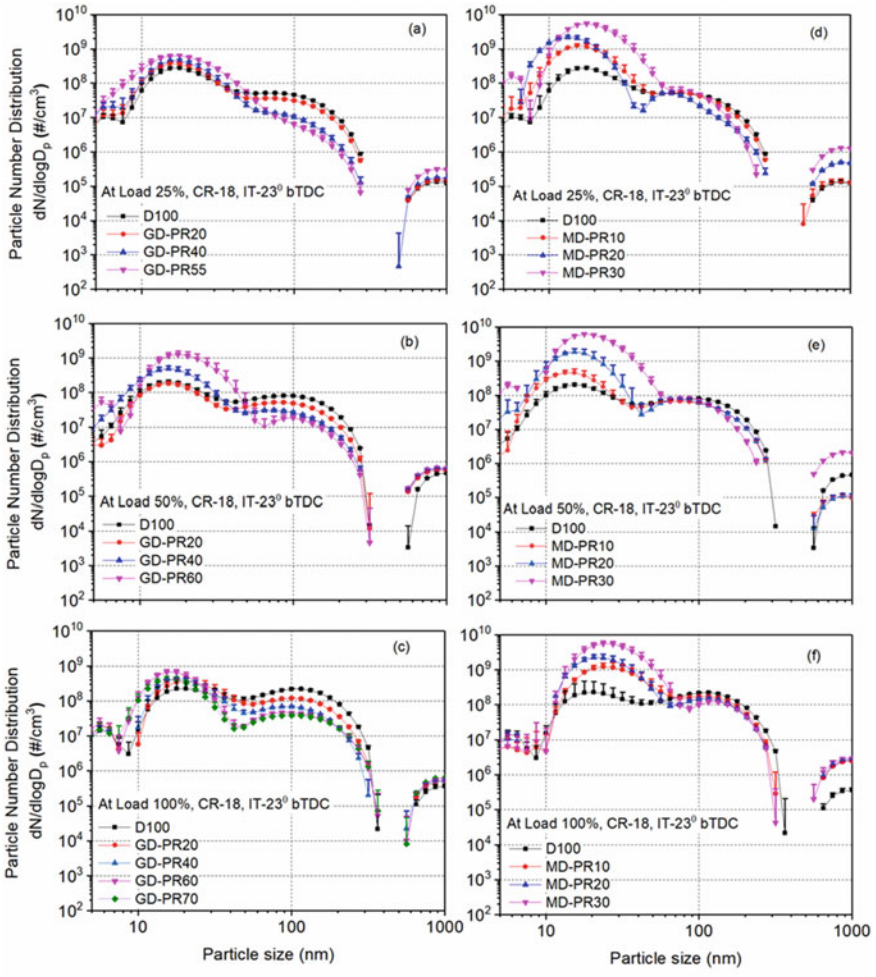

Fig. 11.18 PSD for gasoline–diesel and methanol–diesel dual-fuel CI-engine (Saxena and Maurya 2017)

At lower load, due to the longer ignition delay, more fraction of charge burns in the premixed combustion, which causes the formation of a higher concentration of NMP. The figure indicates that in the case of dual-fuel combustion mode, an increase in the fraction of methanol and butanol causes to increase in the peak of NMP and decreases the peak of AMP (Saxena and Maurya 2020, 2017). The premixing of low-reactivity fuel caused to increase in ignition delay; thus, more amount of mixture combusts in the premixed phase of combustion and results in the formation of a higher concentration of NMP. In addition to this, the figure also indicates that for the same fuel substitution ratio, the peak of NMP is higher for methanol–diesel dual-fuel operation. Higher latent heat of vaporization and lower reactivity of methanol than gasoline leads to longer ignition delay in methanol–diesel dual-fuel operation; thus, comparatively more amount of mixture combusts in the premixed phase of combustion, which results in the formation of more number of NMP.

Increase in the substitution percentage of methanol and butanol caused to increase in total particle concentration, which is due to a higher concentration of NMP (Saxena et al. 2018; Saxena and Maurya 2017). A higher concentration of NMP is attributed to nucleation, condensation, and coagulation of unburnt hydrocarbons. Unburnt HC leads to generate particles and increases the total particle concentration. Total particle number concentration and NMP are higher for methanol–butanol–diesel dual-fuel operation than gasoline-diesel dual-fuel operation (Saxena et al. 2018; Saxena and Maurya 2017).

Along with the regulated emissions (NO_x, CO, HC, soot, and particle numbers), several unregulated emission species (formaldehyde (HCHO), unburned methanol (CH_3OH), formic acid (HCOOH), benzene (C_6H_6) 1,3-butadiene (1,3-C_4H_6), and toluene (C_7H_8)) are also emitted in significant concentration. A study reported that an increase in air intake temperature leads to decrease the methanol emissions (Pan et al. 2015). This is because of improved combustion and higher exhaust gas temperature (Pan et al. 2015). The influence of pilot injection quantity and timing on CH_3OH is presented in Fig. 11.19a, b. It has been observed that the CH_3OH emission is close to zero level for neat diesel operation and increases with an increase in the methanol fumigation. The figure depicts that CH_3OH emission initially increases with an increase in methanol substitution ratio (when increased from M0 to M30) and then decreases with a further rise in methanol substitution ratio (when increased from M30 to M50). This is attributed to at lower methanol substitution ratio, the ignition delay remains almost same for M10 and M30; however, increase in methanol substitution leads to increase the fraction of methanol in the cylinder and decrease the charge temperature at the end of the compression stroke (due to charge cooling effect). This caused the combustion of more fraction of methanol when the piston moves away from the top dead center, where the temperature is comparatively lower. It is difficult to oxidize the methanol fraction completely at lower temperatures and results in higher CH_3OH emission (Wei et al. 2017). Additionally, the equivalence ratio varies with change in methanol substitution ratio and pilot injection (Wei et al. 2017). Injection of methanol displaces some fraction of air during the intake stroke, which caused to increase in the total equivalence ratio with an increase in the substitution percentage of methanol. Moreover, an increase in the percentage of methanol

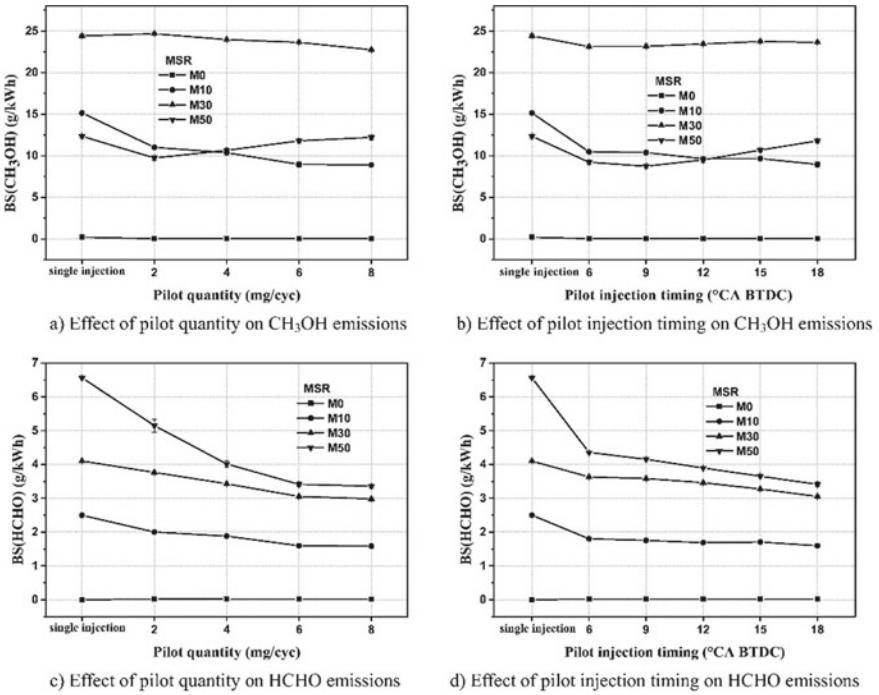

Fig. 11.19 Influence of pilot injection on CH_3OH and HCHO emissions from fumigated methanol–diesel dual-fuel CI-engine (Wei et al. 2017)

substitution leads to an increase in the methanol equivalence ratio and decreases the in-cylinder combustion temperature, which results in higher CH_3OH emissions. Figure 11.19a depicts that with an increase in pilot quantity, the CH_3OH decreases for M10 and M30, whereas increases for M50.

Figure 11.19b depicts that advanced pilot injection leads to reduce CH_3OH emission for M10 operation, whereas it slightly increased to M30 and M50 operation. Advanced pilot injection timing and an increase in pilot injection quantity cause an increase in the charge temperature prior to the main combustion, which enhances the rate of vaporization and early oxidation of methanol. However, shorten delay period of main-injected combustion leads to worse mixing of diesel and the premixed mixture of methanol + air and results in higher CH_3OH emission.

There are various sources of formaldehyde emissions such as some amount of premixed mixture of methanol + air may be escaped during exhaust, quenching of flame near the cylinder wall and piston head (Pan et al. 2015). A study reported that formaldehyde emission decreases with an increase in the air intake temperature (Pan et al. 2015). At higher air intake temperature, the chances of flame quenching are reduced because of the in-cylinder gas temperature (Pan et al. 2015). Higher in-cylinder and exhaust gas temperatures also enhance the oxidation of formaldehyde (Pan et al. 2015). The effect of pilot injection quantity and pilot injection timing on

HCHO emission is shown in Fig. 11.19c, d. The figure indicates that the HCHO emission is very less for neat diesel operation. With an increase in methanol substitution, the HCHO emission increased, possibly due to the reduced in-cylinder charge temperature and increased methanol equivalence ratio, which results in more incomplete combustion of methanol (Wei et al. 2017). The figure indicated that an increase in the pilot injection quantity leads to a decrease in the HCHO emissions, which is possible because of longer high-temperature duration, which enhances the rate of oxidation of HCHO. Additionally, the figure shows that advanced pilot injection results in reduced HCHO emissions. Higher formaldehyde emission for the ethanol–diesel dual-fuel engine is also reported in a study (Júnior and Martins 2015). An increase in diesel injection pressure results in reduced formaldehyde emissions (Júnior and Martins 2015).

Figure 11.20 shows the effect of pilot injection quantity and pilot injection timing on HCOOH and 1,3-C_4H_6 emissions. The influence of pilot injection on HCOOH is shown in Fig. 11.20a, b. HCOOH emission is higher in dual-fuel combustion mode than neat diesel operation, and HCOOH emission increases with an increase in methanol substitution ratio. The HCOOH emission for M10 operation is significantly lower and not very much sensitive to variation in pilot injection. At higher methanol

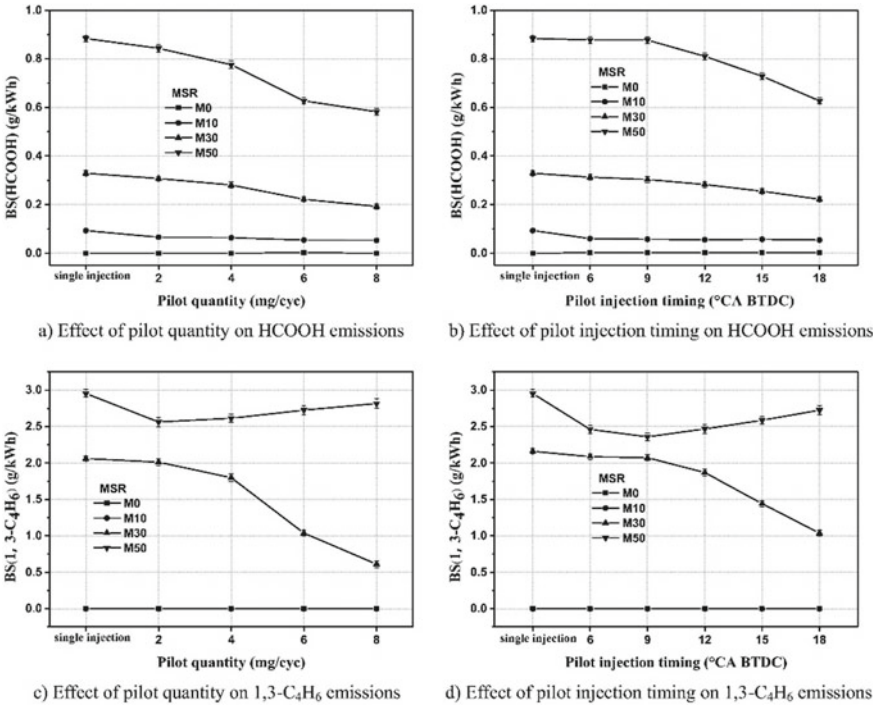

Fig. 11.20 Effect of pilot injection quantity and pilot injection timing on HCOOH and 1,3-C_4H_6 emission from fumigated methanol–diesel dual-fuel CI-engine (Wei et al. 2017)

substitution ratio, advanced pilot injection and an increase in pilot injected mass result in the reduction of HCOOH. This is attributed to the rise in in-cylinder temperature prior to combustion, which enhances the initial rate of oxidation of HCOOH (Wei et al. 2017).

1,3-C_4H_6 is a toxic compound that is classified by EPA (Takada et al. 2003). 1–3 butadiene is a carcinogen and typically emitted from SI, as well as CI-engines (Zhou et al. 2014). The figure indicates that 1,3-C_4H_6 emission is significantly higher in dual-fuel combustion than neat diesel operation. In the case of neat diesel and M10 operation, the 1,3-C_4H_6 emission is very lower. The 1,3-C_4H_6 emission increases with an increase in the methanol substitution ratio. Higher 1,3-C_4H_6 emission with increase methanol fraction also reported in another study (Cheung et al. 2009). 1,3-C_4H_6 emission mainly formed during oxygen-rich combustion and emitted in significantly higher concentration when exhaust gas temperature is higher (Takada et al. 2003). The higher concentration of 1,3-C_4H_6 emission is attributed to the higher oxygen content of methanol even though the dual-fuel temperature has reduced exhaust gas temperature. The figure indicates that in the case of M30 operation, increase in pilot injection quantity and advanced pilot injection lead to decrease the 1,3-C_4H_6 emission, whereas in the case of M50 operation, the 1,3-C_4H_6 emission initially decreases with increase in pilot injection quantity and advanced pilot injection and then increases. For a higher amount of pilot injection and advanced injection timing, the charge temperature prior to combustion is higher, which enhances the oxidation of 1,3-C_4H_6 emission (Wei et al. 2017). When methanol substitution is increased from 30 to 50%, the atomization of fuel becomes poorer. Prior to the main combustion, increased in-cylinder temperature initially enhances the partial oxidation of diesel. An increase in methanol substitution ratio leads to a comparatively lower temperature on which it is difficult to oxidize 1,3-butadiene and results in higher emission (Wei et al. 2017).

Benzene and toluene are classified as mutagenic and carcinogenic. Benzene and toluene are mainly formed from unburned molecules from fuel, structural modifications, and prosynthesis (Wei et al. 2017; Zhao et al. 2011; Correa and Arbilla 2006). Benzene and toluene emissions increase with an increase in methanol substitution ratio (Wei et al. 2017). In dual-fuel operation, an increase in methanol substitution ratio leads to an increase in the oxygen concentration in the charge and reduces the unsaturated hydrocarbons. On the contrary, an increase in the percentage of methanol leads to a decrease in the in-cylinder temperature and exhaust temperature as well, which causes a reduction of oxidation of benzene and toluene and results in increased emissions. Both these reasons are counteracted with each other, caused to higher or reduced emissions with an increase in methanol substitution ratio (Wei et al. 2017).

Summary

This chapter presents the performance, combustion, and emissions characteristics of low and medium carbon alcohol–diesel fueled dual-fuel CI-engine. Methanol, ethanol, and butanol are renewable and clean alternative fuels, which can be produced from various renewable resources. The main findings of the chapter are given below.

- The thermal efficiency of alcohol–diesel dual-fuel CI-engine is relatively lower in comparison with neat diesel operation at the same operating condition. However, efficiency can be improved by using higher air intake temperature with optimal high-reactivity fuel (diesel) injection timing, which further needs to be investigated.
- The lower and medium operating boundary of dual-fuel operation is restricted by the partial burn and misfire, respectively, which limits the alcohol premixing. The excessive alcohol premixing at medium to higher engine load is restricted by higher pressure rise rate.
- The cyclic variations in the combustion cycle also limit the range of fuel premixing. The detailed analysis of combustion variations in dual-fuel CI-engine needs to be investigated in the future.
- Dual-fuel operation has longer ignition delay, which increases with an increase in the substitution percentage of alcohol fuel. The ignition delay period is mainly influenced by in-cylinder temperature, pressure, and oxygen concentration at the time of diesel injection.
- The dual-fuel operation has a relatively lower and slightly retarded peak of HRR in comparison with neat diesel operation. Three-stage HRR is observed for higher air intake temperature operation in dual-fuel operation. Higher diesel injection pressure leads to the increased and advanced peak of combustion pressure and HRR.
- With an increase in the engine load, the PPRR increases, whereas it reduces with an increase in the alcohol premixing. PPRR restricts the range of injection timing. For early injection strategy, the delayed injection timing leads to an increase in the PPRR, which limits the upper limit of PPRR. However, for the late-injection strategy, the delayed injection timing leads to a decrease in the PPRR.
- An increase in the substitution ratio of alcohol in dual-fuel operation leads to a decrease in NO_x and soot emissions, whereas HC and CO emissions significantly increased. For the late-injection strategy, the NO_x emission decreases with an increase in the fraction of exhaust gas recirculation. Soot emission reduced with an increase in the fraction of exhaust gas recirculation. NO_x emission decreases with a decrease of air intake temperature at fixed alcohol–diesel substitution ratio, whereas HC and CO emission decreases with an increase in air intake temperature.
- An increase in the fraction of methanol–butanol causes to increase in the peak of NMP and decreases the peak of AMP in particle size distribution. Increase in the substitution percentage of methanol and butanol caused to increase in total particle concentration, which is due to a higher concentration of NMP.
- The detailed analysis of solid particle numbers from dual-fuel CI-engine needs to be investigated in the future.

References

Austin W, Heutel G, Kreisman D (2019) School bus emissions, student health and academic performance. Econ Educ Rev 70:109–126

Bergmann JC, Trichez D, Sallet LP, e Silva FCDP, Almeida JR (2018) Technological advancements in 1G ethanol production and recovery of by-products based on the biorefinery concept. In: Advances in sugarcane biorefinery. Elsevier, pp 73–95

BP Statistical Review of World Energy (2019). Energy outlook

Britto RF Jr, Martins CA (2014) Experimental analysis of a diesel engine operating in diesel-ethanol dual-fuel mode. Fuel 134:140–150

Chen H, Zhang P, Liu Y (2018) Investigation on combustion and emission performance of a common rail diesel engine fueled with diesel-ethylene glycol dual fuel. Appl Therm Eng 142:43–55

Cheung CS, Zhu L, Huang Z (2009) Regulated and unregulated emissions from a diesel engine fueled with biodiesel and biodiesel blended with methanol. Atmos Environ 43(32):4865–4872

Chmielniak T, Sciazko M (2003) Co-gasification of biomass and coal for methanol synthesis. Appl Energy 74(3–4):393–403

Correa SM, Arbilla G (2006) Aromatic hydrocarbons emissions in diesel and biodiesel exhaust. Atmos Environ 40(35):6821–6826

Datta A, Mandal BK (2016) A comprehensive review of biodiesel as an alternative fuel for compression ignition engine. Renew Sustain Energy Rev 57:799–821

Di Blasio G, Beatrice C, Molina S (2013) Effect of port injected ethanol on combustion characteristics in a dual-fuel light duty diesel engine. SAE technical paper 2013-01-1692. https://doi.org/10.4271/2013-01-1692

Di Blasio G, Viscardi M, Alfè M, Gargiulo V et al (2014) Analysis of the impact of the dual-fuel ethanol-diesel system on the size, morphology, and chemical characteristics of the soot particles emitted from a LD diesel engine. SAE technical paper 2014-01-1613. https://doi.org/10.4271/2014-01-1613

Di Blasio G, Belgiorno G, Beatrice C (2017) Effects on performances, emissions and particle size distributions of a dual fuel (methane-diesel) light-duty engine varying the compression ratio. Appl Energy 204:726–740

Di Iorio S, Magno A, Mancaruso E, Vaglieco BM (2017) Analysis of the effects of diesel/methane dual fuel combustion on nitrogen oxides and particle formation through optical investigation in a real engine. Fuel Process Technol 159:200–210

Directive 2009/28/EC of the European Parliament and of the Council on the promotion of the use of energy from renewable sources (2009)

Fraioli V, Mancaruso E, Migliaccio M, Vaglieco BM (2014) Ethanol effect as premixed fuel in dual-fuel CI engines: experimental and numerical investigations. Appl Energy 119:394–404

Gong C, Li Z, Yi L, Liu F (2019) Comparative study on combustion and emissions between methanol port-injection engine and methanol direct-injection engine with H_2-enriched port-injection under lean-burn conditions. Energy Convers Manage 200:112096

Gong C, Li Z, Huang K, Liu F (2020) Research on the performance of a hydrogen/methanol dual-injection assisted spark-ignition engine using late-injection strategy for methanol. Fuel 260:116403

Hariharan N, Senthil V, Krishnamoorthi M, Karthic SV (2020) Application of artificial neural network and response surface methodology for predicting and optimizing dual-fuel CI engine characteristics using hydrogen and bio fuel with water injection. Fuel 270:117576

Harrod KS, Jaramillo RJ, Berger JA, Gigliotti AP, Seilkop SK, Reed MD (2005) Inhaled diesel engine emissions reduce bacterial clearance and exacerbate lung disease to Pseudomonas aeruginosa infection in vivo. Toxicol Sci 83(1):155–165

Hoogewind A (2014) Production of 2-propanol, butanol and ethanol using Clostridium beijerinckii optonii. A Thesis

Jamuwa DK, Sharma D, Soni SL (2016) Experimental investigation of performance, exhaust emission and combustion parameters of stationary compression ignition engine using ethanol fumigation in dual fuel mode. Energy Convers Manage 115:221–231

Jin C, Yao M, Liu H, Chia-fon FL, Ji J (2011) Progress in the production and application of *n*-butanol as a biofuel. Renew Sustain Energy Rev 15(8):4080–4106

Júnior RFB, Martins CA (2015) Emission analysis of a diesel engine operating in diesel–ethanol dual-fuel mode. Fuel 148:191–201

Kittelson DB (1998) Engines and nanoparticles: a review. J Aerosol Sci 29(5–6):575–588

Krahl J, Munack A, Schröder O, Stein H, Bünger J (2003) Influence of biodiesel and different designed diesel fuels on the exhaust gas emissions and health effects. SAE Trans, 2447–2455

Kreyling WG, Semmler-Behnke M, Möller W (2006) Health implications of nanoparticles. J Nanopart Res 8(5):543–562

Lambe SM, Watson HC (1992) Low polluting, energy efficient CI hydrogen engine. Int J Hydrogen Energy 17(7):513–525

Lata DB, Misra A (2011) Analysis of ignition delay period of a dual fuel diesel engine with hydrogen and LPG as secondary fuels. Int J Hydrogen Energy 36(5):3746–3756

Lata DB, Misra A, Medhekar S (2011) Investigations on the combustion parameters of a dual fuel diesel engine with hydrogen and LPG as secondary fuels. Int J Hydrogen Energy 36(21):13808–13819

Liu H, Wang X, Zheng Z, Gu J, Wang H, Yao M (2014) Experimental and simulation investigation of the combustion characteristics and emissions using *n*-butanol/biodiesel dual-fuel injection on a diesel engine. Energy 74:741–752

Liu J, Yao A, Yao C (2015) Effects of diesel injection pressure on the performance and emissions of a HD common-rail diesel engine fueled with diesel/methanol dual fuel. Fuel 140:192–200

Lu H, Yao A, Yao C, Chen C, Wang B (2019) An investigation on the characteristics of and influence factors for NO_2 formation in diesel/methanol dual fuel engine. Fuel 235:617–626

Maiboom A, Tauzia X, Hétet JF (2008) Experimental study of various effects of exhaust gas recirculation (EGR) on combustion and emissions of an automotive direct injection diesel engine. Energy 33(1):22–34

Mancaruso E, Vaglieco BM (2011) UV-visible spectroscopic measurements of dual-fuel PCCI engine. SAE Int J Fuels Lubr 4(2):271–281

Masimalai SK (2014) Influence of methanol induction on performance, emission and combustion behavior of a methanol-diesel dual fuel engine (No. 2014-01-1315). SAE technical paper

Maurya RK (2018) Characteristics and control of low temperature combustion engines: employing gasoline, ethanol and methanol. Springer, Cham. ISBN 978-3-319-68508-3

McClellan RO (1987) Health effects of exposure to diesel exhaust particles. Annu Rev Pharmacol Toxicol 27(1):279–300

McDonald JD, Reed MD, Campen MJ, Barrett EG, Seagrave J, Mauderly JL (2007) Health effects of inhaled gasoline engine emissions. Inhalation Toxicol 19(Supp 1):107–116

Meng X, Nithyanandan K, Lee T, Li Y, Long W, Lee CF (2016) An experimental study of the combustion, performance and emission characteristics of a CI engine under diesel-1-butanol/CNG dual fuel operation mode (No. 2016-01-0788). SAE technical paper

Niculescu R, Clenci A, Iorga-Siman V (2019) Review on the use of diesel–biodiesel–alcohol blends in compression ignition engines. Energies 12(7):1194

Ning L, Duan Q, Chen Z, Kou H, Liu B, Yang B, Zeng K (2020) A comparative study on the combustion and emissions of a non-road common rail diesel engine fueled with primary alcohol fuels (methanol, ethanol, and *n*-butanol)/diesel dual fuel. Fuel 266:117034

Nour M, Attia AM, Nada SA (2019) Combustion, performance and emission analysis of diesel engine fueled by higher alcohols (butanol, octanol and heptanol)/diesel blends. Energy Convers Manage 185:313–329

OECD/International Transport Forum (2013) ITF transport outlook 2013: funding transport. OECD Publishing/ITF. https://doi.org/10.1787/9789282103937-en

Pan W, Yao C, Han G, Wei H, Wang Q (2015) The impact of intake air temperature on performance and exhaust emissions of a diesel methanol dual fuel engine. Fuel 162:101–110
Panithasan MS, Gopalakichenin D, Venkadesan G, Veeraraagavan S (2019) Impact of rice husk nanoparticle on the performance and emission aspects of a diesel engine running on blends of pine oil-diesel. Environ Sci Pollut Res 26(1):282–291
Park SH, Lee CS (2014) Applicability of dimethyl ether (DME) in a compression ignition engine as an alternative fuel. Energy Convers Manage 86:848–863
Peters A, Veronesi B, Calderón-Garcidueñas L, Gehr P, Chen LC, Geiser M, Reed W, Rothen-Rutishauser B, Schürch S, Schulz H (2006) Translocation and potential neurological effects of fine and ultrafine particles a critical update. Part Fibre Toxicol 3(1):13
Prakash G, Ramesh A, Shaik AB (1999) An approach for estimation of ignition delay in a dual fuel engine. SAE transactions, pp 399–405
Ris C (2007) US EPA health assessment for diesel engine exhaust: a review. Inhalation Toxicol 19(Supp 1):229–239
Saxena MR, Maurya RK (2017) Effect of premixing ratio, injection timing and compression ratio on nano particle emissions from dual fuel non-road compression ignition engine fueled with gasoline/methanol (port injection) and diesel (direct injection). Fuel 203:894–914
Saxena MR, Maurya RK (2018) Performance, combustion, and emissions characteristics of conventional diesel engine using butanol blends. In: Advances in internal combustion engine research. Springer, Singapore, pp 93–110
Saxena MR, Maurya RK (2020) Determination of range of fuel premixing ratio in gasoline/butanol-diesel dual-fuel engine for lower exhaust emissions and higher efficiency (No. 2020–01–1128). SAE technical paper
Saxena MR, Maurya RK, Alex G (2018) Comparative study on characteristics of compression ignition engine in dual fuel mode employing gasoline/butanol and diesel. In: Paper NO-SEEC-2018-141, international conference on sustainable energy and environmental challenges (SEEC-2018). Indian Institute of Science (IISc), India, 01 Jan–03 Jan 2018
Sayin C, Uslu K (2008) Influence of advanced injection timing on the performance and emissions of CI engine fueled with ethanol-blended diesel fuel. Int J Energy Res 32(11):1006–1015
Sharma VC, Ogbeide ON (1982) Pawpaw as a renewable energy resource for the production of alcohol fuels. Energy 7(10):871–873
Song R, Liu J, Wang L, Liu S (2008) Performance and emissions of a diesel engine fuelled with methanol. Energy Fuels 22(6):3883–3888
Swor TA, Kokjohn S, Andrie M, Reitz RD (2010) Improving diesel engine performance using low and high pressure split injections for single heat release and two-stage combustion (No. 2010-01-0340). SAE technical paper
Szulczyk KR (2010) Which is a better transportation fuel–butanol or ethanol? Int J Energy Environ 1(3):501–512
Takada K, Yoshimura F, Ohga Y, Kusaka J, Daisho Y (2003) Experimental study on unregulated emission characteristics of turbocharged DI diesel engine with common rail fuel injection system (No. 2003-01-3158). SAE technical paper
Thring RH (1983) Alternative fuels for spark-ignition engines. SAE Trans 715–725
Tillman DA (1978) Wood as an energy resource. Academic Press, New York
Tsao G, Ladisch M, Ladisch C, Hsu D, Dale B, Chou T (1978) Ant & reports in fermentation processes, part 1, vol 2. Academic Press, New York
Tutak W, Lukacs K, Szwaja S, Bereczky A (2015) Alcohol–diesel fuel combustion in the compression ignition engine. Fuel 154:196–206
Üçtuğ FG, Ağralı S, Arıkan Y, Avcıoğlu E (2014) Deciding between carbon trading and carbon capture and sequestration: an optimisation-based case study for methanol synthesis from syngas. J Environ Manage 132:1–8
Verhelst S, Maesschalck P, Rombaut N, Sierens R (2009) Increasing the power output of hydrogen internal combustion engines by means of supercharging and exhaust gas recirculation. Int J Hydrogen Energy 34(10):4406–4412

Volpato Filho O (2008) Gasoline C made with hydrous ethanol. In: XVI SIMEA 2008—Simpósio Internacional de Engenharia Automotiva. Sao Paolo. Retrieved 10 July 2017

Wang LJ, Song RZ, Zou HB, Liu SH, Zhou LB (2008) Study on combustion characteristics of a methanol—diesel dual-fuel compression ignition engine. Proc Inst Mech Eng Part D J Autom Eng 222(4):619–627

Wang Q, Yao C, Dou Z, Wang B, Wu T (2015a) Effect of intake pre-heating and injection timing on combustion and emission characteristics of a methanol fumigated diesel engine at part load. Fuel 159:796–802

Wang Q, Wei L, Pan W, Yao C (2015b) Investigation of operating range in a methanol fumigated diesel engine. Fuel 140:164–170

Wei H, Yao C, Pan W, Han G, Dou Z, Wu T, Liu M, Wang B, Gao J, Chen C, Shi J (2017) Experimental investigations of the effects of pilot injection on combustion and gaseous emission characteristics of diesel/methanol dual fuel engine. Fuel 188:427–441

Weitekamp CA, Kerr LB, Dishaw L, Nichols J, Lein M, Stewart MJ (2020) A systematic review of the health effects associated with the inhalation of particle-filtered and whole diesel exhaust. Inhalation Toxicol 32(1):1–13

WHO, a United Agency Report (2012) https://www.who.int/mediacentre/news/releases/2014/air-pollution/en/

Yadav J, Ramesh A (2018) Comparison of single and multiple injection strategies in a butanol diesel dual fuel engine. J Energy Resour Technol 140(7)

Yao C, Pan W, Yao A (2017) Methanol fumigation in compression-ignition engines: a critical review of recent academic and technological developments. Fuel 209:713–732

Yousefi A, Birouk M, Lawler B, Gharehghani A (2015) Performance and emissions of a dual-fuel pilot diesel ignition engine operating on various premixed fuels. Energy Convers Manage 106:322–336

Zhao H, Ge Y, Tan J, Yin H, Guo J, Zhao W, Dai P (2011) Effects of different mixing ratios on emissions from passenger cars fueled with methanol/gasoline blends. J Environ Sci 23(11):1831–1838

Zhou JH, Cheung CS, Leung CW (2014) Combustion, performance, regulated and unregulated emissions of a diesel engine with hydrogen addition. Appl Energy 126:1–12

Chapter 12
Impact of Ethanol on Combustion, Performance, and Emission Characteristics of Diesel Engine

Tomesh Kumar Sahu, Ravindra Kshatri, and Pravesh Chandra Shukla

Abbreviations

aTDC	After top dead center
bTDC	Before top dead center
BTE	Brake thermal condition
BSFC	Brake-specific fuel consumption
CAD	Crank angle degree
CD	Combustion duration (°CA)
CI	Compression ignition engine
CO	Carbon monoxide
EOC	End of combustion (°CA)
EGT	Exhaust gas temperature (°C)
CRDI	Common rail direct fuel injection
GHG	Greenhouse gas
HC	Hydrocarbons
HRR	Heat Release Rate
ID	Ignition Delay (°CA)
IMEP	Indicated mean effective pressure
JME	Jatropha methyl ester
NO_x	Nitrogen oxides
PM	Particulate matter
SOC	Start of combustion (°CA)
SOI	Start of ignition (°CA)

T. K. Sahu · R. Kshatri · P. C. Shukla (✉)
Department of Mechanical Engineering, Indian Institute of Technology Bhilai, Raipur, India
e-mail: pravesh@iitbhilai.ac.in

P. C. Shukla et al. (eds.), *Alcohol as an Alternative Fuel for Internal Combustion Engines*, Energy, Environment, and Sustainability,
https://doi.org/10.1007/978-981-16-0931-2_13

12.1 Introduction

Increasing population of the world significantly increases the demand for energy and transport vehicles. Nowadays, most of the transport vehicles and several industries are using internal combustion (IC) engines as their prime power generating units. Diesel engines are one of the most preferred IC engine for its excellent durability and fuel efficiency. It has a wide range of application in different sectors such as agriculture, transport, power generation, etc. Diesel engines emit lower carbon monoxide (CO), hydrocarbons (HC), and carbon dioxide (CO_2) compared to gasoline engines because of lean air–fuel mixtures formation and higher fuel efficiency; however, the oxides of nitrogen (NO_x) and particulate matter (PM) emissions of diesel engines are comparatively high (Gürü et al. 2010). Since, the number of vehicles are increasing continuously, benefaction of transport vehicles to the overall greenhouse gas emissions has been increased (Anyon et al. 2003). Air pollution causes significant problems of health, in particular lungs and hearts, which increases the indirect cost for curement. Search for better alternative fuels to resolve the problem related to exhaust emission and scarcity of fuel are one of the focused area of research (Kessel 2000; Gilbert and Perl 2005; Goldemberg et al. 2001). Mixing of ethanol to prepare ethanol–diesel blend is one of the feasible ways to use ethanol for CI engines in the form of alternative fuels; however, it is limited in proportion due to its issues of miscibility and auto-ignition characteristic. Several experimental study of ethanol–diesel blends have been performed in CI engines. It was observed that the mixing of ethanol in diesel normally increases ignition delay (ID), brake-specific fuel consumption (BSFC), and NO_x emissions, whereas it decreases combustion duration (CD), brake thermal efficiency (BTE), CO, and smoke emissions for a limited proportion of ethanol in diesel. Emiroğlu et al. (2018) have recorded ignition delay was higher for alcohols than mineral diesel for the combustion and performance tests performed in a signle cylinder engine. Peak values of heat releases rate (HRRmax) were also observed higher, and their locations were earlier than regular diesel (Emiroğlu and Şen 2018). Also, they reported increased in NO_x emission in the tail pipe due to the generation of higher locally peak temperature inside the combustion chamber (Emiroğlu and Şen 2018). Jamrozik et al. (2018) have performed experiments for dual fuel mode in a CI engine operating at full load for 1500 rpm. They observed that addition of ethanol increased ignition delay (ID), indicated thermal efficiency (ITE), indicated mean effective pressure (IMEP). Concerning emissions, higher NO_x emission was observed compare to mineral diesel; however, it reduced CO emission in the tail pipe (Jamrozik et al. 2018). Oliveira et al. (2015) have experimented the diesel power generator for different fuel blends of anhydrous ethanol (5, 10, and 15% of ethanol in diesel oil with 7% biodiesel (B7); v/v) at varying loading conditions (5–37.5 kW). The test was performed without any modification in geometry and blend of ethanol–diesel–biodiesel were injected. Result of experiments was compared with baseline B7. They observed increase in ignition delay (ID) and late start of combustion (SOC) with increase in ethanol percentage; however, combustion duration (CD) and exhaust gas temperature (EGT) were reduced (Oliveira et al. 2015). Padala et al.

(2013) conducted an experiment with ethanol manifold injection in a CI engine and reported that ethanol port injection resulted in higher engine efficiency. Park et al. (2011) reported reduction of HC and CO for ethanol mixed fuel in diesel engine. Tutak et al. (2015) conducted an experiment with E85 (85% ethanol + 15% gasoline; v/v) blends with diesel. They reported E85 with diesel increased ignition delay, peak combustion temperature, BTE, total hydrocarbon (THC), and CO emissions, moreover, combustion duration, NO_x, and soot emissions showed reduction.

With studies previously performed, it is evident that the performance and emission values were largely affected by the fraction of ethanol in the blends for CI engines. Although, study related to application and impact of ethanol in CI engine has been studied, further research is still required to optimize the performance and emissions parameters. Aim of the chapter is to provide details about the utilization of different ethanol blends. A comprehensive review related to combustion and emissions properties of ethanol ratios for different engine operating conditions were performed.

12.2 Alcohols as an Alternative Fuels

Lower carbon number alcohols, like methanol and ethanol, have been of more interest because to their ease of production and their inherent oxygen content for alcohol-diesel blends. Utilization of blended fuel in CI engine could increase combustion efficiency and reduce the emissions of exhaust (Asad et al. 2015; Moka et al. 2014). Since low carbon alcohol poses lower cetane number, higher latent heat of vaporization and poor miscibility, these properties restricts the utilization of alcohols of low carbon atoms for utilization as a fuel. Four or more carbon alcohols have other advantages compared to low carbon alcohols as diesel fuel additives. These have higher heating value and higher cetane number than low carbon alcohols; however, difficulty in production and availability limits its utilization in CI engine (Ma et al. 2017). Ethanol (C_2H_5OH), which is renewable and having high oxygen content (~35% m/m), is used as a blend with diesel in CI engine. One of the important aspects for ethanol is that it can be produced from several biomass feedstocks. Production of ethanol and its utilization in transportation may reduce the dependency on conventional fuels, provide fuel security, and result in overall lower CO_2 emission (in a well-to-wheel manner). Ethanol's high oxygen content enhances combustion and decreases exhaust emissions (Rakopoulos et al. 2007). Although due to its hygroscopic nature and lower flashpoint, more care is required during handling, transportation, and storage (Banapurmath and Tewari 2010). Ethanol has lower evaporation temperature compare to diesel fuel; the blend of diesel and ethanol will encourage fuel evaporation and thus accelerate the preparation of the air and fuel mixture. Moreover, poor miscibility of ethanol partially restricts ethanol to have a homogeneous solution with diesel, which, sometimes, results in phase separation (Kumar et al. 2013). Mixing of ethanol and mineral diesel is normally restricted to 15% due to different molecular polarities of fuel. Emulsifier is normally being

used to enable higher ethanol–diesel blending concentration (more than 15% v/v). Ethanol miscibility in mineral diesel largely depends on hydrocarbon, wax content, and temperature of fuel. Lower ethanol percentage shows better consistent solution compare to higher ethanol blends. Also, hygroscopic nature of alcohols allows to absorb moisture quickly from the environment. This phenomenon tends to separate out the ethanol from the ethanol–diesel blends. Separation tendency further increases if the blends are kept at lower temperature (lower than 10 °C) (Kumar et al. 2013); this affects the feasibility of utilization in cold weather conditions. Direct blending of ethanol (more than 15%) into diesel is not desirable because of phase separation. Emulsion method is used to avoid the phase separation problem, which increases blending capacity up to 25% in diesel (Çelebi and Aydın 2019). Moreover, the port injection of ethanol allows the use of even higher concentrations of ethanol (Çelebi and Aydın 2019). Kwanchareon et al. (2007) experimented to study solubility and emissions properties of diesel–biodiesel–ethanol blends in CI engine. They reported 20 °C as an important key point where phase seaparation starts and stated that blending proportion of 80-15-5 for diesel–biodiesel–ethanol shows optimal properties and emission values (Kwanchareon et al. 2007). Lower CO and HC emissions for higher engine load were reported for the same; however, NO_x emission was observed relatively higher compare to diesel (Kwanchareon et al. 2007). Several researchers (Rakopoulos et al. 2008; Labeckas et al. 2014; Ajav et al. 1999) reported utilization of ethanol blends in CI engine. Rakopoulos et al. 2008 (2008) have investigated the use of ethanol and mineral diesel blend (E05, E10, and E15) in a direct injection CI engine at 2000 rpm for four different engine loads. They observed that uses of ethanol–diesel blends reduce CO and smoke emissions significantly, while reduction in NO_x emissions were marginally (Rakopoulos et al. 2008).

12.3 Physico-chemical Properties of Ethanol and Diesel

Physico-chemical properties of ethanol and diesel are shown in Table 12.1. It was noted that ethanol has high auto-ignition temperature ~363 °C (approximately 42% higher than diesel auto-ignition temperature ~254 °C), which shows that it needs significant higher compression ratio than diesel in order to initiate the auto-ignition. Moreover, ethanol is an oxygenated fuel with ~35% m/m inherent oxygen content which may help for its faster combustion compare to mineral diesel, and also, ethanol has 75% less viscosity than diesel which may reduce viscous losses during fuel injection.

Table 12.1
Physico-chemical properties of ethanol and diesel (Zhang et al. 2011; Karabektas et al. 2013; Sahu et al. 2019)

Properties	Ethanol	Diesel (BS-IV)
Molecular formula	C_2H_5OH	C_nH_{2n}
Molecular weight, (g/mole)	46	–
Stoichiometric ratio, (A/F ratio)	9	15
Cetane number	6	51
Flashpoint, (°C)	15	35
Auto-ignition temperature, (°C)	363	254
Viscosity at 20 °C, (mPas)	1.2	2.0–4.5
Density,(kg/m^3)	786	820–845
Lower heating value (MJ/kg)	28.4	45.5
Heat of vaporization (kJ/kg)	840	–
Oxygen content, (wt%)	34.8	0

12.3.1 Effect of Ethanol Blends on In-Cylinder Pressure and Heat Release Rate (HRR)

In-cylinder pressure trace and heat release rate (HRR) are important combustion characteristics. These parameters are useful to understand combustion behavior of fuel–air mixture and to correlate the performance and emission data with combustion. Emiroğlu et al. (2018) have performed experiments to investigate the combustion, performance and emissions parameters of diesel engine fueled with 10% blends of alcohols (methanol, ethanol, and butanol; v/v) for varying engine loading conditions at 1500 rpm. Peak in-cylinder pressure (Pmax), maximum heat release rate (HRRmax), and ignition delay were observed to be higher for alcohols compared to mineral diesel for all loading conditions (Emiroğlu and Şen 2018) (Fig. 12.1).

Ning et al. (2020) have investigated dual fuel injection with diesel as direct injection and alcohols as port injections. The volume fraction of alcohol was maintained at 10, 20, 30, and 40% (v/v) for engine operating condition of 2500 rpm and 0.75 MPa. They observed that increased fraction of port injected alcohols increased the ignition delay, decreased the Pmax, and increased HRRmax (Fig. 12.2). Their results showed decreased combustion duration with delayed SOI when alcohols were port injected (Ning et al. 2020).

Tse et al. (2015) have investigated the varying fraction of ethanol (5, 10, and 20%; v/v) with baseline fuel as diesel–biodiesel blend (15% biodiesel with ultra-low sulfur diesel) for combustion and particulate matter (PM) analysis. They observed that the utilization of ethanol blending with baseline fuel increases the Pmax and HRRmax, reduces the combustion duration (CD), and retards the start of injection (Tse et al. 2015). Ethanol fumigation into the air-intake manifold was studied by Jamuwa et al. (2016) to investigate the combustion, performance, and emissions characteristics of small capacity CI engine. They observed increase in Pmax and

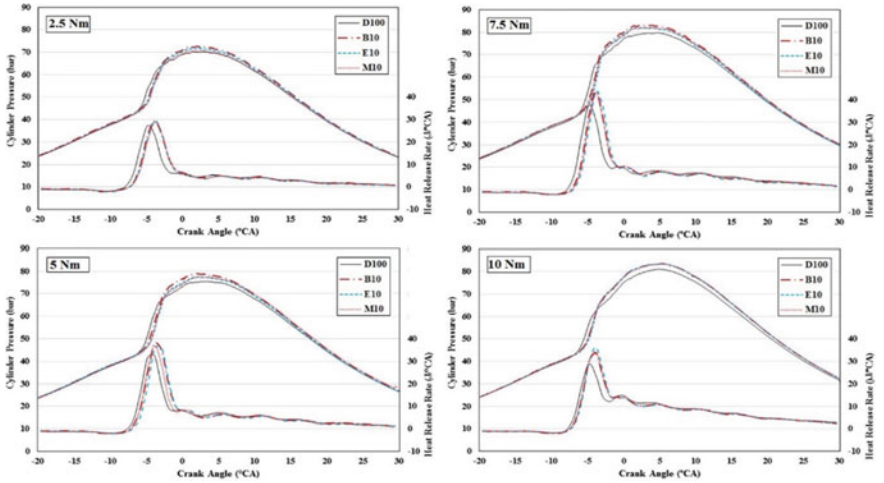

Fig. 12.1 In-cylinder pressure vs CAD and HRR vs CAD curve under different engine loads at 1500 rpm (M10, E10, and B10 are methanol, ethanol, and butanol, respectively, into diesel) (Emiroğlu and Şen 2018)

HRRmax by using ethanol fumigation. It also improved the break thermal efficiency of the engine (Jamuwa et al. 2016) (Fig. 12.3).

Prashant et al. (2016) conducted an experiment to investigate combustion parameters of a four-cylinder (turbocharged and intercooled) duel-fuel diesel engine for different engine loading conditions (10, 20. and 40% of the rated engine load). They reported lower ignition delay (ID) for higher loads (ID at 20% ethanol substitution was 16, 14, and 10° CA for 10, 20, and 40% loading conditions, respectively) (Fig. 12.4) (Prashant et al. 2016).

12.3.2 Effect of Ethanol Blends on Performance Parameter

The brake-specific fuel consumption (BSFC) of the blended fuels relies on some of the physico-chemical characteristics such as calorific value, density, viscosity of the fuel. Typically, BSFC of fuel blend increases as the energy content in the fuel decreases. Ethanol has lower heating value (LHV) which reduces overall heating value of blends upon increasing ethanol blend fraction. Concerning the performance parameters investigated by Emiroğlu et al. (2018), it was observed that BSFC was higher and BTE was lower for alcohol blends (10% blends of butanol, ethanol, and methanol; B10, E10, M10) for tested loading conditions compared to mineral diesel (Fig. 12.5). Comparing the blends of alcohols, butanol performed superior with higher efficiency for a given engine load (Emiroğlu and Şen 2018).

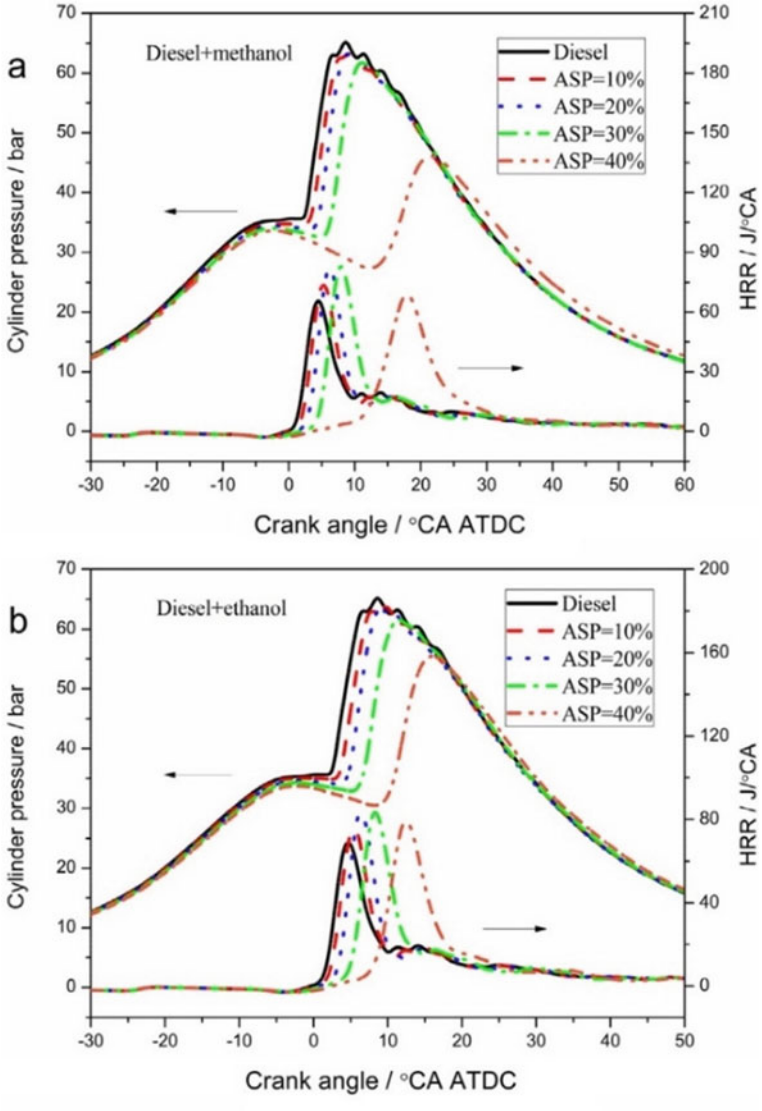

Fig. 12.2 Effects of (**a**) methanol and (**b**) ethanol blendings on in-cylinder pressure vs CAD and heat realease rate vs CAD curve at IMEP = 0.75 MPa at 2500 rpm (Ning et al. 2020)

Jamuwa et al. (2016) have investigated for five different ethanol fumigation rates (0, 0.1, 0.2, 0.3, 0.4, and 0.5 kg/h) assigned as e0, e1, e2, e3, e4, and e5 in a CI engine. They reported increased BTE for higher loading condition up to 6% (Fig. 12.6) with higher fumigation rates compare to e0; however, it showed reduced BTE up to 11.2% at lower engine loads (Jamuwa et al. 2016). They observed BTE for e0

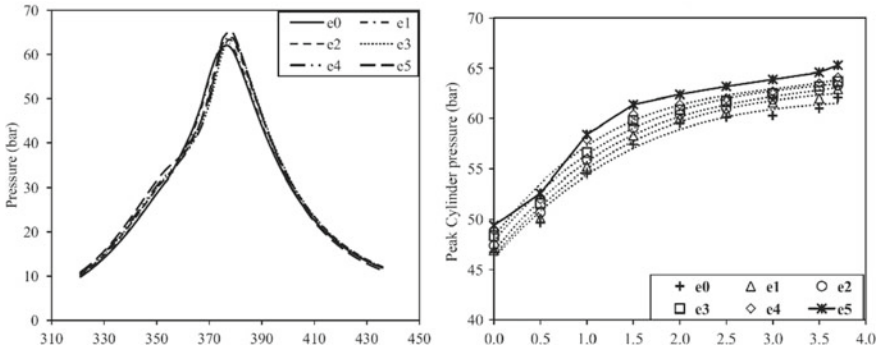

Fig. 12.3 P-Θ and values of Pmax for diesel and different ethanol fumigation rates (0, 0.1, 0.2, 0.3, 0.4, and 0.5 kg/h) assigned as e0, e1, e2, e3, e4, and e5 (Jamuwa et al. 2016)

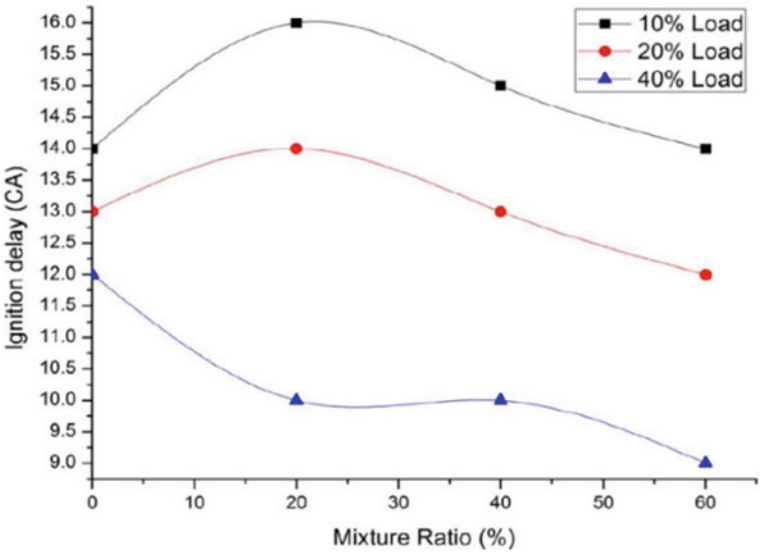

Fig. 12.4 Ignition delay (CA) versus mixture ratio (%) (Prashant et al. 2016)

was 28.3% at full load condition, and with ethanol fumigation, BTE recorded was relatively higher by 3.2%, 4.3%, 5.3%, 6%, and 5% for e1, e2, e3, e4, and e5, respectively (Jamuwa et al. 2016). Four different blends were prepared with 15% blending of methanol, ethanol, biodiesel, and vegetable oil, respectively, with mineral diesel for the performance and emission investigation by Karabektas et al. (2013). Test was performed for different engine speeds, at full load condition. Blends of ethanol and methanol have resulted in reduced brake power and increased specific fuel consumption. At engine maximum torque speed (1400 rpm), BSFC recorded was

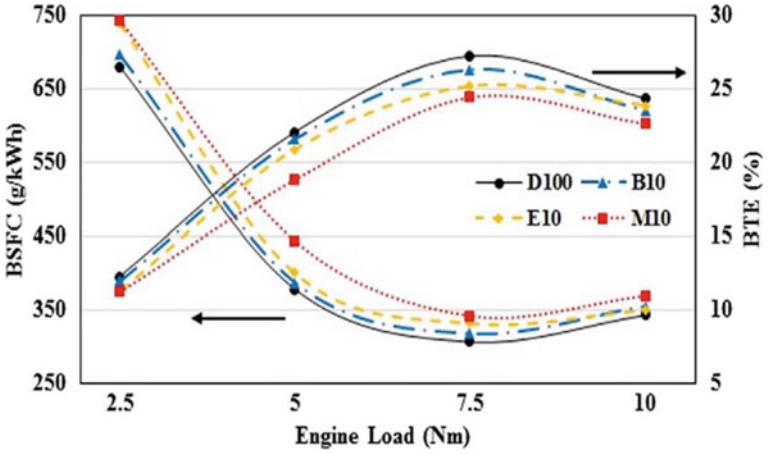

Fig. 12.5 BSFC and BTE vs engine loads plot (1500 rpm) for D100, M10, E10, and B10 (M10, E10, and B10 are methanol, ethanol, and butanol, respectively, into diesel) (Emiroğlu and Şen 2018)

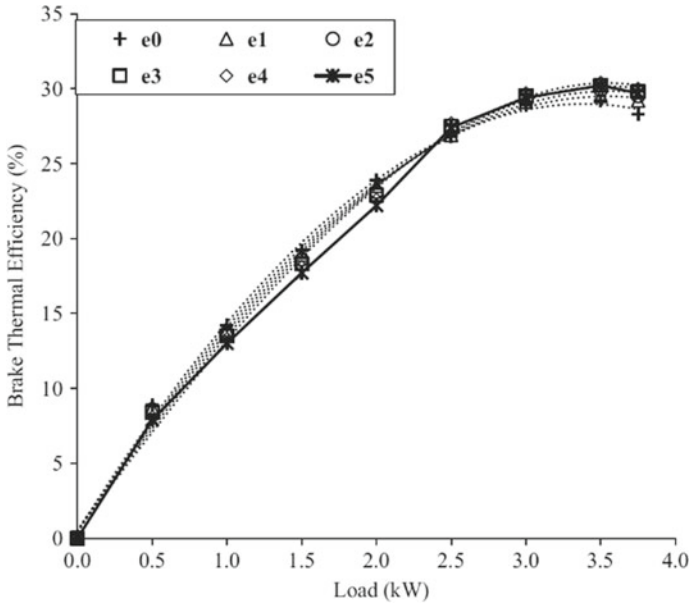

Fig. 12.6 BTE versus load curve for different ethanol fumigation rates (0, 0.1, 0.2, 0.3, 0.4, and 0.5 kg/h) assigned as e0, e1, e2, e3, e4, and e5 (Jamuwa et al. 2016)

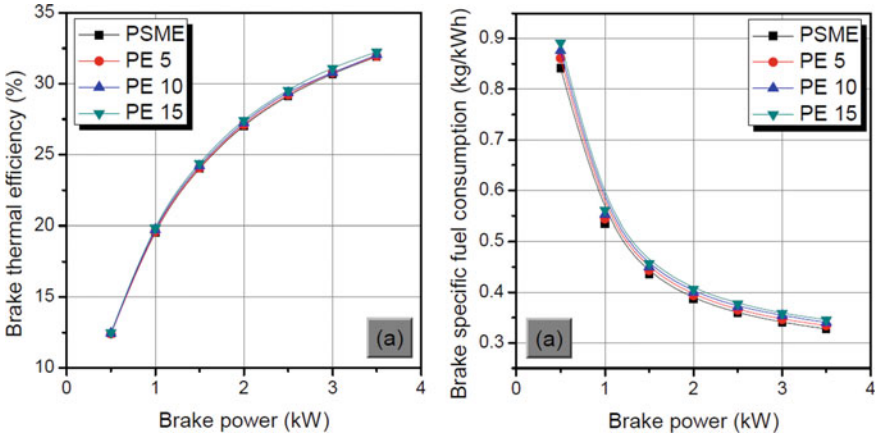

Fig. 12.7 BTE versus brake power (left) and BSFC versus brake power (right) plot for biodiesel (PSME) and biodiesel–ethanol blends (Datta and Mandal 2017)

0.265, 0.292, and 0.281 g/kWh for diesel, M15, and E15, respectively (Karabektas et al. 2013).

The effects of alcohol addition into biodiesel were studied by Datta and Mandal 2017 (2017) for combustion, performance, and emission characterization of the CI engine using diesel RK software. They simulated CI engine fueled with palm stearin biodiesel–ethanol (PSME) and reported that addition to ethanol increases the time of ignition (ignition delay was ~10.0° CA, 14.2° CA, and 15.6° CA for PSME, PE15, and PM15, respectively, at full load condition), higher HRR and a marginally increase in thermal efficiency (BTE observed were 31.91%, 32.24%, and 32.47% for PSME, PE15, and PM15, respectively, at full load condition) (Fig. 12.7) (Datta and Mandal 2017).

Padala et al. (2013) have reported that ethanol injection increases the engine efficiency. They claimed that 10% increase in efficiency was achieved by replacing 60% of diesel with ethanol (Padala et al. 2013). Murcak et al. (2013) have experimented to see effect of ethanol–diesel blends in CI engine. Experiment was conducted with three different blends (5, 10, and 20% of ethanol into mineral diesel) (Murcak and 2013). They found that 5% ethanol blends show highest brake power; however, maximum torque (42.27 Nm) was obtained for 10% ethanol–diesel blend and BSFC was minimum for 20% ethanol–diesel blend (Murcak et al. 2013). Pradelle et al. (2019) conducted an experiment to study the combustion and performance of Euro-3 CI engine for varying blend ratio of diesel–biodiesel–ethanol at different engine speeds. Adding ethanol into fuel increases ignition delay and HRR however decreased the Pmax. They also reported increase in BSFC (approximately 2% increase for each 5% volume of alcohol) (Pradelle et al. 2019).

12.3.3 Effect of Ethanol Blends on Emissions Parameters

Concerning the emission parameters investigated by Emiroğlu et al. (2018), it was noted that NO_x emission increased (Fig. 12.8) due to the generation of higher locally peak temperature because of ignition delay. Smoke and CO emissions decreased (50% reduction for smoke and up to 15% reduction for CO compare to mineral diesel at 10 Nm) due to improvement of combustion quality because low viscosity and presence of inherent oxygen promote combustion. Their study showed that alcohols have a good option for the future alternative of the diesel engines because it significantly reduces exhaust emissions without significantly affecting the performance of the engine. It was suggested in the study that alcohols may lead to the removal of expensive after-treatment devices also. In a study conducted by Kannan et al. (2012) ethanol is injected through port injection and diesel–jatropha methyl ester (JME) blends were injected directly in the combustion chamber. Addition of ethanol in diesel and JME increased fuel consumption (up to 10% higher at low load and 2–4% higher at high engine load compare to mineral diesel), thermal efficiency (7% higher at full load and 1% higher at low load), and NO_x emissions (40% reduced for low load and 30% higher for full load. Significantly, reduction in smoke, CO, and THC was found with increasing fraction of ethanol in diesel–JME at higher loads. These reductions for smoke, CO, and THC were observed to be 4%, 5%, and 8%, respectively (Kannan et al. 2012).

Park et al. (2011) observed lower NO_x emissions (900 ppm, 820 ppm, and 600 ppm for diesel, 10% ethanol, and 20% ethanol blend, respectively, at 1500 rpm and 30 Nm) for the tests performed in a CRDI engine for different ethanol–diesel blends. On the one hand, higher CO and HC emissions were recorded (CO emissions for diesel, 10% ethanol, and 20% ethanol blend were 0.04%, 0.05%, and 0.11%, respectively, at 1500 rpm and 30 Nm) (Park et al. 2011). Padala et al. (2013) conducted an experiment to observe the utilization of ethanol in a CRDI engine. Ethanol injection in the manifold and direct injection of mineral diesel was adopted for their experiments. They reported that the increased fraction of ethanol injection in the manifold, HC, CO, and NO_x emissions was increased; however, smoke emission decreased (Padala et al. 2013). Some of the studies (Zhang et al. 2011; Ning et al. 2020; Tse et al. 2015) focused on the measurement of CO, HC, and PM measurement.

Zhang et al. (2011) have experimented with various alcohol blends in diesel engine; they reported NO_x (up to 16%) and PM emissions reduced (up to 26%) using alcohols blended fuel however increase CO and HC emissions (CO emissions were 3 and 10 g/kW h for mineral diesel and 20% ethanol at mid-load condition) (Fig. 12.9) (Zhang et al. 2011). Ning et al. (2020) have also tested various alcohol blends (ethanol, methanol and butanol with mineral diesel) in a CI engine. They observed alcohols reduced PM emission (by up to ~93%) and CO emission (by up to ~90%); however, NO_x emissions were increased (by up to 60%) (Ning et al. 2020). Concerning the emission parameters investigated by Tse et al. (2015), brake-specific particulate matter (BSPM) emissions were observed lower (~200 mg/kWh) for 20% ethanol blends than other diesel–biodiesel–ethanol blends (Fig. 12.10) at low and

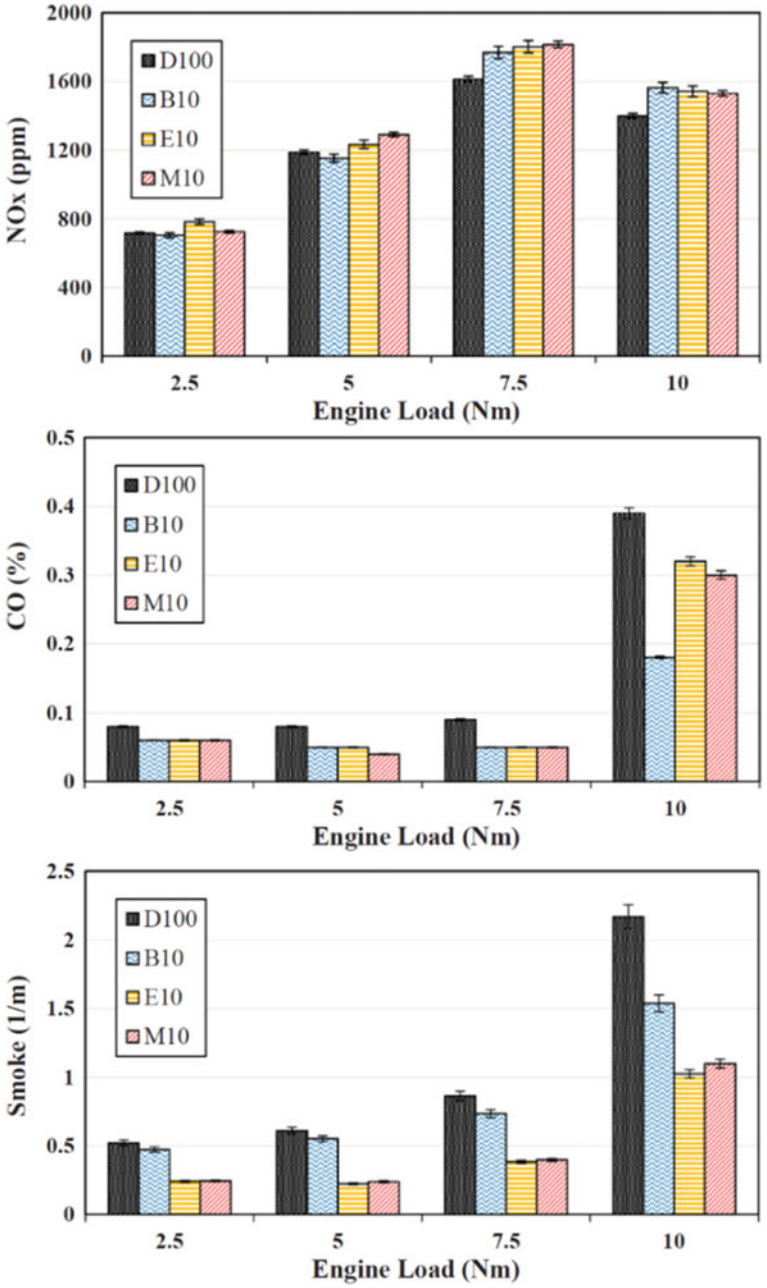

Fig. 12.8 NO_x, CO, and smoke emissions vs engine load for various blends (D100, B10, E10, and M10) (Emiroğlu and Şen 2018)

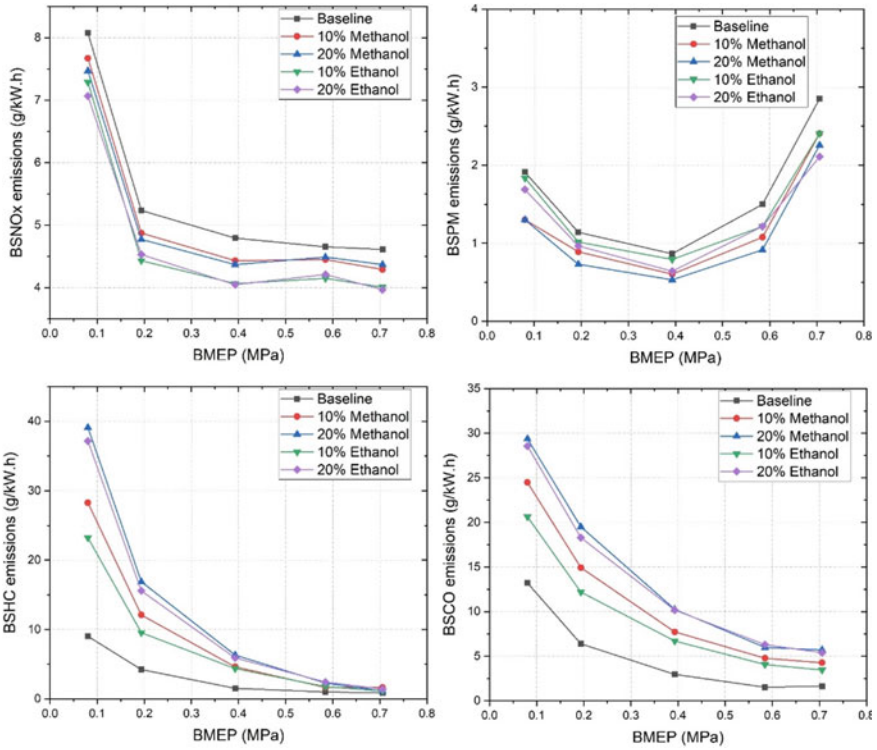

Fig. 12.9 Comparison of BSNOx, BSPM, BSHC, and BSCO emissions for ethanol and methanol blends with diesel (Zhang et al. 2011)

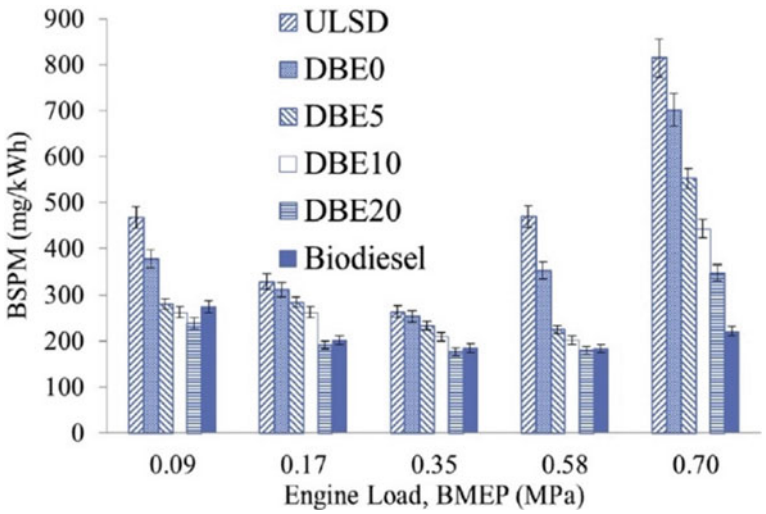

Fig. 12.10 Variation of BSPM with engine load for alternative fuels and ULSD (Tse et al. 2015)

intermediate engine load conditions although biodiesel showed lower BSPM for full load condition (Tse et al. 2015). Mofijur et al. (2015) have reported that the blending of ethanol and biodiesel into diesel showed reduction of NO_x emissions (up to 11.9%), HC emissions (up to 15.1%), and CO emissions (up to 14.7%). Praptijanto et al. (2015) have experimented with ethanol–diesel blend on CI engine. They also reported alcohols blending in base fuel mineral diesel reduce PM, NO_x, and CO emissions in the tailpipe (Praptijanto et al. 2015).

12.4 Conclusions

Continuous utilization of conventional fuels for energy resources is not sustainable, because of limited-continously reducing reserves and higher GHGs emissions. Research in the field of alternative fuel is vital to secure future environmental condition. Alcohols (primarily methanol and ethanol) produced from bio-resources have emerged as one of the best alternative uses in IC engines for a partial or full replacement of diesel fuel. Lower mass fraction of carbon, lower sulfur content and higher inherent oxygen content added advantage for its utilization in IC engines as a fuel. The literature reported in this chapter shows that the indicated thermal efficiency of the engine decreases and brake-specific fuel consumption increases as ethanol fraction increases in fuel blends. This primarily happens becuase of the lower heating value of alcohols. As far as emissions are concerned, CO and HC emissions decrease with ethanol blend percentage due to inherent oxygen and lower viscosity of ethanol; however, NO_x emissions increase due to the locally higher peak in-cylinder temperature. It can be concluded from various studies that ethanol blends tend to reduce the smoke emissions drastically in comparison with mineral diesel. Since PM emission is the critical emission parameter for diesel exhaust, ethanol blends can play an important role in reducing PM emissions. Ethanol-blended fuels may reduce the load on costly after-treatment devices.

References

Ajav EA, Singh B, Bhattacharya TK (1999) Experimental study of some performance parameters of a constant speed stationary diesel engine using ethanol–diesel blends as fuel. Biomass Bioenerg 17:357–365

Anyon P, Pattison B-A, Trompp W (2003) Toxic emissions from diesel vehicles in Australia. Parsons Aust Pty Ltd. 112

Asad U, Kumar R, Zheng M, Tjong J (2015) Ethanol-fueled low temperature combustion: a pathway to clean and efficient diesel engine cycles. Appl Energy 157:838–850

Banapurmath NR, Tewari PG (2010) Performance, combustion, and emissions characteristics of a single-cylinder compression ignition engine operated on ethanol—biodiesel blended fuels. Proc Inst Mech Eng Part J Power Energy 224:533–543

Çelebi Y, Aydın H (2019) An overview on the light alcohol fuels in diesel engines. Fuel 236:890–911. https://doi.org/10.1016/j.fuel.2018.08.138

Datta A, Mandal BK (2017) Engine performance, combustion and emission characteristics of a compression ignition engine operating on different biodiesel-alcohol blends. Energy 125:470–483. https://doi.org/10.1016/j.energy.2017.02.110

de Oliveira A, de Morais AM, Valente OS, Sodré JR (2015) Combustion characteristics, performance and emissions from a diesel power generator fuelled by B7-ethanol blends. Fuel Process Technol 139:67–72

Emiroğlu AO, Şen M (2018) Combustion, performance and emission characteristics of various alcohol blends in a single cylinder diesel engine. Fuel 212:34–40

Gilbert R, Perl A (2005) Energy and transport futures. A report prepared national round table environment economics university calgary, 1–96

Goldemberg J, Johansson TB, Reddy AKN, Williams RH (2001) Energy for the new millennium. Ambio a J Hum Environ 30:330–337

Gürü M, Koca A, Can Ö, Çınar C, Şahin F (2010) Biodiesel production from waste chicken fat based sources and evaluation with Mg based additive in a diesel engine. Renew Energy 35:637–643

Jamrozik A, Tutak W, Gruca M, Pyrc M (2018) Performance, emission and combustion characteristics of CI dual fuel engine powered by diesel/ethanol and diesel/gasoline fuels. J Mech Sci Technol 32:2947–2957

Jamuwa DK, Sharma D, Soni SL (2016) Experimental investigation of performance, exhaust emission and combustion parameters of stationary compression ignition engine using ethanol fumigation in dual fuel mode. Energy Convers Manag 115:221–231

Kannan D, Pachamuthu S, Nabi MN, Hustad JE, Løvås T (2012) Theoretical and experimental investigation of diesel engine performance, combustion and emissions analysis fuelled with the blends of ethanol, diesel and jatropha methyl ester. Energy Convers Manag 53:322–331

Karabektas M, Ergen G, Hosoz M (2013) Effects of the blends containing low ratios of alternative fuels on the performance and emission characteristics of a diesel engine. Fuel 112:537–541. https://doi.org/10.1016/j.fuel.2011.04.036

Kessel DG (2000) Global warming—facts, assessment, countermeasures. J Pet Sci Eng 26:157–168

Kumar S, Cho JH, Park J, Moon I (2013) Advances in diesel–alcohol blends and their effects on the performance and emissions of diesel engines. Renew Sustain Energy Rev 22:46–72

Kumar ST, Gupta S, Chandra SP (2019) Chapter 4. Second generation ethanol.pdf. Altern. Fuels Their Util. Strateg. Intern. Combust. Engines, Springer Nature Singapore Pte Ltd. 2020, pp 49–64. https://doi.org/10.1007/978-981-15-0418-1_4

Kwanchareon P, Luengnaruemitchai A, Jai-In S (2007) Solubility of a diesel–biodiesel–ethanol blend, its fuel properties, and its emission characteristics from diesel engine. Fuel 86:1053–1061

Labeckas G, Slavinskas S, Mažeika M (2014) The effect of ethanol–diesel–biodiesel blends on combustion, performance and emissions of a direct injection diesel engine. Energy Convers Manag 79:698–720

Ma Y, Huang S, Huang R, Zhang Y, Xu S (2017) Ignition and combustion characteristics of n-pentanol–diesel blends in a constant volume chamber. Appl Energy 185:519–530

Mofijur M, Rasul MG, Hyde J (2015) Recent developments on internal combustion engine performance and emissions fuelled with biodiesel-diesel-ethanol blends. Procedia Eng 105:658–664. https://doi.org/10.1016/j.proeng.2015.05.045

Moka S, Pande M, Rani M, Gakhar R, Sharma M, Rani J et al (2014) Alternative fuels: an overview of current trends and scope for future. Renew Sustain Energy Rev 32:697–712

Murcak A, Hasİmoğlu C, Çevik I, Karabektas M, Ergen G (2013) Effects of ethanol-diesel blends to performance of a DI diesel engine for different injection timings. Fuel 109:582–587. https://doi.org/https://doi.org/10.1016/j.fuel.2013.03.014

Ning L, Duan Q, Chen Z, Kou H, Liu B, Yang B et al (2020) A comparative study on the combustion and emissions of a non-road common rail diesel engine fueled with primary alcohol fuels (methanol, ethanol, and n-butanol)/diesel dual fuel. Fuel 266:117034

Padala S, Woo C, Kook S, Hawkes ER (2013) Ethanol utilisation in a diesel engine using dual-fuelling technology. Fuel 109:597–607. https://doi.org/10.1016/j.fuel.2013.03.049

Park SH, Youn IM, Lee CS (2011) Influence of ethanol blends on the combustion performance and exhaust emission characteristics of a four-cylinder diesel engine at various engine loads and injection timings. Fuel 90:748–755

Pradelle F, Braga SL, de Aguiar Martins ARF, Turkovics F, Pradelle RNC (2019) Performance and combustion characteristics of a compression ignition engine running on diesel-biodiesel-ethanol (DBE) blends–potential as diesel fuel substitute on an Euro III engine. Renew Energy 136:586–598

Praptijanto A, Muharam A, Nur A, Putrasari Y (2015) Effect of ethanol percentage for diesel engine performance using virtual engine simulation tool. Energy Procedia 68:345–354

Prashant GK, Lata DB, Joshi PC (2016) Investigations on the effect of ethanol blend on the combustion parameters of dual fuel diesel engine. Appl Therm Eng 96:623–631

Rakopoulos CD, Antonopoulos KA, Rakopoulos DC (2007) Experimental heat release analysis and emissions of a HSDI diesel engine fueled with ethanol-diesel fuel blends. Energy 32:1791–1808. https://doi.org/10.1016/j.energy.2007.03.005

Rakopoulos DC, Rakopoulos CD, Kakaras EC, Giakoumis EG (2008) Effects of ethanol–diesel fuel blends on the performance and exhaust emissions of heavy duty DI diesel engine. Energy Convers Manag 49:3155–3162

Tse H, Leung CW, Cheung CS (2015) Investigation on the combustion characteristics and particulate emissions from a diesel engine fueled with diesel-biodiesel-ethanol blends. Energy 83:343–350

Tutak W, Lukacs K, Szwaja S, Bereczky A (2015) Alcohol–diesel fuel combustion in the compression ignition engine. Fuel 154:196–206

Zhang ZH, Tsang KS, Cheung CS, Chan TL, Yao CD (2011) Effect of fumigation methanol and ethanol on the gaseous and particulate emissions of a direct-injection diesel engine. Atmos Environ 45:2001–2008